THE JOURNAL OF CHEMICAL PHYSICS

VOLUME 14 NUMBER 3

MARCH 1, 1946

Published by the

AMERICAN INSTITUTE OF PHYSICS

Lancaster Press, Inc. New York, N. Y.

...MICAL ...CS

...RS

...itor

...

...

...

THE JOURNAL
OF
CHEMICAL PHYSICS

VOLUME 14, NUMBER 3 MARCH, 1946

Surfaces of Solids XV

First-Order Phase Changes of Adsorbed Films on the Surfaces of Solids: The Film of *n*-Heptane on Ferric Oxide

GEORGE JURA, EDWARD H. LOESER, PAUL R. BASFORD, AND WILLIAM D. HARKINS*
Department of Chemistry, University of Chicago, Chicago, Illinois
and
Physical Chemical Research, Engineering Division, Chrysler Corporation, Detroit, Michigan
(Received November 23, 1945)

Two-dimensional first-order changes, in which a gaseous film of normal heptane is transformed into another phase of lower molecular area with evolution of heat, have been discovered on subphases of ferric oxide, silver, and graphite. All of the critical phenomena observed in three-dimensional systems are found to be duplicated. For *n*-heptane on ferric oxide the critical constants are: σ_c (area) 900A^2 per molecule; π (film pressure) 0.45 dyne cm^{-1}; and T_c, 29°C. The critical constants are found to depend on the nature of the solid as well as on that of the vapor. The heat of transformation at 25°C is estimated to be 12,000±5000 cal. mole^{-1}. This value appears to be considerably higher than the 6150 cal. mole^{-1} required for the formation of three-dimensional liquid *n*-heptane from its vapor at the same temperature. The volume-pressure relations are considered for the adsorption isotherm in the case in which a second- or third-order phase change occurs.

I. INTRODUCTION

IN recent papers from this laboratory the point of view has been adopted that the phases and phase changes of films on solids are similar to those of monolayers on the surface of water. It has been found that those changes which are first order in three dimensions are apt to be second order on either solids or water in two dimensions. One exception to this is in the reversible vaporization-condensation in monolayers of oil on the surface of water, which is usually first order, even though it is in some cases second order.[1]

The earliest first-order change to be found on a solid was that of *n*-heptane on silver.[2] However, that of the same vapor on crystalline ferric oxide, as reported here, has been investigated in much more detail and exhibits at temperature from 15° to 30°C the same general phenomena as those of three-dimensional gases in the vicinity of the critical point.

II. THEORY

Most changes of phase in three dimensions are of the first order, i.e., possess a latent heat of transformation and a discontinuous change in volume. Many transformations, however, are of the second order. The criteria for the order of changes of phase in three dimensions were first

* The writers wish to acknowledge the helpful cooperation in this work of Dr. Orlan M. Arnold of the Chrysler Corporation. This is a part of a larger research project under the general direction of William D. Harkins.

[1] For an illustration of such a second-order change, see N. K. Adam and G. Jessop, Proc. Roy. Soc. **A110**, 423 (1926)

[2] G. Jura, E. H. Loeser, W. D. Harkins, and P. R. Basford, J. Chem. Phys. **13**, 535 (1945).

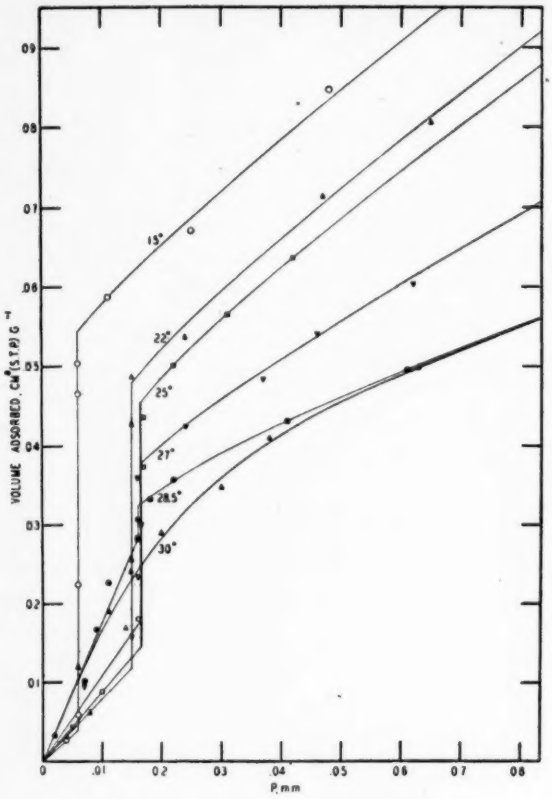

FIG. 1. Low pressure isotherms of *n*-heptane on ferric oxide. The curves at 15°, 22°, 25°, 27°, 28.5°C exhibit a finite discontinuity of v as a function of p.

set down by Ehrenfest.[3] Harkins and Boyd[4] and Dervichian[5] have both developed the criteria for phase changes in two-dimensional films. For films it develops that the compressibility, k, defined by the equation, is sufficient to determine the order of the change.

$$k=\frac{1}{-\sigma}\left(\frac{\partial\sigma}{\partial\pi}\right)_T. \qquad (1)$$

For a first-order change, k becomes infinite for those values of σ for which the transition occurs; for a second-order change there is a *finite* discontinuity in k, while for a third-order change there is a finite discontinuity in $(\partial k/\partial\sigma)_T$.

The observed pressure (p), volume (v) adsorption data can be put into the $\pi-\sigma$ form if π is obtained by the integration of the Gibbs adsorption equation as suggested by Bangham.[6-8]

The area of the surface available per molecule can be calculated from the specific area, Σ, and the volume of gas adsorbed. Likewise, it is possible to express the compressibility as a function of the quantities directly measured in adsorption. This transformation can be carried out by use of the Gibbs adsorption equation. The compressibility is then found to be

$$k=\frac{V_M\Sigma}{RTv^2}\left(\frac{\partial v}{\partial \ln p}\right)_{T,\Sigma}, \qquad (2)$$

where V_M is the molar gas volume, Σ, the specific area, R the gas constant, T the absolute temperature, v the volume of gas adsorbed per gram, and p the equilibrium pressure. Thus, in a first-order change, the volume must vary, without any change in pressure, in a second-order change there is a discontinuity in $(\partial v/\partial p)_T$, and in a

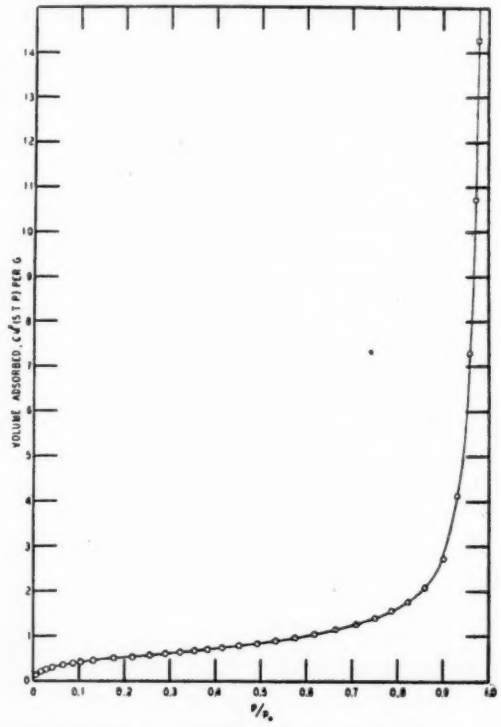

FIG. 2. The complete isotherm of *n*-heptane on ferric oxide at 25°C. $p_0=45.77$ mm.

[3] P Ehrenfest, Proc. Acad. Sci. (Amsterdam) **36**, 115 (1933).
[4] W. D. Harkins and G. E. Boyd, J. Phys. Chem. **45**, 20 (1941)
[5] D. G. Dervichian, J. Chem. Phys. **7**, 932 (1939).
[6] D. H. Bangham, Trans. Faraday Soc. **33**, 805 (1937).
[7] D. H. Bangham and R. I. Razouk, Trans. Faraday Soc. **33**, 1463 (1937).
[8] D. H. Bangham and R. I. Razouk, Proc. Roy. Soc. (London) **A166**, 572 (1938).

third-order change there is a discontinuity in $(\partial^2 v/\partial p^2)_T$. Thus, it is possible to determine if in a film a phase change occurs and the order of the phase change directly from the observed experimental data.

III. MATERIALS AND APPARATUS

The ferric oxide used was Baker and Adamson's reagent grade. The *n*-heptane, apparatus, and method of making the measurements have been described by Jura and Harkins.[9] Temperatures were determined with a mercury thermometer graduated to 0.1°C which had been compared with a similar thermometer calibrated by the Bureau of Standards.

IV. EXPERIMENTAL RESULTS

The isotherms at 15.00°±0.05°, 22.00°±0.02°, 25.00°±0.02°, 27.00°±0.02°, 28.50°±0.02°, and 30.00°±0.02°C up to a pressure of 0.080 mm are exhibited in Fig. 1, while the entire isotherm at 25°C from $p/p_0=0$ to $p/p_0=1$ is shown in Fig. 2. The area of the sample was $7.46 m^2 g^{-1}$ as determined by the relative method of Harkins and Jura.[10] The study of the isotherm in the region of high relative pressures indicates that the sample has some pores, although the small area exhibited indicates that the porosity is of minor importance. The data indicate also that the few pores that are present are large compared to the size of the *n*-heptane molecule. Assuming that the macroscopic constants of *n*-heptane can be used and that the Kelvin equation is valid, the isotherm shows that only a negligible fraction of the area is present in pores whose diameters are less than 200A.

Figure 2 shows that as judged by previous standards the isotherm is "normal." The main interest of this paper, however, lies in Fig. 1.

The important feature of the isotherms shown in Fig. 1 is that *all* the isotherms, except that at 30°, exhibit a finite discontinuity of v as a function of p. The discontinuity becomes smaller as the temperature is increased, and there is a concomitant increase in the value of the pressure from 0.006 mm at 15° to 0.016 mm at 28.5°, at which the discontinuity occurs. *The above are the experimentally observed facts.* Table I lists the pressures at which the discontinuity occurs and the volume of gas adsorbed at the end of each branch of the curve at the discontinuity.

TABLE I. The values of v and p at the discontinuity in the adsorption of *n*-heptane on ferric oxide.

t°C	p mm Hg	cc ads. g^{-1} at low p	cc ads. g^{-1} at high p
15.00	0.006	0.00396	0.0545
22.00	0.014	0.0119	0.0479
25.00	0.016	0.0144	0.0453
27.00	0.016	0.0173	0.0383
28.50	0.016	0.0283	0.0324

Obviously, the values of the volume adsorbed per gram at the point of discontinuity are not very precise since they are obtained by the extrapolation of each branch of the curve. This is especially true of the extrapolation of the branch of the curve from zero pressure. In Fig. 1 the curves on the low pressure side of the discontinuity are shown as straight lines. There is evidence, as illustrated by the 30° isotherm and the later discussion, that the lines are not straight but curved. However, sufficiently accurate data cannot be obtained with the present apparatus to determine the curvature.

Three questions concerning the discontinuity are raised by the experimental work: (1) the reproducibility of the values; (2) do they represent equilibrium? and (3) is the isotherm reversible? As to (1) it was found that the reproducibility of the discontinuity is within the limits of error of the determination of the pressure. For example, the discontinuity shown at 27°C occurs at a pressure of 0.017 mm Hg. A repetition of the experiment on a different sample of the ferric oxide showed the discontinuity to take place at the same pressure. The maximum observed difference of the pressure of the flat was found to be 0.002 mm.

From the experiments on adsorption alone it was not possible to prove without question that the observed values represent equilibrium. It can be shown only that the values do not change with time. After the time when the constancy of the pressure seemed to indicate that equilibrium had been established, it was found that there was no further change on standing for another 24 hours,

[9] G. Jura and W. D. Harkins, J. Am. Chem. Soc. **66**, 1356 (1944).
[10] W. D. Harkins and G. Jura, J. Am. Chem. Soc. **66**, 1366 (1944).

regardless of the position of the point in the isotherm, as follows: at the last point in the lower branch before entering the flat; at the first, middle, and end points in the flat; and in the first point on the upper branch of the curve. All of these remained constant, within experimental error, for a 24-hour period.

The results obtained by desorption at 25°C are exhibited in Fig. 3. The solid line represents the adsorption curve at the same temperature. Because of the low pressures, less than 2×10^{-3} cc of gas could be desorbed at one time. Since as much as 10 grams was used for the determination of the adsorption, it was not feasible to determine the desorption curve on the same sample as that used for adsorption. For the determination of the desorption 8×10^{-3} cc of gas was adsorbed on a sample weighing 0.16 gram. This point is shown as a circle in Fig. 3 at a pressure of 0.022 mm. The points obtained by desorption are shown as rectangles, whose size represents the possible error in the determination. The error in the volume desorbed was estimated on the assumption that the pressure reading could be in error by 0.001 mm. The time test applied to the adsorption was also used for desorption. In desorption the discontinuity occurred at a pressure of 0.014 mm, whereas in adsorption it occurred at 0.016 mm. Equal discrepancies in the pressure of the discontinuity have been observed for duplicate determinations of adsorption. Thus, within experimental error, the isotherm is reversible in the region of the discontinuity.

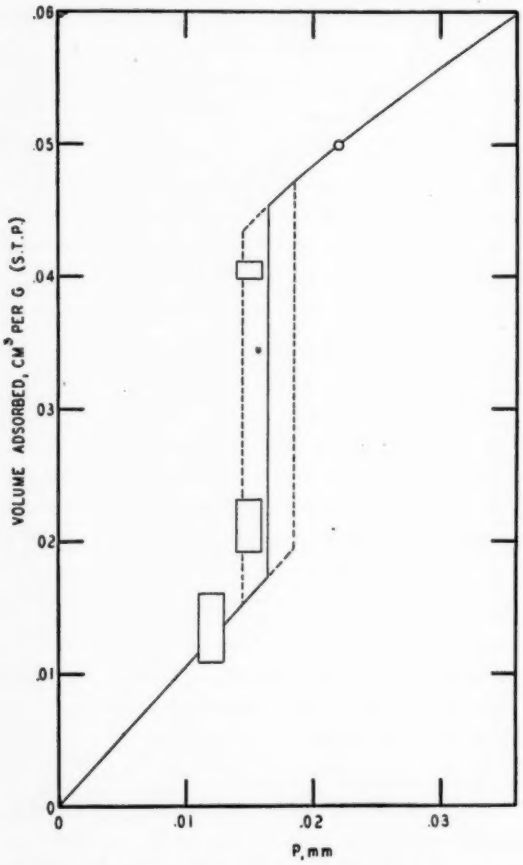

FIG. 3. The reversibility of the adsorption at the discontinuity at 25°C. The solid line represents the adsorption curve. The dotted lines indicate the maximum observed pressure of the "flat" in repeat experiments. The circle represents the adsorption point taken on the small sample for the desorption. The rectangles, whose sizes represent the possible experimental error, are the desorption points.

Both the fact that the values do not change with time and the reversibility of the process indicate that the curves given in Fig. 1 represent equilibrium values. Similar discontinuities have been observed with other systems: *n*-heptane on reduced silver at 15° and other solids at 25°C; nitrogen on several solids at −195.8° to −195.0°C; water on graphite at 25°C; and triptane on silver at 0°C. The above systems have not been investigated in as great detail as that on ferric oxide. Work on other systems indicates that similar discontinuities exist. For example, there is an exceedingly long vertical region in the $p-v$ plot at 0.006 mm when *n*-heptane is adsorbed on graphite containing 0.46 percent ash by weight.

With the exception of the discontinuity of water on graphite, all take place at very low relative pressures. For example, the isotherms of nitrogen were determined on six solids in the low pressure region. The discontinuity was observed on three of them at relative pressures of 0.8, 1.1, and 1.4×10^{-3}. These three solids were alumina-silica cracking catalysts whose areas varied from 120 to $485 m^2 g^{-1}$.

Wooten and Brown[11] have observed and reported discontinuities which bear some resemblance to those reported here when ethylene is adsorbed on alkaline earth oxide-coated cathodes. The discontinuities they observed occur at relative pressures of 0.25 to 0.4. Apart from the difference in the relative pressure at which the discontinu-

[11] L. A. Wooten and C. Brown, J. Am. Chem. Soc. 65, 113 (1945).

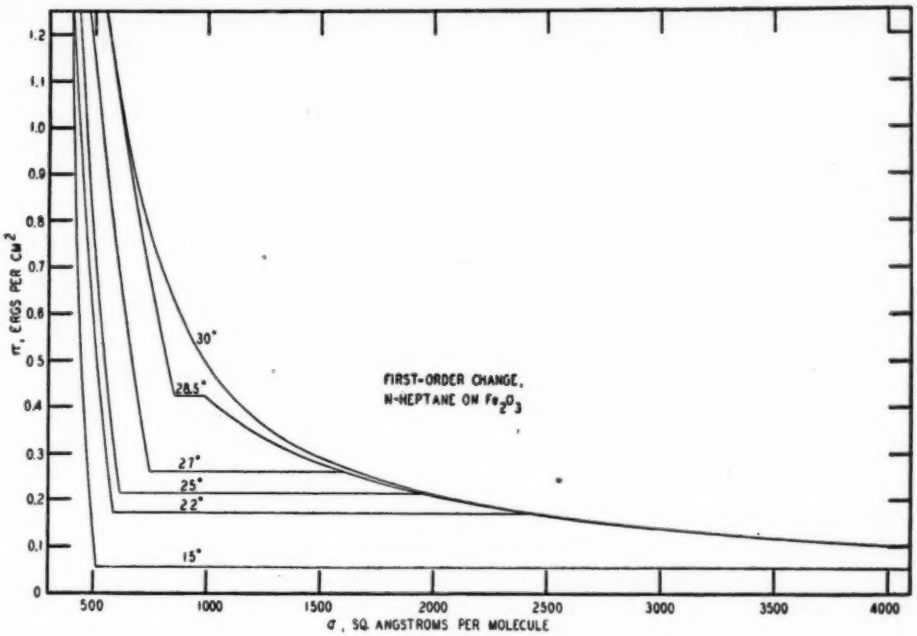

FIG. 4. The pressure-area curves for the films of *n*-heptane on ferric oxide at various temperatures as calculated from the adsorption values of Fig. 1.

ities occur, there are two other differences in their work and the results reported in this paper: (1) their films are polymolecular when the discontinuity occurs, while those reported here exhibit the discontinuity when only a fraction of a monolayer has been adsorbed; and (2) the effect of temperature appears to be in the opposite direction from that observed by the writers. The results of Wooten and Brown strongly suggest a phase transition between two of the nongaseous phases of films. At least, the behavior observed by them is not incompatible with this idea.

V. DISCUSSION

In the previous section the experimental facts concerning the discontinuity have been presented. The only reasonable explanation which adequately explains the observed facts is that the discontinuity represents a first-order phase change of the film adsorbed from the gas phase. The phase formed by the condensation of the vapor phase of the monolayer probably corresponds to the liquid expanded phase of insoluble films on the surface of water.

The most striking evidence that a first-order change is taking place can be seen in Fig. 4, where the film pressure, π, area, σ, curves have been plotted. Figure 4 exhibits all the characteristics of the three-dimensional pressure-area relationships of gases in the neighborhood of the critical temperature. The isotherms at 15°, 22°, 25°, 27°, and 28.5° lie below the critical temperature, while that at 30° is above. There is present the typical van der Waal's area for this transformation, characteristic of this type of transformation in both two and three dimensions.

The available data give for the critical constants: area, 900A² per molecule; temperature, 29°C; and film pressure, 0.5 dynes cm^{-1}. The values for the critical constants depend on the nature of the surface of the solid as well as on that of the gas. For example, the critical temperature of a similar transformation on reduced silver has been found by us to lie between 15° and 25°C. The evidence also indicates that the critical area is lower than that on ferric oxide.[2]

The values for the critical constants are of the order of magnitude to be expected, except that for the area, 900A² per molecule, which appears high. The *n*-heptane molecule lies flat on the surface at these concentrations of the film. If the corresponding area is calculated for the three-dimensional gas at its critical temperature, it is found to be 110A² per molecule. The interaction with the strong surface field should condense the film before it reaches this low area. No explanation has been found as yet for the

TABLE II. The critical constants for *n*-heptane on silver, ferric oxide, and graphite.*

	π_c (dyne cm^{-1})	σ_c (A^2 per molecule)	T_c (°C)
Silver	over 0.18	$310<\sigma_c<2200$	$15°<T_c<25°$
Ferric oxide	0.5	900	29
Graphite*	over 0.6	$200<\sigma_c<600$	over 25°

* Ash less than 0.004 percent.

high molecular area (Fig. 4) at which the transition to a lower area phase is completed. With *n*-heptane on graphite this area is much smaller. It is possible, though there is no evidence for this, that different crystal faces are present and that the first-order transition occurs on only one of these.

Sufficient data are now available to demonstrate that the values of the critical constants are dependent on the nature of the solid as well as that of the vapor. Values of the constants for ferric oxide, with limits of variation for silver and graphite, are given in Table II.

The heat of transformation may in theory be calculated from the Clausius-Clapeyron equation as applied to surfaces:

$$d\pi/dT=\Delta H/T\Delta\sigma,$$

where π is the film pressure of the transition, ΔH the heat of transformation in ergs per molecule, and $\Delta\sigma$ the change in molecular area during the transition. Unfortunately, the data are not sufficiently accurate or sufficiently extensive to make possible an accurate estimate of the heat liberated. At 25°C the heat evolved is 12,000 $\pm$5000 cal. mole^{-1}, while at 28.5° it is 1000$\pm$400 cal. mole^{-1}. The variation of the heat of adsorption in this region is exceedingly interesting and will be considered in a later paper.

The inaccuracy of the heat of transition is due to the inability to determine π and $\Delta\sigma$ more accurately. In obtaining the value of π it has been assumed that the film is a perfect gas before the transition. However, the work at 30°C shows that the film begins to deviate appreciably from the perfect gas law when the molecular area is reduced to 1800A^2 per molecule. The equilibrium vapor pressure cannot be determined sufficiently accurately to determine the curvature of the low pressure branch of the isotherm. Thus, the values for σ on the high area side are probably too low. The probable effect on the value of π is to make it too high. This can be seen from the equation used for integrating the function.

From the statistical point of view Devonshire[12] has calculated for the rare gases, with a number of simplifying assumptions, the ratio of the critical temperature of a two-dimensional film to that of the gas in three dimensions. Although his calculation is in theory not applicable to the present system, a comparison with the experimental values is made below, since this is the first time any experimental values of the ratio have been obtained. He calculated that

$$T_c \text{ of film}/T_c \text{ of gas}=0.53.$$

For the transition of *n*-heptane on ferric oxide this ratio is found to be 0.56 or only 6 percent higher than his value. For *n*-heptane on silver this ratio lies between 0.53 and 0.55. It is not possible to state at the present time how general the above agreement is.

The discussion has shown that the observed experimental facts are in complete accord with the idea that the discontinuity is a first-order transition: (1) the compressibility becomes infinite; (2) there is a ΔH not equal to zero; (3) the results at various temperatures exhibit critical temperature phenomena; and (4) the critical temperature is in agreement with that calculated theoretically. The last of these, (4), is, however, of doubtful significance.

To prove definitely that the observed discontinuity is a first-order change it is necessary to show that other explanations are not satisfactory. Another possible explanation is that capillary condensation is the cause of the discontinuity. On the basis of the theory of capillary condensation the solid would need to possess pores of exactly the same diameters, which are then filled at the pressure of the discontinuity. The application of this idea would then require that the top branch of the curve should depend on the temperature in such a manner that the volume of condensed material is constant, i.e., for the short temperature range covered, 15° to 28.5°, all of the volumes at the top of the flat should be the same within the limits of experimental error. There is a variation from .0545 cc gas at 15°C to .0324 cc gas at 28.5°C. This

[12] A. F. Devonshire, Proc. Roy. Soc. (London) **A163**, 132 (1937).

variation is entirely too large to be accounted for by a change in density of condensed liquid. Also the condensation process cannot explain the disappearance of the discontinuity at 30°. Thus, the results obtained cannot be explained by the assumption of capillary condensation.

It might be assumed that a first-order change does not occur, but that the phenomena are due to the presence on the crystals of more than one type of surface, some of which are more effective than others. This can be shown to be improbable. Each surface would have its own isotherm. If the discontinuity were to take place on only one of the surfaces, then under equilibrium conditions a discontinuity would be observed as a mean of the effects. All of the experimental data, the constancy with time, and the reversibility indicate that the data are equilibrium values. Therefore, the observed discontinuity must be due to a discontinuity on at least *one* of the surfaces present. Therefore, the existence of different types of surfaces does not explain the observed discontinuity.

Other possible explanations are equally as improbable. Thus, the interpretation that the observed discontinuities are due to a first-order change appears certain. What has been designated as *stepwise adsorption* exhibits no obvious relationship to the change considered here.[13] (See Fig. 2.) The discontinuity in the low pressure region is the only one found, and the data do not indicate the presence of any other first-order change.

If the interpretation that the irregularities in stepwise adsorption are due to phase transitions, then it is possible to explain their existence in two ways. For a homogeneous surface each discontinuity would represent a new surface phase. This would lead to an inordinately large number of phases, so many that such an explanation is unreasonable. The other possible explanation from this point of view is that there are present a large number of individual surfaces for which the transitions take place at different pressures. However, the problem of stepwise adsorption has not been studied in sufficient detail to show what is involved.

[13] For a brief review, see: S. Brunauer, *The Adsorption of Gases and Vapors* (Princeton University Press, Princeton, New Jersey, 1943), pp. 346–348.

THE JOURNAL OF CHEMICAL PHYSICS VOLUME 14, NUMBER 3 MARCH, 1946

Absorption Spectrum of Fluorbenzene in the Near Ultraviolet*

S. H. WOLLMAN**
Department of Physics, Duke University, Durham, North Carolina

(December 28, 1945)

The absorption spectrum of C_6H_5F at 2750–2380A was photographed in the first order of a three-meter grating spectrograph. As in C_6H_5Cl the band system corresponds to an electronic transition A_1, B_1. This is an allowed transition and the 0,0 band is stronger than in C_6H_5Cl because of the greater perturbation by the fluorine. Several progressions of totally symmetric vibrations are observed. The vibration whose excitation brings the corresponding benzene spectrum into appearance, and which shows up relatively intensely in C_6H_5Cl, appears in C_6H_5F but is not particularly prominent. In contrast to C_6H_5Cl, transitions to the carbon-halogen vibration in the upper electronic state are quite strong.

INTRODUCTION

THE near ultraviolet absorption spectrum of chlorbenzene has been interpreted[1] as having its origin in two types of transitions, each made possible by a different perturbation of the hexagonally symmetric potential field of benzene's planar carbon ring: a weak transition permitted because of the destruction of the sixfold symmetry by a non-totally symmetric vibration of symmetry β_1, and a somewhat stronger transition permitted because of the destruction of the sixfold symmetry by the presence of the electro-

* Based on a portion of a thesis submitted in partial fulfillment of the requirements for the degree of Doctor of Philosophy in the Graduate School of Arts and Sciences of Duke University, 1941.

** Present address: Bureau of Ordnance, Navy Department, Washington, D. C.

[1] H. Sponer and S. H. Wollman, J. Chem. Phys. 9, 816 (1941).

negative atom of chlorine. A corresponding study has now been made for fluorbenzene to provide additional data to check the above interpretation.

The near ultraviolet absorption spectrum of fluorbenzene has been investigated by Henri;[2] but because of the incompleteness of the published results, it was necessary to rephotograph and remeasure the spectrum.

The analysis shows that the spectrum of fluorbenzene is similar to that of chlorbenzene, but that as might have been expected, the stronger perturbation of the carbon ring by the fluorine enhances the transitions forbidden in benzene but permitted in fluorbenzene because of the presence of the fluorine.

EXPERIMENTAL DETAILS

The absorption spectrum of fluorbenzene was photographed in the near ultraviolet using a three-meter grating in Eagle mounting. The light source was a water-cooled hydrogen discharge tube of conventional design. It gave sufficient intensity to get a satisfactory density on a type II-0 Eastman spectrographic plate in from one and a half hours to three hours, depending on the intensity of the absorption bands.

Samples of pure fluorbenzene[3] were distilled into the absorption tube from an all-glass system. The quartz absorption tube used, 15 cm long, was provided with a side arm to hold the liquid sample. The temperature of the liquid and the vapor could be controlled independently. The vapor was always at room temperature; the temperature of the liquid, controlled by a dry ice and acetone bath, was varied from −55° to 28°C depending on the desired pressure of vapor in the absorption path.

When the liquid was at room temperature the windows of the absorption tube became fogged gradually by photochemical decomposition products. The decomposition could have been predicted from examination of the absorption spectrum since some very diffuse bands (indicating predissociation) occur at the short wave-length end of the spectrum. The absorption of the fogged windows was tested and found to be uniform and continuous in the region of interest, and hence did not introduce any complications.

The bands were measured to the band head. The edges of the sharpest bands were measured to .2 to .3 cm^{-1} while some of the diffuse bands could be measured only to the nearest two cm^{-1}.

Iron lines were used as the comparison spectrum.

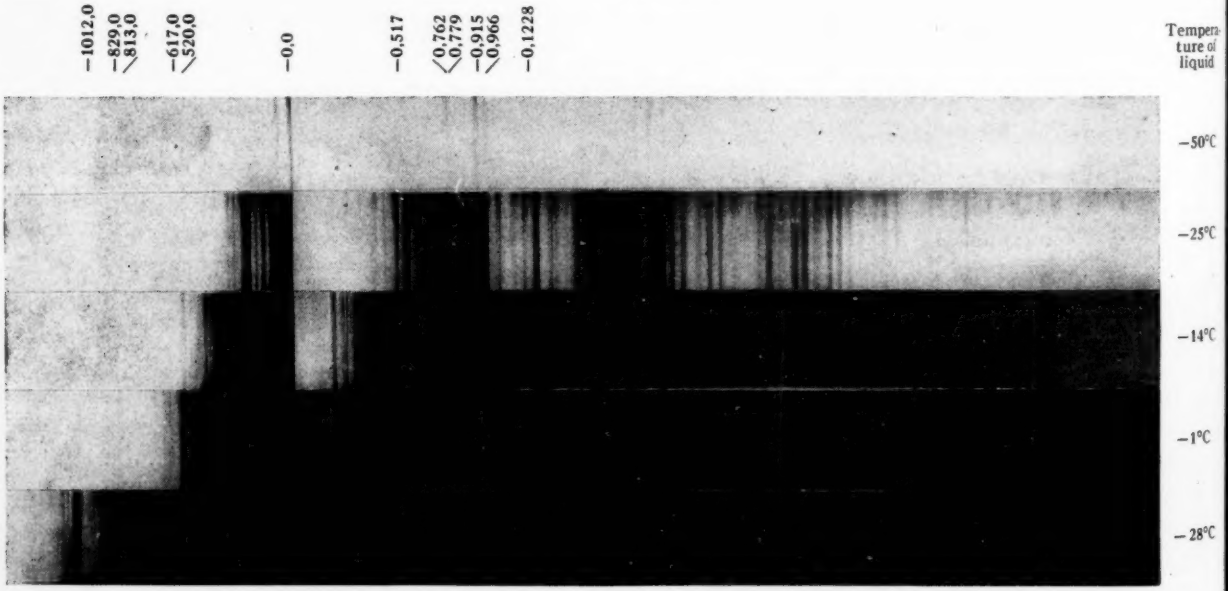

FIG. 1 Ultraviolet absorption spectrum of fluorbenzene vapor.

[2] V. Henri, *Structure des Molécules* (J. Henmann, Paris, 1925).

[3] We are indebted to Dr. Marcus Hobbs of the Chemistry Department for supplying the sample of fluorbenzene.

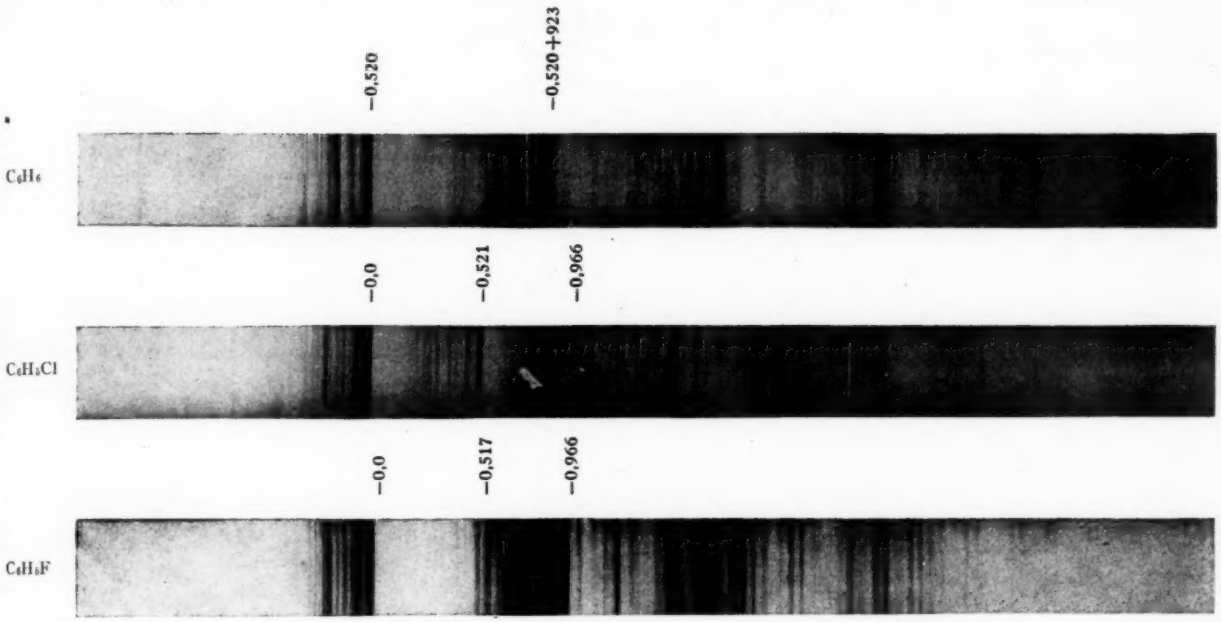

FIG. 2. Ultraviolet absorption spectra of benzene, chlorbenzene, and fluorbenzene.

EXPERIMENTAL RESULTS

The part of the spectrum photographed lies in the region between 2750A and 2380A. A selection of the photographs of the spectrum taken at progressively higher pressures of vapor is shown in Fig. 1. As the pressure increases, more bands appear. Those at the extreme long wave-length end of the spectrum originate in transitions from excited vibrational levels in the ground electronic state.

All the bands are degraded to the red. Most of the band heads are doubled with a spacing of about 2 cm^{-1}. The long wave-length head is the stronger and it seems probable that, if only a single head is observed, it is the long wave-length head. Hence all calculations of wave numbers are made relative to these strong heads.

The wave numbers, intensities, and some assignments of the observed bands are collected in Table I. Wave numbers in parentheses correspond to bands which were observed but not measured. Because of the wide range of intensities under various pressure conditions, the intensity classification refers to the experimental conditions in the remarks column. The notation in the intensity column means: *vw* = very weak, *w* = weak, *m* = medium, *st* = strong, *vst* = very strong, *d* = diffuse.

It is found that the vibrations are somewhat anharmonic, and, therefore, that the frequency of a particular vibration depends to a certain extent on its state of excitation, as well as on vibrations with which it is coupled. For example, the difference frequency, 67 cm^{-1}, varies between 65 cm^{-1} and 70 cm^{-1}. Such fine distinctions have been ignored and a set of representative values has been chosen and listed throughout in the assignment column. The notation used to indicate transitions listed in the assignment column is as follows: Numbers to the left of the comma refer to the wave numbers of vibrations in the ground electronic state, those to the right to wave numbers of vibrations excited in the upper electronic state, except for those preceded by a minus sign which refer to the difference frequencies of 1,1 transitions.

ANALYSIS OF THE SPECTRUM

The symmetry properties of fluorbenzene are the same as those of chlorbenzene.[1] The molecule is planar, with a twofold axis of symmetry through the fluorine atom, and belongs to the symmetry class C_{2v}. The lowest electronic state is totally symmetric as in benzene. It is assumed that the upper electronic state involved in the observed spectrum is of symmetry B_1. The

TABLE I. Bands of fluorbenzene.

Wave number (cm^{-1})	Intensity	Assignment	Remarks
36369	*vw*		Intensities were estimated from plates taken with liquid at 28°C
36395	*vwd*		
36488	*vwd*		
36513.5	*vw*		
36531.9	*w*	1218, −67	
36545	*vw*		
36570.6	*m*	240–1012, 0	
36577.3	*m*		
36590	*wd*		
36601	*m*	1012, −209; 1218, 0	
36603.3	*m*		
36610.5	*w*	1012, −3×67	
36638	*wd*	1012, −172	
(36662)	*wd*	1157, 0	
36677.2	*m*	1012, −2×67	
36710	*md*	1012, −98	
(36725)	*vw*	1027, −67	
36741.6	*st*	1012, −67	
36780.5	*st*	829, −209	
36792	*md*	1027, 0	
36807.0	*vst*	1012, 0	
36809.6	*vst*		
36823	*md*	2×240–520, 0; 996, 0	
36841	*wd*		
36858	*md*	829, −2×67	
36875	*md*	813, −2×67	
36923.1	*m*	829, −67	Intensities were estimated from plates taken with liquid at 18°C
36925.9	*m*		
36939.8	*m*	813, −67	
36942.3	*m*		
36951	*vwd*		
36990.2	*vst*	829, 0	
36992.7	*vst*		
37006.1	*vst*	813, 0	
37008.8	*vst*		
37021	*vwd*		
37036	*vwd*		
37061	*wd*	240–520, 0; 758, 0	
37071.8	*w*	617, −2×67	
37093.8	*m*	520, −209	
37106.5	*vw*		
37120	*vwd*		
37131	*wd*		
37136.9	*m*	617, −67	
37146	*wd*		
(37165)	*vd*	520, −2×67	
37196.3	*m*		
37202.1	*w*	617, 0	Intensities were estimated from plates taken with liquid at −14°C
37221.8	*w*		
37232.9	*w*	520, −67	
37241.6	*w*		
37248.3	*vw*		
37257	*vwd*		
37299.2	*st*	520, 0	
37301.3	*st*		
37329	*md*	490, 0	
37350	*md*		
37369.2	*m*		
37400.0	*st*	0, −2×209	
37402.8	*st*		
37411.8	*m*		
37418.2	*m*		
37421.1	*m*		
37439	*wd*		
37449	*wd*		Intensities were estimated from plates taken with liquid at −32°C
37460.4	*w*		
37470.2	*w*		
37485.2	*w*		
37501.9	*w*		
37512.2	*wm*	240, −67	
37517.7	*vw*		
37524.3	*vw*	813, 520	
37539.2		0, −67−209	
37542.2	*m*		
37553.9	*w*		
37578.6	*m*	240, 0	
37581.1	*w*		
37609.7	*st*	0, −209	
37612.4	*m*		
37619.0	*wm*	0, −3×67	
37629.9	*vw*	0, −19−172	
37646.9	*m*	0, −172	
37649.0	*w*		
37656.4	*w*	0, −67−98	
(37666)	*w*	0, −19−2×67	
37683.4	*st*	0, −2×67	
37685.8	*st*		
37691.0	*w*		
37721	*mstd*	0, −98	
37733	*mstd*	0, −19−67	
37749.4	*vst*	0, −67	
37752.0	*mst*		
37758.5	*m*	0, −60	
37760.6	*w*		
37799	*vst*	0, −19	
37815.8	*vst*		
37818.8	*vst*	0, 0	Main edge
37822.8	*mst*		
37829.2	*vw*	758, 779	Intensities were estimated from plates taken with liquid at −14°C
37839.4	*vw*		
37846.5	*vw*		
37865.7	*w*		
37874	*vwd*		
37883.7	*vw*		
37913	*w*		
37929.3	*w*		
37931.7			
37937.3	*vw*		
37950	*vwd*		Intensities were estimated from plates taken with liquid at −32°C
37959	*vwd*	0, 205−67	
37974	*vwd*	813, 966; 758, 915	
38017.4	*w*	0, 332−2×67	
38023.5	*w*	0, 205; 758, 966	
38026.1	*w*		
38083.9	*w*	0, 332−67	
38128.7	*vw*	0, 517−209	
38137.6	*vw*	0, 517−3×67	
38150.7	*w*	0, 332	
38155.3	*vw*		
38186.8	*w*		
38203.7	*w*	0, 517−2×67	
38213.0	*vw*	520, 915	
38228.6	*wm*	0, 410	
38231.4	*vw*		
38269.6	*w*	0, 517−67	
38278	*vwd*		
38320	*md*		
38335.6	*m*	0, 517	
38359.7	*vw*	240, 779	
38375.7	*m*	0, 762−209	
38383.6	*vw*	0, 762−3×67	
38391.0	*m*	0, 779−209	
38393.3	*vw*		
38410.0	*vw*	0, 205+517−2×67	
38432	*m*	0, 205+410	
38449.2	*m*	0, 762−2×67	
38465	*m*	0, 779−2×67	
38478	*wd*	0, 205+517−67	
38515	*st*	0, 762−67	
38530.9	*st*	0, 779−67	
38532.9	*w*	0, 915−209	
(38541)		0, 205+517; 240, 966	
38580.9	*vst*	0, 762	
38583.6	*m*	0, 966−209	
38597.5	*vst*	0, 779	
38600.0	*w*	0, 915−2×67	
38609.0	*w*		
38616.3	*vw*		
38665	*st*	0, 915−67	
38674	*m*		
38718.0	*vst*	0, 966−67	
38733.6	*vst*	0, 915	
38738.3	*m*		
38766.1	*m*	0, 966−19	
38784.5	*vst*	0, 966	
38787.0	*m*		
38793.0	*vw*		
38796.3	*vw*		
38838.8	*w*	0, 1228−209	
38849.7	*m*		
38852.3	*m*	0, 2×517	
38926.2	*w*		
38935.9	*vw*		
38949.0	*vw*		
38970	*wd*	0, 1218−67	
38978	*wd*	0, 1228−67	
38985	*vwd*		
38993	*vwd*	0, 410+762	
		0, 205+966	
39009	*vwd*	0, 410+779	
39036.8	*mst*	0, 1218	
39043.8			
39046.8	*mst*	0, 1228	
39049.4	*vw*		
39057.8	*vw*	0, 205+2×517	
		0, 517+779−67	
39099.1	*w*	0, 517+762	

TABLE I.—*Continued.*

Wave number (cm^{-1})	Intensity	Assignment	Remarks
39115.7	*wm*	0, 517 +779	
39119.7	*vw*		
39138	*wd*		
39150	*wd*		
39172.3	*w*		
39197	*wd*	0, 410 +966	
39230.7	*vw*		
39237.5	*vw*		
39245.3	*w*		
39251.6	*w*	0, 517 +915	
39257.6	*w*		
(39297)		0, 3 ×517 −67	
39302.4	*m*	0, 517 +966	
39312.5	*m*	0, 2 ×779 −67	
(39342)	*vwd*	0, 2 ×762	
39359.3	*st*	0, 762 +779	
39364.3	*wm*	0, 3 ×517	
39381	*md*	0, 2 ×779	
39405.3	*vw*		
39446	*wd*	0, 779 +915 −67	
39496	*md*	0, 762 +915	
39502	*wmd*	0, 779 +966 −67	
39513	*md*	0, 779 +915	
39550	*md*	0, 762 +966	
39569	*md*	0, 779 +966	
39588	*vwd*		
39653.3	*m*	0, 2 ×915	
39699	*md*	0, 915 +966	
39707.0	*w*		
39740	*wd*		
39753	*md*	0, 2 ×966	
39769	*vwd*	0, 2 ×517 +915	
39802	*wd*		
39817	*wd*	0, 2 ×517 +966	
39825	*vwd*		
39842	*vwd*		
39901	*vwd*		
39916	*vwd*		
39959	*wmd*	0, 915 +1218	
39966	*wmd*	0, 915 +1228	
40014	*wmd*	0, 966 +1228	
40054.6	*vw*	0, 3 ×779	
40084	*vwd*	0, 517 +779 +966	
40103	*vwd*		
40118	*vwd*		
40135	*vwd*		
40166	*vwd*	0, 517 +2 ×915 0, 410 +2 ×966	
		0, 517 +762 +966	
40184	*vwd*	0, 517 +779 +966	
40218	*vwd*	0, 517 +915 +966	
40229	*vwd*		
40234	*vwd*		
40278	*wmd*	0, 2 ×1228 0, 517 +2 ×966	
40300.7	*vw*		
40326	*vwd*	0, 762 +779 +966	
40351	*vwd*	0, 2 ×779 +966	
40370	*vwd*		
40417.2	*m*	0, 762 +2 ×915	
40433.6	*w*	0, 779 +2 ×915	
40482.6	*m*		
40489.3	*m*		
40521	*vwd*	0, 762 +2 ×966	
40537	*vwd*	0, 779 +2 ×966	
40546	*vwd*		
40557	*vwd*		
40568	*vwd*	0, 3 ×915	
40622.2	*w*	0, 2 ×915 +966	
40668.5	*w*	0, 915 +2 ×966	
40675.6	*vw*		
40722	*wd*	0, 3 ×966	
40737	*vwd*	0, 2 ×517 +915 +966	
40814	*vwd*		
40847	*vwd*		
40871	*vwd*		
40905.6	*vw*		
40922	*vwd*	0, 915 ×966 +1228	
40987.8	*vw*	0, 2 ×966 +1228	
41132	*vwd*	0, 517 +2 ×915 +966	
41195	*vwd*	0, 915 +2 ×1228 0, 517 +915 +2 ×966	
41246	*vwd*	0, 517 +3 ×966	
41335.1	*vw*		
41385.0	*vw*		
41401.2	*vw*		
41449	*vwd*	0, 779 +915 +2 ×966	
41534	*vwd*		
41587	*vwd*	0, 2 ×915 +2 ×966	
41634	*vwd*	0, 915 +3 ×966	
41689	*vwd*	0, 4 ×966	
41741	*vwd*		
41762	*vwd*		
41835	*vwd*		
41898	*vwd*		
41947	*vwd*		

symmetry class B_1 in the group C_{2v} corresponds to the class B_{2u} in the group D_{6h} of benzene, and arises when the sixfold axis of symmetry is destroyed by the substitution of a halogen atom for one of the hydrogens. In benzene the corresponding spectrum arises out of a transition to an upper electronic state of symmetry B_{2u}. Transitions between electronic states with symmetries A_1 and B_1 are allowed; the transition moment lies in the molecular plane perpendicular to the carbon-fluorine bond. Transitions with moments in the other two principal directions are "forbidden" unless permitted because of the accompanying transition of a vibration of suitable symmetry. When the transition moment is parallel to the carbon-fluorine bond the accompanying vibration is of symmetry β_1. Only one such vibration was found and it corresponds to the vibration of symmetry ϵ_g^+, which permits the corresponding transition in benzene. When the transition moment is perpendicular to the molecular plane, the accompanying vibration is of symmetry α_2. A few such vibrations seem to be observed.

Since fluorbenzene and chlorbenzene have similar structures, it is to be expected that the absorption spectra will be similar. Comparison of the absorption spectra of fluorbenzene and chlorbenzene presented in Fig. 2 together with that of benzene shows that there is a strong resemblance. The pressure of the vapor and the length of the absorption path are 25 mm and 75 cm for benzene, 1.7 mm and 75 cm for chlorbenzene, and 3 mm and 15 cm for fluorbenzene, respectively. Examination of the spectra indicates that the absorption strength of fluorbenzene is about twice that of chlorbenzene and perhaps ten times that of benzene. Fluorbenzene has a greater absorption strength than benzene because the fluorine perturbs the hexagonal field

TABLE II. Wave numbers and symmetries of some vibrations in the ground electronic state of fluorbenzene.

Ultra-violet vapor	Raman liquid (reference 4)	Infra-red liquid (reference 5)	Depolarization factor (reference 4)	Symmetry (reference 4)	Symmetry (this paper)
240	241		.83	β_2	α_2
520	519	518	.60	α_1	α_1
617	612	610	.92	β_1	β_1
813	807	802	.12	α_1	α_1
829	831			α_2	α_1?
996?	997	997			
1012	1010		.07	α_1	α_1
1027	1024				α_1
(1157)	1157		.65	α_1 or β_1	α_1?
1218	1218		.15	α_1	α_1

of the carbon ring more than the chlorine does. Further evidence indicating that fluorbenzene has a ring field deviating more from hexagonal symmetry than that of chlorbenzene will be presented later in the discussion.

As in chlorbenzene,[1] it is postulated that the 0,0 transition is represented by the strongest band on the short wave-length end of the first strong group.

It is then possible to obtain the values of the wave numbers of vibrations in the ground electronic state by taking wave number differences between the 0,0 band and bands on its long wave-length side. The results, taken from Table I, are listed in Table II along with the corresponding values observed in the Raman effect[4] and the infra-red absorption spectrum[5] in the liquid state. In addition, depolarization factors[4] and symmetries assigned on the basis of Raman effect data[4] are listed as well as symmetries assigned on the basis of a combination of Raman and ultraviolet data.

The main portion of the spectrum, all the bands on the short wave-length side of the 0,0 band, arises from transitions to excited vibrational levels in the upper electronic state. The strongest bands involve totally symmetric carbon vibrations, singly or multiply excited, or excited in combination with other totally symmetric vibrations. The vibrations which are most strongly excited in the upper electronic state have the wave numbers 517, 762, 779, 915, 966, 1218, and 1228 cm^{-1}.

Reasonable assignments can be given for many of these vibrations in the ground and excited electronic states.

The 617 and the 520 frequencies in Table II are closely related to the carbon vibration 606 of symmetry ϵ_g^+ in benzene. When benzene has one hydrogen replaced by a halogen the degeneracy of the 606 vibration is removed and it is expected to split into a vibration of symmetry β_1 with a frequency around 600 and a totally symmetric vibration with a somewhat lower frequency. This is observed: in fluorbenzene the frequencies are 617 and 520, respectively, and similarly, in chlorbenzene they are 615 and 418. Support for the assignment of the 520 is obtained from the value of the depolarization factor of the Raman scattering. Support for the assignment of the 617 is obtained from the following argument: The bands involving transitions from the singly excited 617 vibration, and bands involving transitions to the singly and possibly to the triply excited 517 vibration in the upper electronic state, have a sharpness similar to that of the corresponding bands in the near ultraviolet absorption spectrum of benzene. The 617 and 517 bands in fluorbenzene are significantly sharper than the bands corresponding to transitions involving only totally symmetric vibrations, including the case in which the 517 vibration is doubly excited. Moreover, in benzene, chlorbenzene, and fluorbenzene the difference in frequency of this vibration in the upper and lower electronic states is about the same. It therefore seems reasonable to assume that the 517 is related to the 617, and that the pair correspond to the 520 and the 606 in benzene, and to the 521 and the 615 in chlorbenzene, which show a similar sharpness. Now it is known from Raman spectra that the 606 in benzene is a carbon ring vibration. Hence it is expected that the 617 and 517 vibrations involve a carbon vibration rather than a hydrogen vibration. This interpretation is in contrast to that in a recent Raman study[4] where the 617 is assigned to a β_1 vibration related to the ϵ_u^- hydrogen vibration 1035 in benzene.

The transition of the form 0, $n\times517$, $n=2$, increases in intensity relative to that with $n=1$ as the substituent changes from Br to Cl to F.[6]

[4] K. W. F. Kohlrausch and H. Wittek, Monats. f. Chem. **74**, 1 (1941). See this paper for earlier references.
[5] J. Lecomte, J. de phys. et rad. **8**, 489 (1937).

[6] The fact that a band corresponding to 0, $n\times517$, $n=1, 2$ in fluorbenzene appears also in chlorbenzene and probably

This is an illustration of the decreasing importance of the vibration mechanism in making the transition allowed, or of the increasing perturbation of the ring field by the substituent in the order Br<Cl<F.

The structure of the 517 and the 617 seems to be characteristic not only of the particular vibrations but also of the direction of the transition moment of transitions permitted because of vibrations of symmetry β_1. This is indicated by the fact that the structure of the band corresponding to the transition 0, 2×517 looks like that of a transition involving only totally symmetric vibrations. This is to be expected since the doubly excited vibration is totally symmetric. The dependence of band structure on the direction of the transition moment and hence on the symmetry class of an associated vibration is of help in determining the symmetry class of vibrations in these monosubstituted benzenes. Usually the depolarization factor of the Raman scattering can distinguish between totally symmetric and non-totally symmetric vibrations. If a vibration is non-totally symmetric and occurs in ultraviolet absorption in transitions of the form v, 0 or 0, v (v standing for an arbitrary vibration), it cannot be of symmetry β_2; if the band is sharp and the presented discussion is correct, the transition moment is parallel to the carbon fluorine bond and the symmetry is β_1; in other bands the transition moment is perpendicular to the molecular plane and the symmetry is α_2.

In connection with the vibrations with frequencies of about 1000 cm^{-1}, ultraviolet bands are observed at positions corresponding to the observation of vibrations of frequencies 996, 1012, 1027, (1157), and 1218 cm^{-1} in the ground electronic state. While a reasonable alternative assignment can be given for the band at 36601 cm^{-1}, *viz.* 1012, –209, it is fairly certain that 1218, 0 is also present since the weaker associated transition 1218, –67 is observed. The depolarization factor of the corresponding Raman band shows the vibration to be totally symmetric. There is no obvious assignment of a frequency in the upper electronic state to correspond to the 1218. The bands at 39037 and 39047 corresponding to the transitions 0, 1218, and 0, 1228, respectively, seem to be the best choice although they would involve frequency values equal or slightly higher than the one in the ground electronic state.

It is not certain that the 996 vibration is observed. The band at 36823 may not correspond to the transition 996, 0, since not only is an alternative assignment possible, but no transition of the form 996, –67 is observed.

The frequencies 1012 and 1027 in the ground state are probably carbon vibrations. Several totally symmetric carbon vibrations are to be expected in this region. If these vibrations are related to the 915 and the 966 in the upper electronic state which because of extensive strong progressions are certainly totally symmetric carbon vibrations, the recent assignment of the 1027 to a hydrogen vibration[4] is unlikely.

The 1157 is very probably a hydrogen vibration.

The 813 has been correlated with the carbon-fluorine vibration. The assignment[4] was made after comparison of Raman bands in monosubstituted benzenes. It was found that corresponding bands were strongly dependent on the mass of the substituent. Polarization measurements indicate that the vibration is totally symmetric.

The 829 has been assigned[4] to an out-of-plane vibration of the hydrogens because in a similar comparison the corresponding bands are largely independent of the substituent. It was assumed that the 829 represents the very closely neighbored components α_2 and β_2 resulting mainly from 850 ϵ_g^- in benzene. The ultraviolet absorption data do not indicate a confirmation of this assignment. The single excitation of a β_2 vibration is a forbidden transition and the single excitation of an α_2 vibration should give rise to a relatively weak band. Contrary to these predictions the 829 is a strong band. Since the band appearance indicates that β_1 symmetry is doubtful, the vibration is probably totally symmetric.

The 762 and the 779 frequencies in the upper

in brombenzene indicates that the transition from the ground state to the doubly excited vibration of symmetry β_1 in the upper electronic state can occur, and that the band in chlorbenzene at 38095 cm^{-1} is probably 0, 2×521. The alternative explanation[1] (that the 1043 arises from an accidental degeneracy involving a doubly excited vibration with a fundamental frequency of 525 cm^{-1} and a totally symmetric carbon ring vibration) which was proposed because of the strong intensity of the band now seems doubtful.

electronic state probably correspond to the 813 and the 829 in the ground electronic state, although it is not clear which vibrations are to be paired. Either the 762 or the 779 represents the carbon-fluorine vibration in the excited electronic state. This is in contrast to results in chlorbenzene where the corresponding transition (to a state with a singly excited carbon-chlorine vibration) is not observed. A possible explanation of this difference may lie in the fact that the fluorine atom perturbs the carbon ring field more than a chlorine atom. It has been pointed out[1] that the transition moment may be dependent on the normal coordinate of a vibration. For transitions from the ground state to excited totally symmetric vibrations in the upper electronic state (in molecules in which the upper electronic state involved in the transition has a larger moment of inertia than the lower electronic state), the part of the transition moment independent of the displacement has a sign opposite to the part of the moment proportional to the first power of the displacement of the normal coordinate. In chlorbenzene these contributions probably cancel, since transitions from the ground state to a singly excited carbon-chlorine vibration in the upper electronic state do not seem to occur; in fluorbenzene as indicated by the over-all greater absorption strength, the constant term is larger than in chlorbenzene, and there is only partial cancellation. The transition from the ground state to a singly excited carbon-fluorine vibration in the upper electronic state is observed. The strong intensities of the 762 and the 779 bands and their way of combining with other vibrations suggests that they are both totally symmetric.

The 240 frequency in the ground electronic state is probably of symmetry α_2. It has been assigned[4] to β_2 symmetry related to the $406\epsilon_u^+$ carbon vibration in benzene on the basis of Raman studies. However, the vibration appears in a transition corresponding to 240, 0 with moderate strength in studies on fluorbenzene, chlorbenzene, and brombenzene, and hence cannot be of symmetry β_2, as this transition would then be forbidden. Since the Raman scattering shows the vibration to be non-totally symmetric, and since the ultraviolet band appearance indicates that it is not of symmetry β_1 it is probably of symmetry α_2. The results do not permit a definite correlation of the 240 frequency to a particular mode of vibration.

In addition to the frequencies discussed, others occur, difference frequencies or n,n transitions, in bands to the long wave-length side of the more prominent bands. These difference frequencies have been identified by the fact that they are so low compared to the observed Raman frequencies and to the expected size of vibrational frequencies in this molecule. Confirmation could be obtained by studying the temperature dependence of the intensity of the bands involving them. The prominent difference frequencies are 20, 67, 98, 172, and 209 cm^{-1}. Not much can be said about these difference frequencies at the present time. The 20, 98, and 172, which occur only once and not in progressions are probably to be associated with one of the higher ground-state frequencies. The 209 and the 67 which occur up to 2,2 and 3,3 transitions, respectively, are probably related to low frequencies, perhaps less than 400 cm^{-1}. Probably none of the most prominent vibrations may be associated with the observed difference frequencies. The 98 agrees closely numerically with 617, 517 but the assignment is uncertain since the corresponding difference frequency does not appear in chlorbenzene.

The author wishes to express his appreciation to Professor H. Sponer for suggesting this problem and for many helpful suggestions. This research was supported by a grant-in-aid from the Duke University Research Fund.

Chemical Forms Assumed by C^{14} Produced by Neutron Irradiation of Nitrogenous Substances

P. E. YANKWICH,[1] G. K. ROLLEFSON, AND T. H. NORRIS
Department of Chemistry, University of California, Berkeley, California

(Received December 20, 1945)

The nature of the radioactive compounds formed in the production of C^{14} by neutron irradiation of nitrogen-containing material of various types has been investigated. Of the radioactive compounds sought, carbon dioxide and carbon monoxide were found in all samples which contained oxygen, either in the parent compound or in the solvent water. Formic acid and methanol were found only in water solutions. Hydrogen cyanide, on the other hand, was found in no solution, but was found in all the pure substance samples except ammonium nitrate and aniline. Methane was found only in those hydrogenous substances containing no oxygen. Formaldehyde was never found. An attempt is made to interpret the results in terms of the processes in which the C^{14} atoms must be involved in the dissipation of the recoil energy associated with their formation. The fact that several compounds are produced in radioactive form in the original irradiation eliminates the necessity for the synthesis from radioactive carbon dioxide of these compounds for use in tracer work. A simplified method for the preparation of C^{14} is suggested.

As an extension of the work of Ruben and Kamen[2] on the long-lived radioactive isotope of carbon, C^{14}, we have made chemical fractionations of the C^{14} radioactivity induced by neutron irradiation of several nitrogen-containing compounds of different types with a view to obtaining more detailed information as to the chemical form in which the newly created atom is to be found in a particular case and how this varies with the nature of the material irradiated.

The nuclear reaction involved is

$$_0n^1 + {}_7N^{14} = {}_6C^{14} + {}_1H^1 + Q,$$

where Q has been estimated at about 0.60 Mev.[2,3] The C^{14} nucleus, therefore, acquires a recoil energy of approximately 40,000 ev, far more than enough to rupture any chemical bonds by which the nitrogen atom involved may have been held. The subsequent chemical fate of such an energetic atom is, in itself, a matter of interest, besides being, in the case of C^{14}, a matter of some practical importance.

Rather similar phenomena have been investigated[4] in the cases of several n, γ reactions and nuclear isomeric transitions which similarly yield excited monatomic products. One would expect that, after dissipation of their energy, these product atoms might appear in a new chemical species, in a substitution product of the parent compound, or even in molecules of the parent compound itself. All three possibilities have been realized and attempts have been made to correlate and interpret the results, but few generalizations have been possible. The work has been particularly fruitful, however, in suggesting methods to be used in extracting the induced activity from the irradiated material.

We too have tried to explain our results: certain plausible and interesting correlations have been found possible. The work has potential value, moreover, as an aid in the preparation of C^{14} for use as a tracer, in which connection it was originally undertaken. With a neutron source such as the Berkeley cyclotron, this isotope, because of its long half-life, can be obtained in only small yields, with low specific activities, and these only with considerable labor. Our data are helpful in suggesting the most efficient and least tedious methods of extracting and concentrating the isotope from the bulk of irradiated material.

We hope, moreover, that the information may be useful in another connection as well. One of the principle hindrances to the use of C^{14} as a tracer in research in organic chemistry or the life sciences is the difficulty involved in its incorpora-

[1] From a dissertation submitted in partial satisfaction of the requirements for the degree of Doctor of Philosophy.
[2] S. Ruben and M. D. Kamen, Phys. Rev. **57**, 549 (1940); **59**, 349 (1941).
[3] T. W. Bonner and W. M. Brubaker, Phys. Rev. **49**, 223 (1936).
[4] Szilard and Chalmers, Nature **134**, 462 (1934), and many other workers. For a review see G. T. Seaborg, Chem. Rev. **27**, 199 (1940).

tion into various organic compounds. One must have available a semi-micro synthetic method which uses carbon dioxide as a starting material and produces good yields (usually 50 percent or better) without undue dilution of the radioactivity. Such a situation exists for only a limited number of simple compounds. The possibility of placing the C^{14} in a particular desired compound in the first place, simultaneously with the original production of the radioactivity, cannot fail to be attractive; it was hoped that this work might be suggestive along this line.

In addition to the samples we fractionated, several others were irradiated, but, because of their small size, these failed to accumulate sufficient radioactivity to be handled. Much desirable additional data is, therefore, not yet available.

EXPERIMENTAL

Samples

Three groups of samples were subjected to irregular irradiation with neutrons from the Berkeley 60-inch cyclotron for a period of about two years. The irregularity precludes any estimate of total neutron dosage. However, since the groups were maintained intact for this period, the dosages and hence, roughly, the yields of C^{14} per gram of nitrogen should have been more or less comparable within a given group. As an examination of the data will show, this is borne out only very approximately by experiment. The discrepancy may arise in part from shielding of one sample by another. This should have been particularly true of the large samples in Group I.

Group I consisted of twenty-five stainless steel tanks, 15 to 30 liters in volume, filled with saturated ammonium nitrate solutions. Of these we analyzed only three tanks in detail.

Group II consisted of 500 g of ammonium nitrate crystals, 100 g of hydrazine dihydrochloride, and 330 g of dry aniline, all in sealed containers. The hydrazine contained about 2 percent moisture.

Group III was composed of 170 g of ammonium nitrate crystals, 210 g of urea crystals, a saturated solution of urea containing about 300 g of solute, and a 50 percent pyridine-water solution containing about 100 g of pyridine. The seals on all but the second of the samples in this group were found to have been imperfect, resulting in loss of gaseous activity.

Fractionations

We adopted an analytical procedure designed to locate C^{14} activity present in the form of what seemed the most likely one-carbon compounds: carbon dioxide, carbon monoxide, methane, hydrogen cyanide, formaldehyde, methanol, and formic acid. It would have been of considerable interest to look for substitution compounds, which were, in all probability, formed in certain cases—a probability indicated by the low apparent yields of radio-carbon, particularly in the case of aniline—but the impracticality of extracting such compounds in view of the very low activities involved precluded this possibility.

With variations for the different cases, a more or less general procedure was followed, involving analysis of three fractions: gaseous activity in the gas phase over the sample; gaseous activity trapped within the sample; and non-volatile, water-soluble activity in the sample.

The first fraction, consisting of the activity in the gas phase over the sample, was isolated by connecting the sample vessel to a large evacuated bulb and allowing the pressure to equalize between the two. The large bulb was then shut off, and the sample container allowed to fill with air. The two vessels were again connected and the pressure allowed to equalize. This procedure was repeated until the pressure in the large bulb had reached almost an atmosphere. This bulb, to which 4.2 cc each of carbon dioxide, carbon monoxide, and methane had previously been added as carriers, was now connected to an analytical train, and its contents were swept through the train with oxygen at a rate of 5 to 10 liters per hour. In this train, the gases passed first through a bubbler containing dilute sodium hydroxide, by which the carbon dioxide was removed, then through a copper oxide combustion tube at 315°C in which carbon monoxide was oxidized to carbon dioxide, through another bubbler to absorb this gas, through a second copper oxide tube at 700°C to oxidize methane, and through a final bubbler to absorb the carbon dioxide from this oxidation. Barium carbonate was precipitated from the three alkaline solutions and "counted" as such. This procedure was found

quantitative in blank experiments at the flow rate given.

To separate the second and the third fractions, the solution of the sample (if a solid, it was first dissolved) was acidified with nitric acid, shaken with 4.2 cc each of carbon dioxide, carbon monoxide, and methane, and then aerated with oxygen for a long period, the gas stream being passed through the same analytical train as before. This constituted the second fraction; the third fraction remained in the out-gassed solution, which was then neutralized preparatory to treatment.

This solution containing the third fraction was first examined for radioactive cyanide. To the whole, or an aliquot, one millimole of potassium cyanide carrier was added and then precipitated as silver cyanide. The solution was maintained at 0°C for two hours before filtration. The solid silver cyanide was counted as such. In the cases of the hydrazine, the glycine, the aniline, and the pyridine, this procedure proved unsatisfactory, so chloride ion, if not already present, was added, and a mixed precipitate of silver chloride and silver cyanide was obtained. This precipitate was crushed up thoroughly in water, the suspension made 0.1*N* in sodium hydroxide, and excess potassium permanganate added. Thirty minutes of boiling sufficed for complete oxidation of the cyanide to cyanate, while leaving the chloride unaffected. After destruction of excess permanganate as described below, acidification resulted in hydrolysis of the cyanate to ammonium ion and carbon dioxide, and the latter was then swept out of the solution with a stream of oxygen, absorbed in sodium hydroxide, and precipitated and counted as barium carbonate.

To the filtrate from the cyanide separation was next added a small quantity each of formaldehyde, methanol, and formic acid. The solution was acidified and these compounds separated from the bulk of the original material by distillation of the solution as nearly to dryness as seemed practical. Formaldehyde was separated from the distillate by precipitation as the 2,4-dinitrophenylhydrazone. The distillate was then made alkaline and again distilled down to one-fifth its original volume. The residue contained the formate and the distillate the alcohol. These solutions were made 0.1*N* in sodium hydroxide, excess potassium permanganate was added, and the two compounds were oxidized to carbonate by three minutes of boiling. Excess permanganate was destroyed by dropwise addition of potassium iodide to the solutions to which excess ammonium chloride had also been added, and then, after acidification, carbon dioxide was swept out and converted to barium carbonate for counting.

This was the general procedure followed with all the samples. Certain necessary variations made may be noted. In the cases of three of the samples, the containers were imperfectly sealed and the results for gaseous activities in these instances were consequently of questionable validity. With the urea solution, for this reason, the first and second fractions were combined before analysis. In the case of the aniline, it was convenient for other experimental reasons to do likewise. Moreover, this substance is, of course, not miscible with water, so the procedure for fraction 3 had to be modified. Water-soluble activity was extracted with successive portions of dilute sodium hydroxide containing carrier cyanide, followed by dilute hydrochloric acid, then more base and finally water. These water solutions were combined and silver cyanide and chloride were precipitated and treated as described before. The filtrate was subjected to oxidation by alkaline permanganate and the barium carbonate thus obtained counted as "other water-soluble activity." Finally, in the case of the pyridine, concentrated sulfuric acid was added prior to the distillation of the formaldehyde, methanol, and formic acid from the sample to prevent volatilization of the pyridine itself.

Counting

In this work we have adopted a more satisfactory method for measuring the radioactivity than has hitherto been used for C^{14} in this laboratory. Because of the low energy ($145{,}000 \pm 15$ ev[2]) of its beta-particles, this isotope has, until now, been counted either as a thin layer of solid, e.g., barium carbonate, mounted inside a screen-wall counter[5] or as gaseous carbon dioxide directly introduced into a counter. Both of these methods have their disadvantages in loss of time and lack of accuracy. A rather similar problem exists in

[5] W. F. Libby, Phys. Rev. **46**, 196 (1934).

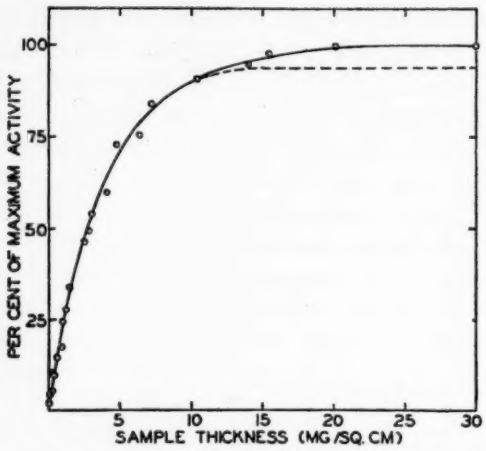

FIG. 1. Increase in apparent activity as increasing weights of a single $BaC^{14}O_3$ sample are counted. Broken line indicates divergence from our results of a curve calculated on the basis of the data of Ruben and Kamen (see reference 2).

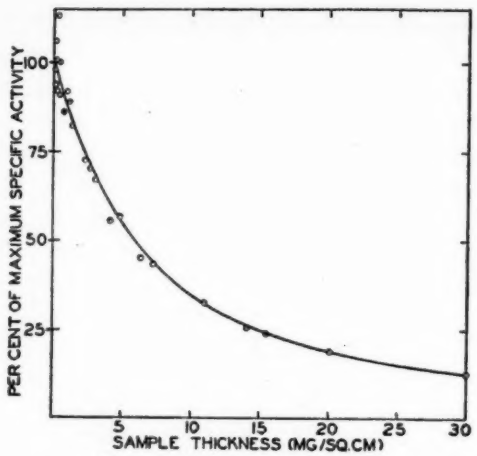

FIG. 2. Specific activity of a $BaC^{14}O_3$ sample *versus* sample thickness.

the case of S^{35}, the upper energy limit of whose beta-particles is 120,000 ev.[6] Workers with this isotope[7] have lately succeeded in counting it as a thin layer of barium sulfate placed just below the thin mica window of a bell-jar type counter, thus avoiding the necessity of refilling the counter tube for each sample. With certain variations, we have adopted their method for C^{14}.

Our counter tube consisted of a bell-jar shaped glass housing, containing a brass cathode and a central tungsten wire, and with a mica window at the bottom. The window was 3.0 mg/sq. cm in thickness, 60 mm in diameter, and was reinforced on the inside by a light-weight, open-mesh brass screen. The cathode, which was one centimeter above the window, was 5.0 cm long and 4.8 cm in diameter. A mixture of 740 mm of helium and 10 mm of ethanol, used as a filling gas in this work, performed satisfactorily. We have lately, however, been using the better argon and alcohol (90 mm and 10 mm) mixture in these counters, despite the difficulty of obtaining windows of sufficient strength to withstand the external pressure.

The samples were isolated as barium carbonate and, in two cases, silver cyanide and were counted as thin layers of these solids mounted on thin aluminum disks (weight about 0.6 g) placed two millimeters below the counter window. The geometry was well standardized, so that reproducible results might be expected. The disks fitted snugly into a machined brass carriage which slipped into a fixed position under the counter. Background determinations were easily made by replacing the sample with a clean disk. (As might be expected, a disk mounted with inactive barium carbonate gave the same background count as a clean disk.) Accurate weighing of the samples was facilitated by the lightness of the disks. The samples were mounted by a technique similar to that used by Hendricks *et al.*[7] for barium sulfate. A brass cup with straight sides and a flat bottom was provided with a thick concentric sleeve fitting snugly inside of it and machined to give a good seal with the bottom when forced down by a screw arrangement. The aluminum disks were of such size as just to cover the bottom of the cup; thus, the sleeve, when inserted, would seal their edges. A suspension of the solid sample in 95 percent ethanol was placed in the cup, allowed to settle, and the excess alcohol evaporated off by gentle warming. The disks were then removed and weighed. The area of the mounted sample being known (11.6 sq. cm), an accurate estimate could be made of the thickness of the sample, which was necessary in order that a correction for self-absorption might be applied. For reproducibility, uniformity of sample layer was essential; our method of mounting gave this, except for very heavy layers (>20 mg/sq. cm), with which thin patches developed, giving an apparent enhance-

[6] M. Kamen, Phys. Rev. 46, 196 (1934).
[7] Hendricks, Bryner, Thomas, and Ivie, J. Phys. Chem. 47, 469 (1943).

ment of activity. In these cases, tamping the dried coating with the flattened end of a glass rod obviated this difficulty.

The self-absorption correction was experimentally determined by measuring the apparent activity of varying weights of a single radioactive barium carbonate sample mounted as described above. As expected, the activity at first increased with increase in size of the specimens, but eventually a maximum activity was obtained which could not be further increased.

The results are shown in Fig. 1, plotted as percent of this maximum activity *vs.* thickness of coating. The experimental curve coincides exactly with a curve calculated on the basis of Ruben and Kamen's[2] data on absorption by aluminum foil up to about 12 mg/sq. cm. The calculated curve (shown as a broken line) comes to a saturation value at 16 mg/sq. cm, however, and at a value about 6 percent below the experimental value. A plot of the percent of that activity which would be observed if the sample layer were of zero thickness is shown in Fig. 2, based on the same data as Fig. 1. This figure enables one to make direct comparison between samples of various thicknesses; we used it to correct all our data to zero thickness. The corrections for silver cyanide were assumed the same as those for barium carbonate.

It would, of course, be quite convenient for work with this isotope if it were available in such quantities that samples of thickness greater than 25 mg/sq. cm only, for instance, might be counted, thus eliminating the necessity for any correction.

RESULTS

The experimental results are shown in Table I. The first column gives the sample fractionated; the group in which it was irradiated is indicated by the Roman numeral in parenthesis. The succeeding seven columns show the total activity in each fraction in counts per minute, in most cases computed from an actual count made on an aliquot of the whole fraction. For carbon dioxide, carbon monoxide, and methane the two figures

TABLE I. Fractional distribution of activity in the samples.

Sample	Activity in fractions (counts per minute) CO_2	CO	CH_4	HCN	HCHO	CH_3OH	HCOOH	Activity per g N
NH_4NO_3								
Soln. (I)	3,300±150	71,500±5000	1700±100	0±60	0±100	1600±200	24,700±2000	38
	62,800±2500	6600±400	2150±500					
	38.0%	44.8%	2.2%			0.9%	14.1%	
Soln. (I)	42,300±600	166,800±4000	450±80	0±1000	0±100	8600±1000	57,700±2500	80
	315,000±7000	11,100±400	0±50					
	59.4%	29.5%	0.1%			1.4%	9.6%	
Soln. (I)	850±150	60,500±3000	600±200	0±150	0±120	3700±1000	lost	13
	14,300±1000	11,700±400	350±100					
	16.5%	78.5%	1.1%			4.0%		
Crystals, 170 g (III)[a]	0±10	0±10	0±10	0±10	0±10	0±20	0±20	10.6
	450±50	185±25	0±10					
Crystals, 500 g (II)	775±40	160±25	0±15	0±15	0±6	0±20	0±20	6.9
	205±20	70±10	0±15					
	81.0%	19.0%						
$(NH_2)_2CO$								
Soln. (III)[a]	0±10	0±10	0±10	0±20	0±10	110±30	455±50	4.0
Crystals (III)	215±15	45±10	0±6	500±100	0±10	0±20	0±20	9.2
	140±20	0±10	0±15					
	39.5%	5.0%		55.5%				
$N_2H_4 \cdot 2HCl$								
Crystals (II)	77±15	36±10	19±5	325±50	0±10	0±20	0±20	17.1
	0±7	0±10	0±10					
	17.8%	7.9%	4.2%	71.1%				
NH_2CH_2COOH								
Crystals (II)	0±6	0±6	0±10	25±8	0±6	(80±20)	(50±10)	12
	13±5	0±4	0±8					
	7.7%			14.9%		47.6%	29.8%	
C_5H_5N								
Soln. (III)[a]	32±6	0±10	0±10	0±12	0±10	0±20	36±20	3.8
$C_6H_5NH_2$								
Liquid (II)	0±6	0±10	41±6	0±12		0±50		.82

[a] Containers were imperfectly sealed.

given represent, respectively, gas phase activity and activity trapped within the sample—solution or crystals as the case may be. The percentages shown indicate the portion of the total activity which the particular fraction represents. The last column gives the total activity isolated divided by the grams of nitrogen in the sample, and, as mentioned before, these figures should be more or less the same within each group. The limits of error shown represent "presumable errors," in most cases somewhat larger than "probable errors" computed on the basis solely of statistical fluctuation of the radioactive decay. They attempt to take into account other, often greater, sources of error, such as variability in counter behavior, non-uniformity of the mounted samples, etc. The use of calculated "probable errors" for these data cannot fail to be misleading. It will be observed that the magnitude of these errors shows a large variation. This arises from the fact that aliquots counted represented very much smaller percentages of the total fraction in some cases than in others. Where an aliquot of a bulky fraction showed little or no activity, the error became quite large.

The data for some of the samples require a certain amount of explanation and amplification.

Ammonium Nitrate Samples

In the saturated ammonium nitrate solutions, methane activity is irregular, varying from zero to about 2 percent; it is, moreover, irregularly distributed between solution and gas phase. We suspect this activity to be apparent only, appearing as a result of incomplete oxidation of carbon monoxide in the first combustion tube, so that a certain amount of the activity associated with it was not absorbed by the alkali, but carried over into the methane fraction. This belief is based in particular on the case of the first ammonium nitrate solution, which shows the highest apparent methane activity. After completion of the analysis of this solution, it was found that gas flow rates through the analytical train of 20 and 26 liters per hour had been used inadvertantly for gas phase activity (fraction I) and dissolved gaseous activity (fraction II), respectively; preliminary experiments had shown a rate of 5 to 10 liters per hour to be satisfactory. A check on the weights of barium carbonate obtained for the carbon monoxide and methane fractions from fraction II indicated that the latter was larger, and the former smaller than the known amounts of "carriers" which had been added by approximately the right amount to account for all the apparent radio-methane. Although lower gas flow rates were subsequently used, it seems quite reasonable to suppose that the small amounts of "radio-methane" found in the other ammonium nitrate solutions are to be accounted for in a similar fashion. Methane should, therefore, probably be considered inactive.

In addition to the compounds shown, radiocarbon in the elemental state was a possibility, although an unlikely one. It was not experimentally practical to look for it on the walls of the tanks, where there might have been the best possibility of finding it, but it was shown to be absent in the solution, a sample of which was filtered several times through a bed of graphite. This graphite, after washing with acid to remove any carbonate, was found inactive.

It is evident that the proportions of carbon monoxide, methanol, and formic acid are roughly the same for the three solutions, which is what might be expected. The percentages of carbon dioxide, however, vary erratically. This is, we think, caused by the fact that there was a good deal of iron rust (from pipe fittings) inside the tanks. The rust was found to be slightly active, presumably as a result of reacting with some of the active carbon dioxide. The distributions of the radioactive gases between the gas phase and solution are interesting to examine in this connection. Knowing the solution and gas space volumes, one may calculate from the observed activity distribution a distribution coefficient for equal volumes. Computed as gas/liquid activity, the values for carbon monoxide are 84, 93, and 73 for the three cases. These compare favorably with an expected value of about 86.[8] For carbon dioxide the values 0.55, 0.83, and 0.84 are obtained, which are to be compared with an expected value of about 2.5.[9] That the carbon dioxide had not become equilibrated between the two phases seems unlikely in view of the carbon

[8] From Winkler, Ber. **34**, 1408 (1901), a distribution coefficient for water at 20°C of 43 is obtained. By analogy with other cases this should be approximately doubled for saturated ammonium nitrate.

[9] Setschenov, Ann. de Chimie [6] **25**, 226 (1892).

monoxide result and the fact that the tanks stood for about eighteen months between the end of their irradiation and their analysis. Rather the preferential absorption by the rust of the gas phase carbon dioxide seems the best explanation. Thus, too, could the wide discrepancy between the three yields shown in the last column be accounted for—although, as mentioned before, this may be explained in part as resulting from shielding of one tank by another.

In the case of the ammonium nitrate crystals, the absence of activity in the gas phase over the 170-g sample is to be ascribed to loss from an imperfectly sealed container. However, the fact that the yield of C^{14} is the greatest for this sample of all those in Group III suggests that this loss was not too large; i.e., most of the activity must have been trapped in the crystals. Yet with the 500-g sample the bulk of the activity was found in the gas phase. These results can perhaps be reconciled by the fact that the crystals of the 170-g sample were considerably coarser than those of the 500-g sample. The much greater surface in the latter case might have resulted in diffusion into the gas space of considerable activity trapped immediately below the surface. It is interesting to note that in these samples there is two to four times as much active carbon dioxide as carbon monoxide, a result not inconsistent with the solution results.

It might be noted that these results amplify those of Ruben and Kamen[1] in that the latter found only gaseous activity in the ammonium nitrate solutions and no gas phase activity over the crystals

Other Samples

The fact that carbon dioxide and carbon monoxide are formed with urea crystals, and that they were found in the ammonium nitrate solutions as well as crystals, suggests that they were also formed in the urea solution. Their absence presumably results from the fact that the container was poorly sealed. We suspect their loss from the badly sealed pyridine solution as well, the small carbon dioxide activity representing only a residue. The appearance of oxygen-containing activity in the hydrazine doubtless results from the fact that the crystals were moist. The presence of this activity in the gas phase only is consistent with this idea. In the case of the glycine, the formic acid activity shown must be taken as a lower limit, since it represents a measurement made on only a portion of the formic acid fraction. The barium carbonate from the remainder became so diluted with inactive barium carbonate resulting from decomposition, in the course of the analysis, of the glycine itself that measurement of the activity of this portion became impossible. In regard to this glycine, it is quite possible that the activity given for methanol and formic acid does not actually belong to these compounds. Our analytical scheme distinguished only between alcohols, acids, and aldehydes. For most of the samples irradiated, the absence of carbon chains made improbable the formation within these classes of any compounds other than methanol, formic acid, and formaldehyde. A glycine molecule could, on the other hand, have reacted with a radioactive carbon atom to produce 2- or 3-carbon compounds, and any of these which were alcohols or acids would have appeared in our scheme as methanol and formic acid.

DISCUSSION

Certain facts in regard to the type of environment favorable to the formation of each of the carbon-containing compounds are immediately apparent from our results; others, while not so obvious, may be inferred.

Carbon dioxide and carbon monoxide are produced in the irradiation of all oxygen-containing material, except glycine where, although there is no apparent carbon monoxide, the expected amount would probably be within experimental error; these gases were presumably lost by leakage from the urea and pyridine solutions. Carbon dioxide tends to appear in considerably greater abundance than carbon monoxide (see above for discussion of disappearance of carbon dioxide from the ammonium nitrate solutions) and these substances together tend to contain the bulk of the activity, except where there exists a good possibility for the formation of addition or substitution compounds with the parent substance, such as in the cases of glycine or pyridine.

Methane, it may be seen, appears only in the absence of oxygen and in the presence of a relatively high hydrogen density (see above in regard to the ammonium nitrate solutions).

Hydrogen cyanide is to be found in the absence of water and of a high oxygen concentration. Formaldehyde formation does not appear to be favored by any of the conditions covered by this work. Methanol and formic acid tend to appear together in the presence of water, the latter in considerably greater abundance.

In the irradiation of the more complicated compounds, glycine, pyridine, and aniline, it is evident that most of the activity has not been properly accounted for. We had originally planned more elaborate fractionations of these substances, but their total C^{14} content did not make such feasible.

The question may be raised as to the influence on the results of thermal exchange reactions, occurring over the long period of time involved in the irradiations. For instance, since, in all solutions, inactive carbon dioxide impurity was undoubtedly large compared to carbon monoxide impurity, an exchange reaction would tend to produce an equilibrium condition in which the bulk of the carbon monoxide activity would have been transferred to carbon dioxide. Although such reactions may perhaps be excluded by the argument given below for thermal reactions in general, they may probably equally well be excluded in most cases solely on the basis of improbability. The exchange mentioned, between carbon dioxide and carbon monoxide, for instance, is known to occur, in the gas phase, at an appreciable rate only at temperatures in the region of 800°C;[10] one may perhaps reasonably infer from this that the occurrence of the exchange in our solutions at a measurable rate at room temperature is unlikely. A detailed examination of other possibilities for exchange which might influence the distribution of the activity suggests that in general they would require a high activation energy and consequently may be considered improbable. We have, therefore, disregarded reactions of this type in the interpretation of our results.

It is interesting to attempt an explanation of the results in terms of the processes in which the C^{14} atoms must be involved immediately after their formation. These atoms are, as mentioned before, more than assured of ejection from any parent molecule by virtue of the recoil energy, ~40,000 ev, associated with their formation, and will, consequently, first appear as swiftly moving single atoms. We say atoms, not nuclei, inasmuch as the particles will probably never be stripped of all their electrons, since the velocity associated with the recoil energy, $\sim 7.4 \times 10^7$ cm/sec., is that of an electron of only 1.6 volts. The question is, now, what will become of such atoms. Their behavior will, in all probability, be rather like that of α-particles which have become reduced to comparable energies. Their kinetic energy will doubtless be dissipated in a succession of collisions with the atoms and molecules of the environment, these collisions leading to a good deal of ionization and radical formation. In this process the particles will travel a considerable distance from the locale of their birth. Along their paths they will probably, by analogy with α-particles, change charge a large number of times, but the predominating tendency will be to gain electrons. Only toward the end of the paths, after most of their initial energy has become dissipated, will there exist a reasonable probability of formation of combinations with other atoms. It seems reasonable to suppose that these first combinations should be diatomic and that the nature of the partner atoms should be more or less randomly determined by the relative abundance of the different atomic species in the medium. A particular combination may or may not be a potentially stable one; it may carry a charge or be a radical. Most important, it will still be quite energetic and will tend to undergo further "high energy" reactions on collision with other molecules. It may add further atoms; it may exchange "partner atoms;" it may change its charge; it may be broken up.

These first reactions may not necessarily lead to a more stable combination. However, the energy level will soon drop below that required for the "high energy" reactions, leaving the radioactive substance, whatever may then be its form, in a state analogous to chemical activation. In this state, it will tend to undergo only reactions which result in a decrease in free energy, i.e., those leading to relatively stable molecules. It seems reasonable to suppose that at this stage most of the radioactive atoms will reach a stable

[10] J. D. Brandner and H. C. Urey, J. Chem. Phys. **13**, 351 (1945).

form and so remain. Free radicals or unstable ions reaching room temperature should still be quite reactive and should soon react to produce stable radioactive compounds. The predominance of relatively stable compounds among the products shown in Table I lends support to these ideas. We suggest, therefore, that thermal reactions occurring over a period of time subsequent to the recoil process will not be important in determining the final chemical form of the radioactivity: almost all such reactions will have occurred toward the end of the recoil process itself.

Let us now see how the experimental results fit into the picture just outlined.

In the ammonium nitrate solutions the first combinations must obviously be with hydrogen, oxygen, or nitrogen, in that order of probability. A C—H combination should be quite unstable and should soon change to one of the other forms or else add another atom, the most probable being another hydrogen, thus giving an excited methylene. This methylene will then either be oxidized to carbon monoxide or carbon dioxide or else become hydrated: thus the formation of methanol is explained. The lack of formation of methane, or at least the very low incidence of it, is easily explained on the basis of the low probability of the addition of two more hydrogens to the methylene, compared to the probability either of oxidation or of hydration. In like manner the absence of formaldehyde may be accounted for. This would most readily be formed by the addition of an oxygen to methylene, but the probability of this process should be low compared to that of the hydration process. The C—O combinations which survive the "high energy" reaction stage may either dissipate their remaining energy, and settle down as normal carbon monoxide molecules, or, in consequence of the high concentration of nitrate ions in a somewhat acid medium may, while excited, be oxidized to carbon dioxide molecules, which then remain as such. The data indicate the higher probability of the latter event, a not unexpected result. The C—N combinations might perhaps be expected to lead to formation of stable hydrogen cyanide; the fact that this compound is not formed may possibly be explained by either of two occurrences. The cyanide while still excited will have a strong tendency toward oxidation to cyanate. This, in the acid medium prevailing, would at once be hydrolyzed. Failing this event, the tendency of hydrogen cyanide toward hydrolysis might lead to the rapid conversion of the radio-cyanide to ammonium formate. The latter alternative would explain nicely the absence of cyanide coupled with the presence of a large amount of formate. In regard to the possible relative importance of the first suggestion, however, our data can give no information, since the radioactive carbon dioxide which would be formed thereby would be indistinguishable from that formed by other mechanisms.

In the case of the ammonium nitrate crystals, there is still a high concentration of oxygen, and as might be expected the two oxides of carbon are formed in large amounts. The CO_2/CO ratio is even larger for the crystals than for the solutions. This may be explained either by the post-irradiation loss of carbon dioxide from the solutions, as already discussed, or by the fact that the solid is probably a stronger oxidizing medium than the solution. As with the solution, no methane is formed, and the explanation of this is doubtless to be found in the high probability of oxidation of methylene, even if formed, in such a medium. The absence of water accounts for the non-formation of methanol. Lacking the possibility of hydration, the methylene presumably is oxidized. One might anticipate the formation of formaldehyde under these circumstances. It is evident from its absence that the oxidation of methylene proceeds beyond the stage of this compound. It is interesting that no cyanide appears in this case. This is most easily explained by supposing that any C—N intermediates are oxidized to cyanate. This substance would, of course, hydrolyze to carbon dioxide and ammonium ion on solution of the crystals in an acid medium. The fact that no formate is to be found is in line with our suggestion that this is formed through the reaction of a not quite de-energized cyanide with the water in the solution.

The first instance of cyanide formation is that of the urea crystals. Here there exists a relatively greater concentration of nitrogen and smaller concentration of oxygen, so the C—N combinations should have a strong tendency toward formation and but a slight one toward oxidation

to cyanate. The non-formation of formate is again to be explained by the absence of water. Carbon dioxide and carbon monoxide are formed, but in much smaller amounts, because of the low concentration of oxygen. Water being absent, methanol is not formed; and methane is again absent because of the improbability of the acquisition by methylene of two additional hydrogens. Comparing with these results those for the solution of urea, we find just the expected changes in distribution of activity. The cyanide disappears and a roughly comparable quantity of formate appears. (The solution and solid contained, respectively, about 300 g and 210 g of urea, and the yields should have been approximately the same since both samples were in Group III.) Methanol again makes its appearance, presumably as a result of the presence of water.

Consequent to the high concentration of nitrogen and the absence of oxygen in the hydrazine, cyanide is the chief product. This activity was presumably trapped within the crystals and despite the small amount of moisture present, no formate was formed. Because of the considerable tendency toward their formation, however, the two oxides of carbon did appear possibly as a result of the presence of the water. The concentration of oxygen in the air within the sample container would not seem sufficient to account for the formation of these compounds (cf. their non-formation in the case of aniline). In this case also, the high hydrogen concentration and absence of oxygen made possible the production of a small amount of methane.

It is evident that the formation of cyanide in the case of the glycine crystals and its non-formation coupled with the appearance of formate in that of the pyridine solution is consistent with our picture. The appearance of methane in the aniline of course results from the absence of oxygen coupled with a high hydrogen concentration.

The foregoing discussion gives a reasonable and self-consistent explanation of our experimental results. Our data cannot be considered sufficiently extensive, of course, to preclude the possibility of an alternative picture. With the neutron sources now available, it should not be difficult to extend our data considerably.

Practical Considerations

In regard to the possibility, mentioned in the introduction, of "on the spot" syntheses, it is evident that a proper choice of material to be irradiated may lead to the production of any one of several desirable C^{14}-containing compound. Radio-cyanide is relatively easy to obtain synthetically from carbon dioxide, but its direct production would obviate the necessity for this operation. Methanol is more difficult to prepare synthetically; it could be quite easily concentrated from the irradiated solutions. Formic acid also might be of considerable value in tracer work. More complicated compounds are doubtless formed in the cases of glycine, pyridine, and aniline, but no definite conclusions can be drawn from our data.

It is also evident from this work that, in the preparation of C^{14} by irradiation of ammonium nitrate with neutrons, the task of separating the activity could be greatly simplified if one were to use a saturated solution in a closed container with an adequate gas space over the solution. The bulk of the activity (in the form of carbon dioxide and carbon monoxide[11]) could be simply pumped off periodically, thus doing away with the laborious task of handling the solution itself. Methanol and formic acid would, of course, accumulate in the solution and, if desired, these could eventually be recovered.

ACKNOWLEDGMENT

We wish to express our thanks to Professor E. O. Lawrence and the Radiation Laboratory staff for the irradiation of the samples and in particular to Dr. Martin Kamen and Miss M. B. Allen, who took an active interest in seeing to this irradiation. We should like also to acknowledge our indebtedness to Professor A. C. Helmholz for much helpful discussion in connection with the interpretation of the results.

[11] If we assume the addition of no carriers, the carbon monoxide can normally be isolated with a very much higher specific activity than the carbon dioxide, since the latter invariably becomes diluted with inactive atmospheric carbon dioxide.

Motions of Molecules in Condensed Systems. II. The Infra-Red Spectra for Benzene Solid, Liquid, and Vapor in the Range from 3 to 16.7μ

RALPH S. HALFORD AND OLIVER A. SCHAEFFER
Mallinckrodt Chemical Laboratory, Harvard University, Cambridge, Massachusetts

(Received December 7, 1945)

Infra-red spectra are compared throughout the interval from 600 to 3300 wave numbers for the same amount of benzene existing separately as solid at 3°, liquid at 8°, and vapor at 20°C. The comparison demonstrates convincingly that (1) predictable selection rules for the solid are obeyed strictly, (2) there are no selection rules operating in the liquid phase, (3) the shift of molecular frequencies induced by successive stages of condensation is small and can be ignored in the approximation that regards the vibrations of an isolated molecule as harmonic ones, (4) the intensification of components of the spectrum accompanying changes of state proceeds as predicted qualitatively in an earlier paper, (5) all proposed complete assignments of the fundamental frequencies of benzene require revision. The components appearing in the several spectra are classified in accordance with a scheme suggested by the selection rules for the vapor and solid.

INTRODUCTION

INFRA-RED absorption bands are characterized by the locations of their centers on the frequency scale, by their fine structures or apparently continuous envelopes, and by their intensities. When a band is observed in the spectrum of a vapor its characteristics can be interpreted readily to a useful degree of approximation in terms of a molecular model wherein vibration and rotation are separable motions. The location of the band center measures the difference in energy between two vibrational states; the envelope[1] or fine structure, as the case may be, reveals information concerning the quantized rotational states; the integrated intensity,[2] when properly interpreted, measures the effective charges on vibrating parts of the molecule. When the molecule enters a condensed phase, its bands become altered; the location of a band is shifted, both the envelope or fine structure and the intensity are changed. Furthermore, new bands may develop in the spectrum of the condensed phase where none appear in the spectrum of the vapor. These phenomena are induced by intermolecular forces; they provide a little used and, in some respects, highly discerning method for studying matter in its condensed states. However, there are few data in the literature that are suitable for such an undertaking. In order to avoid uncertainties arising from differences of either resolving power or calibration, it is necessary to compare spectra obtained for different states with the same instrument; also, for obvious reasons it is desirable to use always the same amount of absorbing material and to work at similar if not equal temperatures.

In this article we shall describe the results of a study of the infra-red spectra for benzene as vapor, liquid, and solid along with the procedures used for obtaining them. The results will be used to test the conclusion drawn in an earlier paper[3] that the qualitative features of spectra in condensed phases can be interpreted by focusing attention upon the motions of one molecule. We shall show also that the vibrations of a molecule retain their individualities in the several phases within about the same degree of approximation that they may be regarded as harmonic in the isolated molecule.

Benzene was chosen for this study because of the ease with which it can be produced in all three states at similar temperatures and because its symmetry provides interpretable band envelopes in the vapor along with comparatively great promise of new developments accompanying condensation.

EXPERIMENTAL

Reagent grade, thiophene-free benzene was purified further by repeated fractional crystal-

[1] S. L. Gerhard and D. M. Dennison, Phys. Rev. **43**, 197 (1933).
[2] A. J. Wells and E. B. Wilson, Jr., J. Chem. Phys. **9**, 659 (1941).
[3] R. S. Halford, J. Chem. Phys. **14**, 8 (1946).

lizations; the resulting specimen represented less than half of the original batch. Water, which influenced greatly the reflectivity of solid specimens, was removed by refluxing the recrystallized material with phosphorous pentoxide. The benzene was stored over this reagent and distilled into an absorption cell as required.

The absorption cells employed for study of liquid and solid specimens were each constructed from two disks, about 3 mm thick and 50 mm in diameter, of optical quality synthetic rocksalt. One disk, serving as a cover, was ground plane and given a high polish on both faces. The other disk was finished similarly on one face before it was attached with wax to a suitably constructed face plate with the rough surface exposed for machining on a lathe. Using a round-nosed tool to minimize marks, the surface was first machined until uniform; then, leaving a rim about 3 mm wide at the edge of the disk, a well was cut to the desired depth. The work was given a high polish before it was removed from the face plate. After dissolving the wax as completely as possible its thorough removal was accomplished by additional light polishing on both faces of the disk.

To assemble the cell, a thin layer of glycerine was applied on the outer portion of the rim, an excess of benzene was distilled into the well, and the cover was lowered, making contact first at one point on the edge, in a manner such that the excess liquid and all bubbles were forced out of the cell. The two disks were pressed tightly together and the upper one was rotated relative to the lower one in order to distribute the glycerine uniformly on the rim and to make a tight seal.

Cells prepared and filled in this way retain their contents indefinitely when stored in any position and can be taken apart only with difficulty. The glycerine does not dissolve appreciably in the benzene, remains confined to the rim, and has very slight action toward the rocksalt. During the course of this work we constructed and used several cells with wells varying from 20 to 100 microns in depth. After they had been in service for some time, two of them, assembled in the usual way, were calibrated by weighing their contents. The depths so determined agreed* with the machining data within the precision of adjustment of the lathe.

The cell was supported rigidly in the light path by a holder consisting of threaded male and female parts arranged within a thermostating jacket. The female part was a shallow cylinder with a flange at the bottom whose aperture excluded the rim of the cell. The cell rested on the flange and was held in place by the male part with matching aperture. The male part advanced on fine threads so that the pressure on the cell was tolerably uniform. Cold air circulated intermittently through the jacket surrounding the cell holder. A thermocouple buried in the flange served to measure temperature and also, by activating a photo-switch in the power supply of a solenoid valve, to control the flow of cold air. The temperature at the site of the thermocouple was thus maintained constant within a range of about one degree. Observations of the melting point of benzene showed that the thermocouple reflected adequately the temperature of the specimen in the cell.

In order to prevent condensation of atmospheric moisture on the cold outer surfaces of the cell the jacketed holder was housed in a waterproofed wooden box fitted with rocksalt windows. The interior of the box was charged with fresh desiccant some hours prior to commencing operation of the cooler. In spite of these precautions occasional difficulties were experienced on excessively humid days and data were discarded routinely whenever subsequent dismantling of the apparatus disclosed any moisture on the cell.

Measurements were made with the automatic recording prism spectrophotometer[4] placed at our disposal through the kindness of Professor Wilson. A polished disk of rocksalt in an identical companion holder, housed adjacent to the absorber in the same cooling jacket, served as the standard for photometry. The spectra were recorded a portion at a time. First, the liquid was brought to 8°C and its spectrum taken over a selected interval of frequencies. Then, after the specimen was frozen, it was annealed just below the melting point until it attained virtually

* We are indebted to Mr. Gene B. Carpenter for this information.

[4] H. Gershinowitz and E. B. Wilson, Jr., J. Chem. Phys. 6, 197 (1938).

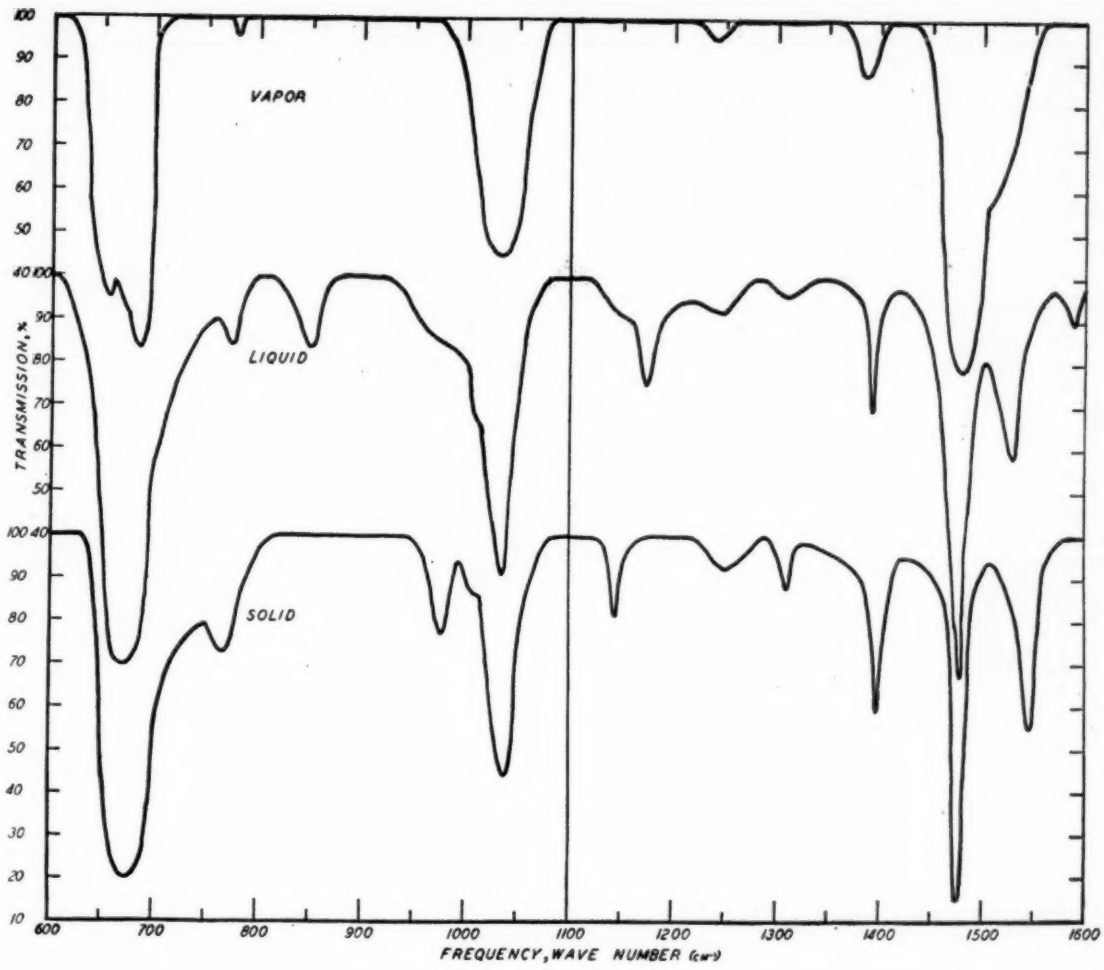

FIG. 1. Infra-red absorption spectra for equivalent absorbing paths of benzene vapor (48 mm in 30-cm cell at 20°C), liquid (0.065 mm thickness at 8°C), solid (same specimen at 3° C). Observations below 1100 wave numbers with rocksalt prism, others with fluorite prism.

constant transmission, the temperature was reduced to 3°C, and the spectrum of the solid was recorded over the same interval of frequencies. The cycle of operations was never repeated with the same specimen; instead, the apparatus was dismantled and inspected for evidences of moisture.

A liquid specimen that has not been frozen previously in the cell shows no evidence of contraction when it is cooled; it remains uniformly distributed over the whole cross section of the cell. Furthermore, rather drastic supercooling is required to produce the solid which then forms suddenly. For this reason, the solid is also distributed uniformly over the cross section of the cell. *This fortuitous circumstance permits reasonably valid comparisons to be made between intensities of absorption by the same specimen in the two different states.* On the other hand, after regeneration from the solid, the liquid specimen exhibits an undesirable centered bubble of vapor. The bubble spans about 10 percent of the cross section and represents the space created by thermal contraction which occurs preferentially

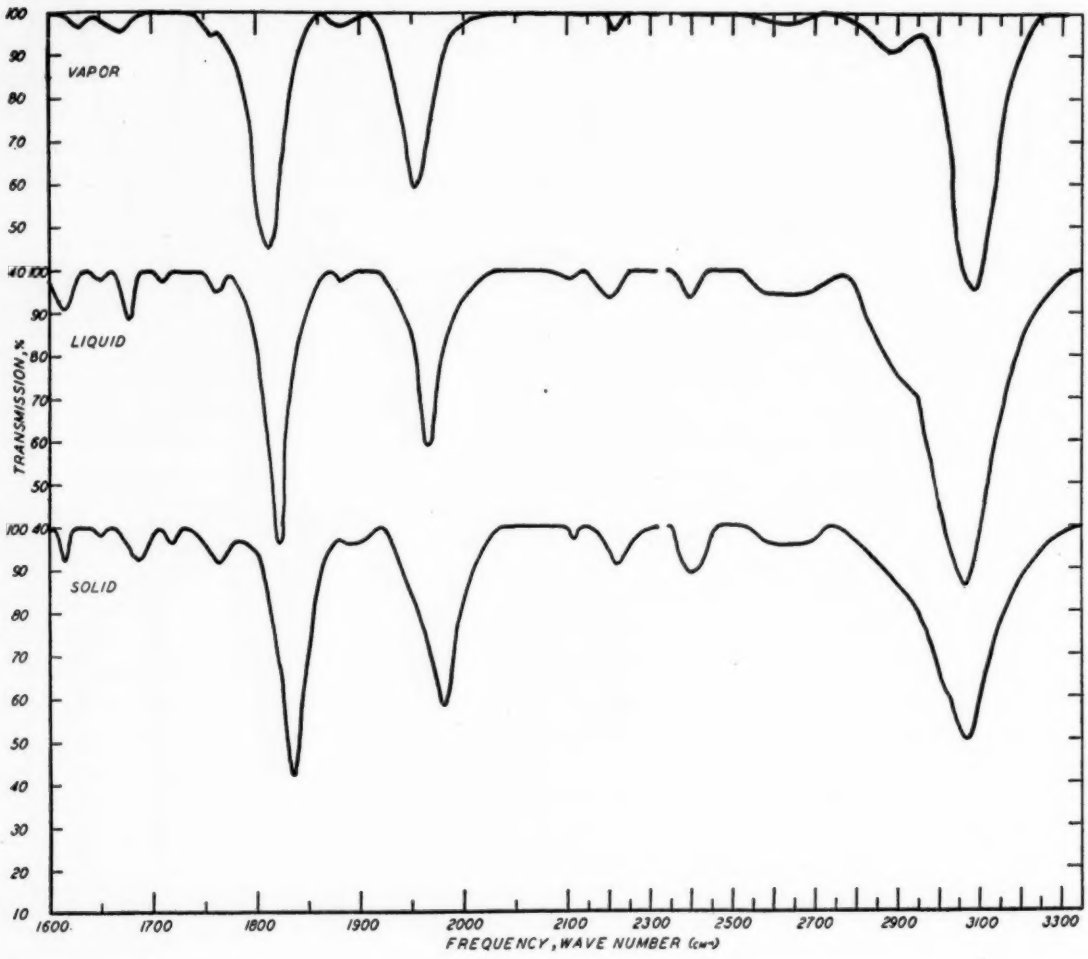

FIG. 2. Infra-red absorption spectra for equivalent absorbing paths of benzene vapor (48 mm in 30-cm cell at 20°C); liquid (0.065 mm thickness at 8°C), solid (same specimen at 3°C). All observations with fluorite prism.

in the cross section. Subsequent resolidification occurs gradually so that the specimen has an opportunity to redistribute itself in the cell. The resulting larger bubble contributes a disproportionate share of the transmitted radiation owing to the large reflection losses that occur elsewhere on the surface of the solid specimen. Consequently, comparisons of intensities of absorption by the two states are now rendered more than ordinarily suspect. The difficulty can be avoided by warming the regenerated liquid until the bubble disappears.

The specimen of vapor was confined in a glass tube 30 cm long, closed at both ends with rock-salt windows; the photometric standard was an identical but empty cell. The pressure of the vapor was adjusted so that the ratio of densities for it and a liquid specimen was equal to the inverse ratio of the lengths of their absorbing paths.

RESULTS

Figures 1 and 2 depict the relative transmissions at different frequencies for the same amount of benzene when it exists separately as vapor, liquid, or solid. The spectra for both liquid and solid were examined with specimens approximately 40, 65, and 100 microns thick, in each case throughout all or part of the range from 600 to 3300 wave numbers. These variations of thickness produce little change in the spectra except for the expected one of uniform intensification. To avoid complicating the figures we have elected to reproduce only the most illuminating results. The spectrum of the vapor was examined with just one specimen, confined in our cell under a pressure of 48 mm Hg, which is equivalent to a liquid sample 65 microns thick. In all cases the spectra have been corrected for losses due to reflection. These were small for the vapor and liquid but ranged for the solid, depending upon its thickness and previous history, between 25 and 60 percent of the incident radiation. The correction was determined from the proportion of the incident light transmitted for frequencies that the specimen was evidently incapable of absorbing. The proportion of light lost by reflection was found to be the same within experimental error throughout the range of frequencies that we traversed with any one specimen but for the solid specimens it changed with age. Annealing produced initially a rapid increase of transmission that was followed by a slow, steady increase persisting over long periods of time. It was not feasible to wait for cessation of this latter effect; instead, the reflection loss was determined, always for the same standard frequency, at the start and at the end of each record made with the solid. The correction for reflection was applied as though its change had occurred linearly; because the increment was never more than a few units of percent this procedure was quite adequate.

Table I supplements Figs. 1 and 2 by showing for the band centers their locations on the frequency scale along with the corresponding measures of *absorption*. All data for liquid and solid were obtained with at least duplicate specimens. The locations of the band centers were reproduced in all cases within the precision afforded by our instrument; this varies somewhat with the dispersion of a prism but is in the neighborhood of a few tenths of one percent of the value given for the frequency. The measures of absorption have not been corrected for stray light traversing the spectrometer. The amount of stray radiation was determined for a few frequencies selected at random and was found to constitute about ten percent of the incident radiation with some variation from place to place. The effective correction should be slightly larger for solid than for liquid specimens owing to some unavoidable inhomogeneity* in the crystalline material. In all other respects the measures of absorption are believed to be reliable for purposes of comparison. They were reproducible for different specimens in the same cell within a few units of percent and, most im-

TABLE I. The locations and the measures of absorption for the band centers in the spectra for vapor, liquid, and solid.

Vapor $\tilde{\nu}$(cm^{-1})	Vapor A(%)	Liquid $\tilde{\nu}$(cm^{-1})	Liquid A(%)	Solid $\tilde{\nu}$(cm^{-1})	Solid A(%)	Type*
671	77	674	90	676	80	*U*
779	4	774	16	766	27	*U*
		849	16			*G*
		~ 980	<15	978	23	*U'*
		~1010	?	~1010	?	?
1032	55	1033	69	1037	56	*U*
		~1150	<10	1145	18	*U'*
		1175	25			*G*
1243	5	1247	8	1252	8	*U*
		1310	4	1309	12	*U'*
1385	13	1393	31	1396	41	*U, U'*
1483	82	1478	93	1485	85	*U*
~1526	<30	1530	42	1546	45	*U*
		1588	11			*G*
1615	4	1614	9	1616	8	*U*
1655	5	1650	3	1650	2	*U*
		1678	12	1686	8	*U*
		1712	3	1715	3	?
1755	5	1760	5	1764	9	*U*
1811	55	1822	64	1836	58	*U*
1880	3	1880	3	1890	4	*U*
1954	41	1965	41	1982	42	*U*
		2110	2	2110	3	?
2215	4	2210	6	2220	9	*U*
		2398	7	2400	11	*U'*
2620	3	2600	7	2600	4	*U*
		2690	7	2670	4	*U*
2880	10	≈2880	?	≈2880	?	*U*
		~2950	<30	~2950	<20	*U'*
3085	65	3065	74	3070	50	*U, G*

~ Indicates shoulder on adjacent band.
* See discussion.

* At 674 and 1480 the absorption is practically complete. At these locations the apparent transmissions are slightly greater for solid specimens than for liquid ones. The comparison permits one to judge the importance of this factor.

portant for the use we wish to make of them, fluctuations were uniform and parallel for both liquid and solid.

The intensities of absorption by vapor and liquid are comparable except in one respect. A spectrograph with limited resolving power, when viewing a sample of line absorptions, will average the transmissions through transparent regions with those through absorbing ones. If the breadth and spacing of the lines is altered, and this is undoubtedly the case upon passing from vapor to liquid, the averaged transmission will likewise be altered even though the true capacity for absorption remains unchanged. It is possible to correct[2] for this error, which could be a large one, but we have deemed it unnecessary to do so. Our present conclusions involving the vapor spectrum are derived solely from the presence or absence of a component there. Furthermore, there are some bands appearing in the spectra for all three states which are expected[3] to have only slightly greater intensities in the condensed phases and this expectation is realized with the uncorrected data. For example, the integrated intensities for the band near 1950 are, in round numbers, 1700 in the vapor and 2200 in the liquid; for the band near 1820 they are 2200 in the vapor and 2700 in the liquid. These changes of approximately twenty percent in each case are not excessive and accordingly we believe that the intensities we have observed for the two states are comparable for our purposes without correction.

The fundamental molecular frequencies of benzene, with one exception, are believed generally to fall within the range we have been discussing. Indirect evidence[5] supports the notion that the exception lies in the vicinity of 400 wave numbers. For sake of completeness we attempted to examine this region. A specimen of liquid was confined in a cell, similar otherwise to the ones we have described but constructed from KBr. The low intensity available from our source forced us to employ an exceptional gain in the amplifier and to work without the cooler in order to attain a maximum aperture. For the former reason, motions in the galvanometer suspension introduced an unusual amount of uncertainty into the results. Furthermore, the results were complicated by a comparatively high proportion of stray radiation. Subject to these reservations, no absorption could be detected in the range from 380 to 450 wave numbers. We conclude that, if our specimen possessed an absorption band in this range, the associated intensity did not exceed fifteen percent. The extremely unfavorable conditions (smaller aperture, losses by reflection) that would attend examination of a solid specimen caused us to abandon the project.

The infra-red spectra of both vapor and liquid have been subjects for a number of prior investigations. Some of these were compared and discussed by Ingold[6] *et al.*; others[7] have been reported subsequently. When allowances are made for the varying resolving powers of different instruments and the influence of sample thickness upon resolution, no noteworthy discrepancies can be detected among the results, including our own, of recent studies with the liquid. We wish to emphasize particularly that the spectrum[8] reported for a highly purified specimen of liquid benzene, NBS Standard 99.95±0.02 mole percent, is virtually identical with the one observed by us. Each spectrum contains two or three extremely weak components, all located above 1600 wave numbers, that do not appear in the other but these are the only respects in which they differ significantly. We conclude therefore that our own specimen was spectroscopically pure; it would also be rated pure if judged[9,10] by other criteria. Different observers are not so well agreed concerning the spectrum of the vapor. Ingold *et al.* have reported weak components at 779, 807, 962, 1143, and 1240, all but one having counterparts in the spectrum of the liquid. We have found the first and last ones without difficulty but have been unable to detect any traces of the others in spite of careful searching.

[5] R. C. Lord, Jr. and D. H. Andrews, J. Phys. Chem. **41**, 149 (1937).

[6] C. R. Bailey, J. B. Hale, C. K. Ingold, and J. W. Thompson, J. Chem. Soc. 931 (1936).

[7] A. P. I. Research Project No. 44, Spectrograms No. 122 and 307, available at National Bureau of Standards, Washington, D. C.

[8] Reference 7, Spectrogram No. 307 contributed by U. S. Naval Research Laboratory, Washington, D. C.

[9] F. S. Fawcett and H. E. Rasmussen, J. Am. Chem. Soc. **67**, 1705 (1945).

[10] G. N. Lewis and M. Kasha, J. Am. Chem. Soc. **66**, 2100 (1944).

The spectrogram[11] reported for a vapor specimen of high purity, API-NBS Standard 99.94±0.03 mole percent, shows only the first one among the list of components; however, the last one falls in a narrow region where, judging from the description provided by the Bureau of Standards, the otherwise powerful instrument employed is comparatively impotent. In our own studies the band at 1240 would escape notice with the rock-salt prism but could not be overlooked with the fluorite prism. The latter prism was used also by us in our unsuccessful search for a band at 1143. We hold no reservations concerning our conclusion that the spectrum of benzene vapor contains weak components near 780 and 1240 but no others in the intermediate range. There are other discrepancies in addition to the ones already noted; however, the only doubtful components in our list are weak ones at 1655 and 1880. Neither of these is likely to have any important role in the interpretation of the data as a whole and so we shall not offer further comments. We believe that ours is the first comprehensive study of the infra-red spectrum for solid benzene.

DISCUSSION

Theoretical principles appropriate for the interpretation of spectra observed with condensed systems were developed in the first paper[3] of this series. In brief, selection rules, usually less strict than the ones governing the vapor spectrum, will operate in the crystalline phase; these are predictable from suitable knowledge of the crystal structure. No selection rules will operate in the liquid state. It is to be expected then that the spectrum for the crystal will be richer than the one for the vapor and that the one for the liquid may be richer still. A glance at the distribution of entries in Table I confirms that this expectation is realized in the case of benzene. Furthermore, the relaxation of selection rules is associated with the development of intermolecular forces; the absorptions that are peculiar to the condensed phases depend for their intensities upon these interactions. Intermolecular forces are more powerful and more concentrated in the crystal than in the liquid; consequently, the components that are added by these forces commonly to the spectra of both states are likely to be more intense in the spectrum for the crystal. On the other hand, intermolecular forces are much weaker than intramolecular ones. Components of the vapor spectrum derive their intensities from the latter source. Therefore these are likely to be the most intense components in the spectra for all three states and, unless they are feeble in the spectrum for the vapor, their intensities should be altered less by changes of state. These predictions are well fulfilled by the data for benzene.

A knowledge of the selection rules for vapor and crystal is prerequisite for further discussion of the spectra. The thirty fundamental modes of vibration in an isolated benzene molecule, presumed to have the point symmetry D_{6h}, will produce twenty distinct frequencies. These are distributed[12] among the irreducible representations of D_{6h} in the pattern: $2A_{1g}$, A_{2g}, $2B_{2g}$, $4E_{2g}$, E_{1g}, A_{2u}, $2B_{1u}$, $2B_{2u}$, $2E_{2u}$, and $3E_{1u}$. Motions associated with A_{1g}, E_{1g}, and E_{2g} will contribute to the Raman spectrum, those associated with A_{2u} and E_{1u} to the infra-red spectrum. All other representations are inactive in both spectra and the two types of spectra are mutually exclusive.

Crystalline benzene is an example of the space group $\mathbf{V}_h^{15}$ with four molecules per unit cell. This information suffices[3] to show that in the crystal the molecules of benzene occupy sites having the symmetries C_i. The components of the spectrum for the crystal can be correlated with the modes of motion of one of its molecules; these are associated with the two irreducible representations A_g and A_u of the site group C_i. The representation A_g receives the lattice modes of rotatory origin and the fifteen molecular modes associated with the *gerade* representations of D_{6h}; A_u receives the lattice modes of translatory origin and the fifteen molecular modes associated with the *ungerade* representations of D_{6h}. The modes associated with A_g contribute to the Raman spectrum, those with A_u to the infra-red spectrum; the two types of spectra continue to be mutually exclusive. In principle the fifteen molecular modes in each representation will pro-

[11] Reference 7, Spectrogram No. 122 contributed by The Texas Company, Beacon, New York.

[12] E. B. Wilson, Jr., Phys. Rev. **45**, 706 (1934).

duce fifteen distinct frequencies owing to the removal by intermolecular forces of degeneracies that prevail in the isolated molecule; in practice the resulting doublets will probably not be resolved and only ten frequencies will need to be considered.

All twenty resoluble fundamental frequencies can contribute to both types of spectra for the liquid. However, even though the two types of spectra are no longer mutually exclusive for this state, they will doubtless present contrasting intensity patterns.

The foregoing considerations suggest the utility of designating three types of components that may be encountered in the infra-red spectra for benzene in the three different states. Components of type U derive from the representations A_{2u} and E_{1u} of D_{6h}; they will appear in the infra-red spectra for all three states and will usually show comparatively little intensification accompanying a change of state. Those of type U' will appear in the infra-red spectra for both condensed states but not in the spectrum for the vapor and will show comparatively great intensification accompanying solidification; they derive from the other *ungerade* representations of D_{6h}. Components of type G will appear in the infra-red spectrum for the liquid state only; they derive from the *gerade* representations of D_{6h}. The last type can be subdivided when discussing Raman spectra but the distinctions are without value except when implemented by more data than are now available. From the experimental point of view the distinction between types U and U' is not completely sharp since feeble components of the former type, if overlooked in the spectrum of the vapor, could be mistaken for ones of the latter type. However, it is to be hoped that the exceptions will not be too numerous. With this reservation the components observed by us have been classified according to types as shown in the last column of Table I.

Perhaps the most striking features that emerge from even a casual comparison of the spectra for the three states are the absorptions shown by the liquid, but not by either vapor or solid, in the vicinities of 849, 1175, and 1588. A thorough scrutiny of the figures shows that a similar pattern of behavior is exhibited also in the vicinities of 990 and 3060, accounting in the first instance for the improved resolution achieved between the bands at 978 and 1037 in the spectrum of the solid and in the second instance for the unusual loss of intensity that accompanies solidification. The conclusions developed in the preceding paragraphs require unequivocally that these five locations must be associated with components of type G. The opportunity presents itself now to conduct a rather exacting test of the validity of our theoretical considerations. Potential components of type G will include the most prominent contributors to the Raman spectrum of liquid benzene. The latter are found[13] at 606, 850, 992, 1178, 1586, 1604, 3048, and 3062 and account for all five of our locations. The result of this test is a spectacular success for the theory, showing in particular that the selection rules deduced for the crystal are indeed obeyed strictly and that there are no selection rules operating in the liquid phase. It is apparently true for benzene, and perhaps in general too, that prominent components in one type of spectrum are especially prone to enter the other type of spectrum whenever permitted to do so by relaxation of the selection rules. This empiricism is supported not only by the cases already cited but also by the apparent entry[13] of components of type U into the Raman spectrum for the liquid.

All components observed in the spectrum of the vapor can be assigned to type U without further comment. The remaining bands, excluding those of type G, cannot be classified with the same degree of certainty. We have assigned them regularly to type U' except for the ones that failed to intensify upon solidification. Among the latter cases the shoulder near 2950 is almost certainly of type U' but its intensification is obscured by the behavior of the neighboring component of type G; the bands at 1678 and 2690 are assigned to type U because we can be certain in these instances that they are not intensified by the change of state; the others are too weak to justify any assignment and these have been left unclassified. Finally, we have indicated our belief that the component in the vicinity of 1390 may contain contributions of

[13] N. R. Angus, C. K. Ingold, and A. H. Leckie, J. Chem. Soc. 925 (1936).

both types since the degree of its intensification by the changes of state seems somewhat unusual.

Almost all of the entries listed in Table I are shifted toward higher frequencies by the successive stages of condensation. However, even the most pronounced shift is not much greater than one percent of the value of the mean frequency. This is comparable with the error, deduced from applications of the product rule to the spectra[14] of benzene and its deuterated derivatives, that results commonly from the assumption that the vibrations in the isolated molecule are harmonic. Also, the two errors are in opposed directions and tend to compensate. Therefore, shifts of frequency induced in molecular vibrations of benzene by intermolecular forces may be ignored to the degree of approximation that the motions of the isolated molecule are considered to be harmonic ones. Evidently the molecular vibrations retain their individualities in the condensed phases to a very high degree.

The resolving power of our instrument is apparently inadequate to exhibit the branched structure expected in the band envelopes for the vapor. Consequently we have been unable to explore the status of molecular rotation in the condensed phases. The most fruitful objects for such a study would be the prominent bands of type *U* for which the structure is interpretable in the spectrum of the vapor. The basis for interpreting intensities in terms of intermolecular forces is insufficiently developed to permit of any conclusions. It is obvious, however, that such studies will be most productive when directed toward the components of types *G* and *U'* in the condensed phases.

[14] A. Langseth and R. C. Lord, Jr., Kgl. Danske Vid. Sels., Math.-Fys. Medd. [6] **16**, 1 (1938).

FUNDAMENTAL MOLECULAR FREQUENCIES

Although it is incidental to our main purpose, we are aware that the new data reported here are capable, when properly interpreted, of contributing significantly to the identification of the fundamental frequencies of vibration in the benzene molecule. For example, our results invalidate, in one respect or another, all of the recently offered[14–16] attempts to achieve a complete assignment of fundamental frequencies.

[15] W. R. Angus, C. R. Bailey, J. B. Hale, C. K. Ingold, A. H. Leckie, C. G. Raisin, J. W. Thompson, and C. L. Wilson, J. Chem. Soc. 971 (1936).

[16] K. S. Pitzer and D. W. Scott, J. Am. Chem. Soc. **65**, 803 (1943).

Heat-Capacity Lag in Gas Dynamics*,[1]

ARTHUR KANTROWITZ
National Advisory Committee for Aeronautics, Langley Field, Virginia
(Received December 17, 1945)

The existence of energy dissipations in gas dynamics, which must be attributed to a lag in the vibrational heat capacity of the gas, has been established both theoretically and experimentally. The flow about a very small impact tube is discussed. It is shown that total-head defects due to heat-capacity lag during and after the compression of the gas at the nose of an impact tube are to be anticipated. Experiments quantitatively verifying these anticipations in carbon dioxide are discussed. A general theory of the dissipations in a more general flow problem is developed and applied to some special cases. It is pointed out that energy dissipations due to this effect are to be anticipated in turbines. Dissipations of this kind might also introduce errors in cases in which the flow of one gas is used in an attempt to simulate the flow of another gas. Unfortunately, the relaxation times of most of the gases of engineering importance have not been studied. A new method of measuring the relaxation time of gases is introduced in which the total-head defects observed with a specially shaped impact tube are compared with theoretical considerations. A parameter is thus evaluated in which the only unknown quantity is the relaxation time of the gas. This method has been applied to carbon dioxide and has given consistent results for two impact tubes at a variety of gas velocities.

INTRODUCTION

THE possibility of dispersion and absorption of sound due to parts of the heat capacity lagging behind the rapid temperature changes accompanying the propagation of a sound wave in a gas was first discussed theoretically by Jeans and Einstein. Dispersion and absorption in carbon dioxide observed by Pierce were shown by Herzfeld and Rice to be attributable to lagging of the vibrational heat capacity of the gas. Kneser was able to account quantitatively for dispersion and absorption in CO_2 and oxygen on the assumption that the vibrational heat capacity lagged.

The dispersion and absorption of sound in several gases have been investigated and a fairly complete bibliography is available in Richards' paper.[2] It is found, in general, that dispersion and absorption many times larger than those attributable to viscosity and heat conduction are to be expected in gases with vibrational heat capacity. These effects can be described by relations such as those given by Kneser and can be attributed to the vibrational heat capacity of the gas.

All the measurements of dispersion and absorption have demonstrated that most impurities markedly reduce the relaxation time of a gas; for example, Kneser[3] and Knudsen[4] concluded that the adjustment of the vibrational heat capacity of oxygen was dependent entirely on the action of impurities. Various experiments with CO_2 have shown that, at room temperature, collisions with water molecules are 500 times as effective as collisions with CO_2 molecules in exciting vibration in CO_2 molecules. This strong dependence on purity has produced great discrepancies among the relaxation times measured by the various workers in this field. There has been much better agreement among the measurements of the effectiveness of impurities. Sonic measurements in CO_2 are discussed in appendix A. A quantum-mechanical theory of relaxation times developed by Landau and Teller is discussed in appendix B. Two conclusions, which are verified by the sonic work in CO_2, are important to the present subject: (1) All the vibrational states of a single normal mode adjust with the same relaxation time and (2) the logarithm of the relaxation time (expressed in molecular collisions) is proportional

* Submitted in partial fulfillment of the requirements for the degree of Doctor of Philosophy at Columbia University. Publication assisted by the Ernest Kempton Adams Fund for Physical Research of Columbia University.

[1] This work was done at the Langley Memorial Aeronautical Laboratory of the National Advisory Committee for Aeronautics. A somewhat more complete version was first published as an advance restricted report No. 4A22 by the NACA. The restriction has since been removed, and the author is grateful to the NACA for permission to publish this report.

[2] W. T. Richards, Rev. Mod. Phys. **11**, 36–64 (1939).

[3] H. O. Kneser, J. Acous. Soc. Am. **5**, 122–126 (1939).

[4] V. O. Knudsen, J. Acous. Soc. Am. **5**, 112–121 (1933).

to $T^{-\frac{1}{2}}$. Verification of conclusion (2) is presented in Fig. 6.

EFFECTS IN GAS DYNAMICS

In the flow of gases about obstacles, compressions and rarefactions accompanied by temperature changes occur. The time in which these temperature changes take place is controlled by the dimensions of the obstacles and the velocity of flow. If these time intervals are comparable with or shorter than the time required for the gas to absorb its full heat capacity, the gas will depart from its equilibrium partition of energy. In this case, the transfer of energy from parts of the heat capacity that have more than their share to parts that have less than their share will be an irreversible process and will increase the entropy of the gas. If the time intervals involved are comparable with the relaxation time of the gas, this increase in entropy can be used to measure the relaxation time of the gas.[5]

Turbine-working fluids such as steam, air, and exhaust gas have appreciable vibrational heat capacity at high temperatures. If these gases have relaxation times comparable with or shorter than the intervals during which temperature changes occur in the gas, losses attributable to heat-capacity lag must be anticipated. A rough estimate has indicated that, unless the relaxation times of the working fluids are very short, the losses at high temperatures due to heat-capacity lag can be comparable with the losses due to skin friction. Unfortunately, no measurements of the relaxation times of the usual turbine-working fluids exist.

Various persons have proposed, in wind-tunnel tests and in tests of rotating machinery, the substitution of gases that have properties enabling tests to be made more conveniently at a given Mach number or Reynolds number than with the actual working fluid. In such cases, care must be taken to ensure that an error due to differences in heat-capacity lag behavior of the fluid used and the working fluid is not introduced. For example, according to a rough calculation, a wing in pure CO_2 might have a drag coefficient twice as large as the same wing in air at the same Mach number and Reynolds number.

[5] A. R. Kantrowitz, "Letter to the Editor," J. Chem. Phys. **10**, 145 (1942).

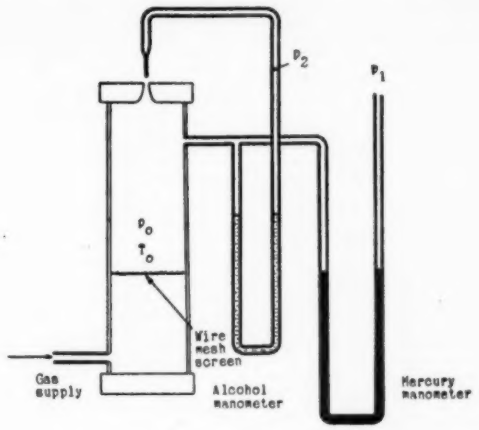

FIG. 1. Schematized experimental arrangement. The gas enters the chamber and flows through the fine mesh screen, which reduces the turbulence of the flow, then out the faired orifice impinging on the impact tube. It is found that, in gases with no vibrational heat capacity, it is possible by reducing the turbulence in the chamber and correctly aligning the impact tube with the flow to reduce the reading of the alcohol manometer to zero. When this adjustment is made, this apparatus provides a sensitive method of measuring any internal irreversibility in the expansion or compression of the gas. The provision of a small orifice at the point where the gas enters the chamber helps to make the manometer readings steady. The screen should be 100 or 200 mesh or can be replaced by a wad of tightly packed steel or glass wool. (See Fig. 5.)

In the following discussion, the existence of these dissipations in gas dynamics is demonstrated and a gas-dynamics method of measuring the relaxation times is developed. The application of this method to the measurement of the relaxation times of gases of engineering importance is proposed.

FLOW ABOUT A VERY SMALL IMPACT TUBE

As a first example of the energy dissipations to be expected from heat-capacity lag, consider the total head measured by an impact tube in a perfect gas. For definiteness, consider the apparatus illustrated schematically in Fig. 1. The gas enters the chamber and settles at the pressure p_0 and the temperature T_0. It then expands to a pressure p_1 and a temperature T_1 out of the faired orifice, which is designed to give a temperature drop gradual enough that the expansion through the orifice is isentropic. The gas that flows along the axial streamline of the impact tube is then brought to rest at the nose of the tube and, during this process, its pressure rises to p_2 and its temperature rises to T_2. If this second process is slow

enough to be isentropic also, the entropy and the energy of the gas that has reached equilibrium at the nose of the impact tube are equal to the values in the chamber and hence the pressure p_2 equals p_0 and the reading on the alcohol manometer is zero.

Consider, however, the other extreme case in which the compression time—that is, the time required for the gas to undergo the greater part of its temperature rise at the nose of the impact tube—is small compared with the time required for the gas to absorb its full heat capacity. The orifice is considered large enough that, during the expansion through it, the gas maintains equilibrium. A part of the heat capacity of the gas c_{vib} does not follow the rise in temperature during the compression as the gas is brought to rest at the nose of the impact tube and comes to equilibrium irreversibly after the compression is over. The resultant increase of entropy in this case means that the pressure p_2 is lower than p_0. We shall now calculate this increase in entropy. All temperature changes are assumed small enough that the heat capacities of the gas can be taken as constants.

At the beginning of the adjustment, the lagging part of the heat capacity c_{vib} is still in equilibrium with a thermometer at the temperature T_1 while the translational and other degrees of freedom with heat capacities totaling c_p', the relaxation time of which can be neglected, are in equilibrium with a thermometer at some higher temperature T. Energy then flows from the heat capacity c_p' to the heat capacity c_{vib}, increasing the temperature T_{vib} associated with c_{vib} from T_1 to the final equilibrium temperature, which is T_0. Conservation of energy gives the following relation between T and T_{vib}:

$$c_{\text{vib}}T_{\text{vib}}+c_p'T=c_pT_0, \tag{1}$$

where c_p is the total heat capacity at constant pressure. The entropy increase when an element of energy dq flows from T to T_{vib} is

$$dS=\frac{dq}{T_{\text{vib}}}-\frac{dq}{T}=c_{\text{vib}}dT_{\text{vib}}\left(\frac{1}{T_{\text{vib}}}-\frac{1}{T}\right). \tag{2}$$

Eliminating T in Eq. (2) from Eq. (1) and integrating over the whole process gives

$$\Delta S=\int_{T_1}^{T_0}c_{\text{vib}}dT_{\text{vib}}\left(\frac{-c_p'}{c_pT_0-c_{\text{vib}}T_{\text{vib}}}+\frac{1}{T_{\text{vib}}}\right),$$

$$=\log\left[\frac{\dfrac{c_p}{c_{\text{vib}}}-1}{\dfrac{c_p}{c_{\text{vib}}}-\dfrac{T_1}{T_0}}\right]^{c_p'}\left(\frac{T_0}{T_1}\right)^{c_{\text{vib}}}. \tag{3}$$

Equation (3) gives the entropy difference between the gas in the chamber and the gas at equilibrium at the nose of the impact tube. Because the energy and hence the temperature is the same at the beginning and at the end of the process, the ratio of chamber pressure to impact-tube pressure can readily be computed from the perfect gas relation

$$S=c_p\log T-R\log p+\text{Constant},$$

which gives

$$\Delta S=R\log(p_0/p_2)$$

and

$$\frac{p_0}{p_2}=\left[\frac{\dfrac{c_p}{c_{\text{vib}}}-1}{\dfrac{c_p}{c_{\text{vib}}}-\dfrac{T_1}{T_0}}\right]^{c_p'/R}\left(\frac{T_0}{T_1}\right)^{c_{\text{vib}}/R}. \tag{4}$$

It may be instructive to derive this relation by considering the isentropic parts of the process. During the slow expansion, the enthalpy theorem* gives $c_pT+u^2/2=\text{Constant}$ (u is flow velocity) and, during the instantaneous compression, $c_p'T+u^2/2=\text{Constant}$, c_{vib} being omitted because it takes no part in the compression. Com-

* If no energy is transmitted across the walls of a stream tube, the total energy (internal energy E plus kinetic energy per unit mass $u^2/2$) plus the work done by pressures pV must be the same at any cross section of the tube; that is,

$$E+\tfrac{1}{2}u^2+pV=\text{Constant}. \tag{a}$$

In the case of a perfect gas with constant heat capacity and with equilibrium partition of energy, Eq. (a) becomes

$$c_pT+\tfrac{1}{2}u^2=\text{Constant}, \tag{b}$$

where c_p is the heat capacity at constant pressure and T is the absolute temperature. Whenever equilibrium partition exists, even though non-equilibrium states have been passed through, Eq. (a) is applicable in the absence of viscosity and heat conduction and Eq. (b) can be applied to perfect gases, provided the heat capacity of the gas can be considered constant.

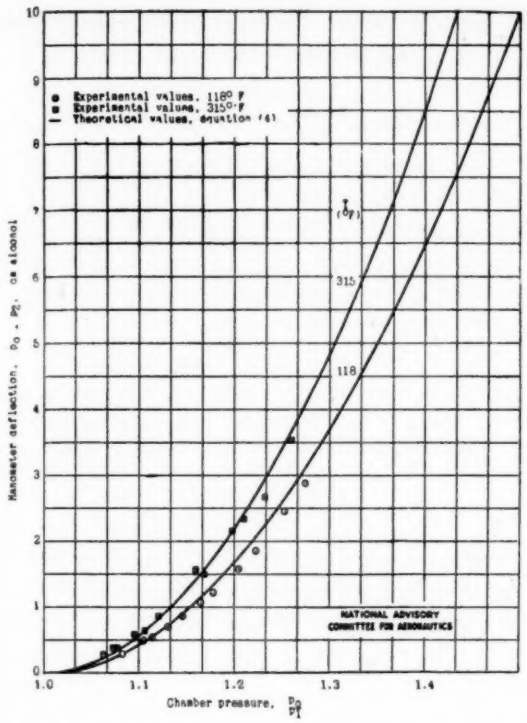

FIG. 2. Total-head defects measured using CO_2 with the apparatus schematized in Fig. 1. The orifice is $\frac{1}{2}$ inch thick and the impact tube is .005 inch in diameter, which meant that the expansion was slow and the compression fast compared to the relaxation time of the gas. The theoretical values were obtained by assuming the expansion to be reversible and the compression to be instantaneous.

bining these equations gives

$$c_p(T_0-T_1)=c_p'(T_2-T_1), \qquad (5)$$

where T_2 is the temperature reached by the translational degrees of freedom before the adjustment period starts. The adiabatic-compression relation can be applied to both the expansion and the compression with the appropriate heat capacities to calculate p_2; thus,

$$\left(\frac{p_2}{p_1}\right)^{R/c_p'}=\frac{T_2}{T_1}; \quad \left(\frac{p_0}{p_1}\right)^{R/c_p}=\frac{T_0}{T_1}. \qquad (6)$$

Combining Eqs. (5) and (6) gives, after several manipulations, a result identical with Eq. (4).

The apparatus schematized in Fig. 1 was used to check Eq. (4) for CO_2 where the vibrational heat capacity would be expected to lag. The orifice was a hole in a $\frac{1}{2}$-inch plate with its diameter variation designed for constant time rate of temperature drop. The last $\frac{1}{16}$ inch of the flow passage was straight in order that the streamlines in the jet would be straight and axial and hence the static pressure at the orifice exit would equal atmospheric pressure. The glass impact tube was 0.005 inch in diameter, and its end was ground square on a razor hone. The chamber pressures used were such that the gas velocities at the orifice exit were between 300 and 600 feet per second. The expansion therefore took place in times ranging between 1.4×10^{-4} and 2.8×10^{-4} second. The compression at the nose of an impact tube takes place while the gas flows a distance of the order of 1-tube radius. The compression times then ranged between 7×10^{-7} and 14×10^{-7} second. Commercial CO_2 was used and, because it was fairly dry, a relaxation time of the order of 10^{-5} second was expected. It seemed likely, therefore, that this set-up would approach the case of an isentropic expansion and an instantaneous compression closely enough for the results to bear at least a qualitative resemblance to Eq. (4).

Preliminary to the investigation of heat-capacity lags, it was necessary to make sure that hydrodynamic effects other than heat-capacity lag would not produce a reading on the alcohol manometer. Air and, later, nitrogen at room temperature were therefore substituted for CO_2 at the beginning of each run. It was always found in these preliminary tests that, when the tube was properly aligned, the difference in pressure measured by the alcohol manometer was very small and could be accounted for entirely by lags in the small vibrational heat capacity of air (about 0.02R).

Carbon dioxide was then introduced into the apparatus and the observations shown in Fig. 2 were made. The gas was heated before entering the chamber, and its temperature was measured by a small thermocouple inserted in the jet close to the impact tube. In accordance with aerodynamic experience, the temperature measured by the thermocouple was assumed to be $0.9T_0+0.1T_1$. The difference between T_0 and T_1 was always less than 30°F, corresponding to a difference in c_{vib} of less than 8 percent, and was thus considered accurate enough to assume a constant c_{vib} and to compute this value at a temperature $\bar{T}=(T_0+T_1)/2$.

The pressure p_0-p_1 was read by the mercury manometer, p_1 by a barometer, and p_0-p_2 by the

alcohol manometer, which was fitted with a microscope to make possible readings to 0.001 inch.

In Fig. 2, the reading of the alcohol manometer is plotted against the chamber pressure p_0/p_1. The experimental values at both temperatures agree with the theoretical values more closely than could have been anticipated. It will become clear later that the theoretical and experimental values agreed so closely because small entropy increases in the orifice, attributable to too-rapid expansion, just about compensated for the fact that the compression was not quite instantaneous compared with the relaxation time of the gas. It should be pointed out that ordinary hydrodynamic effects such as misalignment of the impact tube would be expected to produce a total-head defect which would vary directly as p_0/p_1-1.

GENERAL THEORY OF ENERGY DISSIPATIONS IN GASES EXHIBITING HEAT-CAPACITY LAG

In the general case in which the temperature changes may be neither very fast nor very slow compared with the relaxation time of the gas, the temperature history of a gas particle as it flows along a streamline must be considered. The problem is greatly simplified if the effect of heat-capacity lag on velocity distribution is neglected in order to get the effect of the lag on energy dissipation. This procedure can be regarded as the first step in an iteration process and is probably adequate for the applications now contemplated. We shall also retain the restriction that the temperature changes involved in the flow are small enough for the heat capacities to be considered constant.

Assume, therefore, that the velocity distribution in the field of flow is determined by standard gas-dynamics methods. The velocity distribution is usually given as a function of space coordinates $u(x, y, z)$ or along the σ streamline as $u_\sigma(s)$, where s is the distance along the streamline. This expression can be converted to a function of time $u_\sigma(t)$ by integration of $dt=ds/u(s)$ along a streamline. The function $u_\sigma(t)$ is taken for granted and the entropy increase in the flow along a streamline is determined.

By introducing the variable ϵ, which represents the excess energy per unit mass in the lagging heat capacity over the energy at equilibrium partition at the translational temperature T, it is seen that

$$c_pT+\tfrac{1}{2}u^2+\epsilon=\text{Constant}. \tag{7}$$

The assumption is now introduced that there is only one type of heat energy in the gas E_{vib} which lags appreciably behind the translational temperature and that its time rate of adjustment is proportional to its departure from equilibrium; that is,

$$dE_{\text{vib}}/dt=-k\epsilon.$$

This assumption is in agreement with the sonic theories previously discussed. From the definition of ϵ,

$$\epsilon=E_{\text{vib}}-c_{\text{vib}}T,$$

because $c_{\text{vib}}T_{\text{vib}}$ is the equilibrium value of E_{vib} (measured from an arbitrary zero). By combining these equations, E_{vib} can be eliminated to yield

$$\frac{d\epsilon}{dt}=-c_{\text{vib}}\frac{dT}{dt}-k\epsilon. \tag{8}$$

The meaning of k can be made clear if the variation of ϵ with time is examined for the case in which the total heat energy of the gas remains constant. In this case,

$$c_pT+\epsilon=\text{Constant}.$$

Eq. (8) then becomes

$$\frac{d\epsilon}{dt}=\frac{c_{\text{vib}}}{c_p}\frac{d\epsilon}{dt}-k\epsilon$$

or

$$\frac{d\epsilon}{dt}=-k\frac{c_p}{c_p'}\epsilon,$$

from which kc_p/c_p' is the reciprocal of the relaxation time τ of the gas. It will be seen that these equations are restricted to gases with only one relaxation time.

In order to simplify later expressions and to clarify their physical meaning, we introduce the dimensionless variables

$$\left.\begin{aligned}\epsilon'&=\epsilon\Big/\frac{c_{\text{vib}}}{c_p'}\frac{U^2}{2} & t'&=\frac{t}{h/U}\\ u'&=u/U & K&=h/\tau U\end{aligned}\right\}, \tag{9}$$

where h and U are a typical length and a typical

velocity in the flow and K is a dimensionless parameter that is a measure of the ratio of the times in which temperature changes occur in the gas to the relaxation time of the gas. It will be seen later that ϵ' is defined to make it become unity after an instantaneous expansion which starts from rest with equilibrium energy partition and ends with the velocity U. Eliminating T between Eqs. (7) and (8) and introducing the non-dimensional quantities gives

$$\frac{d\epsilon'}{dt'}+K\epsilon'=\frac{du'^2}{dt'}. \tag{10}$$

If $u'(t')$ is known, the integral of Eq. (10) can be written as

$$\epsilon'=e^{-\int K dt'}\left(\int \frac{du'^2}{dt'}e^{\int K dt'}dt'+\text{Constant}\right). \tag{11}$$

The rate of entropy increase in the flow can now be calculated from Eq. (11). The rate of heat flow from the temperature T_{vib} to T is $k\epsilon$; hence,

$$\frac{dS}{dt}=k\epsilon\left(\frac{1}{T}-\frac{1}{T_{\text{vib}}}\right). \tag{12}$$

Now $\epsilon=c_{\text{vib}}(T_{\text{vib}}-T)$ and Eq. (12) can be written as

$$\frac{dS}{dt}=k\epsilon\left(\frac{1}{T}-\frac{1}{T+(\epsilon/c_{\text{vib}})}\right).$$

The entropy increase along the streamline in question between the starting time t_0 and the time t is

$$\Delta S=\int_{t_0}^{t} k\epsilon\left(\frac{1}{T}-\frac{1}{T+(\epsilon/c_{\text{vib}})}\right)dt. \tag{13}$$

In order to obtain the total entropy increase, Eq. (13) would have to be integrated over all the streamlines in the flow with the use of Eq. (7).

Similarity Law for Low Velocity Flows

The calculation of energy dissipations can be simplified if the restriction to flows involving pressure and temperature changes that are small compared with ambient pressure and temperature is adopted. The greatest advantage of this procedure is that the flow pattern obtained in an incompressible fluid can be used as an approximation. This fact is important because few compressible fluid flows are known accurately. If this restriction is accepted, k and hence K can be assumed constant for the flow. Equation (11) then becomes

$$\epsilon'=\exp(-Kt')\times\left(\int \frac{du'^2}{dt'}\exp(Kt')dt'+\text{Constant}\right). \tag{14}$$

Now both ϵ/c_{vib} and variations of T are small compared with T and Eq. (13) becomes

$$\Delta S=\frac{k}{c_{\text{vib}}\bar{T}^2}\int_{t_0}^{t}\epsilon^2 dt. \tag{15}$$

We can now show that there is a simple relation among the dependencies of the energy dissipation in a low velocity flow on the scale of the flow, on the typical velocity, and on the relaxation time of the gas. This relation is that the entropy increase, reduced to non-dimensional form, depends in geometrically similar flows on a single parameter K.

Equation (15) can be rewritten as

$$\Delta S=\frac{c_p' K}{c_p c_{\text{vib}}\bar{T}^2}\left(\frac{U^2}{2}\frac{c_{\text{vib}}}{c_p'}\right)^2\int_{t_0'}^{t'}\epsilon'^2 dt'.$$

Introducing the non-dimensional entropy increase $\Delta S'$ by dividing ΔS by the entropy increase following an "instantaneous" compression gives

$$\Delta S'=2K\int_{t_0'}^{t'}\epsilon'^2 dt'. \tag{16}$$

From Eq. (14), it is known that ϵ' and hence from Eq. (16) $\Delta S'$ depends only on K for similar flows.

Approximations for Large and Small Values of K

The integrations of Eqs. (14) and (16) are sometimes difficult to perform analytically and laborious to evaluate numerically. For the special cases in which the relaxation time is either long or short compared with the times in which temperature changes take place in the gas, it is possible to use approximations that considerably reduce the numerical labor. In these cases, it is possible to express $\Delta S'$ in terms of integrals in which K does

not appear under the integral sign; thus, these integrals need be evaluated only once to determine $\Delta S'$ for all values of K for which the approximation is valid.

The case of short relaxation time, when K is large, will be treated first. In order to avoid confusion, the symbol t_a' is introduced into Eq. (14), which becomes

$$\epsilon'(t_a') = \int_{t_0'}^{t_a'} \frac{du'^2}{dt'} \exp\left[-K(t_a'-t')\right]dt'. \quad (17)$$

For a large value of K, most of the contribution to this integral comes from values of t' so close to t_a' that the following approximations can be made:

$$\frac{du'^2}{dt'} = \left(\frac{du'^2}{dt'}\right)_a; \quad t'-t_a' = \frac{u'^2-u_a'^2}{\left(\frac{du'^2}{dt'}\right)_a},$$

and the lower limit of the integral in Eq. (17) can be replaced by $\pm\infty$. Equation (17) then becomes

$$\epsilon'(t_a') = \int_{\pm\infty}^{u_a'^2} \exp\left[\frac{K}{\left(\frac{du'^2}{dt'}\right)_a}(u'^2-u_a'^2)\right]du'^2,$$

where the sign of the lower limit is opposite that of $(du'^2/dt')_a$. Hence for $K \gg 1$,

$$\epsilon'(t_a') = \frac{1}{K}\left(\frac{du'^2}{dt'}\right)_a; \quad \Delta S' = \frac{2}{K}\int\left(\frac{du'^2}{dt'}\right)^2 dt'. \quad (18)$$

The case of long relaxation time, when K is small compared with 1, will now be considered. In the usual flow problem, the gas velocity changes appreciably during a certain time interval—say, from 0 to t_1'—and then settles to a new steady value. The problem can be divided into two parts: $0<t'<t_1'$ and $t'>t_1'$. If K is small enough, the change in ϵ' due to the ϵ' term in Eq. (10) is small compared with the change due to the du'^2/dt' term and can be neglected in the calculation of the entropy increase $\Delta S_1'$ during the first interval; thus,

$$\epsilon' = u'^2 - u_0'^2,$$

where $u_0'^2$ is the velocity squared at $t'=0$. Hence,

$$\Delta S_1' = 2K\int_0^{t_1'} \epsilon'^2 dt' = 2K\int_0^{t_1'} (u'^2-u_0'^2)^2 dt'.$$

In order to compute the value of ϵ' at t_1', the total contribution of the ϵ' term in Eq. (10) is added to the total change in the square of the velocity during the first interval $\Delta u'^2$. Thus,

$$\epsilon_1' = \Delta u'^2 - K\int_0^{t_1'} \epsilon' dt' = \Delta u'^2 - K\int_0^{t_1'} (u'^2-u_0'^2)dt'.$$

In the period after t_1',

$$\epsilon' = \epsilon_1' \exp\left[-K(t'-t_1')\right],$$

and the entropy increase in this second period $\Delta S_2'$ is

$$\Delta S_2' = 2K\epsilon_1'^2\int_{t_1'}^{\infty} \exp\left[-2K(t'-t_1')\right]dt' = \epsilon_1'^2.$$

The total entropy increase in the flow is therefore, for $K \ll 1$,

$$\Delta S' = 2K\int_0^{t_1'} (u_0'^2-u'^2)^2 dt' + \left[K\int_0^{t_1'} (u_0'^2-u'^2)dt' + \Delta u'^2\right]^2.$$

Calculation of Total-Head Defect in Flow about a "Source-Shaped" Impact Tube

The total-head defect to be anticipated in a compression at the nose of an impact tube of a special shape is calculated to be used in the measurement of the relaxation time of gases. The restriction to low velocities adopted previously is retained, chiefly to permit the use of incompressible-fluid theory and of the similarity theorem.

The flow about bodies of revolution in a uniform stream is usually calculated by considering the flow about sources in the fluid.[6] It is possible to find a surface in the flow across which no fluid flows. If a solid body shaped like this surface is substituted for the sources, no alteration outside

[6] O. G. Tietjens, *Fundamentals of Hydro- and Aeromechanics* (McGraw-Hill Book Company, Inc., New York, 1934), p. 146.

the surface occurs; the flow about the solid body is thus identical with that about the sources. The flow about a single source in a uniform flow has been calculated by Tietjens.[6] The total-head defect to be anticipated for a tube of this shape is calculated as follows:

The velocity along the central streamline is required. This velocity has been given as:[7]

$$u(x) = U(1-d^2/16x^2),$$

where x = distance along central streamline from source, U = velocity far from body, and d = diameter of impact tube. This expression can be converted to the following non-dimensional form by using U as the typical velocity and d as the typical dimensions:

$$u'(x') = 1 - \frac{1}{16x'^2}. \tag{19}$$

The next step is to find $u'(t')$. The quantity t' can be found as a function of u' by integrating

$$dt' = \frac{dx'}{u'(x')} = -\frac{1}{8}\frac{du'}{u'(1-u')^{\frac{1}{2}}}.$$

The choice of the zero of t' is arbitrary. For convenience, if $t'=0$ when $u'=0.99$, then

$$t' = -\frac{1}{8}\int_{0.99}^{u'} \frac{du'}{u'(1-u')^{\frac{1}{2}}},$$

$$= -\frac{1}{8}\left[\log\left(\frac{11}{9}\frac{1-(1-u')^{\frac{1}{2}}}{1+(1-u')^{\frac{1}{2}}}\right) + \frac{2}{(1-u')^{\frac{1}{2}}} - 20\right]. \tag{20}$$

The next step is to determine $\epsilon'(t')$ from Eq. (14).

TABLE I. Results of numerical calculations of $\Delta S'$ for source-shaped impact tube.

K	$\Delta S'$
10	0.1685
3	.405
2	.516
1	.676
0.3	.868
0.1	.952

[7] See reference 6, p. 147.

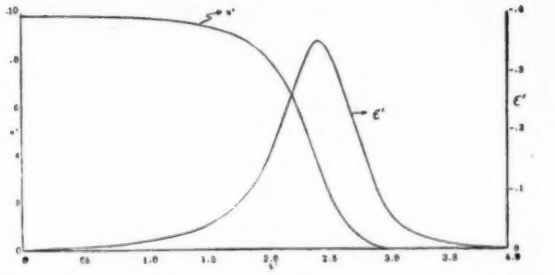

FIG. 3. Flow about a source-shaped impact tube. u', which is obtained from Eq. (20), is the velocity divided by the undisturbed gas velocity. ϵ' is the excess energy in vibration divided by the amount which would be present immediately following an instantaneous expansion from rest to the undisturbed gas velocity. The values of ϵ' were obtained from Eq. (22) for the case where the impact tube diameter is three times the distance the undisturbed gas travels during its relaxation time ($K=3$).

Then, by the use of Eq. (19),

$$\frac{du'^2}{dt'} = 2u'^2\frac{du'}{dx'} = -16u'^2(1-u')^{\frac{1}{2}}. \tag{21}$$

Because ϵ' is zero initially ($t' = -\infty$) and remains zero until u' begins to vary rapidly with time, if K is not too small, the lagging heat capacity can be assumed to follow the temperature changes in the gas up to the point $u'=0.99$; that is, $\epsilon'=0$ can be used for $t'=0$. Combining this fact with Eqs. (14) and (21) yields

$$\epsilon'(t') = -\exp(-Kt') \times \int_0^{t'} 16u'^2(1-u')^{\frac{1}{2}} \exp(Kt')dt'. \tag{22}$$

In view of the partly transcendental nature of Eq. (20), it was necessary to integrate Eq. (22) numerically. Equation (20) was plotted (Fig. 3) in such a way that the values of u' corresponding to regularly spaced values of t' could be found easily. By Simpson's rule, $\epsilon'(t')$ was then found for a series of values of K. An example of the result of such a calculation is given in Fig. 3 for $K=3$. The entropy increase along the central streamline was then found from Eq. (16).

Values of $\Delta S'$ found from integrating Eq. (22) by Simpson's rule and Eq. (16) with a planimeter are plotted in Fig. 4 and are given in Table I. For large and small values of K, the approximations developed earlier were used to reduce the labor of calculations and yielded the result $\Delta S' = 1.743/K$ when K is large and $\Delta S' = 1.452K$

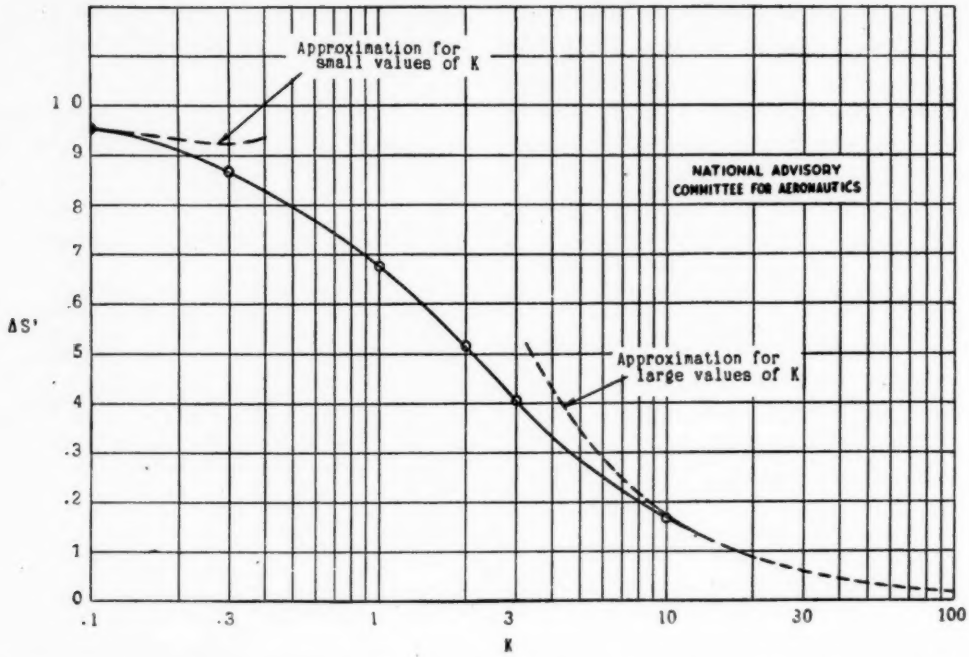

FIG. 4. The non-dimensional entropy increase in the flow approaching a source-shaped impact tube. $\Delta S'$ is the ratio of the entropy increase to that which would be obtained following an instantaneous compression to rest. $K=d/U\tau$ and is the ratio of the diameter of the impact tube to the distance traveled by the undisturbed gas during its relaxation time. The circles show the results of numerical calculations.

$+(1-1.008K)^2$ when K is small. These results are plotted in Fig. 4; this figure thus indicates the range of applicability of these approximations.

Calculation of Entropy Increase in Flow through a Nozzle of Special Design

For the measurements of the relaxation time in CO_2, a nozzle is employed in which the gases expand and accelerate before meeting the impact tube. This expansion cannot always be made slow enough—that is, the nozzle long enough—so that the expansion through the nozzle involves a really negligible entropy increase; hence, the results of Fig. 4 must be corrected for the entropy increases in the nozzle. In order to simplify the calculations, the nozzle was so designed that the time rate of temperature drop was constant. It can be shown that the entropy increase in a nozzle of this design is

$$\Delta S'=\frac{4}{3K_N}-\frac{16}{9K_N^2}(1-\exp(-\tfrac{3}{2}K_N))+\frac{4}{9K_N^2}(1-\exp(-3K_N)),$$

where $K_N=l/Ut$ and U is the final velocity attained by the flow in a nozzle of length l. It must be remembered that the calculations for the impact tube presumed ϵ' to be zero initially. This condition is the case only if $K_N\gg 1$, and hence the calculation given here is valid only for this case.

From the definitions of K and K_N, it is seen that $K_N=lK/d$ and hence the total entropy increase

$$\Delta S_T'=\Delta S_{\text{tube}}'+\Delta S_N' \qquad (23)$$

can be expressed as a function of K alone for a given l/d.

MEASUREMENT OF RELAXATION TIME OF CO_2

We shall now apply the theory just developed to the measurement of the relaxation time of CO_2. This work was undertaken both to test the theory and to develop a technique that would supplement the sonic methods previously used for measuring relaxation times. The method essentially consists in expanding the gas through a known pressure ratio in a nozzle and compressing it again at the nose of a source-shaped impact tube. The resultant total-head loss is

divided by the total-head loss that would be obtained in a very slow expansion and a fast compression (Eq. (4)). This non-dimensional total-head loss is compared with a theoretical result such as the one derived previously (Eq. (23)) and the value of K appropriate to the flow is found. From this value of K, the relaxation time of the gas can be easily computed if the velocity before compression and the diameter of the impact tube are known.

During the compression of the gas, the temperature and pressure rise from T_1 and p_1 to T_2 and p_2, respectively. The relaxation time and the heat capacity of the gas thus change along a streamline. The procedure previously outlined then gives an average relaxation time for the flow. It is assumed that this average relaxation time is the relaxation time appropriate to conditions halfway between compressed and expanded conditions. Because p_2 is close to p_0 and $T_2=T_0$, these conditions $\bar{p}$ and $\bar{T}$ can be found from

$$\bar{p}=(p_0+p_1)/2$$

and

$$\bar{T}=(T_0+T_1)/2.$$

The errors introduced in this way certainly are no greater than those due to the low velocity assumption introduced earlier in the theory.

Gas

The gas used in these experiments was commercial "bone-dry" CO_2. This gas was dried by passing it through calcium chloride and then dehydrite while it was at a pressure greater than 40 atmospheres. The purification procedure was not so thorough as methods used in some previous investigations, and it is to be expected that somewhat shorter relaxation times would be obtained. The primary object of this work is to establish the self-consistency of this test method rather than to obtain an accurate relaxation time for pure CO_2.

Apparatus

The apparatus used is essentially the same as that schematized in Fig. 1. A longitudinal section through a chamber of the most recent design is shown in Fig. 5. (The chamber used in the tests discussed in the next section did not incorporate

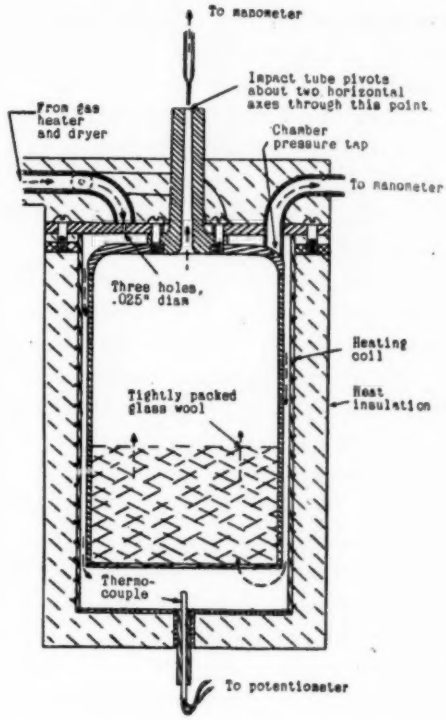

FIG. 5. Longitudinal section through chamber used to measure the relaxation time of heated gases.

the liner and the gas entered from the bottom.) The gas enters through three holes that were made small to stabilize the gas flow into the chamber. The glass wool is necessary to remove turbulence from the gas in the chamber and contributes materially toward reducing the total-head defects obtained in gases without heat-capacity lag. It was found that total-head defects traceable to non-uniformities in temperature existed and could be reduced by the use of the lined chamber shown. The fact that the gas flows around the inner chamber before entering helps to keep the gas in the inner chamber at uniform temperature.

The temperature non-uniformities can be almost eliminated if the gas entering the outer chamber is at the same temperature as the chamber. A mechanism was used to adjust the alignment of the impact tube without moving the tip from the center of the nozzle. The impact tube must be adjustable in order that small errors in shape near the hole will not give spurious total-head defects (in helium, for example). The gas and the chamber were heated electrically and a

thermocouple inside the chamber was used to measure the gas temperature.

The nozzle used had a circular cross section, was 1.6 inches long, and was designed according to the methods previously described to give a constant time rate of temperature drop; that is, du^2/dt = Constant for the first 1.5 inches, the last 0.1 inch being straight.

Two impact tubes with diameters 0.0299 inch and 0.0177 inch were used in these experiments. They were made by drawing out glass tubing until a piece of appropriate diameter and hole was obtained. The hole was kept larger than about 0.004 inch and the fine section not too long ($\approx\frac{1}{4}$ in.) to prevent the response of the alcohol manometer from being too sluggish. The ends of the tubes were ground to a source shape on a fine stone. During the grinding process, a silhouette of the tube was cast on the screen of a projecting microscope and the contour superimposed on a source-shaped curve. By this technique, the contour could be ground to the source shape within 0.0005 inch, except for the hole, in a short time.

Tests and Computations

The total-head defect in CO_2 was measured with the two impact tubes over a range of chamber pressures. The consistency of relaxation times obtained at various pressure ratios and with various impact tubes serves as a check on this method of measuring relaxation time and on the theory on which the method is based.

Before each series of measurements, nitrogen, which has only a negligible vibrational heat content at room temperature, was run through the chamber to be sure that no spurious effects and leaks were present. In the results reported herein, the errors due to these effects were kept to less than 0.01 percent of the chamber pressure; therefore, the resultant error in relaxation time due to these causes was less than 4 percent. In subsequent work (not reported herein), it was found that most of these total-head aberrations could be eliminated by ensuring uniform temperature in the issuing gases. If care is taken to eliminate temperature non-uniformities, tube misalignments, and turbulence in the chamber, the total-head aberrations can be reduced to 0.002 percent or less.

The total-head defects obtained were divided by the result of Eq. (4) to reduce them to non-dimensional form. The appropriate value of K was found by referring to plots of Eq. (23). The gas velocity was computed from the reading of the mercury manometer by the enthalpy theorem with adiabatic expansion assumed. The relaxation time was then computed from the definition of K by Eq. (9). The relaxation times thus obtained were expressed in collisions per molecule. The number of molecular collisions per second in CO_2 was assumed to be 8.888×10^9 at 15°C and 1 atmosphere.[8] At all other temperatures and pressures, the number of collisions was assumed to vary inversely with $\sqrt{T}$ and directly with pressure. The number of molecular collisions per second and the heat capacity of the gas were computed at temperature $\bar{T}$ and pressure $\bar{p}$. The data and results obtained are given in Tables II and III for the 0.0299- and 0.0177-inch tubes, respectively.

The results indicate that the relaxation time in collisions is nearly independent of pressure ratio and impact-tube size. This consistency constitutes the desired verification of this test method. It was expected that a variation at high pressure ratios would appear in view of the assumption of low velocity made at several points in the theoretical development.

A large part of the scatter of the results, in particular the apparent drop at low pressures, is attributed to the fact that in the tests the average temperature (half-way between chamber and expanded temperatures) was not held constant during the run.

The average number of collisions obtained with the 0.0299-inch tube was 33,100; with the 0.0177-inch tube, 32,000. The final result at 105°F thus is 32,600, which is somewhat lower than the result of recent investigations in which the CO_2 has been much more carefully purified than in the present investigation (compare with Fig. 6).

IMPACT-TUBE METHOD OF MEASURING RELAXATION TIME OF GASES

The impact-tube method of measuring the relaxation time of gases rests essentially on the

[8] E. H. Kennard, *Kinetic Theory of Gases* (McGraw-Hill Book Company, Inc., New York, 1938), Tables, pp. 26 and 149.

TABLE II. Data and calculations for 0.0299-inch tube.

1 Chamber pressure, p_0/p_1 (atmos.)	2 Total-head defect, $100\frac{(p_0/p_2)-1}{(p_0/p_1)-1}$ (percent)	3 Average temperature, $\bar{T}$ (°F)	4 Total-head defect from inst. compression theory, $100\frac{(p_0/p_2)-1}{(p_0/p_1)-1}$ (percent)	5 Total $\Delta S'$ $\left(\frac{\text{Col. 2}}{\text{Col. 4}}\right)$	6 K from plots of Eq. (23)	7 Gas velocity at end of nozzle, U (in./sec.)	8 Relaxation time, $\tau=\frac{d}{Uk}$ (microsec.)	9 Collisions ($\tau\times$collisions per molecule per sec.)
1.185	0.321	115.0	0.611	0.525	2.03	5640	2.61	24,000
1.253	.482	109.8	.815	.591	1.58	6464	2.93	27,800
1.323	.669	107.5	1.024	.653	1.23	7188	3.38	33,200
1.388	.805	100.7	1.198	.672	1.13	7731	3.42	34,700
1.464	.966	101.6	1.412	.684	1.07	8336	3.35	35,100
1.527	1.088	98.2	1.577	.690	1.05	8761	3.25	35,000
1.580	1.193	96.1	1.706	.699	1.01	9090	3.26	35,900
1.672	1.344	93.9	1.934	.695	1 025	9611	3.04	34,700
1.734	1.445	92.6	2.076	.696	1.02	9936	2.95	34,500
1.738	1.467	92.4	2.084	.704	.982	9955	3.06	35,900
1.295	.586	107.8	.941	.623	1.38	6910	4.17	30,400
1.350	.721	105.4	1.098	.656	1.21	7423	3.33	33,100
1.364	.758	111.5	1.152	.658	1.21	7591	3.25	32,400
1.422	.880	107.2	1.312	.671	1.14	8051	3.26	33,300
1.499	1.025	99.2	1.502	.682	1.075	8573	3.25	34,500
1.552	1.130	98.1	1.641	.688	1.05	8926	3.19	34,700
								Av. 33,100

fact that the total-head defect not traceable to heat-capacity lag can be reduced to a very small value—say, 0.002 percent. Very small dissipations due to heat-capacity lag are therefore measurable. For example, a gas having a lagging heat capacity $0.1R$ with a relaxation time of 10^{-7} second could give a total-head defect of 0.05 percent. If the gas had a lagging heat capacity as large as R, a relaxation time as short as 10^{-8} second would be measurable.

This method seems to be easier to carry out than the sonic methods previously discussed and

TABLE III. Data and calculations for 0.0177-inch tube.

1 Chamber pressure, p_0/p_1 (atmos.)	2 Total-head defect, $100\frac{(p_0/p_2)-1}{(p_0/p_1)-1}$ (percent)	3 Average temperature, $\bar{T}$ (°F)	4 Total-head defect from inst. compression theory, $100\frac{(p_0/p_2)-1}{(p_0/p_1)-1}$ (percent)	5 Total $\Delta S'$ $\left(\frac{\text{Col. 2}}{\text{Col. 4}}\right)$	6 K from plots of Eq. (23)	7 Gas velocity at end of nozzle, U (in./sec.)	8 Relaxation time, $\tau=\frac{d}{Uk}$ (microsec.)	9 Collisions ($\tau\times$collisions per molecule per sec.)
1.442	1.014	97.7	1.342	0.756	0.73	8146	2.98	31,700
1.315	.765	127.3	1.041	.735	.81	7232	3.02	29,700
1.334	.748	106.1	1.057	.708	.92	7289	2.64	26,700
1.389	.900	98.8	1.196	.753	.74	7723	3.11	32,400
1.278	.633	100.8	.876	.723	.85	6687	3.11	30,800
1.229	.519	110.1	.742	.699	.97	6182	2.95	28,400
1.205	.480	121.1	.683	.704	.93	5940	3.20	30,200
1.467	1.100	103.4	1.429	.770	.67	8377	3.15	33,700
1.686	1.521	95.2	1.972	.772	67	9703	2.72	32,000
1.612	1.383	96.0	1.788	.774	.67	9283	2.85	32,500
1.665	1.495	95.0	1.919	.779	.65	9585	2.84	33,100
1.581	1.317	95.1	1.708	.771	.67	9088	2.91	32,800
1.556	1.283	96.1	1.644	.780	.64	8937	3.09	34,500
1.548	1.276	99.2	1.637	.780	.64	8912	3.10	34,400
1.531	1.244	100.9	1.594	.781	.64	8807	3.14	34,600
1.515	1.216	104.3	1.564	.778	.65	8728	3.12	34,000
1.482	1.123	102.9	1.468	.765	.69	8482	3.00	32,600
1.417	.986	107.3	1.298	.760	.71	8013	3.11	32,500
								Av. 32,000

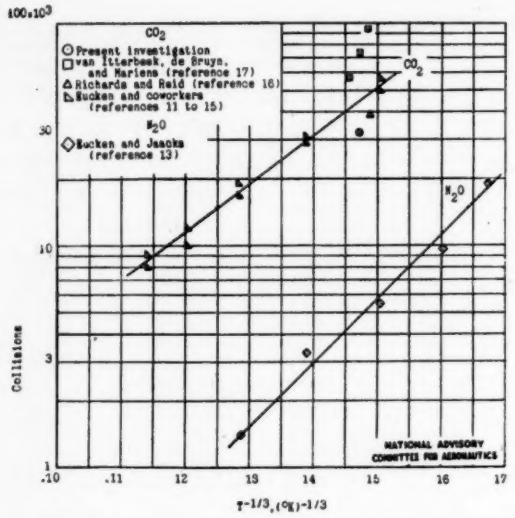

FIG. 6. Landau and Teller (reference 18) have predicted that the logarithm of the relaxation time of a gas expressed in molecular collisions should be proportional to $T^{-\frac{1}{3}}$. It will be seen that the results of Eucken and his co-workers confirm the theory of Landau and Teller very well.

can be used to measure relaxation times with comparable precision. The quantity of gas required to make a measurement will be larger than for the sonic methods (a standard tank of CO_2 lasts about 5 hr. in this apparatus) and thus may make it more difficult to attain high purity.

If the gas to be studied has a long relaxation time, greater than 50 microseconds, for example, it should be possible to measure the relaxation time in an apparatus similar to the one discussed by comparing the total-head defects obtained with a calculation of the entropy increase in the nozzle. In this case, the time taken for the gas to flow through the nozzle is compared with the relaxation time of the gas. The shape of the impact tube would be unimportant in this case as long as it was small enough that $K \ll 1$.

CONCLUSIONS

The existence of energy dissipations in gas dynamics, which must be attributed to a lag in the vibrational heat capacity of the gas, has been established both theoretically and experimentally.

An approximate method of calculating the entropy increase in a general flow problem has been developed. The special case in which a gas at rest expands out of a specially shaped nozzle and is compressed at the nose of a source-shaped impact tube near the mouth of the nozzle has been treated, and the dependence of the resultant total-head defect on the relaxation time of the gas has been found.

The total-head defect in this flow has been applied to measure the relaxation time of CO_2. The results obtained with two impact tubes were in agreement within about 3 percent. The consistency of these results is regarded as a check on the general theory developed and on this measurement method.

Dr. Vannevar Bush helped to initiate this work by asking the writer a stimulating question. The author also is very grateful to Professor E. Teller, Mr. E. N. Jacobs, and Dr. Robert E. Street for helpful discussion.

APPENDIX A

Sonic Measurements in Carbon Dioxide

Much careful work has been done on the lag in the vibrational heat capacity of CO_2. Carbon dioxide is a linear molecule and thus has a translational and rotational heat capacity of $5/2R$. It has four normal modes in vibration that are diagrammed with their frequencies as follows:[9]

$$\begin{array}{lcll} O\rightarrow & C & \leftarrow O & \nu_1 = 4.164\times 10^{13}, \\ & \uparrow & & \\ O & C & O & \nu_2 = 2.003\times 10^{13}, \quad 2 \text{ modes}, \\ \downarrow & & \downarrow & \\ \leftarrow O & C\rightarrow & \leftarrow O & \nu_3 = 7.050\times 10^{13}. \end{array}$$

The heat capacity of CO_2 is somewhat complicated by the fact that the second excited state of the oscillation ν_2 has almost the same energy as the first excited state of ν_1. The near resonance results in a strong interaction through the first-order perturbation (the first-order departure of the potential energy from the square law) between the two states involved, as was pointed out by Fermi.[10] This perturbation produces significant disturbances (≈ 50 cm^{-1}) of the level involved but does not have a large effect on the heat capacity of the gas. The heat capacity of CO_2 was computed by Kassel[11] and his results are used in the present calculations.

[9] D. M. Dennison, Phys. Rev. **41**, 304–312 (1932).
[10] E. Fermi, Zeits. f. Physik **71**, 250–259 (1931).
[11] L. S. Kassel, J. Am. Chem. Soc. **56**, 1838–1842 (1934).

Eucken and his co-workers have carefully studied over a period of years the dispersion of sound in CO_2.[12–15] One conclusion of this work—that the vibrational energy levels in CO_2 adjust with the same relaxation time—is demonstrated by showing that the dispersion curves obtained fit a simple dispersion formula such as Kneser's.

Küchler, for example, obtained a simple dispersion curve at 410°C, at which appreciable heat capacity due to all three normal modes would be expected. Richards and Reid[16] and others[17] have maintained that the symmetrical valence vibration ν_1 of CO_2 does not adjust at 9 kilocycles in some dispersion measurements made near room temperature. As they point out, this fact is remarkable because the second excited state of ν_2 strongly perturbs the first excited state of ν_1. In any case, the contribution of this normal mode to the heat capacity is very small at room temperature and the effects found are near the limits of the accuracy of Richards and Reid.

The relaxation time of CO_2 in molecular collisions, as given by Eucken and his co-workers, is plotted against $T^{-\frac{1}{3}}$ (T in °K) in Fig. 6 for comparison with the theory discussed in appendix B. van Itterbeek, de Bruyn, and Mariëns[18] measured the absorption at 599 kilocycles in very carefully purified CO_2. Their measurements, which are also given in Fig. 6, show a longer relaxation time than the measurements of Eucken and his co-workers. They attribute this increased relaxation time to careful purification of the gas.

All the measurements with CO_2 have indicated that the relaxation time is inversely proportional to the pressure of the gas. This result shows that the process responsible for the interchange of energy between vibrational and other degrees of freedom is bimolecular.

[12] A. Eucken and R. Becker, Zeits. f. physik. Chemie **20**, 467 (1933); **27**, 219–262 (1934).
[13] A. Eucken and H. Jaacks, Zeits. f. physik. Chemie **30**, 85–112 (1935).
[14] A. Eucken and E. Numaan, Zeits. f. physik. Chemie **36**, 163–183 (1937).
[15] L. Küchler, Zeits. f. physik. Chemie **41**, 199–214 (1938).
[16] W. T. Richards and J. A. Reid, J. Chem. Phys. **2**, 193–205 (1934); **2**, 206–214 (1934).
[17] See bibliography of reference 2.
[18] A. van Itterbeek, P. de Bruyn, and P. Mariëns, Physica **6**, 511–518 (1939).

APPENDIX B

Theory of Excitation of Molecular Vibration by Collisions

Landau and Teller[19] have given an approximate calculation of the probability of the excitation of a vibrational quantum in a molecular collision. Assuming that the interaction energy which induces the vibration depends linearly on the normal coordinate of a harmonic vibration, they make a first-order perturbation calculation. The matrix element for the transition from the lth to the $(l+1)$th or from the $(l+1)$th to the lth vibrational state is then proportional to $(l+1)^{\frac{1}{2}}$. The transition probabilities k_{ij} are proportional to the square of matrix elements and therefore

$$k_{01}:k_{12}:k_{23}=k_{10}:k_{21}:k_{32}=1:2:3,$$

and, when $i-j\neq\pm1$, $k_{ij}=0$. This result is shown[19] to lead to the prediction that all the allowed transitions in a given normal mode have the same relaxation time. Landau and Teller next examine the collision process classically, assuming the interaction energy between translation and vibration to be proportional to $e^{-x/a}$, where x is the distance between the molecules and a is an undetermined constant. They also assume that the translational energy of the molecules—that is, the collision—is adiabatic. The amount of energy transferred to vibration in a collision is then calculated and used to estimate the transition probability k_{01} and the relaxation time of the gas. They conclude that the temperature variation of the relaxation time expressed in molecular collisions is given by

$$\text{Collisions}\approx\exp\left(3T^{-\frac{1}{3}}\left(\frac{(\pi a\nu)^2M}{2R}\right)^{\frac{1}{3}}\right),$$

where M is molecular weight.

In Fig. 6, experimental results for the relaxation time in collisions of CO_2 and nitrous oxide N_2O are plotted against $T^{-\frac{1}{3}}$. The theoretical results are seen to be straight lines, within experimental error. The value of a can be found from the slope of the straight line. For CO_2 with $\nu=2.003\times10^{13}$, $a=0.22\times10^{-8}$ cm and, for N_2O

[19] L. Landau and E. Teller, Phys. Zeits. Sowjetunion **1**, 34–43 (1936).

with $\nu = 1.773 \times 10^{13}$, $a = 0.36 \times 10^{-8}$ cm. These reasonable values for a are a further check on this theory.

It should be pointed out that the temperature variation of catalytic effects is quite different from that of pure gases, the number of collisions required being nearly independent of temperature.[15] Various attempts have been made to associate the effectiveness of catalysts with their physical or chemical properties but no generally successful rule seems to have been proposed. Gases that have some chemical affinity, gases with large dipole moments, and gases with small moments of inertia are usually most effective.

THE JOURNAL OF CHEMICAL PHYSICS VOLUME 14, NUMBER 3 MARCH, 1946

Application of the Methods of Molecular Distribution to Solutions of Large Molecules

BRUNO H. ZIMM
Polytechnic Institute of Brooklyn, Brooklyn, New York
(Received December 17, 1945)

The equations for the thermodynamic potentials of the solvent in solutions of ordinary organic molecules are extended to solutions of large molecules by methods using continuous molecular distribution functions. Particular attention is given to the coefficient, A_2, of the second term in the expansion of the osmotic pressure in terms of the concentration, since this coefficient has a simple molecular meaning and is sufficient to describe the deviation of the system from ideality at low concentrations. A_2 is calculated by direct integration for two rigid shapes, the sphere and the long thin rod. A general expression is then developed for A_2 for flexible chain molecules in terms of the interactions of the segments of the chains. In favorable cases it is found possible to relate A_2 for a chain molecule to the solution properties of its small molecule homologues by an equation very similar to those developed by Flory, Huggins, and Miller. In general, however, interactions that depend both on the local structure and also on the over-all shape of the chain molecules seriously modify such a relationship. The nature of these interactions, including the effects of branching and of limited flexibility, is discussed. It is also shown that higher coefficients in the expansion of the osmotic pressure in terms of concentration can be treated in a similar way. Comparison with experimental data confirms the general predictions of the theory both for proteins and chain polymers.

I. INTRODUCTION

IT is a task of statistical mechanics to relate the thermodynamics of solutions to the properties of the molecules that compose them. One problem in this field is the investigation of the extraordinary deviations from Raoult's law that are frequently shown by solutions of high polymers and other large molecules. Several papers in recent years[1-3] have contributed greatly to our understanding of the phenomenon, but they are limited in some respects; they have all been based on a highly idealized lattice model, and they are restricted to treating linear chain polymers only, leaving the status of the more rigid protein molecules obscure. Moreover the numerical agreement with experiment has not been satisfactory, for reasons that have remained unelucidated.*

The treatment in this paper aims to divest the theory of as many assumptions as possible and to develop it as an extension of the better understood theories of ideal and regular solutions of small organic molecules. Certain inherent limitations should be noted at the outset, however. The theory is not applicable directly to solutions of ionized particles and is therefore not suitable as

[1] P. J. Flory, J. Chem. Phys. **9**, 660 (1941); **10**, 51 (1942).
[2] M. L. Huggins, J. Chem. Phys. **9**, 440 (1941); J. Phys. Chem. **46**, 151 (1942); J. Am. Chem. Soc. **64**, 1712 (1942); Ann. N. Y. Acad. Sci. **43**, 1 (1942).
[3] A. R. Miller, Proc. Camb. Phil. Soc. **39**, 54 (1942).

* Note added in proof: A recent article by P. J. Flory (J. Chem. Phys. **13**, 453(1945)) contributes greatly to the clearing up of these discrepancies. Many of the conclusions reached therein are similar to those of this paper.

it stands for aqueous protein solutions, except at their iso-electric points. Moreover, the theory is convenient for the discussion of the partial molar free energy and related quantities of only one component, the solvent, in dilute solutions. (Fortunately these are also the quantities and concentrations most accessible experimentally.)

The essential step in obtaining the partial molar free energy of the solvent is the estimation of the change in the phase integral or partition function of the system, that is, its probability, as the relative amounts of the components are varied.

The statistical method used in this paper for calculating the probabilities of the system is quite different in appearance from the lattice approach since it involves operation with continuous distribution functions. This treatment is based on a recent investigation of the theory of non-electrolyte solutions by McMillan and Mayer[4]; without the simplifications achieved by these authors (fortunately at no loss of accuracy) the continuous method would probably be impracticable.

Because these methods have not yet been widely used, the fundamental equations will be reviewed at some length in the following section.

II. FUNDAMENTAL EQUATIONS[4,5]

II.1. Symbolism

Since we must operate with systems of many particles all influencing each other directly or indirectly, it is necessary to adopt a shorthand to represent sets of many coordinates. The conventions are as follows:

- (i) represents all the coordinates of the ith particle
- $\{n\}$ represents the coordinates of a set of n particles
- $\{n\pm m\}$ represents the coordinates of a set of n plus (or minus) m particles. (The particles are assumed to be distinguishable.)
- $d(i)$, $d\{n\}$, $d\{n\pm m\}$ are the respective volume elements in hyperspace.

[4] W. G. McMillan and J. E. Mayer, J. Chem. Phys. **13**, 276 (1945).

[5] J. E. Mayer and E. Montroll, J. Chem. Phys. **9**, 2 (1941).

II.2. Molecular Distribution Functions and Related Quantities[4,5]

In a fluid, or indeed in a real crystal above absolute zero, the molecules are not fixed in a rigid pattern but instead may be found with varying probability at any point in the containing vessel. In line with the fundamental philosophy of quantum-statistical mechanics, one is led to postulate that the most exact description possible of a real system can only give the probabilities of the molecules occurring in certain positions and configurations. For a system containing many molecules in a volume V these probabilities are conveniently expressed by a set of functions, $[F_n\{n\}]$, defined as follows:

$$\frac{1}{V^n}F_n\{n\}d\{n\}, \tag{1}$$

is the probability that the n specified molecules are each at the positions and have the internal configurations specified by $\{n\}$ in the infinitesimal range of these coordinates represented by $d\{n\}$.

The functions are so normalized that when integrated over the complete range of all the coordinates they are unity:

$$\frac{1}{V^n}\int F_n\{n\}d\{n\}=1 \tag{2}$$

(meaning that the probability of finding the n molecules somewhere in V is unity).

If the system contains N molecules altogether, $(1/V^N)F_N\{N\}d\{N\}$ specifies the probability that all these molecules will appear in the configuration symbolized by $\{N\}$. If we are interested in the probability that a certain small group containing n of these N molecules will have the configuration $\{n\}$, irrespective of where the rest of the $N-n$ molecules are, we can obtain it by averaging $(1/V^N)F_N\{N\}d\{N\}$ over all the positions of the $N-n$ undesired molecules. This probability is by definition $(1/V^n)F_n\{n\}d\{n\}$ so that Eq. (3) arises to connect the distribution functions of different sized groups of molecules.

$$F_n\{n\}=\frac{1}{V^{N-n}}\int F_N\{N\}d\{N-n\}. \tag{3}$$

For non-electrolyte fluid systems there are no long range forces or structures, and a single

molecule is as likely to be found in one place as another, so that its distribution function depends on its internal coordinates only. If it is integrated over these, the integral must then be a constant; this is equal to unity as a result of (2).

$$\int F_1(j)d(j)_i = 1. \tag{4}$$

(The symbol $(j)_i$ stands for the internal coordinates of molecule j.)

Also, since there is no long range structure, all the higher distribution functions become equal to a simple product of the F_1's of the molecules involved when the distances between all of them are large. It is convenient to make a transformation to a set of functions, the "g-functions," which become zero in like circumstances.

The first two g-functions are explicitly defined here (for the general definition see McMillan and Mayer[4] and Mayer and Montroll:[5]

$$g_2(i, j) = F_2(i, j) - F_1(i)F_1(j), \tag{5a}$$

$$g_3(i, j, k) = F_3(i, j, k) - F_2(i, j)F_1(k) - F_2(j, k)F_1(i) - F_2(k, i)F_1(j) + 2F_1(i)F_1(j)F_1(k). \tag{5b}$$

Actually the functions so defined do not quite become zero at large distances, but instead approach small values of order $1/N$. The g-functions used later in this paper should therefore be considered to be very slightly modified by the subtraction of a constant so that they go rigorously to zero. The otherwise trivial difference could have been avoided at the cost of simplicity by taking the system as part of an infinite volume of fluid.[4,5]

The function g_2 measures the divergence of the pair distribution function, $F_2(i, j)$, from a simple product of $F_1(i)F_1(j)$; in other words, it is a measure of the effect of the interaction of the two molecules on one another. The higher g-functions have similar meanings for larger groups of molecules.

In this paper it so happens that all the distribution functions are those of the solute molecules in infinitely dilute solution only; the distribution functions of the solvent molecules or those of the solute at finite concentrations are never used.

II.3. Equation for the Osmotic Pressure

By transformation of the grand partition function, appropriately generalized, McMillan and Mayer were able to derive rigorously a series expansion for the osmotic pressure in terms of concentration, which we shall write as

$$\pi = RT\left(\frac{1}{M_2}c + A_2c^2 + A_3c^3 + \cdots\right), \tag{6}$$

where c is the concentration of solute in mass per unit volume of solution, π the osmotic pressure (pressure increment required to make the activity of the solvent in a solution of concentration c equal to that of the pure solvent at its own vapor pressure), M_2 the molecular weight of the solute, and the A_n are constants at constant temperature. This series converges and is valid with constant coefficients at any concentration between an infinitely dilute and a saturated solution.

The coefficients, A_n, are related to the molecular distribution functions. If the forces between the molecules are of the ordinary van der Waals type, that is, not capable of being saturated, the first coefficients may be obtained from the following equations:

$$A_2 = -\frac{N_0}{2VM_2^2}\int g_2\{2\}d\{2\}, \tag{7a}$$

$$A_3 = -\frac{N_0^2}{3VM_2^3}\int g_3\{3\}d\{3\} + 4M_2A_2^2; \tag{7b}$$

N_0 is Avogadro's number and V is the volume of the system. The reader is referred to McMillan and Mayer's paper for the general formula.

In words, the coefficient of the second term in the expansion of the osmotic pressure in terms of concentration is an integral involving the g-function of a pair of solute molecules; the third coefficient is an integral involving the g-functions of a triplet of solvent molecules; all the functions are to be evaluated in the infinitely dilute solution. The higher terms involve larger groups of molecules in a similar way.

It is interesting to note the exact formal correspondence between Eqs. (6) and (7) and the equation of state of an imperfect gas. If π were replaced by the pressure and the g-functions in (7) were defined for the infinitely rarified gas instead of the infinitely dilute solution, the two would be identical. The first term of the series in

each case describes the situation when the molecules do not interact with one another, giving the perfect gas law and van't Hoff's law, respectively, while the higher terms correct successively for the interaction of pairs, triplets, and larger groups of molecules.

III. IDEAL AND REGULAR SOLUTIONS

III.1. Ideal Solutions

If the molecules of the two components are alike in size, shape, and force fields, the distribution functions and hence the integrals over them must be the same for both components. In this case the solution is "ideal" and obeys the well-known equation

$$\pi = -\frac{\Delta\bar{F}_1}{\bar{V}_1} = -\frac{RT}{\bar{V}_1}\ln(1-N_2). \tag{8}$$

$\Delta\bar{F}_1$ is the molar free energy dilution, i.e., $\langle\Delta\bar{F}\rangle_1 = \bar{F}_1 - \bar{F}_1^0$ where $\bar{F}_1$ is the partial molar free energy of the solvent and $\bar{F}_1^0$ is the same quantity at infinite dilution, $\bar{V}_1$ is the solvent's partial molar volume, and N_2 the mole fraction of solute. Equation (8) may be derived from the fundamental Eqs. (6) and (7), but to do so would take us too far afield. It is better here to work backward from Eq. (8) to calculate the values of the coefficients in the general Eq. (6) for this special case.

For the dilute solutions in which we are hereafter interested, it suffices to replace the mole fraction N_2 by its approximate equivalent, $\bar{V}_1 c/M_2$. The logarithm in (8) may then be expanded and the series compared with (6). From this comparison we find the following values for the coefficients A_m for ideal solutions:

$$A_2 = \bar{V}_1/2M_2^2, \tag{9a}$$

$$A_3 = \bar{V}_1^2/3M_2^3, \tag{9b}$$

$$\vdots$$

$$A_n = \bar{V}_1^{n-1}/nM_2^n. \tag{9c}$$

III.2. Regular Solutions

In an *ideal* solution there is no heat of dilution and the entropy (times T) is equal to the negative of the free energy as given by Eq. (8). In a *regular* solution, after the definition of Hildebrand,[6] the heat of dilution is different from zero, but the entropy still has the ideal value. It has been found experimentally that many solutions of organic compounds where the molecules are approximately the same size fit into this classification. The equations of the regular solution therefore form a foundation on which to develop a theory for polymer solutions.

Derivation of the theory of regular solutions themselves from fundamental equations is outside the scope of this paper; here we will content ourselves with setting up formulae to describe the experimental facts.

The partial entropy of dilution equals the negative of the ideal free energy over T and will be given, using (9), by (10)

$$\Delta\bar{S}_1 = R\bar{V}_1\left(\frac{1}{M_2}c + \sum_{n=2}^{\infty}\frac{\bar{V}_1^{n-1}}{nM_2^n}c^n\right). \tag{10}$$

If we follow Hildebrand[6] and Scatchard,[7] we express the corresponding heat in the form

$$\Delta\bar{H}_1 = \sum_{n=2}^{\infty} B_n c^n, \tag{11}$$

where the coefficients B_n are presumably nearly independent of temperature.

The omission of a term in the first power of c has been discussed theoretically by other authors[6,7] and justified by experiment.[6] It can be simply derived starting with Eq. (6) and calculating $\Delta\bar{H}_1$ thermodynamically (assuming the product, $V_1 c$, to be independent of T):

$$\Delta\bar{F}_1 = -\pi\bar{V}_1 = -RT\bar{V}_1\left(\frac{1}{M_2}c + \sum_{n=2}^{\infty}A_n c^n\right), \tag{12}$$

$$\Delta\bar{H}_1 = \frac{\partial(\Delta\bar{F}_1/T)}{\partial(1/T)} = -R\sum_{n=2}^{\infty}\frac{\partial(A_n/\bar{V}_1^{n-1})}{\partial(1/T)}(\bar{V}_1 c)^n. \tag{13}$$

B_n thus equals

$$-R\bar{V}_1^n\frac{\partial(A_n/\bar{V}_1^{n-1})}{\partial(1/T)}.$$

The free energy is obtained by adding the heat and entropy contributions:

$$\Delta\bar{F}_1 = \Delta\bar{H}_1 - T\Delta\bar{S}_1 = -RT\bar{V}_1\left[\frac{1}{M_2}c + \sum_{n=2}^{\infty}\left(\frac{\bar{V}_1^{n-1}}{nM_2^n} - \frac{B_n}{RT\bar{V}_1}\right)c^n\right]. \tag{14}$$

[6] J. H. Hildebrand, *Solubility* (Reinhold Publishing Corporation, New York, 1936); Chem. Rev. **18**, 315 (1935).
[7] G. Scatchard, Chem. Rev. **8**, 321 (1931).

For the purposes of this paper we will express the osmotic pressure of a regular solution in the form (15).

$$\pi=-\frac{\Delta\bar{F}_1}{\bar{V}_1}=RT\left[\frac{1}{M_2}c+\sum_{n=2}^{\infty}\frac{\bar{V}_1{}^{n-1}}{nM_2{}^n}(1-\zeta_n)c^n\right]. \quad (15)$$

The heat coefficients, ζ_n, are given by

$$\zeta_n=\frac{nB_nM_2{}^n}{RT\bar{V}_1{}^n}. \quad (16)$$

Comparing (15) with (6), the assumption of a regular solution is seen to be equivalent to expressing the osmotic coefficients A_n in terms of the heat coefficients and molar volume:

$$A_n=\frac{\bar{V}_1{}^{n-1}}{nM_2{}^n}(1-\zeta_n). \quad (17)$$

While there is certainly a theoretical basis for this relation (17), it should be understood that its use here is purely empirical, justified by a large amount of experimental data on small-molecule organic compounds.

IV. APPLICATION TO SOLUTIONS OF LARGE MOLECULES

In most of the ensuing discussion only the coefficient A_2 will be considered, since this characterizes the most important deviations from Raoult's law. The succeeding coefficients contribute little in dilute solutions. We will find it convenient to treat first two simple cases, whose results can be used to good advantage in the more complicated treatment of the chain molecule. These two cases are those of large spherical and long rigid rod-like molecules suspended in an effectively continuous and structureless solvent. We will assume that the range of the intermolecular forces is negligible compared to the diameters of the particles.

It is then easy to predict the form of the distribution functions; they will be a constant (determined by Eq. (2)) except for those configurations where the molecules interpenetrate, and since the molecules are assumed to be rigid, the functions, which give the probabilities of these configurations, must be zero there.

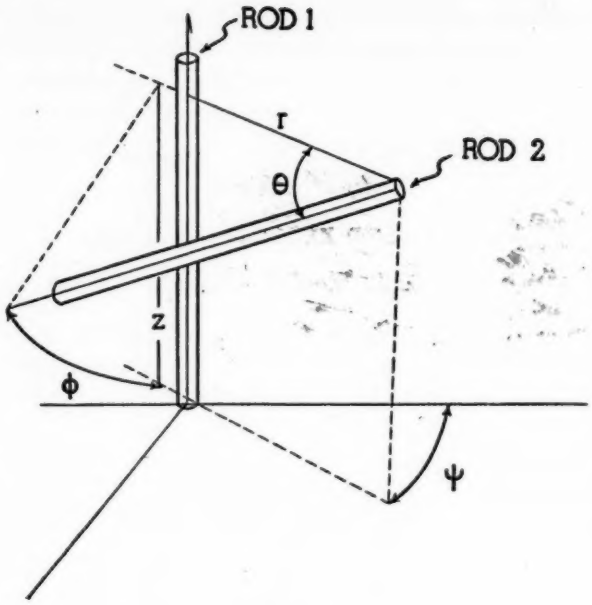

FIG. 1.

IV.1. Rigid Spheres

The spatial distribution function $F_2(1, 2)$, which gives the probability of sphere *1* and sphere *2* being a given distance apart, will be unity because of (2) except when the distance between the centers is less than the diameter a of the spheres.

$$\begin{aligned} F_2(1,2)&=1 \quad \text{when} \quad r_{12}>a, \\ F_2(1,2)&=0 \quad \text{when} \quad r_{12}<a, \end{aligned} \quad (18)$$

$$\begin{aligned} g_2(1,2)&=0 \quad \text{when} \quad r_{12}>a, \\ g_2(1,2)&=-1 \quad \text{when} \quad r_{12}<a, \end{aligned} \quad (19)$$

$$A_2=-\frac{N_0}{2VM_2{}^2}\int g_2(1,2)d(1)d(2)=\frac{2\pi a^3N_0}{3M_2{}^2}. \quad (20)$$

The volume, $\pi a^3/6$, of one sphere will presumably be proportional to the molecular weight, $\pi a^3/6 = M_2v_0$, where v_0 is the volume per unit molecular weight, so that

$$A_2=4N_0v_0/M_2. \quad (21)$$

IV.2. Long Rigid Rods

Consider two long cylindrical rods, numbered *1* and *2*, respectively, of diameter d and length l, with l much greater than d. To describe the positions of this system requires ten coordinates,

three external and two internal for each rod. The distribution function, $F_2(1, 2)$, must be zero when these coordinates have such values that the rods interpenetrate one another.

The ten coordinates may be conveniently chosen as follows (see Fig. 1); the three cartesian coordinates, X, Y, and Z, of one end of rod (*1*); two polar angles, Θ and Φ, to specify the direction of the axis of rod (*1*); a system of normal cylindrical coordinates, a height, z, a radius, r, and an azimuth, ψ, to give the position of a selected end of rod (*2*) with respect to rod (*1*), with z taken in the direction of the axis of rod (*1*) and ψ measured from an arbitrary reference plane through the axis; two polar angles, ϑ and φ, to give the orientation of rod (*2*) with respect to the radius r; ϑ is the angle between the axis of (*2*) and r, and φ is the angle determined by the two planes through r and the axes of (*1*) and (*2*). The volume element in this ten-dimensional space is $dXdYdZ \sin\Theta d\Theta d\Phi dz r dr d\psi \sin\vartheta d\vartheta d\varphi$.

Our problem is to specify those regions of ten-dimensional space in which superposition of the two molecules occurs. For a given value of ϑ less than $\pi/2$, it may be seen from Fig. 1 that the rods only overlap when r is less than $l\cos\vartheta$ and simultaneously φ lies between approximately $d/r\tan\vartheta$ and $-d/r\tan\vartheta$ with z between $-r\tan\vartheta$ and $l-r\tan\vartheta$, or φ between $\pi-d/r\tan\vartheta$ and $\pi+d/r\tan\vartheta$ with z between $r\tan\vartheta$ and $l+r\tan\vartheta$. The distribution function, $F_2(1, 2)$, must be zero in these regions. Outside of these regions it must be constant, since no attractive forces are assumed to act. The value of the constant is determined by the normalization equation, Eq. (2), at $1/16\pi^2$.

Also from Eq. (2) it is found that $F_1(1) = F_1(2) = 1/4\pi$. $F_2(1, 2)$ as well as $g_2(1, 2)$ may now be written down.

$$\left.\begin{aligned} F_2(1,2) &= 0 \\ g_2(1,2) &= -1/16\pi^2 \end{aligned}\right\} \left\{\begin{aligned} &\text{when } 0<r<l\cos\vartheta \\ &\quad 0<\vartheta<\pi/2, \\ &\text{and} \begin{cases} -d/r\tan\vartheta<\varphi<d/r\tan\vartheta \\ r\tan\vartheta<z<l+r\tan\vartheta, \end{cases} \\ &\text{or} \begin{cases} \pi-d/r\tan\vartheta<\varphi<\pi+d/r\tan\vartheta \\ -r\tan\vartheta<z<l-r\tan\vartheta; \end{cases} \end{aligned}\right.$$

$$\left.\begin{aligned} F_2(1,2) &= 1/16\pi^2 \\ g_2(1,2) &= 0 \end{aligned}\right\} \left\{\begin{aligned} &\text{in all other ranges of the} \\ &\quad \text{coordinates.} \end{aligned}\right. \qquad (22)$$

The integral, A_2, is the integral of $g_2(1, 2)$ over that region where it is different from zero.

$$A_2 = \frac{N_0}{32\pi^2 M_2^2 V}\int\!\!\int\!\!\int_V dXdYdZ \int\!\!\int_{4\pi} \sin\Theta d\Theta d\Phi$$
$$\times\int_0^{\pi/2}\sin\vartheta d\vartheta\int_0^{l\cos\vartheta} r dr\int_0^{2\pi} d\psi\left(\int_{r\tan\vartheta}^{l+r\tan\vartheta} dz\right.$$
$$\left.\times\int_{-d/r\tan\vartheta}^{d/r\tan\vartheta} d\varphi+\int_{-r\tan\vartheta}^{l-r\tan\vartheta} dz\int_{\pi-d/r\tan\vartheta}^{\pi+d/r\tan\vartheta} d\varphi\right), \qquad (23)$$

$$A_2 = \pi N_0 d l^2/4M_2^2. \qquad (24)$$

The evaluation is not difficult, but when l and d are of the same order of magnitude, the result must be taken with a grain of salt because of the approximations in the limits on φ. However these limits should be quite adequate when l is greater than d by a factor of ten or more.

It is interesting to note that A_2 is the same constant for a series of rods of the same diameter but of differing lengths, since in this case M_2 is proportional to l. Such constancy is experimentally found for solutions of homologous linear polymers, but does not appear for solutions of the more compact protein molecules. It will be found to arise again in the theory of chain-molecule solutions which follows.

The tremendous difference between the behavior of A_2 for spherical and elongated molecules is also important. With spherical molecules the deviations from Raoult's law are relatively no greater for large molecules than for small ones. With elongated molecules, however, size alone causes *relatively* larger deviations from ideality.

IV.3. Flexible Chain Molecules

A direct extension of the preceding integration to a flexible chain molecule of n links would be very difficult, since the number of coordinates involved would be at least $3n$. However, with the high polymer molecules usually encountered, their length and flexibility are such that the forces of interaction between two such molecules commonly involve only short lengths of the two chains. The parts of the two chains away from the point of collision are out of each other's force fields and have no direct action on one another.

This picture suggests that the pair interaction integral, A_2, depends on two independent things: a function of the size of the molecules only, and a quantity describing the interaction of short segments of the two chains. The following more detailed analysis supports this idea and gives it precise formulation.

IV.4. The Distribution Function F_2 and the Integral A_2 of a Pair of Chain Molecules

For two molecules in solution the form of the distribution function is:

$$F_2(1, 2) = C^2 \exp\left[-U_2(1, 2)/kT\right], \qquad (25)$$

with a C a normalization constant. The energy quantity $U_2(1, 2)$ is the potential of average force in the infinitely dilute solution.[4,8]

The potential of two isolated molecules, when ordinary van der Waals forces are acting, is known

[8] J. G. Kirkwood, J. Chem. Phys. **3**, 300 (1935).

to be almost exactly representable as the sum of the potentials between pairs of atoms or groups of atoms in the two molecules. This assumption of superposition of potential probably does not hold as well for the potential of average force in liquids, but it is still a common and most useful assumption.[8] If we then divide the molecules into small parts, or "segments," the intermolecular potential will be closely equal to a sum of the interaction potentials of all the pairs of segments formed with one member from each molecule. In addition to this, the total potential must include a term which depends on the shape and internal coordinates of each molecule alone, irrespective of the state of the other. In symbols,

$$U_2(1,2)=U_1(1)+U_2(2)+\sum_{\mu_1=1}^{n}\sum_{\nu_2=1}^{n}u(\mu_1,\nu_2). \quad (26)$$

The functions $U_1(1)$ and $U_1(2)$ are the internal energies of *1* and *2*, respectively, while the functions $u(\mu_1, \nu_2)$ are interaction potentials of segment μ_1 of molecule *1* with segment ν_2 of molecule *2*.

It is necessary to interject here a word about symbolism. In this paper it will often be necessary to distinguish between the coordinates of whole molecules and those of their constituent segments. In general, numerals will be used for whole molecules and Greek letters for segments. Thus (*1*) and (*2*) represent all the coordinates, internal and external, of the molecules *1* and *2*, while (μ) and (ν) represent the same thing for the segments μ and ν. Where it is desired to show that a segment belongs to a particular molecule, the symbol for the molecule will follow that for the segment; thus (μ_1) represents the coordinates of segment μ of molecule *1*. This double symbol will be avoided where there is no danger of ambiguity.

Classical statistical mechanics also states similar equations for F_1.

$$\begin{aligned}F_1(1)&=C\exp\left[-U_1(1)/kT\right];\\ F_1(2)&=C\exp\left[-U_1(2)/kT\right].\end{aligned} \quad (27)$$

If we then define a function $\varphi(\mu, \nu)$, such that

$$\varphi(\mu,\nu)=\exp\left[-u(\mu,\nu)/kT\right], \quad (28)$$

we can write $F_2(1, 2)$ as a product, Eq. (29),

$$F_2(1,2)=F_1(1)F_1(2)\prod_{\mu_1}\prod_{\nu_2}\varphi(\mu_1,\nu_2). \quad (29)$$

It is now desired to transform (29) to a form that separates the interactions of the segments into separate terms.

It was remarked earlier that if *1* and *2* are separated in space by a considerable distance, $F_2(1, 2)$ must be equal to a simple product of $F_1(1)$ and $F_1(2)$, as a result of the lack of long range forces in the liquid.

$$\lim_{r_{12}\to\infty}F_2(1,2)=F_1(1)F_1(2). \quad (30)$$

Therefore,

$$\lim_{r_{\mu\nu}\to\infty}\varphi(\mu,\nu)=1. \quad (31)$$

Let us define by Eq. (32) a function, $\chi(\mu, \nu)$, which bears the same relation to $\varphi(\mu, \nu)$ that g_2 bears to F_2.

$$\varphi(\mu,\nu)=1+\chi(\mu,\nu). \quad (32)$$

If we substitute (32) in (29), and expand the product, we obtain the desired sum, as follows:

$$\begin{aligned}F_2(1,2)=F_1(1)F_2(2)\Big[1&+\sum_{\mu_1}\sum_{\nu_2}\chi(\mu_1,\nu_2)\\ &+\sum_{\kappa_1\le\mu_1;\,\lambda_2\le\nu_2}\sum\sum\chi(\kappa_1,\lambda_2)\chi(\mu_1,\nu_2)+\cdots\Big].\end{aligned} \quad (33)$$

By Eq. (5a) $g_2(1, 2)$ is found.

$$\begin{aligned}g_2(1,2)=F_1(1)F_2(2)\Big[&\sum_{\mu_1}\sum_{\nu_2}\chi(\mu_1,\nu_2)\\ &+\sum_{\kappa_1\le\mu_1;\,\lambda_2\le\nu_2}\sum\sum\chi(\kappa_1,\lambda_2)\chi(\mu_1,\nu_2)+\cdots\Big].\end{aligned} \quad (34)$$

To get A_2, we integrate over $g_2(1, 2)$, eliminating the F_1's from the first term of the sum with the aid of Eq. (4).

$$A_2=-\frac{N_0}{2M_2^2}\left[\sum_{\mu_1}\sum_{\nu_2}\int\chi(\mu_1,\nu_2)d(\nu_2)+\cdots\right]. \quad (35)$$

The exact procedure in eliminating the functions F_1 from one of the terms of the first sum is as follows. With μ_1 held fast the function is integrated over all the other coordinates of molecule *1*. These occur only in the function $F_1(1)$, so that the rest of the integrand is a constant. $F_1(2)$ is treated in a similar way, holding ν_2 fast. The results of these two integrations are unity by Eq. (4). All that remains, then, is the integration of $\chi(\mu, \nu)$ over $d(\mu_1)d(\nu_2)$. If the coordinates of ν_2 are chosen relative to those of μ_1 as origin, so that the relative positions of μ_1 and ν_2 do not change as that of μ_1 is varied, then $\chi(\mu, \nu)$ is independent of the value of the coordinates (μ_1). Hence the integration over μ_1 leads only to the volume, V, as a multiplicative constant.

Up to this point the discussion has been applicable to any type of large molecule. Henceforth we will restrict ourselves more specifically to chain molecules, *all of whose segments are alike.*

The actual size of the segments is still unchosen, however; they may consist of two, four, ten, or more links of the chain, as long as they are replicas of one another.

When the segments are all alike, the integrals $\int\chi(\mu,\nu)d(\nu)$ are identical for all pairs and are a constant which we shall write $\int\chi d\nu$ for brevity. If there are n segments in each of the molecules, there are n^2 pairs formed with one member from each molecule, and A_2 is given by

$$A_2=-\frac{N_0n^2}{2M_2^2}\left(\int\chi d\nu+\cdots\right),$$
$$=-\frac{N_0}{2m^2}\left(\int\chi d\nu+\cdots\right), \tag{36}$$

where $m=M_2/n$ is the molecular weight of a segment.

IV.5. Evaluation of the Constant, $\int\chi d\nu$

As far as $\int\chi d\nu$ itself is concerned, it is possible to evaluate it readily if the segments of the chain can be chosen to be of nearly the same size and shape as the molecules of the solvent.

The functions $\varphi(\mu,\nu)$ are actually defined for liquid solutions only by Eq. (29), but we must nevertheless attempt to evaluate them independently if they are to be of any use. Comparison of Eqs. (28) and (25) suggests that they would be the distribution functions, $F_2(\mu,\nu)$, of the segments μ and ν if μ and ν were cut loose from the rest of their chains and allowed to roam about as free molecules.[9] Therefore,

$$\chi(\mu_1,\nu_2)=g_2(\mu,\nu), \tag{37a}$$

$$-\frac{N_0}{2m^2}\int\chi d\nu=A_{2,\mu\nu}, \tag{37b}$$

where $g_2(\mu,\nu)$ is the g-function and $A_{2,\mu\nu}$ the second osmotic coefficient of two free molecules whose constitution is the same as that of the segments μ_1 and ν_2.

We can now use Eq. (17) for $A_{2,\mu\nu}$ and obtain an expression for $\int\chi d\nu$ in this case where the segments are nearly of the same size as the solvent molecules.

$$N_0\int\chi d\nu=\bar{V}_1(1-\zeta_2). \tag{38}$$

If now the situation is such that the higher integrals in (36) can be neglected, A_2 for the polymer is evaluated:

$$A_2=\frac{\bar{V}_1}{2m^2}(1-\zeta_2). \tag{39}$$

Since the segment molecular weight, m, is not precisely defined, it is more convenient to introduce a dimensionless parameter, β, defined as the ratio of the molecular volume of a segment to that of a solvent molecule. If ρ_2 is the density of the polymer segments, A_2 can be written as follows:

$$A_2=\frac{(1-\zeta_2)}{2\beta^2\bar{V}_1\rho_2^2}. \tag{40}$$

This equation is very similar to one derived by Flory[1] from a quasi-lattice picture; the only difference is that the segment size, β, is squared in our equation whereas it appears to the first power only in Flory's. In view of the rather indefinite meaning of β, however, this is probably not an important difference.

A really serious defect of Eq. (40), at least when applied to solutions where the solvent molecules are small, is the neglect of the higher terms in (36), which, unfortunately, are not so easily evaluated.

IV.6. Discussion of the Higher Segment Interaction Integrals

The significance of the integrals involving products of several χ-functions will become clearer from an examination of the meaning of the various terms in Eq. (33) for the pair distribution function, $F_2(1,2)$. The probability of a given configuration of the two molecules is equal to the product of the internal distribution functions of the two plus a series of correction terms. The first group of these, the double sum over the set of $\chi(\mu,\nu)$, corrects the probability of finding a segment of one molecule at a particular place for the chance that a segment of the other molecule will interfere with its being at that

[9] We are assuming that the breaking of their bonds to set them free would have a negligible effect on the van der Waals and repulsive potentials between μ and ν.

place. The chance that the segment of the other molecule will be there is assumed to be independent of where the remaining segments are. This last assumption obviously requires correction in its turn, since the segments of a molecule are not independent of one another. The correction is made automatically by the succeeding terms in the series; for example, the term $\chi(\kappa_1, \lambda_2)\chi(\mu_1, \nu_2)$ can be considered to describe the effect of the interaction of segments κ_1 and λ_2 on the probability of a meeting between segments μ_1 and ν_2.

Most of these higher integrals must always be small, as can be seen from the following argument: If several pairs of segments are picked at random from two freely coiling chains, in an overwhelming preponderance of the configuration space, at least one pair will be far apart and its χ-function will be zero. As a result the integral over a product of randomly selected χ-functions is chiefly an integral over zero and has a very small value which we will discuss later. Only if the segments are so tied together that when one pair is close the other pairs must be close also is the product of the χ-functions different from zero over an appreciable region. In such a case the integral will not be negligible.

Tying together of this sort can occur if the segments are short and are adjacent to one another on the two chains. It can be seen that when the χ-function between one pair of segments is large as a result of the segments being close, the χ-functions between the neighboring segments will be large also. We might expect then that the integral over this product of χ-functions would be of the same order of magnitude as $\int \chi d\nu$ itself.

Moreover, it may well occur that at least some of the integrals that involve an *even* number of χ-functions will be positive, while $\int \chi d\nu$ and others involving an odd number will be negative (because of the predominately negative character of χ), so that the sum will be smaller than $\int \chi d\nu$ alone. It will be seen that there is both theoretical and experimental evidence for such an effect.

It should be noted that the number of such terms that are tied close together and are not small is proportional to the number, n^2, of pairs of segments that can be formed between the chains, so that even with these terms included A_2 is still practically independent of chain length.

The group of higher terms is thus broken into two subgroups that have similar origins but different effects on A_2. The subgroup we have just considered is proportional to n^2 like the simplest terms, $\sum \int \chi d\nu$; this has the important consequence that A_2 is independent of the molecular weight of the solute. The remaining subgroup, arising from the interactions of distantly connected pairs of segments, will be seen to increase more rapidly with n and to be small for the molecular weights generally investigated. Discussion of these is deferred to Section **VI.2.**

We reemphasize the physical meaning of the important first sub-group of terms. These arise because any pair of segments, e.g., μ_1 and ν_2, are hindered in their motions by interferences between the neighboring segments that are bonded to them. If $\int \chi d\nu$ is negative, meaning that the segments repel one another on the average more than they attract, as is generally the case, the over-all effect of these interferences will be to keep μ_1 and ν_2 apart, thus reducing their contribution to A_2. Therefore it is physically reasonable that many of the terms describing these interferences will be different in sign from $\int \chi d\nu$. The previous neglect of this effect has led to discrepancies between experiment and theory.

It is important to know when this subgroup of the terms after $\sum \int \chi d\nu$ in (36) may be negligible. This will happen if the segments themselves are so long that two adjacent pairs on the two chains are seldom close enough to have their χ-functions simultaneously different from zero. Equation (36) may be restricted to the first term, then, if the segments are many times longer than their width (and the effects discussed in Section **VI.2** are negligible.)

We are thus faced with a dilemma in calculating A_2. If we wish to restrict ourselves to calculating $\int \chi d\nu$, we must divide the chains into long and complicated segments, but if we wish to use small simple segments, we must consider the higher integrals. Two examples will illustrate this point.

Polystyrene,

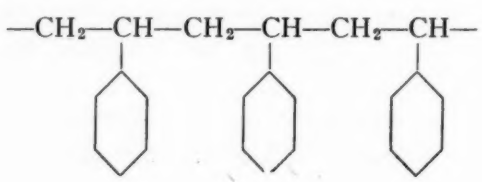

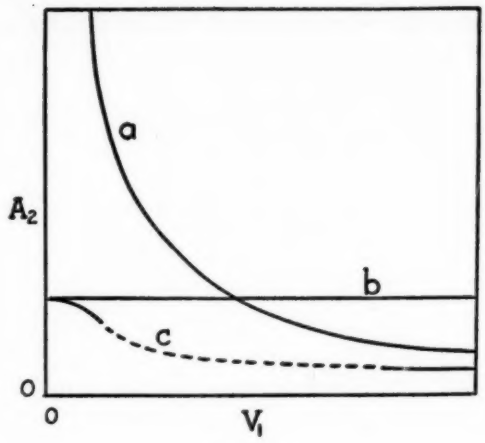

FIG. 2.

dissolves readily in toluene,

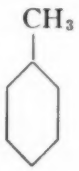

to form solutions in which it would be expected that the heat of dilution, $\Delta\bar{H}_1$, and hence ζ_2, would be very small. It would also seem reasonable to choose the styrene units as the segments, so that β is approximately unity. Nevertheless, Eq. (40) with these constants fails to agree with experimental data quoted in Section V by factors varying from eight to ten. A little consideration shows that it is precisely in a case of this kind where the segments are short and bulky that the higher integrals should be largest.

As a second example, consider the following simple case: A pair of model molecules is made by stringing spherical beads on two straight wires. Let the diameter of the beads be d and the length of the wires be l. There are l/d beads on each wire. Suppose the models to be floating in a continuous fluid. If the beads are taken as the segments, then by (20), (36), and (37),

$$\int \chi d\nu = -4\pi d^3/3,$$

$$A_2 = \frac{N_0(l/d)^2}{2M_2} \cdot \frac{4\pi d^3}{3} = \frac{2\pi N_0 d l^2}{3M_2^2}. \tag{41}$$

However, it is also possible to calculate A_2 approximately from Eq. (24) for a pair of stiff rods, using d as the approximate diameter of the rods. In this case A_2 is found to be $\pi N_0 d l^2/4M_2^2$.

The discrepancy, a factor of about three, must be due to the neglect of the higher terms.

Before further discussion we will develop an alternative approach, useful when the diameter of the chains is much greater than the solvent molecules, in the following section.

IV.7. Evaluation of A_2 for a Chain Molecule in a Continuous Solvent

Let us first find out what happens when a pair of rod molecules, such as were considered in Section **IV.2**, are made flexible by introducing universal joints at intervals along the rods. Provided the segments between the joints are still long enough to be treated as thin rods themselves, the constant $\int \chi d\nu$ is obtained by analogy to Eq. (24) as $\pi d\lambda^2/2$ with λ the length of the segment. Since the segments are long in this case, we can neglect the higher terms and obtain A_2 directly:

$$A_2 = \pi N_0 n^2 d\lambda^2/4M_2^2. \tag{42}$$

But since $n\lambda$ is equal to l, the length of the whole chain,

$$A_2 = \pi N_0 d l^2/4M_2^2. \tag{43}$$

This is identical with formula (24) for a pair of rods without joints. Therefore the introduction of a moderate number of joints in a stiff molecule has no appreciable effect on A_2.[10]

It might be worth while to use this formula, (43), for chain molecules when the solvent molecules are small compared with the diameter of the chain, as, for example, the cellulose esters in volatile solvents.

IV.8. General Discussion

Two formulae have now been derived, each of which is a good approximation to the true formula under different special conditions. Equation (40), involving the neglect of interactions between any groups of segments more complicated than pairs, should work best when the segments are very long and extended compared with their diameters. In this case higher inter-

[10] M. L. Huggins (see reference 2) has arrived at a similar conclusion on the basis of the quasi-lattice picture.

actions are improbable. Since a segment in this equation is defined as the section of polymer chain most nearly equivalent to the solvent molecules in size, Eq. (40) should then be valid in solvents whose molecules are large compared to the diameter of the chain.

On the other hand, the rod formula, Eq. (42), should be true when the polymer chain is moderately extended and the solvent is effectively continuous, that is, consists of molecules much smaller than the diameter of the chain.

The situation is illustrated in Fig. 2, where A_2 for a given polymer is plotted against V_1 for a series of homologous solvents. (The heat coefficient, ζ_2, is assumed to be constant throughout the series.) The curve a is a plot of Eq. (40) (with β assumed constant); the horizontal line b is Eq. (42); the probable course of the true curve is given by c. At very large values of $\bar{V}_1$ the true curve approaches (40) and at small values (42). In the dotted transition region it probably lies below a because of the negative signs of most of the higher integrals in (36). The exact course of the function here can, however, only be guessed at present.

V. COMPARISON WITH EXPERIMENT

V.1. Three General Parameters

Although there is insufficient data in the literature to test all the conclusions drawn from the theory, there is enough to confirm some of its main features. In order to compare different systems on a common basis, it seems best to write A_2 in terms of three experimentally defined parameters, σ, ζ, and λ, corresponding respectively to the entropy, heat and free energy of dilution, as follows:

$$A_2=\frac{\sigma(1-\zeta)}{2\bar{V}_1\rho_2^2}=\frac{\lambda}{2\bar{V}_1\rho_2^2}. \tag{44}$$

The heat coefficient, ζ, is defined as the ratio of the coefficient of c^2 in the expansion of the molar heat of dilution, $\Delta\bar{H}_1$, to the corresponding coefficient in the expansion for $T\Delta\bar{S}_1$. ζ has the special significance of describing the relative contributions of the heat and entropy to the deviation of the free energy of dilution from van't Hoff's law. Experimentally, ζ may be determined from either of the following (equivalent) relations:

$$\zeta=\lim_{c\to 0}\frac{1}{T}\left(\frac{\partial^2\Delta\bar{H}_1}{\partial c^2}\Big/\frac{\partial^2\Delta\bar{S}_1}{\partial c^2}\right), \tag{45a}$$

$$\zeta=T\frac{\partial(A_2/\bar{V}_1)}{\partial T}\Big/\frac{\partial(TA_2/\bar{V}_1)}{\partial T}. \tag{45b}$$

If the segments are chosen so long that higher integrals of the type discussed in Section **IV.6** are negligible, and at the same time the other type of higher integrals which lead to the molecular weight dependence of A_2 discussed in Section **VI.2** are negligible, ζ can be identified with the heat coefficient of the segments, ζ_2, which was employed in developing the theory of the preceding sections. If the higher order interactions are not negligible, as is usually the case in practice, ζ will depend on these interactions and the heat of dilution characteristics of the polymer may not always be identical with those of its small molecule homologues.[11]

On the other hand the parameter, σ, is proportional to the coefficient of the square term in the expansion of $\Delta\bar{S}_1$ in terms of concentration. If the segments are long and the higher integrals negligible, it should be equal to $1/\beta^2$, where β is the ratio of segment to solvent molecule size as used in Eq. (40). In other cases it will depend not only on the size but also on the shape of the segments and where A_2 varies with the molecular weight it will depend on the shape and size of the molecule as a whole (Eq. (60)). Since σ can be considered to be a function of the way in which the segments of one molecule shield each other from other molecules, the name "internal shielding factor" seems appropriate.

In Fig. 2, σ is β^2 times the ratio of the ordinates of curves c and a.

Experimentally, the internal shielding factor,

[11] Cases are well-known where the difference in $\Delta\bar{H}_1$ causes striking differences in the solubility characteristics of the polymer and monomer. This is especially true for highly polar materials, where the intermolecular forces are especially sensitive to small changes in the relative positions of the molecules. For example, polyvinylchloride and polyacrylonitrile are quite insoluble in their respective monomers, although both are amorphous materials and soluble in other solvents. The presence of a double bond, which usually has very little effect on $\Delta\bar{H}_1$, can hardly cause all this difference.

σ, may be defined as follows:

$$\sigma = \lim_{c \to 0} \frac{2\rho_2^2}{R}\left(\frac{\partial^2 \Delta \bar{S}_1}{\partial c^2}\right), \tag{46a}$$

$$\sigma = 2\rho_2^2 \bar{V}_1{}^2 \frac{\partial (TA_2/\bar{V}_1)}{\partial T}. \tag{46b}$$

It seems reasonable that the molecular structure of the solution will be independent of temperature to a first approximation. To the same degree of approximation $\Delta \bar{S}_1$ and $\Delta \bar{H}_1$ will not change with the temperature. Therefore, by Eqs. (45a) and (46a), σ will be constant and ζ will vary as $1/T$.[12]

Thus it appears that ζ is of considerable importance for the description of the nature of the forces between the molecules of the solvent and solute, while σ is principally determined by the shape of the segments.*

The free energy parameter, $\lambda = \sigma(1-\zeta)$, is useful mainly as a dimensionless empirical constant to describe the deviation of the free energy of dilution from the classical ideal solution laws.[13]

V.2. Chain Molecules

Sufficient data are available on at least five systems to calculate the three parameters, λ, σ, and ζ. A_2 has been determined for polyisobutylene in cyclohexane,[14] and polystyrene in toluene.[15]

Table I.

System	Reference	A_2 cm^3 g^{-2}	λ	ζ	σ
Polyisobutylene-Cyclohexane	14				
Fraction B(0-3), Mol. Wt. 844,000		7.1×10^{-4}	0.13	(0)*	0.13
Fraction B(9-13), Mol. Wt. 79,200		7.1×10^{-4}	0.13	(0)*	0.13
Polystyrene (Polymerized at 120°)—Toluene	15				
Fraction 120-1, Mol. Wt. 340,000		3.82×10^{-4}	0.090	(0)*	0.090
Fraction 120-4, Mol. Wt. 108,000		3.72×10^{-4}	0.088	(0)*	0.088
Polystyrene (Polymerized at 180°)—Toluene	15				
Fraction 180-1, Mol. Wt. 169,000		4.78×10^{-4}	0.124	(0)*	0.124
Fraction 180-4, Mol. Wt. 110,000		4.53×10^{-4}	0.118	(0)*	0.118
Rubber-Benzene	16	9.5×10^{-4}	0.12	0.54	0.26
Rubber-Toluene	17	13.4×10^{-4}	0.21	0.3	0.3
Polyvinyl Chloride-2-Butanone	18	4.9×10^{-4}	0.18	0.0	0.18

* The values in parentheses have been estimated to be zero because both components have similar internal pressures.

Although the heat of dilution has not been measured, it is tentatively assigned the value zero because of the non-polar character and chemical similarity of the solvent and solute. On the systems rubber-benzene,[16] rubber-toluene,[17] and polyvinylchloride-methylethylketone,[18] both the osmotic pressure and its temperature coefficient have been determined. The data and values of the parameters are summarized in Table I.

In the first place, A_2 is actually found to be independent of molecular weight in at least two of these systems. In the second place, σ is uniformly much smaller than unity, as would be expected from the argument of the foregoing sections. The values for polystyrene are of particular interest. Since σ is here affected by the method of polymerization of the material, but not by the molecular weight, it follows that the local structure of the chains must depend on the method of polymerization. One is tempted to guess that the higher values of σ, corresponding to smaller amounts of internal shielding, go with the chains that are more extended because of the arrangement of their carbon skeletons.

V.3. Proteins

Although the experimental data on proteins are even less complete than for chain polymers, the following two examples serve to illustrate the osmotic properties of this interesting class of compounds.

[12] T. Alfrey and P. Doty, J. Chem. Phys. **13**, 77 (1945) and W. C. Orr, Trans. Faraday Soc. **40**, 320 (1944) have considered the effect of temperature-sensitive liquid structure on $\Delta \bar{S}_1$ and $\Delta \bar{H}_1$, using the lattice model.

* It may be helpful to point out the significance of the various values of ζ. If $\zeta = 0$, the heat of dilution is zero and the solvent is indifferent to the solute. If ζ is positive, heat is absorbed on dilution, meaning that the solvent and solute molecules tend to associate in groups containing others of their own kind. If $\zeta > 1$, this heat effect contributes more to A_2, which determines the deviations of the free energy from Raoult's law, than the entropy of dilution and the system tends to separate into two phases. (A quantitative discussion of the separation of phases requires the investigation of the higher A_n, which is omitted from this paper, except for the few remarks in section **VI.4.**) On the other hand, if ζ is negative, heat is evolved on dilution and the attraction between unlike molecules is greater than between those of the same kind.

[13] Other authors (references 1 and 2) have introduced a constant, usually designated μ, where $\lambda = 1 - 2\mu$, for the same purpose. If σ were unity, 2μ would equal ζ. Since σ is usually found to be rather far from unity, the author prefers to use λ, which is directly proportional to the deviation in the free energy, rather than μ.

[14] P. J. Flory, J. Am. Chem. Soc. **65**, 372 (1943).

[15] T. Alfrey, A. Bartovics, and H. Mark, J. Am. Chem. Soc. **65**, 2319 (1943).

[16] G. Gee and L. R. H. Treloar, Trans. Faraday Soc. **38**, 147 (1942).

[17] K. H. Meyer and C. G. Boissonnas, Helv. Chim. Acta **23**, 430 (1940)

[18] P. Doty, private communication.

Hemoglobin has been studied by Adair[19] and serum albumin by Burk.[20] The osmotic pressure was measured as a function of concentration at the isoelectric point in strong salt solution, where the long range forces between the protein molecules should be at a minimum. For this reason the heat coefficient, ζ, is probably not large. For purposes of illustration it is assumed to be zero.

Ultracentrifugal measurements in Svedberg's laboratory[21] have shown that both these materials have compact molecules; it is stated that they may be approximated by prolate ellipsoids whose axis ratio is no greater than four. Therefore the internal shielding factor, σ, should be very small, and A_2 should approximate the value of $4N_0v_0/M_2^2$ calculated for spherical molecules (Eq. (21)). From the data given in Table II, it can be seen that the materials behave as predicted.

VI. REFINEMENTS AND EXTENSIONS OF THE THEORY FOR CHAIN MOLECULES

VI.1. Polymers of Heterogeneous Molecular Weight[22]

Since the coefficient A_2 is independent of the molecular weight of the solute to the approximation heretofore considered, it is to be expected that it will be unchanged if the solute is a mixture of chain molecules differing only in length. This can, however, be proved directly, as will be shown now.

McMillan and Mayer[4] give an equation for the osmotic pressure of a solution of mixed solutes

TABLE II.

Substance	Reference	Solvent	A_2 cm³ g⁻²	σ	$4N_0v_0/M_2$*
Hemoglobin (Mol. Wt. 67,000)	19	KH_2PO_4, 0.033M; Na_2HPO_4, 0.033M; KCl, 0.1M, in Water; pH 6.8	5.6×10^{-5}	0.0037	4.4×10^{-5}
Serum Albumin (Mol. Wt. 75,000)	20	$(NH_4)_2SO_4$, 0.74M; 0.05M Acetate Buffer in Water; pH 4.8	6.5×10^{-5}	0.0043	4.0×10^{-5}

* The volume per unit molecular weight, v_0, was calculated from a partial specific volume of 0.75.

which can be written as follows:

$$\pi=RT[\textstyle\sum_i c_i/M_i+\sum_i\sum_j A_{ij}c_ic_j+\cdots]; \quad (47)$$

c_i is the concentration of the ith species of solute, whose molecules consist here of chains of n_i links, M_i is its molecular weight, and the coefficients A_{ij} are defined by the following equation:

$$A_{ij}=-\frac{N_0}{M_iM_jV}\int g_2(i,j)d(i)d(j). \quad (48)$$

Here i stands for a molecule of the ith species and j for one of the jth species.

By applying exactly the same procedure as previously, these coefficients are immediately found to be

$$A_{ij}=-\frac{N_0}{2m^2}\int\chi dv. \quad (49)$$

Inserting these values in (47) the desired relation is obtained.

$$\pi=RT\left[\sum_i c_i/M_i+\frac{N_0}{2m^2}\left(-\int\chi dv\right)\times(\textstyle\sum_i\sum_j c_ic_j)+\cdots\right], \quad (50)$$

$$\pi=RT\left[c/\bar{M}+\frac{N_0}{2m^2}\left(-\int\chi dv\right)c^2+\cdots\right]; \quad (51)$$

$c=\sum c_i$ is the total concentration and

$$\bar{M}=\textstyle\sum c_i/\sum c_i/M_i=\sum N_iM_i/\sum N_i$$

(where $N_i=c_i/M_i$ is the number of moles of the ith species present) is the so-called "number-average" molecular weight.

VI.2. Dependence of A_2 on Molecular Weight

Previously we have considered only the integral of terms of the type $\chi(\mu,\nu)$ and those of the higher terms whose χ-functions were closely tied together by the chain skeleton. The question now arises as to what effect the interaction of segments far down the chains from the two involved in $\chi(\mu,\nu)$ has on the over-all integral, A_2. Any one of these terms will be small as a result of the argument in Section **IV.6**, but there are very large numbers of them.

[19] G. S. Adair, Proc. Roy. Soc. London **120A**, 573 (1928).
[20] N. F. Burk, J. Biol. Chem. **98**, 353 (1932).
[21] T. Svedberg and K. O. Pedersen, *The Ultracentrifuge* (Oxford University Press, Oxford, 1940).
[22] Lattice theory discussions of this topic have been given by P. J. Flory, J. Chem. Phys. **12**, 425 (1944) and by R. L. Scott and M. Magat, *ibid.* **13**, 172 (1945).

Intuitively it can be seen that the more tightly the chains are curled, the more important will be terms of this type, involving the interaction of distant segments. This conclusion is supported by the calculation of the following section, which predicts that A_2 will depend on the molecular weight to a degree determined by the internal distribution function, that is, the average shape, of the molecules. The group of terms we now desire to evaluate in Eq. (35) begins with the following quadruple sum,

$$\sum_{\kappa_1 \leq \mu_1;\ \lambda_2 \leq \nu_2} \sum \sum \sum \frac{1}{V} \int\int \cdots \int F_1(1) F_1(2) \times \chi(\kappa_1, \lambda_2)\chi(\mu_1, \nu_2) d(1) d(2), \quad (52)$$

in which μ_1 and ν_2 are not simultaneously equal to κ_1 and λ_2, respectively. Consider a typical term of this sum. The integral may obviously be factored as shown:

$$\frac{1}{V} \int \left[\int F_1(1) d(1-\kappa, \mu) \right] \times \left[\int F_1(2) d(2-\lambda, \nu) \right] \times \chi(\kappa_1, \lambda_2)\chi(\mu_1, \nu_2) d(\kappa_1) d(\mu_1) d(\lambda_2) d(\nu_2). \quad (53)$$

(The symbol $(1-\kappa, \mu)$ stands for all the coordinates of molecule *1* except those involving segments κ and μ.) By definition (in analogy to Eq. (3)) the partial integral $\int F_1(1) d(1-\kappa, \mu)$ is the distribution function of segments κ and μ with respect to one another, averaged over all the positions of the other segments. If κ and μ are separated by several links of the chain, this distribution function must be the well-known Gaussian distribution widely used in the theory of rubber elasticity.[23] Therefore,

$$\int F_1(1) d(1-\kappa, \mu) = (3/2\pi R_{\kappa\mu}^2)^{\frac{3}{2}} \times \exp(-3r_{\kappa\mu}^2/2R_{\kappa\mu}^2). \quad (54)$$

In this equation $r_{\kappa\mu}$ is the distance between segments κ and μ, while $R_{\kappa\mu}$ is the root-mean-square value of this distance, that is $R_{\kappa\mu}$ satisfies the identity

$$R_{\kappa\mu}^2 = (3/2\pi R_{\kappa\mu}^2)^{\frac{3}{2}} \int_0^\infty 4\pi r_{\kappa\mu}^4 \times \exp(-3r_{\kappa\mu}^2/2R_{\kappa\mu}^2) dr_{\kappa\mu}. \quad (55)$$

A similar equation holds for the segments λ and ν, provided there are several links of the chain of molecule *2* between them.

In order to simplify the integral further, use may be made of the special properties of the χ-functions. In (53) we hold the position of segment κ fixed and integrate over the positions of segment λ. In the first place, $\chi(\kappa, \lambda)$ is zero except in the narrow region where λ is very close to κ; in the second place, the only other part of the integrand that depends on the position of λ, $\int F_1(2) d(2-\lambda, \nu)$, is a slowly varying function of (λ) and therefore may be considered to be a constant for practical purposes whenever $\chi(\kappa, \lambda)$ is different from zero. As a result the integration over the positions of λ may be considered to involve $\chi(\kappa, \lambda)$ alone in the integrand. A similar conclusion is reached concerning segment ν if segment μ is considered fixed. Also, it is noticed that $r_{\lambda\nu}$ must nearly equal $r_{\kappa\mu}$, since either $\chi(\kappa, \lambda)$ or $\chi(\mu, \nu)$ will be zero if this is not so.

Making use of these facts, together with Eq. (54), the integral (53) can now be written in a manageable form, as follows:

$$4\pi \left(\int \chi d\nu \right)^2 \left(\frac{3}{2\pi R_{\kappa\mu} R_{\lambda\nu}} \right)^3 \int_0^\infty r_{\kappa\mu}^2 \times \exp\left\{ -\left[\frac{3(R_{\kappa\mu}^2 + R_{\lambda\nu}^2) r_{\kappa\mu}^2}{2R_{\kappa\mu}^2 R_{\lambda\nu}^2} \right] \right\} dr_{\kappa\mu}. \quad (56)$$

(Choosing the coordinates of the segment κ as the origin for all the other coordinates of the system, it is obvious that the integrand as a whole will not depend on (κ); therefore the integration over (κ) yields a factor V which cancels that in the denominator of (53). The coordinates of segment μ are now referred to those of κ as origin and are therefore written explicitly in polar form as $4\pi r_{\kappa\mu}^2 dr_{\kappa\mu}$).

It may be objected that these two approximations (of using Eq. (54) for the internal distribution functions and assuming that they vary negligibly slowly compared to the χ-functions)

[23] W. Kuhn, Kolloid Zeits. **68**, 2 (1934).

are not valid for those quartets of segments of which any pair are close together on one chain. This is quite true, if the segments are short, as has been remarked previously, but if the segments are long, the size of all such terms is small compared to the aggregate of the terms for which all segments on the same molecule are separated by a considerable length of chain and for which these approximations hold. *Therefore it is to be understood in this section that the χ-functions refer to long segments.* The definition of a segment as the part of chain most nearly equivalent to a solvent molecule, which was used conveniently elsewhere, does *not* apply here.

Equation (56) may be integrated immediately to give:

$$\left[\frac{3}{2\pi(R_{\kappa\mu}^2+R_{\lambda\nu}^2)}\right]^{\frac{1}{2}}\left(\int\chi d\nu\right)^2. \qquad (57)$$

It is now necessary to subject this expression to the quadruple summation indicated in (52). The variables in this process are the root-mean-square distances, $R_{\kappa\mu}$ and $R_{\lambda\nu}$. It is well known[23] that the squares of these are proportional to the number of segments between κ and μ, or between λ and ν, if the chains are flexible enough to coil at random. In other words, if the segments are numbered consecutively,

$$R_{\kappa\mu}^2=b^2(\mu-\kappa). \qquad (58)$$

The proportionality constant, b, is related to the microscopic structure of the chains. We can now replace the sum by an integral and finish the calculation by simple calculus.

$$(3/2\pi b^2)^{\frac{1}{2}}\left(\int\chi d\nu\right)^2\sum_{\kappa\leq\mu;\,\lambda\leq\nu}\sum\sum\sum\sum 1/(\mu-\kappa+\nu-\lambda)^{\frac{1}{2}}$$

$$=(3/2\pi b^2)^{\frac{1}{2}}\left(\int\chi d\nu\right)^2\int_0^{\mu}d\kappa\int_0^{n}d\mu$$

$$\times\int_0^{\nu}d\lambda\int_0^{n}1/(\mu-\kappa+\nu-\lambda)^{\frac{1}{2}}d\nu$$

$$=(4/15)(28-16\sqrt{2})(3/2\pi b^2)^{\frac{1}{2}}n^{5/2}\left(\int\chi d\nu\right)^2$$

$$=0.47n^{5/2}b^{-3}\left(\int\chi d\nu\right)^2. \qquad (59)$$

When this is introduced into Eq. (36) the following amplification of our previous expression for A_2 results:

$$A_2=-\frac{N_0}{2m^2}$$

$$\times\left[1+0.47\frac{M_2^{\frac{1}{2}}\int\chi d\nu}{m^{\frac{1}{2}}b^3}+\cdots\right]\int\chi d\nu. \qquad (60)$$

Although this equation should not be considered fit for quantitative use until some of the succeeding terms in the series are worked out, it at least shows roughly how A_2 depends on the solute molecular weight. The extent to which this dependence is significant is determined not only by the molecular weight itself but also by the size of the chain-stiffness parameter, b. It is possible, therefore, that A_2 might yield interesting information on the extension of the chains.

However, there seems to be no experimental evidence in the literature to indicate that A_2 depends on M_2 to an important extent. This can only be true if b^3 is larger than $\int\chi d\nu$ by a factor greater than $(M/m)^{\frac{1}{2}}$. It has been calculated,[23] however, that if there were free rotation about the bonds in the backbone of the chain, b should be of the order of magnitude of the length of one of these bonds. We have seen that $\int\chi d\nu$ is generally somewhat smaller than the molecular volume of the solvent, which would be of the order of magnitude of b^3. The fact that a marked change of A_2 with the molecular weight has not been observed is therefore evidence that free rotation about the chain bonds is not of common occurrence.

VI.3. Effect of Branching of the Chains

It is apparent that the presence of a moderate amount of branching in a chain molecule would not affect $\int\chi d\nu$, which depends only on the constitution of the segments. It would, however, increase the dependence of A_2 on the molecular weight, being similar in effect to a tighter coiling of the chain.

The theory therefore predicts a continuous change in the properties of A_2 as the shape of the molecules is varied. When the molecules are rods

or extended chains, the intermolecular interaction is mainly through pairs of segments, so that A_2 is large and independent of the molecular weight in an homologous series. When chain molecules become less extended and more compact, either because of coiling or branching, A_2 is decreased algebraically and becomes dependent on the molecular weight. At the extreme of compactness we have solid spherical molecules (Section **IV.1**), where A_2 is relatively small and varies inversely as the molecular weight.

VI.4. The Coefficient A_3

An equation for A_3 may be obtained from the general form given by McMillan and Mayer (Eq. (7b) of this paper). In the present case where the intermolecular potential is expressed as a sum of pair terms this reduces to

$$A_3=-\frac{N_0}{3M_2{}^3V}\times\int\frac{g_2(1,2)g_2(2,3)g_2(3,1)}{F_1(1)F_1(2)F_1(3)}d(1,2,3). \quad (61)$$

If the expanded form (34) of g_2 is introduced and the same simplifications carried through as before, A_3 can be expanded in series as follows.

$$A_3=-\frac{N_0{}^2}{3M_2{}^3V}\Big[n^3\int\chi(\lambda_1,\mu_2)\chi(\mu_2,\nu_3)\chi(\nu_3,\lambda_1)d(\lambda_1,\mu_2,\nu_3)+\sum_{\kappa_1\le o_1;\,\lambda_2\le\mu_2;\,\nu_3\le\xi_3}\sum\sum\sum\sum\sum\sum\int F_1(1)F_1(2)F_1(3)\chi(\kappa_1,\lambda_2)\chi(\mu_2,\nu_3)\chi(\xi_3,o_1)d(1,2,3)+\cdots\Big]. \quad (62)$$

By an analogous argument to that in Section **IV.5** the integral in the first term is approximately the coefficient A_3 for a solution of free molecules whose constitution is the same as that of the segments of the polymer. This coefficient is therefore given by Eq. (17) for regular solutions. When we substitute it in Eq. (62) for A_3 for the polymer we get

$$A_3=\frac{\bar V_1{}^2(1-\zeta_3)}{3m^3}-\frac{N_0{}^2}{3M_2{}^3V}\Big(\Sigma\cdots\int\cdots\Big). \quad (63)$$

The first term in this equation may thus be handled in a way analogous to that used for the expression $\int\chi d\nu$ which was encountered in A_2. This is likewise the only term in A_3 obtained by the quasi-lattice method (as used at present; see especially Huggins[2]).

As with A_2, there are also numerous higher terms whose importance may be considerable. In addition to those whose χ-functions are associated with segments adjoining each other on the chains, and which can be absorbed into the first term if the segments are made long enough, there is another group, the sixfold sum in Eq. (61), associated with segments far removed from each other. Presumably this group can be treated by the same methods used on the similar group in A_2 (Section **VI.2**), and will depend similarly on the lengths and the internal distribution functions of the chains. The integrations have not been carried out, but one fact is immediately evident; this group in A_3 is proportional to $(\int\chi d\nu)^3$, just as the corresponding group in A_2 was proportional to $(\int\chi d\nu)^2$. As the first step in simplifying the integrals the χ-functions are assumed to vary rapidly as compared to the internal distribution functions, F_1. The integral can therefore be factored and the integrations over the χ-functions carried out separately, leading to $(\int\chi d\nu)^3$ as a factor.

It seems probable in view of these results that not only A_2 and A_3, but also all the higher A_n, are closely related to one another in value, and may perhaps all be characterized by a small number of parameters, or even only one. Huggins[2] and Gee[24] have indeed shown that one parameter is sufficient to describe the deviations from ideality of the experimental data of several rubber-solvent systems over a wide range of concentrations.

ACKNOWLEDGMENT

The author gratefully wishes to acknowledge the continued interest in this work of Professor Walter H. Stockmayer of the Massachusetts Institute of Technology. It was originally planned to write this paper in collaboration, but the obstacles interposed by the distance between Cambridge and New York have proved insurmountable.

[24] G. Gee, Trans. Faraday Soc. **41**, 345 (1945).

THE JOURNAL OF CHEMICAL PHYSICS VOLUME 14, NUMBER 3 MARCH, 1946

The Statistical Mechanical Theory of Transport Processes

I. General Theory

JOHN G. KIRKWOOD
Baker Laboratory, Cornell University, Ithaca, New York

(Received October 13, 1945)

See Errata p. 347

Outlines are sketched for a general statistical mechanical theory of transport processes; e.g., diffusion, heat transfer, fluid flow, and response to time-dependent external force fields. In the case of gases the theory leads to the Maxwell-Boltzmann integro-differential equation of transport. In the case of liquids and solutions, it leads to a generalized theory of Brownian motion, in which the friction constant is explicitly related to the intermolecular forces acting in the system. Specific applications are postponed for treatment in later articles.

I. INTRODUCTION AND GENERAL THEORY

Part A: Introductory Remarks

THE equilibrium theory of statistical mechanics has achieved a satisfactory general formulation at the hands of Gibbs and of later investigators. It provides a systematic interpretation from the molecular standpoint of the equilibrium behavior of thermodynamic systems. Of equal physico-chemical importance are the irreversible processes by which thermodynamic systems attain equilibrium in response to changes in external restraints. In addition to chemical reaction, the most common irreversible processes are the transport processes; diffusion, heat transfer, fluid flow, and response to external forces dependent upon time. Although much has been written on the interpretation of transport processes from the molecular standpoint, no systematic statistical mechanical theory has yet been formulated. In the present article, we shall suggest certain lines of thought on which we believe such a general theory of transport processes might be based. Since we shall formulate the theory within the frame of classical statistical mechanics, we shall not treat chemical reactions, which require the introduction of quantum-mechanical ideas and which are tolerably well described by the transition state theory of Eyring and Polanyi.[1] Quantum-mechanical generalization of the methods to be discussed will be postponed for later treatment.

Since the literature on transport processes is extensive and varied, we shall give here only a few key references and limit our preliminary remarks to a brief mention of the principal methods which have been used in investigating them. An exact and rigorous theory of transport exists for gases at sufficiently low density to be amenable to binary collision analysis. This theory is based upon the Maxwell-Boltzmann integro-differential equation, the consequences of which have been worked out in detail by Chapman and Enskog.[2] A satisfactory theory also exists for transport in dilute solutions, based upon the theory of Brownian motion, the foundations of which are due to Einstein.[3] The theory has been used very successfully in the treatment of irreversible processes in electrolyte solutions by Debye, Onsager, Falkenhagen, and others.[4] Recently Chandrasekar[5] has written an elegant review of the foundations and methods of the theory of Brownian motion, containing many new results, as well as an extensive bibliography. Although self-consistent, the theory of Brownian motion suffers from the defect that it contains an empirical friction constant related to intermolecular forces and molecular structure in a manner not described by the theory. A semi-phenomenological discussion of the Thomson reciprocal relations in coupled transport processes has been given by Onsager[6] and is recommended

[1] See Gladstone, Laidler, and Eyring, *Theory of Rate Processes* (McGraw-Hill Book Company, Inc., New York, 1941).

[2] See Chapman and Cowling, *The Mathematical Theory of Non-Uniform Gases* (Cambridge University Press, New York, 1939).

[3] Einstein, Ann. d. Physik **17**, 549 (1905); **19**, 371 (1906).

[4] See L. Onsager and R. T. Fuoss, J. Phys. Chem. **36**, 2689 (1932).

[5] S. Chandrasekar, Rev. Mod. Phys. **15**, 1–89 (1943).

[6] L. Onsager, Phys. Rev. **37**, 405 (1931); **38**, 2265 (1931).

for its perspectives on the general aspects of the problem of transport. Finally, there have been developed numerous model theories of transport processes, which are based upon simplified representations of the underlying elementary mechanisms. Significant results along these lines have been obtained in recent years by Eyring[1] and his co-workers using the transition state theory.

In the theoretical developments to be presented here, we shall attempt to integrate many of the ideas latent in the kinetic theory of gases and in the theory of Brownian motion into a systematic formulation. Although the notation is necessarily rather complicated, we have written from the physical rather than the mathematical standpoint. Although many mathematical problems are raised, the solution of which would require special and detailed investigation, none but relatively simple mathematical operations are employed in the development of the theory.

Part B: Basic Concepts and Definitions

The macroscopic state of a system of molecules is specified by a small number of molar variables, for example temperature, composition, and parameters of external force. Since its dynamical state is incompletely defined by the molar variables, the macroscopic behavior of the system requires interpretation from the standpoint of statistical mechanics, if a description in molecular terms is desired.

On the other hand, a phenomenological description of macroscopic behavior, without reference to the molecular structure of the system, is possible. Equilibrium behavior is described by thermodynamics. When the values of the molar variables are inconsistent with the conditions for thermodynamic equilibrium, transport processes occur, for example diffusion, heat transfer, and fluid flow. The most common transport processes are macroscopically described by the hydrodynamic equations of continuity, motion, and energy transport, supplemented by certain empirically established relations connecting the mass and heat currents and the stress tensor with the gradients of the molar variables or functions of those variables, for example, the chemical potential gradients, temperature gradient, and rate of strain. The supplementary relations, constituting in their simplest form the laws of diffusion, heat conduction, and viscous fluid flow, contain certain material constants, the coefficients of diffusion, thermal conductivity, and viscosity, which depend upon the local macroscopic state of the system. The differential equations of transport, together with a specification of initial and boundary values of the molar variables, determine the macroscopic state as a function of time and position in the interior of the system.

The principal objectives of the statistical mechanical theory of transport are the formulation of the macroscopic differential equations of transport from the standpoint of molecular dynamics, the investigation of the limits of validity of the empirical laws of diffusion, heat conduction, and viscous flow, and the determination of the coefficients of diffusion, thermal conductivity, and viscosity, from the structure of the system on the molecular scale in terms of the forces acting between the molecules of which it is composed. A second important objective is the molecular interpretation of the linear stimulus-response theory* (based upon the concept of a relaxation time spectrum), describing departures from thermodynamic equilibrium, produced by time dependent external forces. This aspect of the theory is pertinent to such important problems as those of dielectric and mechanical loss.

As a preliminary step in the formulation of the theory of transport, it is necessary to examine the operation of measurement of a property in a system, the macroscopic state of which is changing with time. Since the dynamical state of a system of many degrees of freedom is incompletely defined by the small number of molar variables characterizing its macroscopic state, the first step in an operation of measurement consists in sampling a system at time t from an ensemble representing an initial distribution among accessible microscopic dynamical states. Although the initial distribution is arbitrary, we shall generally be concerned with distributions departing but slightly from statistical equilibrium, to be represented by the canonical or

* See, for example, Kármán and Biot, *Mathematical Methods in Engineering* (McGraw-Hill Book Company Inc., New York, 1940), Chap. X.

microcanonical ensembles of Gibbs, according to convenience. The second step in the operation or measurement consists in recording a time average of the property in question in the sample of the ensemble,** with specified dynamical state at time t, over an interval of time τ, macroscopically short, but microscopically long in a sense presently to be made more precise. If, as is customarily true for systems of many degrees of freedom, the fluctuation of the time averaged property in the ensemble is sufficiently small, the complete operation of measurement yields a value differing by quantities of negligible order from a group average in the ensemble of the time average of the property over a microscopically long but macroscopically short interval τ. A third averaging operation is occasionally necessary, if the property in question is a point function in the three-dimensional configuration space of an individual molecule. This is an average over a macroscopically small domain of configuration space having a representative linear dimension large relative to the range of intermolecular force. The latter average is necessary in the formulation of the hydrodynamic equations of motion and energy transport and in the definition of such quantities as the stress tensor and the heat current.

Although we are forced to defer a detailed analysis of the time average and the magnitude of the interval τ until after the quantitative aspects of the theory have been developed, a few comments seem desirable at this point. To obtain an adequate macroscopic description of the secular variation of the observable properties of a system, it is necessary to select τ of sufficient magnitude to smooth out microscopic fluctuations in molecular distribution. For systems of suitable dynamical structure, the macroscopic description will then be independent of τ, as long as the periods of secular variation are long relative to τ. In the case of gases of such low density that molecular motion can be adequately analyzed in terms of binary collisions, the general theory leads to the Maxwell-Boltzmann integro-differential equation. Here it is obvious that τ must be long relative to the duration of a representative collision. In the case of liquids and liquid solutions where the collision analysis fails or becomes unduly complicated, the general theory may be cast in the form of the theory of Brownian motion, but extends this theory by explicitly relating the friction constant to the intermolecular forces acting in a system of molecules. Here it is found that τ must be long relative to the interval within which there is appreciable correlation between the total intermolecular force acting on a representative molecule at the beginning and end of that interval.

In classical statistical mechanics the dynamical states of a system of N molecules constitute a phase space and the ensemble representing a distribution in initial conditions, incompletely specified by the molar variables, is characterized by a probability density $f^{(N)}(\mathbf{p}, \mathbf{q}; t)$ in phase space, $\mathbf{p}$ representing the momentum coordinates and $\mathbf{q}$ the configuration coordinates of the system. In order to simplify our analysis somewhat, we shall suppose that the molecules possess only translatory degrees of freedom. The vector $\mathbf{p}$ is then defined in $3N$-dimensional momentum space and is composed of N vectors $\mathbf{p}_1 \cdots \mathbf{p}_N$, its projections on the 3-momentum spaces of the several molecules. Likewise $\mathbf{q}$ is a vector in $3N$-dimensional configuration space with components $\mathbf{R}_1, \cdots \mathbf{R}_N$ specifying the positions of the molecular centers of gravity in the 3-configuration spaces of the several molecules. The extension of the results which we shall obtain to molecules possessing internal degrees of freedom, for example rotational, will be obvious providing such internal degrees of freedom

** From the logical point of view, we shall regard the class of macroscopic properties to be defined by the two operations described. That properties experimentally defined by thermodynamic measurements fall into this class, and involve the time as well as group average is fairly obvious. For example, instruments designed for the measurement of a representative property such as the pressure in a fluid in equilibrium automatically record a time average over an interval of the order of magnitude, say, of a second, a millisecond, or perhaps a microsecond. If the area of the surface on which the normal force is recorded is sufficiently small and the time resolution of the instrument sufficiently fine, fluctuations will of course be observed which are independent of the characteristics of the instrument. These fluctuations are, as is well known, responsible for the Brownian motion of colloidal particles. With sufficiently fine resolution, the force acting on unit area, therefore, ceases to be a macroscopic property in the sense in which we have defined this class. Thus, when we speak of pressure in a fluid as a macroscopic property, we mean the normal force per unit area averaged over a macroscopic interval of time of such a magnitude that the recorded average is not sensibly dependent on the magnitude of the interval.

are of the low frequency type in the sense of van Vleck and are therefore amenable to classical statistics to an adequate degree of approximation.

We shall denote by $\mathbf{X}_i$, dependent only on the coordinates of that molecule, the external force acting on a molecule i of the system. If $\mathbf{X}_i$ is time dependent, we shall suppose that this dependence is secular, that is to say, $\mathbf{X}_i$ is not sensibly affected by an average over the microscopic interval τ. We shall denote by $\mathbf{F}_i$ the intermolecular force exerted on a specified molecule i by the other molecules of the system. Although many of our results will be independent of the assumption, we shall further assume that the potential of intermolecular force $V^{(N)}$ has the form

$$V^{(N)}=\sum_{k<l} V_{kl}(R_{kl}),$$
$$R_{kl}=|\mathbf{R}_l-\mathbf{R}_k|, \tag{1}$$

where V_{kl} depends only on the distance R_{kl} of the molecular pair consisting of molecules of types k and l. For the potential of Eq. (1), the intermolecular force is expressible in the form,

$$\mathbf{F}_i=\sum_{l=1\neq i}^{N}\mathbf{F}_{li},$$
$$\mathbf{F}_{li}=-\nabla_l V_{li}=(\mathbf{R}_{il}/R_{il})\frac{dV_{il}}{dR_{il}}, \tag{2}$$
$$\mathbf{R}_{il}=\mathbf{R}_l-\mathbf{R}_i.$$

By Liouville's theorem, embodying the equation of continuity in phase space and the laws of mechanics, it is well known that the probability distribution function, $f^{(N)}(\mathbf{p},\mathbf{q};t)$, satisfies the partial differential equation,

$$Lf^{(N)}+i\frac{\partial f^{(N)}}{\partial t}=0,$$
$$L=i\sum_{l=1}^{N}\left\{\frac{\mathbf{p}_l}{m_l}\cdot\nabla_{\mathbf{R}l}+(\mathbf{X}_l+\mathbf{F}_l)\cdot\nabla_{\mathbf{p}l}\right\}, \tag{3}$$

where m_l is the mass of molecule l. By introducing the factor i, the imaginary unit, the operator L is made self-adjoint when applied to a suitably restricted class of functions, a property to be used at a later stage of our discussion. Although $\mathbf{X}_l$ might be defined to include wall forces confining each molecule to a finite region of configuration space, say the interior of a containing vessel, we shall not include these forces in $\mathbf{X}_l$, but shall take them into account by requiring $f^{(N)}$ to vanish exterior to a region of volume v in the configuration space of each molecule, bounded by the walls of the container.

The characteristics of the partial differential Eq. (3) have the equations of motion of the dynamical system.

$$m_l(d\mathbf{R}_l/dt)=\mathbf{p}_l,$$
$$(d\mathbf{p}_l/dt)=\mathbf{X}_l+\mathbf{F}_l, \tag{4}$$
$$(d/dt)=(\partial/\partial t)_{\mathbf{p}0\mathbf{q}0},$$

where $\mathbf{p}_0$ and $\mathbf{q}_0$ are the coordinates of the system at an arbitrarily selected initial instant of time. If the ensemble is viewed from the hydrodynamical standpoint $\mathbf{p}_0$ and $\mathbf{q}_0$ may also be interpreted as the Lagrange coordinates of an element of the representative fluid in phase space.

The solutions of the partial differential Eq. (3) may be expressed in the form,

$$f^{(N)}(\mathbf{p},\mathbf{q};t+s)=f^{(N)}(\mathbf{p}_0,\mathbf{q}_0;t),$$
$$\mathbf{p}=\exp(-isL_0)\mathbf{p}_0, \tag{5}$$
$$\mathbf{q}=\exp(-isL_0)\mathbf{q}_0,$$

where the operator $\exp(-isL_0)$ is defined as follows.* If $\varphi(\mathbf{p},\mathbf{q})$ is a function of $\mathbf{p}$ and $\mathbf{q}$ not explicitly dependent on time,

$$\psi(\mathbf{p}_0,\mathbf{q}_0;s)=\exp(-isL_0)\varphi(\mathbf{p}_0,\mathbf{q}_0), \tag{6}$$

is defined as the solution of the partial differential equation

$$i(\partial\psi/\partial s)=L_0\psi,$$
$$\psi(\mathbf{p}_0,\mathbf{q}_0;0)=\varphi(\mathbf{p}_0,\mathbf{q}_0), \tag{7}$$

which satisfies the initial condition $\psi_0=\varphi$. In domains of phase space free from singularities of L_0, the formal power series,

$$\exp(-isL_0)=\sum_{n=0}^{\infty}\frac{(-is)^n}{n!}L_0{}^n, \tag{8}$$

may frequently be employed to obtain useful

---

* We note that the operator L of Eq. (3) is a function

$$L(\mathbf{p},\mathbf{q},\nabla_p,\nabla_q)$$

of $\mathbf{p}$, $\mathbf{q}$, ∇_q, and ∇_p. By L_0 we mean

$$L(\mathbf{p}_0,\mathbf{q}_0,\nabla_{p_0},\nabla_{q_0})$$

where $\mathbf{p}_0$ and $\mathbf{q}_0$ are the Lagrange coordinates of the system at an arbitrary initial instant t preceding the interval s under discussion.

results. We note also the property

$$\exp(-isL_0)\varphi(\mathbf{p}_0, \mathbf{q}_0) = \varphi(\mathbf{p}, \mathbf{q}),$$
$$\mathbf{p} = \exp(-isL_0)\mathbf{p}_0, \qquad (9)$$
$$\mathbf{q} = \exp(-isL_0)\mathbf{q}_0.$$

The mathematical theory of the operator $\exp(-isL_0)$ may be formulated from a rigorous standpoint by the methods of spectral theory in Hilbert space.[7] In the analysis to follow, we shall find it sufficient to use the formal operator notation without reference to spectral theory. It should be remembered that explicit application of the operator $\exp(-isL_0)$ requires the construction of the solutions of the equations of motion, Eq. (4), and that the operation is merely a symbolic expression of the finite transformation, associated with the infinitesimal transformation L_0, implied in the solution of the equations of motion. An additional property, which will presently be used, is embodied in the well-known statement of Liouville's theorem that the transformation determinant or Jacobian for $\mathbf{p}_0 \rightarrow \mathbf{p}$; $\mathbf{q}_0 \rightarrow \mathbf{q}$ is unity

$$[\partial(\mathbf{p}, \mathbf{q})]/[\partial(\mathbf{p}_0, \mathbf{q}_0)] = 1, \qquad (10)$$

which follows from the fact that $\exp(-isL_0)$ is a contact transformation.

We now proceed to formulate the averaging operations implied in a macroscopic measurement of a property, $\varphi(p, q)$ not explicitly dependent on time. The time average over the microscopic interval τ will be denoted by α_τ and is expressible in the form

$$\alpha_\tau\varphi = \frac{1}{\tau}\int_0^\tau \varphi(\exp(-isL_0)\mathbf{p}_0, \exp(-isL_0)\mathbf{q}_0)ds, \qquad (11)$$

where $\mathbf{p}_0$ and $\mathbf{q}_0$ are the coordinates of the system at time t. The average in the ensemble from which the system is sampled for observation will be denoted by α_ϵ and is expressible in the form

$$\alpha_\epsilon\varphi = \int\int \varphi(\mathbf{p}_0, \quad) f^{(N)}(\mathbf{p}_0, \mathbf{q}_0; t)d\mathbf{p}_0 d\mathbf{q}_0. \qquad (12)$$

at time t, where $d\mathbf{p}_0$ and $d\mathbf{q}_0$ denote volume elements in momentum and configuration space.

[7] von Neumann, Proc. Nat. Acad. Sci. **18**, 70 (1932); Koopman and von Neumann, Proc. Nat. Acad. Sci. **18**, 255 (1932).

We identify the observed value $(\varphi)_{\text{obs}}$ with $\alpha_\epsilon\alpha_\tau\varphi$

$$(\varphi)_{\text{obs}} = \alpha_\epsilon\alpha_\tau\varphi,$$
$$\alpha_\epsilon\alpha_\tau\varphi = \frac{1}{\tau}\int\int\int_0^\tau \varphi[\exp(-isL_0)\mathbf{p}_0, \exp(-isL_0)\mathbf{q}_0]f^{(N)}(\mathbf{p}_0, \mathbf{q}_0; t)dsd\mathbf{p}_0 d\mathbf{q}_0 \qquad (13)$$

in accordance with our earlier analysis of the operation of macroscopic measurement. We now calculate $\alpha_\tau\alpha_\epsilon$ in which the averaging operations have been commuted.

$$\alpha_\tau\alpha_\epsilon\varphi = \int\int \varphi(\mathbf{p}_0, \mathbf{q}_0) \times \bar{f}^{(N)}(\mathbf{p}_0, \mathbf{q}_0; t)d\mathbf{p}_0 d\mathbf{q}_0, \qquad (14)$$
$$\bar{f}^{(N)}(\mathbf{p}_0, \mathbf{q}_0; t) = \frac{1}{\tau}\int_0^\tau f^{(N)}(\mathbf{p}_0, \mathbf{q}_0; t+s)ds,$$

where $\bar{f}^{(N)}$ is the time-smoothed probability density of the ensemble. Returning to Eq. (13), transforming the variables of integration, and using Eqs. (9) and (10), we obtain

$$\alpha_\epsilon\alpha_\tau\varphi = \int\int \varphi(\mathbf{p}, \mathbf{q})\bar{f}^{(N)}(\mathbf{p}, \mathbf{q}; t)d\mathbf{p}d\mathbf{q}, \qquad (15)$$

the right-hand side of which is identical with that of Eq. (14). We have therefore demonstrated that α_τ and α_ϵ commute and we may write,

$$(\varphi)_{\text{obs}} = \alpha_\epsilon\alpha_\tau\varphi = \alpha_\tau\alpha_\epsilon\varphi,$$
$$\alpha_\epsilon\alpha_\tau - \alpha_\tau\alpha_\epsilon = 0. \qquad (16)$$

In an ensemble representing statistical equilibrium, for example the canonical ensemble of Gibbs, for which the distribution function is

$${}^0f^{(N)} = e^{\beta(A-H)}, \qquad (17)$$

where H is the Hamiltonian function and β is equal to $1/kT$, we obtain from Eq. (15), since ${}^0f^{(N)}$ is independent of time,

$$\alpha_\epsilon\alpha_\tau\varphi = \alpha_\epsilon\varphi, \quad (\varphi)_{\text{obs}} = \alpha_\epsilon\varphi. \qquad (18)$$

Here the group average of the time average is equal to the group average, and $(\varphi)_{\text{obs}}$ is equal to the group average, the usual assumption of the equilibrium theory of statistical mechanics. The justification of Eqs. (16) and (18) as representations of a macroscopically observed property of course require a further step, the demonstration that the fluctuation in the ensemble of

$\alpha_\tau\varphi$ is sufficiently small to reduce to a negligible value the expectation of an observation departing from $\alpha_\epsilon\alpha_\tau\varphi$ by an amount exceeding the precision of measurement.

It might be surmised that Eq. (18) would apply to observations in systems undergoing stationary transport processes, as well as in systems in thermodynamic equilibrium. Such a surmise would not in general be true, since stationary transport processes are stationary in the secular sense but not in the microscopic sense. That is to say, $\bar{f}^{(N)}$ may be independent of time although $f^{(N)}$ is not.

For brevity, we shall henceforth use the following notation

$$\begin{gathered}\alpha_\tau\varphi=(\varphi)_\tau, \quad \alpha_\epsilon\varphi=\langle\varphi\rangle, \\ \alpha_\epsilon\alpha_\tau\varphi=\langle(\varphi)_\tau\rangle, \\ \alpha_\tau\alpha_\epsilon\varphi=(\langle\varphi\rangle)_\tau=\langle\varphi\rangle_{Av},\end{gathered} \tag{19}$$

to represent the results of the several averaging operations. The commutability of α_τ and α_ϵ has been demonstrated when α_ϵ denotes an average over all degrees of freedom of the system. We shall presently find that α_τ and α_ϵ do not in general commute when α_ϵ represents a partial average over some but not all coordinates. This lack of commutability is closely associated with the dissipative mechanism by which, in the drift toward equilibrium, energy is distributed among the degrees of freedom in the system.

If we desire to determine the average value of a function $\varphi(\mathbf{p}, \mathbf{q})$ depending not on all coordinates in phase space, but only on these of a subset of n molecules, we may conveniently employ a distribution function of lower order. If we now let $\mathbf{p}$ and $\mathbf{q}$ denote the coordinates of the subset n alone and $\mathbf{P}$ and $\mathbf{Q}$ those of the set of $N-n$ molecules comprising the remainder of the system, the distribution function of order n is defined in the form

$$\begin{gathered}f^{(n)}(\mathbf{p}, \mathbf{q}; t)=\int\int f^{(N)}(\mathbf{p}, \mathbf{q}, \mathbf{P}, \mathbf{Q}; t)d\mathbf{P}d\mathbf{Q}, \\ \bar{f}^{(n)}(\mathbf{p}, \mathbf{q}; t)=\frac{1}{\tau}\int_0^\tau \bar{f}^{(n)}(\mathbf{p}, \mathbf{q}; t+s)ds.\end{gathered} \tag{20}$$

By Eqs. (15) and (16), we obtain, after integration over those coordinates $\mathbf{P}$ and $\mathbf{Q}$ on which $\varphi(\mathbf{p}, \mathbf{q})$ does not depend,

$$(\langle\varphi\rangle)_\tau=\langle\varphi\rangle_{Av}=\int\int\varphi(\mathbf{p}, \mathbf{q})\bar{f}^{(n)}(\mathbf{p}, \mathbf{q}; t)d\mathbf{p}d\mathbf{q}. \tag{21}$$

If the system consists of several components, the molecular types represented in the set n will be represented by subscripts. Thus

$$f_{i\cdots l}{}^{(n)}(\mathbf{p}_1, \cdots\mathbf{p}_n, \mathbf{R}_1, \cdots\mathbf{R}_n; t)$$

denotes a distribution function of order n in a set comprising n specified molecules $1, \cdots n$ of respective types $i\cdots l$, the coordinates $(\mathbf{p}, \mathbf{q})$ of which have the components $\mathbf{p}_1\cdots\mathbf{p}_n$, $\mathbf{R}_1\cdots\mathbf{R}_n$ in the phases spaces of the individual molecules of the set.

The distribution functions $f^{(N)}$ and $f^{(n)}$ are related in the following way

$$\begin{aligned}&f^{(N)}(\mathbf{p}, \mathbf{q}, \mathbf{P}, \mathbf{Q}; t) \\ &\quad=f^{(n/N)}(\mathbf{p}, \mathbf{q}/\mathbf{P}, \mathbf{Q}; t)f^{(n)}(\mathbf{p}, \mathbf{q}; t),\end{aligned} \tag{22}$$

to a third type of distribution function $f^{(n/N)}$ defining the relative probability density in the phase space of the set of $N-n$ molecules, if the set n is situated at a point $(\mathbf{p}, \mathbf{q})$ in its phase sub-space.

The distribution function $\bar{f}_i{}^{(1)}(\mathbf{R}, \mathbf{p}; t)$ represents the probability density of any specified molecule of type i, contained in the system, in the 6-dimensional phase space $(\mathbf{p}, \mathbf{R})$ of that molecule. The microscopic time average of the concentration of molecular species i at a point $\mathbf{R}$ in the vessel containing the system is

$$C_i(\mathbf{R}, t)=N_i\int\bar{f}_i{}^{(1)}(\mathbf{p}, \mathbf{R}; t)d\mathbf{p}, \tag{23}$$

where N_i is the total number of molecules of type i in the system. The mass current density of species i at point R is given by

$$\mathbf{j}_i=N_i\int\mathbf{p}\bar{f}_i{}^{(1)}(\mathbf{p}, \mathbf{R}; t)d\mathbf{p}. \tag{24}$$

The local temperature $T(\mathbf{R}, t)$ is defined in classical statistical mechanics by the relation

$$\begin{gathered}T(\mathbf{R}, t)=[\langle\mathbf{p}^2\rangle_{Av}-\langle\mathbf{p}\rangle_{Av}{}^2]/3mk, \\ \langle\mathbf{p}^2\rangle_{Av}=(N/C)\int\mathbf{p}^2\bar{f}^{(1)}(\mathbf{p}, \mathbf{R}; t)d\mathbf{p}, \\ \langle\mathbf{p}\rangle_{Av}=(N/C)\int\mathbf{p}\bar{f}^{(1)}(\mathbf{p}, \mathbf{R}; t)d\mathbf{p},\end{gathered} \tag{25}$$

where k is Boltzmann's constant. The temperature is thus determined by $\bar{f}^{(1)}$.

The distribution function $\bar{f}^{(2)}$ defines the probability density in the 12-dimensional phase space of a molecular pair. It may be regarded as a function of $\mathbf{R}_1$ and $\mathbf{R}_2$ or of $\mathbf{R}_1$ and $\mathbf{R}$, the position $\mathbf{R}_2-\mathbf{R}_1$ of molecule 2 of the pair relative to molecule 1. Thus $\bar{f}_{il}^{(2)}(\mathbf{p}_1, \mathbf{p}_2, \mathbf{R}_1, \mathbf{R}; t)$ is the distribution function of order 2 for a pair of molecules of types i and l, respectively. Its importance in the theory of transport will presently be made clear.

The central problem in the statistical mechanical theory of transport consists in the determination of the sequence of time averaged lower order distribution functions $\bar{f}^{(n)}(\mathbf{p}, \mathbf{q}; t)$, of which $\bar{f}^{(1)}$ and $\bar{f}^{(2)}$ play a role of particular importance. When the lower order distribution functions are known, pertinent average values of the properties of the system may be calculated by Eq. (21). In the investigation of mass transport by diffusion and convection, the mass current densities $\mathbf{j}_i$, related to the distribution functions $\bar{f}_i^{(1)}$ by Eq. (24), are of special importance.

In the investigation of fluid flow and the equation of motion of hydrodynamics from the molecular standpoint, the relation between the stress tensor $\boldsymbol{\sigma}$ and the potentials of intermolecular force is of special importance. For a system of one component composed of N molecules, with intermolecular forces of the type described by Eq. (1), contained in volume v, the stress tensor $\boldsymbol{\sigma}$ at a point $\mathbf{r}$ in the region v is found to be

$$\begin{aligned}
\boldsymbol{\sigma} &= -\frac{C}{m}[\langle \mathbf{pp}\rangle_{Av} - \langle \mathbf{p}\rangle_{Av}\langle \mathbf{p}\rangle_{Av}] + \frac{C^2}{2}\int \frac{\mathbf{RR}}{R}\frac{dV}{dR}\bar{g}^{(2)}(\mathbf{r}, \mathbf{R}; t)d\mathbf{R}, \\
\bar{g}^{(2)}(\mathbf{r}, \mathbf{R}; t) &= \frac{N^2}{C^2}\int\int \bar{f}^{(2)}(\mathbf{p}_1, \mathbf{p}_2, \mathbf{r}, \mathbf{R}; t)d\mathbf{p}_1 d\mathbf{p}_2, \\
C(\mathbf{r}, t) &= N\int \bar{f}^{(1)}(\mathbf{p}, \mathbf{r})d\mathbf{p}, \\
\langle \mathbf{pp}\rangle_{Av} &= \frac{N}{C}\int \mathbf{pp}\bar{f}^{(1)}(\mathbf{p}, \mathbf{r}; t)d\mathbf{p},
\end{aligned} \tag{26}$$

where $V(R)$ is the potential of intermolecular force for a molecular pair, m is the molecular mass, $\mathbf{r}$ the position of one molecule of the pair, held fixed in the averaging operation, and $\mathbf{R}$ is the position $\mathbf{R}_2-\mathbf{R}_1$ of the second member of the pair relative to the first. The integral of the second term in $\boldsymbol{\sigma}$ extends over the relative coordinates of the pair. The stress tensor is thus determined by the distribution functions $\bar{f}^{(1)}$ and $\bar{f}^{(2)}$. The first term arising from momentum transport is identical with that customarily encountered in the kinetic theory of gases, for example in the Chapman-Enskog formulation. The second term, arising from intermolecular forces, becomes of dominant importance in liquids and solids.

In the investigation of heat transfer on the molecular scale, the relation between the heat current density $\mathbf{j}_q$ and the distribution functions and intermolecular forces is of primary significance. Again in a system of one component, this relation is found to be,

$$\begin{aligned}
\mathbf{j}_q = \frac{C}{2m^2}\langle(\mathbf{p}-\langle \mathbf{p}\rangle_{Av})(\mathbf{p}-\langle \mathbf{p}\rangle_{Av})^2\rangle_{Av} - \frac{N^2}{2m}\int\int\int \{\mathbf{R}(\mathbf{p}_1-\langle \mathbf{p}\rangle_{Av})\cdot\nabla V - V(\mathbf{p}_1-\langle \mathbf{p}\rangle_{Av})\} \\
\times \bar{f}^{(2)}(\mathbf{p}_1, \mathbf{p}_2, \mathbf{r}, \mathbf{R}; t)d\mathbf{p}_1 d\mathbf{p}_2 d\mathbf{R}.
\end{aligned} \tag{27}$$

The heat current thus depends upon the distribution functions $\bar{f}^{(1)}$ and $\bar{f}^{(2)}$. The first term, associated with kinetic energy transport, is the familiar term of the kinetic theory of gases. The second term, associated with energy transport by intermolecular forces, becomes of dominant importance in liquids and solids.

The macroscopic hydrodynamic equations of motion and energy transport will be treated from the molecular standpoint in separate articles on

viscous fluid flow and heat transfer. In these articles, Eqs. (26) and (27) will be derived from fundamental principles and the ordinary laws of viscosity and thermal conduction will be shown to be valid under suitable conditions by expansion of the distribution functions $\bar{f}^{(1)}$ and $\bar{f}^{(2)}$ in the velocity and temperature gradients. The phenomenon of diffusion will also be treated in detail in a later article.

II. THE THEORY OF BROWNIAN MOTION

In liquids and other condensed systems, we shall find it convenient to use the concepts of the theory of Brownian motion in the formulation of the partial differential equations describing the behavior of the sequence of distribution functions $\bar{f}^{(n)}$. It is therefore desirable to examine the concepts of this theory from the molecular standpoint before proceeding to the problem of determining the distribution functions.

The theory of Brownian motion, which describes transport processes in dilute solution, is based upon the Langevin equation describing the motion of a molecule in an environment in statistical equilibrium. The Langevin equation has the form,

$$\frac{d\mathbf{p}_i}{dt}+\frac{\zeta_i^0}{m_i}\mathbf{p}_i=\mathbf{X}_i+\mathbf{G}_i, \tag{28}$$

where $\mathbf{p}_i$ is the momentum of a specified molecule i, m_i its mass, $\mathbf{X}_i$ the external force acting on it, and $\mathbf{G}_i$ a fluctuating intermolecular force, the time average of which vanishes over a macroscopically short interval τ, and which is uncorrelated in successive intervals of magnitude τ. In the dissipative term $\zeta_i^0\mathbf{p}_i/m_i$ the friction constant ζ_i^0 is a phenomenological constant, recognized to be determined by intermolecular forces, but the precise relationship between ζ_i^0 and the intermolecular forces in the system has not heretofore been established. Estimates of ζ_i^0 have therefore been limited to macromolecules dispersed in solvents of low molecular weight, where macroscopic hydrodynamics may reasonably be expected to apply. For a spherical molecule of radius a, in solvent of viscosity coefficient η, Stokes law yields the estimate $6\pi\eta a$ for the friction constant ζ_i^0.

We shall now attempt to show how the Langevin equation may be obtained from statistical mechanics and how the friction constant is related to the intermolecular forces. If $\mathbf{p}_i$ is the momentum of a specified molecule i in a system with completely specified coordinates $\mathbf{p}_{i0}$, $\mathbf{R}_{i0}$, $\mathbf{P}_0$, $\mathbf{Q}_0$, the latter being those of the remaining $N-1$ molecules, at an arbitrary initial instant of time t, the equation of motion for the molecule in question is

$$\frac{d\mathbf{p}_i}{dt}=\left(\frac{\partial\mathbf{p}_i}{\partial t}\right)_{\mathbf{p}_{i0}\ldots\mathbf{Q}_0}=\mathbf{X}_i+\mathbf{F}_i, \tag{29}$$

where $\mathbf{X}_i$ is the external force and $\mathbf{F}_i$ the intermolecular force acting on molecule i.

We now define $\mathbf{G}_i$ by the relation

$$\begin{aligned}\mathbf{G}_i&=\mathbf{F}_i-{}^i\langle(\mathbf{F}_i)_\tau\rangle,\\ {}^i\langle(\mathbf{F}_i)_\tau\rangle&={}^i\alpha_t\alpha_\tau\mathbf{F}_i,\end{aligned} \tag{30}$$

where the left superscript i denotes an average in the ensemble, from which the system is sampled, with fixed initial coordinates $\mathbf{p}_{i0}$ and $\mathbf{R}_{i0}$ of molecule i. By the definitions of Part I, we have

$${}^i\langle(\mathbf{F}_i)_\tau\rangle=\frac{1}{\tau}\int\int\int_0^\tau\mathbf{F}_i(t+s)f_i^{(1/N)}(\mathbf{p}_{i0}\mathbf{R}_{i0}/\mathbf{P}_0,\mathbf{Q}_0;t)ds d\mathbf{P}_0 d\mathbf{Q}_0, \tag{31}$$

where $\mathbf{F}_i(t+s)$ is used for brevity to denote $\mathbf{F}_i(R_i, Q)$ considered as a function of $\mathbf{R}_{i0}$, $\mathbf{Q}_0$, and s, and $f_i^{(1/N)}$ is the relative probability density in the ensemble at time t in the phase space of the $N-1$ molecules other than i, if i has the coordinates $\mathbf{p}_{i0}$ and $\mathbf{R}_{i0}$. We remark that $\mathbf{G}_i$ has the first property assigned to the fluctuating force in the Langevin equation, that is,

$${}^i\alpha_t\alpha_\tau\mathbf{G}_i=0, \tag{32}$$

but in the somewhat extended sense that average in the ensemble of the time average of $\mathbf{G}_i$ vanishes. This extension is necessary to give precision to the concept of the fluctuating force. The second property, that of no correlation in successive τ intervals, will presently be discussed.

We now examine the average force $\langle(\mathbf{F}_i)_\tau\rangle$. If we make the hypothesis that the environment of molecule i is in statistical equilibrium, or can be regarded to be so to a sufficient degree of approximation, we may write Eq. (30) in the form

$$
\begin{aligned}
{}^i\langle(\mathbf{F}_i)_\tau\rangle &= \frac{1}{\tau}\int\int\int_0^\tau \mathbf{F}_i(t+s)\,{}^0f_i^{(1/N)}(\mathbf{p}_{i0}\mathbf{R}_{i0}/\mathbf{P}_0,\,\mathbf{Q}_0)\,ds\,d\mathbf{P}_0\,d\mathbf{Q}_0, \\
{}^0f_i^{(1/N)} &= \left(\frac{\beta}{2\pi m_i}\right)^{\frac{1}{2}}\frac{1}{v}\exp\left[\beta(A^N-H_0^N)+\beta p_{i0}^2/2m_i+\beta W_i^{(1)}(\mathbf{R}_{i0})\right],
\end{aligned}
\tag{33}
$$

where ${}^0f_i^{(1/N)}$ is the relative probability density in the canonical ensemble representing statistical equilibrium and defined by Eq. (22). The potential of the equilibrium average force* acting on molecule i is denoted by $Wi^{(1)}$. We next consider the average force $({}^i\langle\mathbf{F}_i\rangle)_\tau$ in which the order of the averaging operations α_τ and ${}^i\alpha_\epsilon$ is interchanged and we find,

$$
({}^i\langle\mathbf{F}_i\rangle)_\tau = {}^i\langle\mathbf{F}_l\rangle^0 = \int\int F_i(\mathbf{R}_{l0},\,\mathbf{Q})\,{}^0f_i^{(1/N)}(\mathbf{p}_{l0},\,\mathbf{R}_{l0}/\mathbf{P},\,\mathbf{Q})\,d\mathbf{P}\,d\mathbf{Q}, \tag{34}
$$

if ${}^i\langle\mathbf{F}_i\rangle^0$, the equilibrium intermolecular force has only secular dependence on time so that it is not affected by an average over the microscopic interval τ. It will be shown in a later article on diffusion that in the equilibrium ensemble corresponding to specified composition gradients

$$
{}^i\langle\mathbf{F}_i\rangle^0 = -\nabla\mu_i + kT\nabla\log C_i, \tag{35}
$$

where μ_i is the chemical potential of a molecule of type i and C_i is its concentration. Thus ${}^i\langle F_i\rangle^0$ will be secular for gradients appreciable only over distances of macroscopic magnitude and will in fact vanish if molecule i is a solute component of an ideal dilute solution. It also vanishes identically if the hypothesis of thermodynamic equilibrium is strictly fulfilled and there are no external forces $\mathbf{X}_i$ acting on the system.

If ${}^i\alpha_\epsilon$ and α_τ were commutable as are α_ϵ and α_τ, ${}^i\langle(\mathbf{F}_i)_\tau\rangle$ would be identical with ${}^i\langle\mathbf{F}_i\rangle^0$. This, however, is not the case. In order to establish the relation between ${}^i\langle(\mathbf{F}_i)_\tau\rangle$ and ${}^i\langle\mathbf{F}_i\rangle^0$, we rewrite Eq. (33) in the following form,

$$
{}^i\langle(\mathbf{F}_i)_\tau\rangle = \frac{1}{\tau}\int_0^\tau\int\int\int\int\int \mathbf{F}_i(t+s)\,\delta(\mathbf{p}_{i0}'-\mathbf{p}_{i0})\,\delta(\mathbf{R}_{i0}'-\mathbf{R}_{i0})\,{}^0f_i^{(1/N)}(\mathbf{p}_{i0}',\,\mathbf{R}_{i0}'/\mathbf{P}_0,\,\mathbf{Q}_0)\,d\mathbf{p}_{i0}'\,d\mathbf{R}_{i0}'\,d\mathbf{P}_0\,d\mathbf{Q}_0\,ds, \tag{36}
$$

where the order of integration over time and phase space has been interchanged (this is permissible and has nothing to do with the commutation of ${}^i\alpha_\epsilon$ and α_τ), and the integration has extended over all of phase space at time t by introducing the delta functions $\delta(\mathbf{p}_{i0}'-\mathbf{p}_{i0})$ and $\delta(\mathbf{R}_{i0}'-\mathbf{R}_{i0})$, each the product of three delta functions for each component of the vector arguments. We next note the following properties of the functions appearing in the integrand of Eq. (36).

$$
\begin{aligned}
{}^0f_i^{(1/N)}(\mathbf{p}_{i0}',\,\mathbf{R}_{i0}'/\mathbf{P}_0,\,\mathbf{Q}_0) &= {}^0f_i^{(1/N)}(\mathbf{p}_i',\,\mathbf{R}_i'/\mathbf{P},\,\mathbf{Q})\,{}^0f_i^{(1)}(\mathbf{p}_i',\,\mathbf{R}_i')/{}^0f^{(1)}(\mathbf{p}_{i0}',\,\mathbf{R}_{i0}'), \\
\frac{{}^0f_i^{(1)}(\mathbf{p}_i',\,\mathbf{R}_i')}{{}^0f_i^{(1)}(\mathbf{p}_{i0}',\,\mathbf{R}_{i0}')} &= \exp\left\{-\beta(p_i'^2-p_{i0}'^2)/2m_i-\beta[W_i^{(1)}(\mathbf{R}_i')-W_i^{(1)}(\mathbf{R}_{i0}')]\right\}, \\
&= 1-\frac{\beta\mathbf{p}_i'}{m_i}\cdot\Delta\mathbf{p}_i'+O[(\Delta\mathbf{p}_i')^2]+O(\Delta\mathbf{R}_i'), \\
\Delta\mathbf{p}_i' &= \mathbf{p}_i'-\mathbf{p}_{i0}' = \int_0^s \mathbf{F}_i(t+s')\,ds'+\mathbf{X}_i s, \\
\Delta\mathbf{R}_i' &= \mathbf{R}_i'-\mathbf{R}_{i0}' = \int_0^s (\mathbf{p}_i'/m_i)\,ds'.
\end{aligned}
\tag{37}
$$

* Note: For a discussion of equilibrium average forces and distribution functions, see J. G. Kirkwood, J. Chem. Phys. 3, 300 (1935).

These relations follow at once from Eqs. (17), (20), (22), and (29) and the invariance of $H^{(N)}$ the complete Hamiltonian of the system under the transformation $(\mathbf{p}_{i0}', \mathbf{R}_{i0}', \mathbf{P}_0, \mathbf{Q}_0) \rightarrow (\mathbf{p}_i', \mathbf{R}_i', \mathbf{P}, \mathbf{Q})$ by the operator $\exp(-isLo)$. We further note

$$\begin{aligned} \mathbf{F}_i(t+s) &= \mathbf{F}_i(R_i', Q), \\ \delta(\mathbf{p}_{i0}' - \mathbf{p}_{i0}) &= \delta(\mathbf{p}_i' - \mathbf{p}_{i0} - \Delta\mathbf{p}_i'), \\ &= \delta(\mathbf{p}_i' - \mathbf{p}_{i0}) + \Delta\mathbf{p}_i' \cdot \nabla_{\mathbf{p}_{i0}} \delta(\mathbf{p}_i' - \mathbf{p}_{i0}) + O[(\Delta\mathbf{p}_i')^2], \\ \delta(\mathbf{R}_{i0}' - \mathbf{R}_{i0}) &= \delta(\mathbf{R}_i' - \mathbf{R}_{i0}) + O(\Delta\mathbf{R}_i'). \end{aligned} \tag{38}$$

The expansions of the delta functions in power series in $\Delta\mathbf{p}_i'$ and $\Delta\mathbf{R}_i'$ are formal operations which can be justified by more tedious methods of calculation which circumvent their use. Substitution of the relations of Eqs. (37) and (38) into the integral of Eq. (36) after transformation to the new variables $\mathbf{p}_i'$, $\mathbf{R}_i'$, $\mathbf{P}$, $\mathbf{Q}$ yields, after some calculation,

$$\begin{aligned} {}^i\langle(\mathbf{F}_i)_\tau\rangle &= {}^i\langle\mathbf{F}_i\rangle^0 - \boldsymbol{\zeta}_i \cdot \mathbf{p}_{i0}/m_i + kT\nabla_{\mathbf{p}_{i0}} \cdot \boldsymbol{\zeta}_i + O(\tau). \\ \boldsymbol{\zeta}_i &= \frac{\beta}{\tau} \int\int\int\int_0^\tau \int_0^s \mathbf{F}_i(t+s)\mathbf{F}_i(t+s')\ {}^0f_i^{(1/N)}(\mathbf{p}_i, \mathbf{R}_i/\mathbf{P}, \mathbf{Q}) ds' ds d\mathbf{P} d\mathbf{Q}, \end{aligned} \tag{39}$$

where in the expression for $\boldsymbol{\zeta}_i$, resulting from the calculation, $\mathbf{p}_{i0}$ and $\mathbf{R}_{i0}$ have been replaced by $\mathbf{p}_i$ and $\mathbf{R}_i$ and the remainder included in the term $O(\tau)$. If the tensor $\boldsymbol{\zeta}_i$ has a plateau value, not sensibly dependent on τ, for a microscopic interval τ of sufficient length, in a sense to be discussed presently, the remainder terms arising from the terms $O[(\Delta\mathbf{p}_i')^2]$ and $O[\Delta\mathbf{R}_i']$ in the integrand of Eq. (36) may be shown to be of order τ. In fluid systems such as liquids and liquid solutions, it is apparent that $\boldsymbol{\zeta}_i$ must be isotropic.

$$\boldsymbol{\zeta}_i = \zeta_i \mathbf{1},$$

$$\zeta_i(\tau) = \frac{\beta}{3\tau} \int_0^\tau \int_{-s}^0 \int\int \mathbf{F}_i(t+s) \cdot \mathbf{F}_i(t+s+s')\ {}^0f_i^{(1/N)}(\mathbf{p}_i, \mathbf{R}_i/\mathbf{P}, \mathbf{Q}) d\mathbf{P} d\mathbf{Q} ds' ds, \tag{40}$$

where a permissible change in the order of integration has been made and a change of time variable introduced.

If the structure of the dynamical system is such that in the equilibrium ensemble there exists a microscopic time interval τ_i, of sufficient length that the integral

$$\frac{\beta}{3} \int_{-s}^0 \int\int \mathbf{F}_i(t) \cdot \mathbf{F}_i(t+s')\ {}^0f_i^{(1/N)}(\mathbf{p}_{i0}, \mathbf{R}_{i0}/\mathbf{P}_0, \mathbf{Q}_0) d\mathbf{P}_0 d\mathbf{Q}_0 ds'$$

possesses a plateau value ζ_i given by

$$\zeta_i = \frac{\beta}{3} \int_{-\tau_i}^0 \int\int \mathbf{F}_i(t)\mathbf{F}_i(t+s)\ {}^0f_i^{(1/N)}(\mathbf{p}_{i0}, \mathbf{R}_{i0}/\mathbf{P}_0, \mathbf{Q}_0) d\mathbf{P}_0 d\mathbf{Q}_0 ds, \tag{41}$$

in the sense that for values of s greater than τ_i, but small on the macroscopic scale, the integral differs in absolute value from ζ_i by an amount less than the precision error of a macroscopic measurement of the quantity, then $\zeta_i(\tau)$ possesses the same plateau value ζ_i in the same sense for $\tau > \tau_i'$ where $\tau_i/\tau_i' \ll 1$. This may be expressed more precisely in the form,

$$|\zeta_i(\tau) - \zeta_i| = O(\epsilon); \quad \tau_i' < \tau < \tau^* \tag{42}$$

where ϵ is less than the precision error in the macroscopic measurement of ζ_i and τ^* is a macroscopic interval of time certainly of smaller magnitude than the representative period of the Poincaré cycles of the system. We have intentionally avoided identifying $\zeta_i(\tau)$, for sufficiently long τ, with its asymptotic value $\zeta_i(\infty)$, since the latter value may be shown to vanish for systems confined to a

finite region of configuration space. The apparent paradox encountered here is precisely the paradox between dynamical reversibility and thermodynamic irreversibility. The dissipative processes appearing to operate in thermodynamic systems provide a valid description of macroscopic behavior only if the time over which the properties of the system are averaged in a macroscopic observation is long relative to the periods of microscopic fluctuation but short relative to the periods of Poincaré cycles,* within which secular changes in state may be spontaneously reversed. It is for these reasons that we are forced to speak of a plateau value for $\zeta_i(\tau)$ rather than of its asymptotic value at $\tau\rightarrow\infty$, in discussing macroscopic transport processes. Whether such a plateau value exists will depend upon the dynamical structure of the system, that is upon the particular form of its Hamiltonian.

We shall investigate the friction constant ζ_i in greater detail in Part IV. Anticipating a result to be obtained there, we remark that the integrand of Eq. (41) is found to be an even function of s.† This allows us to express ζ_i in the following form,

$$\zeta_i=\frac{1}{6kT}\int_{-\tau_i}^{+\tau_i}{}^{i}\langle\mathbf{F}_i\cdot e^{-is\,L}\mathbf{F}_i\rangle^0 ds,$$

$${}^{i}\langle\mathbf{F}_i\cdot e^{-is\,L}\mathbf{F}_i\rangle^0=\int\int[\mathbf{F}_i(\mathbf{R}_i,\mathbf{Q}_i)\cdot e^{-is\,L}\mathbf{F}_i(\mathbf{R}_i,\mathbf{Q}_i)]\,{}^{0}f_i^{(1/N)}(\mathbf{p}_i,\mathbf{R}_i/\mathbf{P},\mathbf{Q})d\mathbf{P}d\mathbf{Q}. \tag{43}$$

Although it is apparent that in fluid systems ζ_i will not depend upon the position $\mathbf{R}_{i0}$ of the molecule in configuration space, ζ_i may depend upon the momentum $\mathbf{p}_{i0}$ of the molecule. It will be shown in Part IV that ζ_i does not sensibly depend upon momentum, if the mass of molecule i is large relative to those of the other molecules of the system, for example, when i is a macromolecule in a solvent of low molecular weight. Also, even when molecule i has a mass comparable with those of its environment, ζ_i may not depend sensibly on momentum in condensed systems such as liquids or liquid solutions. When ζ_i does depend upon momentum it is an even function of this variable.

Returning now to Eq. (29), introducing Eqs. (30), (39), and (40) and neglecting the terms of order τ in Eq. (39), after selecting τ of sufficient magnitude to achieve the plateau value of $\zeta_i(\tau)$, we obtain the equation of motion,

$$\frac{d\mathbf{p}_i}{dt}+\zeta_i{}^0\mathbf{p}_i/m_i=\mathbf{X}_i+\mathbf{G}_i,\quad \zeta_i{}^0=\zeta_i-2kT\frac{d\zeta_i}{dp_i{}^2}, \tag{44}$$

where we have suppressed ${}^{i}\langle\mathbf{F}_i\rangle^0$, shown to vanish for an ideal dilute solution, and have identified $\mathbf{p}_{i0}$ in Eq. (39) with $\mathbf{p}_i$, since the instant of time t, in the neighborhood of which the average ${}^{i}\langle(\mathbf{F}_i)_\tau\rangle$ is made is properly to be taken as identical with the instant t at which the acceleration $d\mathbf{p}_i/dt$ is to be calculated. If the plateau value ζ_i exists, it is evident that

$${}^{i}\langle\mathbf{F}_i(t)\cdot\mathbf{F}_i(t+\tau)\rangle^0=0, \tag{45}$$

is valid to the same degree of approximation, that is τ exceeds the time interval during which there is sensible correlation between the total intermolecular force acting in molecule at instants of time separated by that interval. This implies that, with neglect of terms of order τ, there is no correlation between the force $\mathbf{G}_i$ acting on molecule i at successive instants t and $t+\tau$.

Equation (44) thus becomes identical with the Langevin equation, if ζ_i and therefore $\zeta_i{}^0$ is independent of $\mathbf{p}_i$. When ζ_i depends upon $\mathbf{p}_i$, a generalized Langevin equation containing a friction

* Poincaré has stated the theorem that in a system of particles in which the forces depend only upon the spatial coordinates, a given initial state must recur to any specified degree of accuracy, an infinite number of times if the system is confined to a finite region of phase space. The term Poincaré cycle period is used to designate the time of recurrence of a given state to within a specified degree of accuracy in such "quasi-periodic" motion. For systems of molecules such periods are very long on the macroscopic time scale. It may therefore seem that we have placed undue emphasis on the rather obvious point that τ_i should be short relative to such periods. We have done so in order to call attention to the circumstance that the apparently innocent mathematical procedure of letting $\tau_i\rightarrow\infty$ in evaluating the friction constant leads to serious physical difficulties. For a more detailed discussion of these points, see S. Chandrasekar, Rev. Mod. Phys. **15**, 1–89 (1943), Appendix V.

† This may be regarded as a consequence of the principle of microscopic reversibility.

constant dependent on the velocity of the molecule is obtained. We have by means of our analysis suggested the conditions under which the Langevin equation may be expected to be valid, and, what is more significant, have established a relation, Eq. (41), between the friction constant and the intermolecular forces acting in a system of molecules. Many mathematical points call for further investigation, particularly the specification of the properties of the class of systems for which a plateau value ζ_i exists, an investigation of the magnitude of the correlation time τ_i, and an examination of the magnitude of the neglected terms of order τ in Eq. (39). Some of these points will be discussed in Part IV.

Having established the Langevin equation, the details of the conventional theory of Brownian motion may be developed by the Markoff method or known alternative methods, which we do not need to discuss here

III. THE DISTRIBUTION FUNCTIONS

We here return to the problem of determining the sequence of distribution functions $\bar{f}^{(n)}$ from which the average values characterizing macroscopic transport processes are to be calculated. We shall proceed from the Liouville differential equation, Eq. (3), and the definitions, Eq. (20), of the distribution functions $\bar{f}^{(n)}$. Our general method leads on the one hand to the Maxwell-Boltzmann integro-differential equation for gases of sufficiently low density to permit analysis by binary collisions, and, on the other hand to a generalized Fokker-Planck equation, by methods closely related to those of the theory of Brownian motion developed in Part II, for liquids and liquid solutions.

The Liouville equation and the definition of the distribution function $\bar{f}^{(n)}$ are conveniently summarized in the form

$$\sum_{l=1}^{N}\left\{\frac{\mathbf{p}_l}{m_l}\cdot\nabla_{\mathbf{R}_l}f^{(N)}+(\mathbf{X}_l+\mathbf{F}_l)\cdot\nabla_{\mathbf{p}_l}f^{(N)}\right\}+\frac{\partial f^{(N)}}{\partial t}=0,$$

$$f^{(n)}(\mathbf{p},\mathbf{q};t)=\int\int f^{(N)}(\mathbf{p},\mathbf{q},\mathbf{P},\mathbf{Q};t)d\mathbf{P}d\mathbf{Q}, \tag{46}$$

$$\bar{f}^{(n)}(\mathbf{p},\mathbf{q};t)=\frac{1}{\tau}\int_0^\tau f^{(n)}(\mathbf{p},\mathbf{q};t+s)ds,$$

where, as before, $\mathbf{p}$ and $\mathbf{q}$ denote the coordinates of the set of molecules n and $\mathbf{P}$ and $\mathbf{Q}$ those of the set $N-n$, constituting the other molecules of system. In our preliminary remarks, we shall repress subscripts indicating the molecule types comprised in the set n. Integrating the Liouville equation over the partial phase space $(\mathbf{P},\mathbf{Q})$, and restricting our analysis to distributions $\bar{f}^{(N)}$ for which the surface integrals of the currents vanish on the boundary of the phase space accessible to the system, we obtain with use of Green's theorem,

$$\frac{\partial\bar{f}^{(n)}}{\partial t}+\frac{\mathbf{p}}{m}\cdot\nabla_{\mathbf{q}}\bar{f}^{(n)}+\mathbf{X}\cdot\nabla_{\mathbf{p}}\bar{f}^{(n)}=\nabla_{\mathbf{p}}\cdot\boldsymbol{\Omega}^{(n)},$$

$$\boldsymbol{\Omega}^{(n)}=-\frac{1}{\tau}\int_0^\tau\int\int\mathbf{F}(\mathbf{q},\mathbf{Q})f^{(N)}(\mathbf{p},\mathbf{q},\mathbf{P},\mathbf{Q};t+s)d\mathbf{P}d\mathbf{Q}ds, \tag{47}$$

where $\mathbf{X}$ denotes the total external and $\mathbf{F}$ the total intermolecular force, regarded as vectors in the n-configuration space of set n, and $\mathbf{p}/m$ represents a vector in the n-momentum space with projections $\mathbf{p}_1/m_1\cdots\mathbf{p}_n/m_n$ on the 3-spaces of the several molecules of the set. If the intermolecular force has the form, Eq. (2), we may express the mean currents due to intermolecular forces as

$$\boldsymbol{\Omega}^{(n)}=-\sum_{i,k=1}^{n}\mathbf{F}_{ki}\bar{f}^{(n)}+\sum_{i=1}^{n}\sum_{l=n+1}^{N}\boldsymbol{\Omega}_{li}{}^{(n)},$$

$$\boldsymbol{\Omega}_{li}{}^{(n)}=-\int\int\mathbf{F}_{li}(R_{li})\bar{f}^{(n+1)}(\mathbf{p},\mathbf{q},\mathbf{p}_l,\mathbf{R}_l;t)d\mathbf{p}_l d\mathbf{R}_l, \tag{48}$$

where $\mathbf{F}_{ki}$ and $\mathbf{\Omega}_{li}^{(n)}$ are to be treated as vectors in the 3-configuration space of molecule i of the set n (not as vectors in a common 3-space). Eqs. (47) and (48) provide a system of integro-differential equations for the sequence of distribution functions $\bar{f}^{(n)}$, in which the dissipative mechanism affecting their behavior is concealed in time-averaged function of highest order $\bar{f}^{(N)}$. It is therefore necessary to transform the terms $\mathbf{\Omega}_{li}^{(n)}$ with the aid of solutions, Eq. (5) of the Liouville equation for $f^{(N)}$ in order to obtain useful results.

To avoid undue complication, we shall now specialize the analysis to the distribution function $f_i^{(1)}$, the distribution function of order one for a molecule of type i. The extension of the method to distribution functions of higher order will be obvious. Eq. (47) now reduces to

$$\frac{\partial \bar{f}_i^{(1)}}{\partial t}+\frac{\mathbf{p}_i}{m_i}\cdot\nabla_{\mathbf{R}_i}\bar{f}_i^{(1)}+\mathbf{X}_i\cdot\nabla_{\mathbf{p}_i}\bar{f}_i^{(1)}=\nabla_{\mathbf{p}_i}\cdot\mathbf{\Omega}_i^{(1)},$$

$$\mathbf{\Omega}_i^{(1)}=\sum_{l=1}^{\nu}N_l\mathbf{\Omega}_{li}^{(1)}, \tag{49}$$

$$\mathbf{\Omega}_{li}^{(1)}=-\frac{1}{\tau}\int_0^\tau\int\cdots\int\mathbf{F}_{li}(R_{il})f^{(N)}(\mathbf{p}_i,\mathbf{R}_i,\mathbf{p}_l,\mathbf{R}_l,\mathbf{P},\mathbf{Q};t+s)d\mathbf{P}d\mathbf{Q}d\mathbf{p}_ld\mathbf{R}_lds,$$

where $\mathbf{P}$ and $\mathbf{Q}$ here denote the coordinates of all molecules except those of a specified pair of molecules i and l of types i and l respectively (subscripts on coordinates denote specified molecules; on functions $\mathbf{\Omega}_{li}$, $\mathbf{F}_{li}$, etc., they denote molecular types). Using Eqs. (5) and (22) we may write

$$\begin{aligned}
&f^{(N)}(\mathbf{p}_i,\mathbf{R}_i,\mathbf{p}_l,\mathbf{R}_l,\mathbf{P},\mathbf{Q};t+s)=f^{(N)}(\mathbf{p}_{i0},\mathbf{R}_{i0},\mathbf{p}_{l0},\mathbf{R}_{l0},\mathbf{P}_0,\mathbf{Q}_0;t),\\
&f^{(N)}(\mathbf{p}_{i0},\mathbf{R}_{i0},\mathbf{p}_{l0},\mathbf{R}_{l0},\mathbf{P}_0,\mathbf{Q}_0;t)=f_{il}^{(2/N)}(\mathbf{p}_{i0},\mathbf{R}_{i0},\mathbf{p}_{l0},\mathbf{R}_{l0},\mathbf{P}_0,\mathbf{Q}_0;t)f_{il}^{(2)}(\mathbf{p}_{i0},\mathbf{R}_{i0},\mathbf{p}_{l0},\mathbf{R}_{l0};t),\\
&f_{il}^{(2)}(\mathbf{p}_{i0},\mathbf{R}_{i0},\mathbf{p}_{l0},\mathbf{R}_{l0};t)=\varphi_{il}^{(2)}(\mathbf{p}_{i0},\mathbf{R}_{i0},\mathbf{p}_{l0},\mathbf{R}_{l0};t)f_i^{(1)}(\mathbf{p}_{i0},\mathbf{R}_{i0};t)f_l^{(1)}(\mathbf{p}_{l0},\mathbf{R}_{l0};t),
\end{aligned} \tag{50}$$

where $f_{il}^{(2/N)}$ is the relative probability density in the partial phase space $(\mathbf{P},\mathbf{Q})$ when a pair of molecules of type i and l have specified coordinates. The correlation function $\varphi_{il}^{(2)}$ is defined by the last of Eq. (50). In the last of Eq. (49) defining $\mathbf{Q}_{li}^{(1)}$ we extend the integration over all of phase space with the use of delta functions, transform the variables of integration from $\mathbf{p}_i\cdots\mathbf{Q}$ to $\mathbf{p}_{i0}\cdots\mathbf{Q}_0$, and introduce the relations of Eq. (50). We then obtain

$$\begin{aligned}
&\mathbf{\Omega}_{li}^{(1)}=\int\cdots\int\mathbf{K}_{li}(\mathbf{p}_{i0}\cdots\mathbf{R}_{l0};t)f_l^{(1)}(\mathbf{p}_{l0},\mathbf{R}_{l0};t)f_i^{(1)}(\mathbf{p}_{i0},\mathbf{R}_{i0};t)d\mathbf{p}_{l0}d\mathbf{R}_{l0}d\mathbf{p}_{i0}d\mathbf{R}_{i0},\\
&\mathbf{K}_{li}=-\frac{1}{\tau}\int_0^\tau\int\int\mathbf{F}_{li}(t+s)\delta(\mathbf{p}_{i0}+\Delta\mathbf{p}_i-\mathbf{p}_i)\delta(\mathbf{R}_{i0}+\Delta\mathbf{R}_i-\mathbf{R}_i)\varphi_{il}^{(2)}(\mathbf{p}_{i0}\cdots\mathbf{R}_{l0};t)\\
&\qquad\qquad\times f^{(2/N)}(\mathbf{p}_{i0},\mathbf{R}_{i0},\mathbf{p}_{l0},\mathbf{R}_{l0}/\mathbf{P}_0,\mathbf{Q}_0;t)d\mathbf{P}_0d\mathbf{Q}_0ds,\\
&\mathbf{F}_{li}(t+s)=\mathbf{F}_{li}(R_{il})=\mathbf{F}_{li}(p_{i0}\cdots Q_0;s),\quad \Delta\mathbf{p}_i=\int_0^s\mathbf{F}_ids'+\mathbf{X}_is;\quad \Delta\mathbf{R}_i=\int_0^s\mathbf{p}_i/m_ids'.
\end{aligned} \tag{51}$$

An integral of the type of $\mathbf{K}_{li}$ vanishes for sufficiently large τ if, in place of $\varphi_{il}^{(2)}$, the integrand contains a factor which is a short range function of the distance between molecules i and l, diminishing say with distance in the same order as $\mathbf{F}_{li}$. If we use the identity

$$\varphi_{il}^{(2)}=\exp(-\beta W_{il}^{(2)})[1+(\varphi_{il}^{(2)}\exp(\beta W_{il}^{(2)})-1)], \tag{52}$$

where $W_{il}^{(2)}$ is equilibrium potential of mean force acting on the pair il and restrict our analysis to distributions for which $(\varphi_{il}^{(2)}\exp(\beta W_{il}^{(2)})-1)$ is a short range function of the intermolecular distance, we may express $\mathbf{K}_{li}$ in the form

$$\begin{aligned}
\mathbf{K}_{li}=-\frac{1}{\tau}\int_0^\tau\int\int\mathbf{F}_{li}(t+s)\delta(\mathbf{p}_{i0}+\Delta\mathbf{p}_i-\mathbf{p}_i)\delta(\mathbf{R}_{i0}+\Delta\mathbf{R}_i-\mathbf{R}_i)\exp(-\beta W_{il}^{(2)})\\
\times f_{il}^{(2/N)}(\mathbf{p}_{i0},\mathbf{R}_{i0},\mathbf{p}_{l0},\mathbf{R}_{l0}/\mathbf{P}_0,\mathbf{Q}_0;t)d\mathbf{P}_0d\mathbf{Q}_0ds,
\end{aligned} \tag{53}$$

where the factor $\exp(-\beta W_{il}^{(2)})$, although convenient for later use, is arbitrary to the extent that it might be replaced by unity or any function differing from unity by short range terms.

An analytical development of the Maxwell-Boltzmann integro-differential equation may be based on Eq. (53) and the assumption of binary molecular collisions, namely that for configurations in which $\mathbf{F}_{li}$ differs from zero, $d(\Delta\mathbf{p}_i)/dt=\mathbf{F}_{li}$. Since the derivation is somewhat complicated, we shall postpone it for special treatment in a later article. The derivation is worth while, since it clarifies certain important points left obscure by the usual physical argument used to establish the Maxwell-Boltzmann equation.

We shall here employ the methods of the theory of Brownian motion to evaluate $\mathbf{K}_{li}$, writing

$$\mathbf{K}_{li}=\mathbf{K}_{li}{}^{0}+\Delta\mathbf{K}_{li},$$

$$\mathbf{K}_{li}{}^{0}=\frac{1}{\tau}\int_0^{\tau}\int\int\mathbf{F}_{li}(t+s)\delta(\mathbf{p}_{i0}+\Delta\mathbf{p}_i-\mathbf{p}_i)\delta(\mathbf{R}_{i0}+\Delta\mathbf{R}_i-\mathbf{R}_i)\exp\left[-\beta W_{il}^{(2)}(R_{il})\right]\times{}^{0}f_{il}^{(2/N)}(\mathbf{p}_{i0},\mathbf{R}_{i0},\mathbf{p}_{l0},\mathbf{R}_{l0}/\mathbf{P}_0,\mathbf{Q}_0)d\mathbf{P}_0d\mathbf{Q}_0ds, \tag{54}$$

$${}^{0}f_{il}^{(2/N)}=\left(\frac{\beta^2}{(2\pi)^2m_im_l}\right)^{\frac{1}{2}}\frac{1}{v^2}\exp\left\{\beta[A^N-H_0{}^N+p_{i0}{}^2/2m_i+p_{l0}{}^2/2m_l+W_{il}^{(2)}(R_{il0})]\right\},$$

where ${}^{0}f_{il}^{(2/N)}$ is the equilibrium distribution function in the phase space of the molecules constituting the environment of the molecular pair il, and $\Delta\mathbf{K}_{li}$ is the contribution to $\mathbf{K}_{li}$ arising from the departure of $f_{il}^{(2/N)}$ from the equilibrium distribution ${}^{0}f_{il}^{(2/N)}$. Introducing the following relations,

$$\exp\left[-\beta W_{il}^{(2)}(R_{il0})\right]{}^{0}f_{il}^{(2/N)}(\mathbf{p}_{i0},\mathbf{R}_{i0},\mathbf{p}_{l0},\mathbf{R}_{l0}/\mathbf{P}_0,\mathbf{Q}_0)=\exp\left[-\beta W_{il}^{(2)}(R_{il})\right]{}^{0}f_{il}^{(2/N)}(\mathbf{p}_i,\mathbf{R}_i,\mathbf{p}_l,\mathbf{R}_l/\mathbf{P},\mathbf{Q})\times\left\{1-\frac{\beta\mathbf{p}_{i0}}{m_i}\cdot\Delta\mathbf{p}_i-\frac{\beta\mathbf{p}_{l0}}{m_l}\cdot\Delta\mathbf{p}_l+\cdots\right\}, \tag{55}$$

$$\delta(\mathbf{p}_{i0}+\Delta\mathbf{p}_i-\mathbf{p}_i)=\delta(\mathbf{p}_{i0}-\mathbf{p}_i)-\Delta\mathbf{p}_i\cdot\nabla_{\mathbf{p}_i}\delta(\mathbf{p}_{l0}-\mathbf{p}_i)+\cdots,$$

$$\delta(\mathbf{R}_{i0}+\Delta\mathbf{R}_i-\mathbf{R}_i)=\delta(\mathbf{R}_{i0}-\mathbf{R}_i)+\cdots,$$

based upon the invariance of H^N under the transformation $(\mathbf{p}_{0i}\cdots\mathbf{Q}_0)$ to $(\mathbf{p}_i\cdots\mathbf{Q})$, and expansion of the delta functions, we finally obtain for $\mathbf{\Omega}_{li}^{(1)}$,

$$\mathbf{\Omega}_{li}^{(1)}={}^{0}\mathbf{\Omega}_{li}^{(1)}+\Delta\mathbf{\Omega}_{li}^{(1)},$$

$${}^{0}\mathbf{\Omega}_{li}^{(1)}=-({}^{i}\langle\mathbf{F}_{li}\rangle^{0}+\zeta_l{}^{i}\mathbf{v}_l{}^{*})f_i^{(1)}(\mathbf{p}_i,\mathbf{R}_i;t)+\zeta_i{}^{l}\{\mathbf{p}_i/m_i+kT\nabla_{\mathbf{p}_i}\}f_i^{(1)}(\mathbf{p}_i,\mathbf{R}_i;t)+O(\tau),$$

$$\zeta_i{}^{l}=\frac{1}{6kT}\int_{-\tau_i}^{+\tau_i}{}^{i}\langle\mathbf{F}_{li}\cdot e^{-is_iL}\mathbf{F}_i\rangle^{0}ds,\quad {}^{i}\langle\mathbf{F}_{li}\rangle^{0}=\frac{1}{v}\int\mathbf{F}_{li}\exp\left(-\beta W_{il}^{(2)}\right)d\mathbf{R}_l, \tag{56}$$

$$\mathbf{v}_l{}^{*}=(N_l/C_l)\int(\mathbf{p}_l/m_l)\chi_{il}f_l^{(1)}(\mathbf{p}_l,\mathbf{R}_i;t)d\mathbf{R}_ld\mathbf{p}_l,$$

$$\chi_{il}=\frac{\exp\left(-\beta W_{il}^{(2)}\right)}{6kT\zeta_l{}^{i}}\int_{-\tau_i}^{+\tau_i}{}^{il}\langle\mathbf{F}_{li}\cdot e^{-is_iL}\mathbf{F}_l\rangle^{0}ds,$$

where the methods of Part II have been used to simplify the plateau values of the partial friction constant $\zeta_i{}^{l}$, and departures of $f_l^{(1)}$ from ${}^{0}f_l^{(1)}$ have been ignored in the expressions for $\zeta_i{}^{l}$ and ${}^{i}\langle\mathbf{F}_{li}\rangle^{0}$, since we are interested here in obtaining relations valid only to the first order in parameters determining departures from equilibrium. Since the gradient of $f_l^{(1)}(\mathbf{p}_l,\mathbf{R}_l;t)$ in configuration space is supposed to be appreciable only over distances of macroscopic magnitude, and since χ_{il} is a short range function of the intermolecular distance R_{il}, we may write $f_l^{(1)}(\mathbf{p}_l,\mathbf{R}_i;t)$ in the integral defining

$\mathbf{v}_l^*$. If χ_{il} is independent of $\mathbf{p}_l$, the integral $\int \chi_{il} d\mathbf{R}_l$ is unity and the velocity $\mathbf{v}_l^*$ reduces after time smoothing to the mean particle velocity, $\mathbf{v}_l$, of the molecular species l at point $\mathbf{R}_i$,

$$\mathbf{v}_l(\mathbf{R}_i, t) = (N_l/C_l) \int (\mathbf{p}_l/m_l) f_l^{(1)}(\mathbf{p}_l, \mathbf{R}_i; t) d\mathbf{p}_l. \tag{57}$$

The term $\Delta\boldsymbol{\Omega}_{li}^{(1)}$ represents the contribution to $\boldsymbol{\Omega}_{li}^{(1)}$ arising from the departure of the molecules of the environment of the pair il from statistical equilibrium. For convenience in notation, it will be convenient to define a supplementary force $\mathbf{F}_{li}^+$ by the relation

$$\Delta\boldsymbol{\Omega}_{li}^{(1)} = \mathbf{F}_{il}^+ f_i^{(1)}. \tag{58}$$

The calculation of $\mathbf{F}_{li}^+$ of course requires a knowledge of distribution functions of higher order than $f^{(1)}$. If we had calculated $\boldsymbol{\Omega}_{li}^{(1)}$ under the assumption, not that the pair environment was in equilibrium, but in a lower order of approximation, that the environment of molecule i alone was in equilibrium, we would have obtained all terms in Eq. (56) except those involving the $\mathbf{v}_l^*$.

Introducing Eqs. (56) and (58) into Eq. (49), and neglecting terms of order τ, and performing a second time average over the interval τ on the terms of Eq. (56), which will not affect terms already smoothed and possessing only secular time dependence, we obtain the following partial differential equation for $\bar{f}_i^{(1)}$,

$$\frac{\partial \bar{f}_i^{(1)}}{\partial t} + \frac{\mathbf{p}_i}{m_i} \cdot \nabla_{\mathbf{R}_i} \bar{f}_i^{(1)} + \nabla_{\mathbf{p}_i} \cdot (\mathbf{F}_i^* + \mathbf{X}_i) \bar{f}_i^{(1)} = \nabla_{\mathbf{p}_i} \cdot \zeta_i \left\{ \frac{\mathbf{p}_i}{m_i} \bar{f}_i^{(1)} + kT \nabla_{\mathbf{p}_i} \bar{f}_i^{(1)} \right\},$$

$$\mathbf{F}_i^* = {}^i\langle F_i \rangle^0 + \sum_{l=1}^{\nu} N_l \zeta_l{}^i \mathbf{v}_l^* + \mathbf{F}_i{}^+,$$

$${}^i\langle F_i \rangle^0 = \sum_{l=1}^{\nu} N_l \, {}^i\langle \mathbf{F}_{li} \rangle^0 = -\nabla \mu_i + kT \nabla \log C_i, \quad \mathbf{F}_i^+ = \sum_{l=1}^{\nu} N_l \mathbf{F}_{li}^+, \tag{59}$$

$$\zeta_i = \sum_{l=1}^{\nu} N_l \zeta_i{}^l = \frac{1}{6kT} \int_{-\tau_i}^{+\tau_i} {}^i\langle \mathbf{F}_i \cdot e^{-is\,L} \mathbf{F}_i \rangle^0 ds,$$

where, of course, $\mathbf{F}_i^+$ requires further analysis for its calculation. Equation (59) differs from the generalized Fokker-Planck equation of Chandrasekar[8] in the appearance of the force $\mathbf{F}_i^*$ and in the fact that we have related the friction constant to the intermolecular forces in an explicit manner. If the equation is formulated under the assumption that molecule i is a solute component of an ideal dilute solution with an environment in statistical equilibrium, $\mathbf{F}_i^*$ vanishes. In order to relate ζ_i to intermolecular forces, it is necessary to employ statistical mechanics to construct the Brownian motion kernel of Chandrasekar's Eq. (241). This is, in effect, what we have attempted here, although we have made the Liouville equation our starting point rather than the formal integral equation, Chandrasekar (241).

The second group of terms, involving the $\mathbf{v}_l^*$, are of importance in the theory of diffusion. They give rise to macroscopic interactions by means of which a chemical potential gradient of one component of a solution may cause transport of another component. These questions will be treated in detail in a later article on diffusion.

The method employed in the formulation of Eq. (59) for the distribution function $\bar{f}^{(1)}$ may be applied to distribution functions of higher order $\bar{f}^{(n)}$, if the number of degrees of freedom of the set n is small relative to the total number of degrees of freedom of the entire system. Otherwise, it appears that the plateau values of the friction tensors will not in general exist. With slightly more tedious algebraic details, the method yields for the distribution function $\bar{f}_{i\ldots k}^{(n)}(\mathbf{p}, \mathbf{q}; t)$ in a set of n

[8] S. Chandrasekar, Rev. Mod. Phys. **15**, 1–89 (1943), Eq. (249).

molecules of types $i\cdots k$, respectively,

$$\frac{\partial \bar{f}_{i\cdots k}^{(n)}}{\partial t}+\frac{\mathbf{p}}{m}\cdot\nabla_{\mathbf{q}}\bar{f}_{i\cdots k}^{(n)}+\nabla_{\mathbf{p}}\cdot(\mathbf{F}_{i\cdots k}^{*}+\mathbf{X}_{i\cdots k})\bar{f}_{i\cdots k}^{(n)}=\nabla_{\mathbf{p}}\cdot\zeta_{i\cdots k}^{(n)}\cdot\left\{\frac{\mathbf{p}}{m}\bar{f}_{i\cdots k}^{(n)}+kT\nabla_{\mathbf{p}}\bar{f}_{i\cdots k}^{(n)}\right\},$$

$$\mathbf{F}_{i\cdots k}^{*}={}^{i\cdots k}\langle\mathbf{F}_{i\cdots k}\rangle^{0}+\sum_{l=1}^{\nu}N_l\int\zeta_l{}^{i\cdots k}\cdot\frac{\mathbf{p}_l}{m_l}\bar{f}_l^{(1)}(\mathbf{p}_l,\mathbf{R}_l;t)d\mathbf{R}_l d\mathbf{p}_l+\mathbf{F}_{i\cdots k}^{+},$$

$$\zeta_l{}^{i\cdots k}=\frac{1}{2kT}\left\{\sum_{\alpha=1}^{n}\int_{-\tau_{i\cdots k}}^{+\tau_{i\cdots k}}{}^{i\cdots kl}\langle\mathbf{F}_\alpha e^{-isL}\mathbf{F}_l\rangle^{0}ds\right\}\exp\left(-\beta W_{i\cdots kl}^{(n+1)}\right), \tag{60}$$

$$\zeta_{i\cdots k}^{(n)}=\frac{1}{2kT}\sum_{\alpha=1}^{n}\int_{-\tau_{i\cdots k}}^{+\tau_{i\cdots k}}{}^{i\cdots k}\langle\mathbf{F}_\alpha' e^{-isL}\mathbf{F}_\alpha'\rangle^{0}ds,$$

$$\mathbf{F}_\alpha'=\sum_{l=n+1}^{N}\mathbf{F}_{l\alpha},\qquad {}^{i\cdots k}\langle\mathbf{F}_{i\cdots k}\rangle^{0}=-\nabla_{\mathbf{q}}W_{i\cdots k}^{(n)},$$

where $W_{i\cdots k}^{(n)}$ is the equilibrium potential of average force in the set n, and $\mathbf{F}_{i\cdots k}^{+}$ is the average force due to the departure from equilibrium of the environment of the set of $n+1$ molecules of types $i\cdots k$ and l. The friction tensor $\zeta_{i\cdots k}^{(n)}$ is not in general isotropic in the momentum space of the set n as was $\zeta_i^{(1)}$, which we denoted simply by $\zeta_i 1$, for fluid systems. Since ${}^{i\cdots k}\langle\mathbf{F}_{i\cdots k}\rangle^{0}$ may have gradients in configuration space which are appreciable over distances of molecular magnitude, Eq. (60) requires for its validity the additional conditions, not necessary in the case of $\bar{f}_i^{(1)}$, that the correlation time $\tau_{i\cdots k}$, be sufficiently short that the changes in configuration of the set n, with representative velocities in the neighborhood of the equilibrium mean thermal velocities, are negligible in the interval $\tau_{i\cdots k}$, in comparison with the range of intermolecular force. Although this question requires more careful examination, we remark here that the condition is probably fulfilled to an adequate degree of approximation in condensed systems such as liquids and liquid solutions.

In a series of later articles treating specific transport processes, diffusion, heat conduction, and viscous fluid flow, we plan to suggest an approximation based upon the neglect of $\mathbf{F}_{ik}^{+}$ for pairs, namely the average force arising from the departure of the environment of sets of three molecules from equilibrium.

IV. THE FRICTION CONSTANT

The statistical mechanical theory of transport processes which we have outlined leads to a generalized theory of Brownian motion for small sets of n molecules forming a part of a large system of N molecules. The most significant result of the the theory is the relation which it provides between the friction constant, entering into the Langevin equation and into the differential equations for the distribution functions of lower order, and the intermolecular forces acting in the system. We shall attempt here to transform the expression for the friction constant ζ_i into a form suitable for its calculation from the potential of intermolecular force. The method which we shall propose is to be regarded as tentative and the possibility that it may in the future have to be superseded by more refined methods should be kept in mind.

We repeat the expression, Eq. (43), for the friction constant ζ_i, introducing the canonical distribution for ${}^{0}f_i^{(1/N)}$

$$\zeta_i=\frac{1}{6kT}\int_{-\tau_i}^{+\tau_i}{}^{i}\langle\mathbf{F}_i\cdot e^{-isL}\mathbf{F}_i\rangle^{0}ds,$$

$${}^{l}\langle\mathbf{F}_i\cdot e^{-isL}\mathbf{F}_i\rangle^{0}=\int\int\{\mathbf{F}_i\cdot e^{-isL}\mathbf{F}_i\}({}^{0}f_i^{(1)})^{-1}e^{\beta(A-H)}d\mathbf{P}d\mathbf{Q},$$

$${}^{0}f_i^{(1)}=\left(\frac{\beta}{2\pi m_i}\right)^{\frac{3}{2}}\frac{1}{v}\exp\left[-\beta p_i^{2}/2m_i-\beta W_i^{(1)}\right], \tag{61}$$

$$L=i\sum_{l=1}^{N}\left\{\frac{\mathbf{p}_l}{m_l}\cdot\nabla_{\mathbf{R}_l}+\mathbf{F}_l\cdot\nabla_{\mathbf{p}_l}\right\},$$

where in the expression for the operator L, as also in the Hamiltonian H, we omit terms arising from the external forces $\mathbf{X}_l$, since the latter will contribute at most terms of the second order to the distribution functions, the external forces being assumed small, of the first order, in systems to which the theory is applicable. We recall that the friction constant may be a function $\zeta_i(\mathbf{R}_i, \mathbf{p}_i)$ of the coordinates of molecule i, although in fluid systems we would expect no sensible dependence on $\mathbf{R}_i$. It will be found to be convenient to introduce a friction constant $\langle\zeta_i\rangle_{Av}$, the mean value of ζ in the phase space of molecule i.

$$\langle\zeta_i\rangle_{Av}=\int\int\zeta_i(\mathbf{p}_i,\mathbf{R}_i)^0 f_i^{(1)}(\mathbf{p}_i,\mathbf{R}_i)d\mathbf{p}_i d\mathbf{R}_i$$

$$=\frac{1}{6kT}\int_{-\tau_i}^{\tau_i}\langle\mathbf{F}_i\cdot e^{-isL}\mathbf{F}_i\rangle^0 ds, \tag{62}$$

$$\langle\mathbf{F}_i\cdot e^{-isL}\mathbf{F}_i\rangle^0=\int\cdots\int\{\mathbf{F}_i\cdot e^{-isL}\mathbf{F}_i\}e^{\beta(A-H)}d\mathbf{p}_1\cdots d\mathbf{R}_N.$$

If ζ_i is independent of $\mathbf{p}_i$ as well as $\mathbf{R}_i$, it is of course identical with $\langle\zeta_i\rangle_{Av}$.

If we assume that the correlation $\langle\mathbf{F}_i \exp(-isL)\mathbf{F}_i\rangle^0$ between the intermolecular forces acting on molecule i at instants of time separated by the interval s is a monotone decreasing function of time in the neighborhood of $s=0$, it is reasonable to try to represent the decay by a Gaussian factor determined by the second moment of the operator L. If we denote by $\mu_n^{(i)}$ the n'th moment of the operator L, defined as follows

$$\mu_n^{(i)}=\frac{1}{\Delta F_i}\int\cdots\int\{\mathbf{F}_i\cdot L^n\mathbf{F}_i\}e^{\beta(A-H)}d\mathbf{p}_1\cdots d\mathbf{R}_N,$$

$$\Delta F_i=\langle F_i^2\rangle^0=\int\cdots\int F_i^2 e^{\beta(A-H)}d\mathbf{p}_1\cdots d\mathbf{R}_N, \tag{63}$$

$$\omega_i^2=\mu_2^{(i)},$$

where L^n denotes n successive applications of the operator L, we find that the $\mu_n^{(i)}$ are positive for even n and vanish for odd n. Using the formal power series, Eq. (8), for the operator $\exp(-isL)$ in the integrand of Eq. (62) defining $\langle\mathbf{F}_i\cdot e^{-isL}\mathbf{F}_i\rangle^0$ and factoring the function $\exp(-\omega_i^2 s^2/2)$ from the resulting power series, ω_i^2 being used in place of $\mu_2^{(i)}$, the second moment, we obtain,

$$\langle\mathbf{F}_i\cdot e^{-isL}\mathbf{F}_i\rangle^0=\Delta F_i\exp(-\omega_i^2 s^2/2)\sum_{n=0}^{\infty}\frac{\kappa_n^{(i)}(\omega_i^2 s^2)^n}{(2n)!},$$

$$\kappa_n^{(i)}=\sum_{r=0}^{n}\frac{(2n)!(-1)^r}{(2r)!(n-r)!2^{n-r}}\frac{\mu_{2r}^{(i)}}{\mu_2^{(i)r}}. \tag{64}$$

Substitution of the series (64) into the time integral of Eq. (62) yields the plateau value,

$$\langle\zeta_i\rangle_{Av}=\frac{(2\pi)^{\frac{1}{2}}\Delta F_i}{6kT\omega_i}\left\{1+\sum_{n=2}^{\infty}\frac{\kappa_n^{(i)}}{2^n n!}\right\}, \tag{65}$$

with the neglect of terms of $O[\exp(-\omega_i^2\tau_i^2/2)]$. Assuming the formal procedure leading to Eq. (65) to be valid, we are able to specify more precisely the magnitude of the microscopic time interval τ_i, over which the integral defining the friction constant $\langle\zeta_i\rangle_{Av}$ must be extended in order to attain the plateau value. The correlation time is of the order of $1/\omega_i$ and τ_i must evidently be large relative to $1/\omega_i$.

We shall not here attempt to give a mathematical justification of the formal procedure leading to Eq. (65), but tentatively accept the result as plausible for systems of molecules with intermolecular

forces of known types. Properly, the class of dynamical systems, for which the procedure is valid, should be characterized by suitable restrictions on their Hamiltonians. We should probably be prepared to find that, in cases of interest, the series of Eq. (65) is an asymptotic series and not a convergent series.

The variance or fluctuation of intermolecular force Δ_{F_i} may, for intermolecular forces of the type of Eq. (2), be expressed as follows

$$\Delta_{F_i}=\sum_{l=1}^{\nu} N_l\langle F_{li}^2\rangle^0+\sum_{l=1}^{\nu}\sum_{l'=1}^{\nu} N_l N_{l'}\langle \mathbf{F}_{li}\cdot\mathbf{F}_{l'i}\rangle^0, \tag{66}$$

where $\mathbf{F}_{li}$ is the force exerted on a molecule of type i by a molecule of type l. In the absence of long range forces, for example Coulomb forces acting between ions in solution, the average values of Eq. (66) may be transformed with the aid of Green's theorem to give,

$$\Delta_{F_i}=kT\sum_{l=1}^{\nu} c_l\Delta_{il}, \quad \Delta_{il}=N\int\nabla^2 V_{il}(R)\exp\left(-\beta W_{il}^{(2)}\right)dv, \tag{67}$$

where $W_{il}^{(2)}$ is equilibrium potential of average force between a pair of type il, V_{il} the potential of intermolecular force between the pair, and the integral is to be extended over all values of their relative coordinates; N is here Avogadro's number and c_l is the concentration of component l in moles per unit volume. The function $\exp\left(-\beta W_{il}^{(2)}\right)$ is the radial distribution function for a pair il in the equilibrium ensemble.

The characteristic frequency ω_i^2 may be expressed in the following form,

$$\omega_i^2=\frac{1}{\Delta_{F_i}}[\langle L^*\mathbf{F}_i\cdot L\mathbf{F}_i\rangle^0], \tag{68}$$

by virtue of the fact that L is self-adjoint. Integration over momentum space leads to the result

$$\omega_i^2=\frac{kT}{\Delta_{F_i}}\sum_{l=1}^{N}(1/m_l)\langle(\nabla_l\mathbf{F}_i):(\nabla_l\mathbf{F}_i)\rangle^0 \tag{69}$$

where $(\nabla_l\mathbf{F}_i):(\nabla_l\mathbf{F}_i)$ denotes the inner product of the dyadic $\nabla_l\mathbf{F}_i$, equal to the sum of the squares of its nine components. For intermolecular forces of the type of Eq. (2), a further reduction is possible, in the absence of long range Coulomb forces,

$$\begin{aligned}
\omega_i^2&=\frac{kT}{\Delta_{F_i}}\left\{\sum_{l=1}^{\nu}\left(\frac{1}{M_l}+\frac{1}{M_i}\right)C_l I_l^{\,i}+\frac{1}{M_i}\sum_{l=1}^{\nu}\sum_{l'=1}^{\nu} C_l C_{l'} I_{ll'}^{\,i}\right\},\\
I_l^{\,i}&=N^2\int\left\{\left(\frac{d^2V_{il}}{dR^2}\right)^2+\frac{2}{R^2}\left(\frac{dV_{il}}{dR}\right)^2\right\}\exp\left(-\beta W_{il}^{(2)}\right)dv,\\
I_{ll'}^{\,i}&=N^3\int\int\left\{\cos^2\gamma\frac{d^2V_{il}}{dR^2}\frac{d^2V_{il'}}{dR'^2}+\sin^2\gamma\left[\frac{1}{R}\frac{dV_{il}}{dR}\frac{d^2V_{il'}}{dR'^2}+\frac{1}{R'}\frac{d^2V_{il}}{dR^2}\frac{dV_{il'}}{dR'}\right]\right.\\
&\qquad\left.+\frac{3-\cos^2\gamma}{RR'}\frac{dV_{il}}{dR}\frac{dV_{il'}}{dR'}\right\}\exp\left(-\beta W_{ill'}^{(3)}\right)dv'dv,\\
\cos\gamma&=(\mathbf{R}'\cdot\mathbf{R})/R'R,
\end{aligned} \tag{70}$$

where M_i and M_l are the molecular weights of components i and l respectively, and $V_{il}(R)$ and $V_{il'}(R')$ are the potentials of the force between pairs of types il and il', respectively. The potential $W_{ill'}^{(3)}$ is the equilibrium potential of average force acting on molecules l' and l situated at points R' and R from the fixed molecule i. The average values in configuration space have been simplified for fluid systems in which $W_i^{(1)}$ the equilibrium potential of mean force on any molecule i is zero.

Returning to the friction constant ζ_i, which may depend upon $\mathbf{p}_i$ and thus differ from $\langle\zeta_i\rangle_{Av}$, we make the hypothesis that the time decay of the mean value ${}^i\langle\mathbf{F}_i\cdot e^{-isL}\mathbf{F}_i\rangle^0$ is also of the order of $\exp(-\omega_i^2 s^2/2)$ with the ω_i^2 of Eqs. (68)–(70). Using the power series, Eq. (8) for $\exp(-isL)$ in Eq. (61), again factoring $\exp(-\omega_i^2 s^2/2)$, and integrating with respect to time, we obtain the plateau value,

$$\zeta_i=\frac{(2\pi)^{\frac{1}{2}}\Delta_{F_i}}{6kT\omega_i}\left\{1+\sum_{n=1}^{\infty}\frac{{}^i\kappa_n{}^{(i)}}{2^n n!}\right\},\quad {}^i\kappa_n{}^{(i)}=\sum_{r=0}^{n}\frac{(2n)!(-1)^r}{(2r)!(n-r)!2^{n-r}}\frac{{}^i\mu_{2r}{}^{(i)}}{\mu_2{}^{(i)r}},\tag{71}$$

$${}^i\mu_{2r}{}^{(i)}=(1/\Delta_{F_i})\ {}^i\langle\mathbf{F}_i\cdot L^{2r}\mathbf{F}_i\rangle^0,$$

where ${}^i\kappa_1{}^{(i)}$ depends upon $\mathbf{p}_i$ and does not vanish as did $\kappa_1{}^{(i)}$. The moments ${}^i\mu_n{}^{(i)}$ depend upon $\mathbf{p}_i$ and therefore differ from the $\mu_n{}^{(i)}$. The coefficients $\kappa_n{}^{(i)}$ and ${}^i\kappa_n{}^{(i)}$ can be expressed in terms of semi-invariants, frequently used in statistics, instead of directly in terms of the moments, if desired.

Assuming that moments of L higher than the second can be neglected and calculating the pertinent average values, we obtain the following approximation to the friction constant ζ_i.

$$\zeta_i=\frac{(2\pi)^{\frac{1}{2}}\Delta_{F_i}}{6kT\omega_i}[1-\alpha_i(1-\beta p_i^2/3m_i)],\quad \alpha_i=\frac{(kT)^2}{2M_i\Delta_{F_i}\omega_i^2}\sum_{l=1}^{\nu}C_l{\alpha_l}^i,$$

$${\alpha_l}^i=N^2\int(\nabla^4 V_{il})\exp(-\beta W_{il}{}^{(2)})dv,\tag{72}$$

where Δ_{F_i} and ω_i are given by Eqs. (67) and (70). Green's theorem has again been used in calculating α_i under the restriction of short range intermolecular forces. We surmise and will later investigate by explicit calculation that in condensed systems such as liquids and liquid solutions, where the second group of terms of Eq. (70) involving the $I_{ll'}{}^i$ make the dominant contribution to ω_i^2, that α_i will be sufficiently small to neglect the dependence of ζ_i on p_i for values of p_i in the neighborhood of its equilibrium root mean square. In this case our approximation to the friction constant becomes

$$\zeta_i=\frac{(2\pi)^{\frac{1}{2}}\Delta_{F_i}}{6kT\omega_i}.\tag{73}$$

If molecule i is a macromolecule of high molecular weight M_i in a solvent of low molecular weight, we shall expect ζ_i to be effectively independent of p_i, since ω_i by Eq. (70) becomes independent of M_i and thus α_i diminishes with M_i, vanishing with the ratio of M_s/M_i, where M_s is the solvent molecular weight.

For a macromolecule in a solvent of low molecular weight we conclude from Eq. (73) and the asymptotic independence of ω_i on M_i that ζ_i will be also independent of M_i, depending only on the mass of the solvent molecules. The relation between Eq. (73) and the hydrodynamic estimate of ζ_i by Stokes law for macromolecules is connected with the boundary condition of no slip at an interface with a rigid surface, which is used in the hydrodynamics of viscous fluids. The resistance $\zeta_i\mathbf{p}_i/m_i$ experienced by a macroscopic sphere i, when determined by our method with the ζ_i of Eqs. (61) and (73) is due to a surface layer of molecules of solvent of thickness of the order of the range of intermolecular forces. If the hypothesis of no slip in this layer is made, the resistance $\zeta_i\mathbf{p}_i/m_i$ experienced by sphere will be equal to the hydrodynamic resistance $6\pi\eta m_i\mathbf{p}_i$ exerted by the fluid on the surface layer. This argument might be made the basis for a molecular theory of the viscosity coefficient η, but it turns out not to be the most convenient or consequential approach to this problem.

A few further remarks concerning the dependence of the friction constant ζ_i on the mass of molecule i are of interest. Only when the mass of molecule i is large relative to those of the molecules of its environment will ζ_i be independent of M_i. In fact from Eqs. (70) and (73), one observes that if the mass of i is very small relative to those of its environment, ζ_i is proportional to $M_i^{\frac{1}{2}}$. This circumstance suggests, contrary to the conclusion to be drawn from the hydrodynamic estimate of ζ_i based on Stoke's law, that isotope separations by thermal dif-

fusion or electrolysis might be practicable in liquids and liquid solutions, provided the solvent consists of molecules of mass not small relative to the masses of the molecules to be separated.

We remark that we have not proved the existence of a plateau value of the friction constant for systems of molecules interacting with intermolecular forces of the usual type. We have only outlined a method for estimating ζ_i which appears feasible, if the plateau value exists. It is therefore of interest to examine two cases, the crystal with harmonic lattice vibrations and the gas with binary collisions, for which the integral Eq. (61), defining ζ_i, can be evaluated directly.

Although we shall not here reproduce the details of the analysis, we remark that the friction constant appears to have no plateau value for the crystal with harmonic lattice vibrations. This is evidently due to the fact that the motion is multiply periodically. We do not conclude from this that no dissipative mechanism exists whereby a molecule moving in the lattice can exchange energy with the harmonic lattice vibrational modes, but only that anharmonic terms must be considered in describing the dissipative mechanism. Nor does this necessarily imply that Eqs. (67), (70), and (71), although they involve derivatives of the potentials of intermolecular force no higher than the second, do not provide an adequate approximation to the friction constant in crystals (of course, in crystals ζ_i is a function of $\mathbf{R}_i$ and requires a supplementary average over a domain of linear dimensions large relative to the lattice parameters before use in macroscopic transport theory). That is to say, the anharmonic terms may assure the approach to a plateau value, by affecting the wings of the force correlation, without sensibly affecting its value.

Although transport in gases of low density is most accurately described by the Maxwell-Boltzmann integro-differential equation, the theory developed here is applicable to a certain degree of approximation. Using binary collision analysis, we find that ζ_i does indeed have a plateau value for values of τ_i, long relative to the representative duration of a molecular collision. For simplicity, we give the result for a system of one component, easily generalized to an arbitrary number of components.

$$\begin{aligned}
\zeta &= \frac{N}{6vkT}\int\int \Phi(\mathbf{R}_0, \alpha, \epsilon)\left(\frac{dV}{dR_0}\right) \\
&\qquad \times \exp\left(-\beta V - \beta p_{20}^2/2m\right) d\mathbf{R}_0 d\mathbf{p}_{20}, \\
\Phi &= \frac{m}{2\alpha}\int_0^{\vartheta^*} \cos(\vartheta - \vartheta_0) R^2 \frac{dV}{dR} d\vartheta, \\
\alpha &= |\mathbf{R}_0 \times \mathbf{p}_{12}^0|; \\
\vartheta^* &= 2\int_b^\infty \frac{(\alpha/r^2)dr}{[m(\epsilon - V(r) - \alpha^2/mr^2)]^{\frac{1}{2}}}, \\
\epsilon &= p_{12}^{02}/m + V(R_0),
\end{aligned} \tag{74}$$

where b is largest positive root of

$$\epsilon - V(b) - \alpha^2/mb^2 = 0,$$

and $\mathbf{p}_{12}^0$ and $\mathbf{R}_0$ are the relative momentum and position of a molecular pair, m the molecular mass, and V the potential of intermolecular force. In the integral defining Φ, R is to be evaluated as a function of ϑ, from the equation of the orbit,

$$\begin{aligned}
\vartheta &= \int_R^\infty \frac{(\alpha/r^2)dr}{[m(\epsilon - V - \alpha^2/mr^2)]^{\frac{1}{2}}}; \quad 0 \leqq \vartheta \leqq \vartheta^*/2, \\
\vartheta &= \vartheta^* - \int_R^\infty \frac{(\alpha/r^2)dr}{[m(\epsilon - V - \alpha^2/mr^2)]^{\frac{1}{2}}}; \\
&\qquad \vartheta^*/2 < \vartheta \leqq \vartheta^*
\end{aligned} \tag{75}$$

for a binary collision. A comparison of ζ evaluated by Eqs. (74) and (75) with the approximation, Eq. (71), would be desirable. However, it should be kept in mind in making such a comparison that the peak approximation, upon which Eq. (71) is based is without doubt much better in liquids and liquid solutions than in gases.

We close our survey of the general theory by a remark about $\zeta_i(\infty)$, the asymptotic value of $\zeta_i(\tau)$ for $\zeta \to \infty$. In the case of gases, we would find that $\zeta_i(\infty)$ is vanishing or undeterminate, if we were so unwise as to let $\tau_i \to \infty$, since after a time of the order of the period of a Poincaré cycle, the contribution, Eq. (73), to ζ would be cancelled by that from a collision in which the orbit was traversed in the reverse sense. Using spectral theory (see Appendix I), we have convinced ourselves that in a system of molecules

with arbitrary central forces, the only invariants of which are energy, total linear momentum, and total angular momentum, $\zeta_i(\infty)$ always vanishes. As we have already pointed out, this circumstance is related to the failure of thermodynamic dissipative mechanisms over very long periods comparable with those of Poincaré cycles.

Applications of the general theory, which we have presented here, to special transport processes will follow in later articles.

In conclusion, we wish to express our thanks to Professor Joseph E. Mayer for his kindness in reading this article in manuscript and for providing much illuminating criticism.

APPENDIX: REMARKS ON THE MATHEMATICAL THEORY OF THE OPERATOR $\exp(-isL)$

Although we shall not attempt an exhaustive justification of our manipulations of the operator $\exp(-isL)$, we wish to call attention to the basic mathematical theory[9] underlying the use of this operator. We first consider the eigenvalue problem

$$L\psi_\lambda = \lambda\psi_\lambda, \tag{A1}$$

where the domain of the operator L is restricted to functions $g(p, q)$ in phase space which form a Hilbert space. Since L is self adjoint, the eigenvalues λ are real. The inner product (f, g) of two such functions is defined as

$$(f, g) = \int\int f^* g d\mathbf{p} d\mathbf{q}, \tag{A2}$$

where if f, g are vectors in phase space f^*g in the integrand is to be replaced by $\mathbf{f}^* \cdot \mathbf{g}$. If $E(\lambda)$, the canonical resolution of the identity appropriate to L, is defined as the operator which projects any function g on the linear manifold in Hilbert space spanned by the eigenfunctions of L corresponding to eigenvalues less than λ, the operator $\exp(-isL)$ may be represented by the Stieltjes integral,

$$e^{-isL} = \int_{-\infty}^{+\infty} e^{-i\lambda s} dE(\lambda). \tag{A3}$$

[9] See von Neumann, Proc. Nat. Acad. Sci. **18** (1932). Also *Quantenmechanik* (Verlagsbuchhandlung Julius Springer, Berlin, 1932); Stone, *Linear Transformations in Hilbert Space* (American Mathematical Society Publication, 1932).

Using Eq. (A3) in Eq. (62) defining the mean friction constant $\langle\zeta_i\rangle_{Av}$, we have

$$\begin{aligned} \langle\zeta_i\rangle_{Av} &= \frac{1}{6kT}\int_{-\tau_i}^{+\tau_i}\int_{-\infty}^{+\infty} e^{-i\lambda s} dz_i(\lambda) ds, \\ z_i(\lambda) &= (E(\lambda)\mathbf{\Lambda}_i, \mathbf{\Lambda}_i), \\ \mathbf{\Lambda}_i &= \exp\left[\beta(A-H)/2\right]\mathbf{F}_i, \end{aligned} \tag{A4}$$

where the invariance of H under $\exp(-isL)$ has been used to symmetrize the expression. The fluctuation of intermolecular force is evidently given by

$$\Delta F_i = \int_{-\infty}^{+\infty} dz_i(\lambda) = (\mathbf{\Lambda}_i, \mathbf{\Lambda}_i), \tag{A5}$$

and the moments of L, with respect to $Z(\lambda)$, of Eq. (63) are expressible in the form,

$$\mu_n^{(i)} = \frac{1}{\Delta F_i}\int_{-\infty}^{+\infty} \lambda^n dz_i(\lambda). \tag{A6}$$

The justification of the peak approximation,

$$\langle\zeta_i\rangle_{Av} = \frac{(2\pi)^{\frac{1}{2}}\Delta F_i}{6kT\omega_i}, \quad \omega_i^2 = \mu_2^{(i)}, \tag{A7}$$

employed in Part IV to represent $\langle\zeta_i\rangle_{Av}$, therefore must rest upon a study of the structure of the projection operator $E(\lambda)$ for the special dynamical system in question, and a verification that the integral,

$$\int_{-\infty}^{+\infty} e^{-is\lambda} dz_i(\lambda),$$

is adequately approximated by

$$\Delta F_i \exp(-\omega_i^2 s^2/2)$$

in the neighborhood of $s=0$ and for subsequent intervals of time of microscopic duration (small relative to the representative interval of macroscopic observation).

A brief discussion of the asymptotic value $\langle\zeta_i\rangle_{Av}(\infty)$ for $\tau_i \to \infty$ is of some interest here. Let us suppose that the spectrum of L is continuous in the neighborhood of $\lambda=0$, and that the operator E_0' defined by

$$E_0' = \lim_{\lambda\to 0} \frac{E(\lambda) - E(-\lambda)}{2\lambda} \tag{A8}$$

exists. Then, commuting the order of integra-

tions in Eq. (A4) and letting $\tau_i \to \infty$, we get

$$\zeta_i(\infty) = \frac{\pi}{6kT}(E_0'\mathbf{\Lambda}_i, E_0'\mathbf{\Lambda}_i), \tag{A9}$$

where E_0' is the operator projecting a function in Hilbert space on the linear manifold spanned by the eigenfunctions of L per unit λ-interval in the vicinity of $\lambda = 0$. The functions spanning this manifold are functions of the invariants of L, that is the constants of the motion. For arbitrary central intermolecular forces, with energy, total linear momentum, and total angular momentum the only invariants, explicit calculation shows that $\langle \zeta_i \rangle_{Nv}(\infty)$ vanishes, a fact to which attention has already been called.

Other uses of the spectral resolution of L may be mentioned. For example, the solution $\varphi(\mathbf{p}, \mathbf{q}; t)$ of the inhomogeneous equation,

$$\begin{aligned} L\varphi + i\frac{\partial \varphi}{\partial t} &= A(\mathbf{p}, \mathbf{q}; t), \\ \varphi(\mathbf{p}, \mathbf{q}; 0) &= \varphi_0(\mathbf{p}, \mathbf{q}), \end{aligned} \tag{A10}$$

may be expressed in the form

$$\begin{aligned} \varphi(\mathbf{p}, \mathbf{q}; t) = &\int_{-\infty}^{+\infty} e^{-i\lambda t} d(E(\lambda)\varphi_0) \\ &+ \int_0^t \int_{-\infty}^{+\infty} e^{-i\lambda(t-s)} d(E(\lambda)A) ds \end{aligned} \tag{A11}$$

which is useful in the treatment of time dependent external forces under certain circumstances.*

* This method is being studied by Dr. F. W. Boggs in connection with the general theory of dielectric loss.

A Note on the Theory of Diffusion Controlled Reactions with Application to the Quenching of Fluorescence

ELLIOTT W. MONTROLL*
Department of Chemistry, Polytechnic Institute of Brooklyn, Brooklyn, New York
(Received September 26, 1945)

The principles of Smoluchowski's collision theory of reactions in solution are outlined. This theory is applicable to reactions which occur immediately on the collision of two reactant particles; that is, diffusion controlled reactions. The rate of such reactions depends on the collision frequency of reactants. In this paper an expression for the collision frequency is derived as a function of time when initially there is a Boltzmann distribution of particles around any particular reactant molecule. Both the Brownian motion of and the forces between reactant molecules are considered in the calculation. The general results are applied to the theory of quenching of fluorescence. It is shown that the quenching constant, k_Q, defined by

$$\left(\frac{I_0}{I}-1\right)\Big/ n_Q=k_Q,$$

(where I_0 is the intensity of fluorescence in the absence of quencher and I the intensity in the presence of quencher of concentration n_Q) can be expressed as a sum of two terms, one proportional to the reciprocal of the viscosity of the solvent and the other to the reciprocal of the square root of the viscosity.

RECENTLY there has been a renewal of interest in Smoluchowski's collision theory of reaction rates in solutions. This theory,[1] which is applicable to those reactions which occur instantaneously upon collision of two molecules or ions (diffusion controlled reactions) was originally developed to explain the process of coagulation of colloids. It assumes that any pair of colloidal particles adhere to each other after they collide and behave as a single larger particle. Thus, after many collisions giant coagulated particles are formed. The collision frequency calculations required for this theory were shown to be equivalent to the calculation of the rate of diffusion of particles into the sphere of influence of a single particle in the solution. In Smoluchowski's work the effect of forces between particles was neglected. Zsigmondy[2] and Tuorila[3] obtained reasonable experimental agreement with Smoluchowski's theory. Some deviation was to be expected because of the assumptions that were made to avoid the complications caused by the wide variety of shapes of coagulated particles formed by collisions.

In 1935 Sveshnikoff[4] developed a theory of quenching of fluorescence using Smoluchowski's methods. Qualitatively the explanation of quenching is based on the idea that a molecule or ion in solution which has been excited by the absorption of a photon returns to its ground state by the emission of light (fluorescence) or by collision with a foreign particle called a quencher. An increase in quencher concentration causes more collisions, lowering the intensity of fluorescence. Sveshnikoff derived an expression for the collision frequency of excited particles with quencher from a study of the diffusion of quencher into the sphere of influence of the excited particles. Usually one assumes that this sphere has a radius equal to the sum of the radii of the two colliding particles.

Frequently the excited particles and quencher are ions, in which case Coulomb forces interfere with the normal diffusion process. Debye[5] has evaluated the influence of these forces on the *steady-state* collision frequency. As will be discussed later in this paper, the transient collision frequency (collision frequency before the steady

* Present address, Division of Research in Natural Sciences, University of Pittsburgh, Pittsburgh, Pennsylvania.

[1] M. Smoluchowski, Physik. Zeits. **17**, 557, 585 (1916); Zeits. f. physik. Chemie **92**, 129 (1917).
[2] R. Zsigmondy, Zeits. f. physik. Chemie **92**, 600 (1917).
[3] Tuorila, Kolloid-Chem. Beihefte **22**, 191 (1926).
[4] B. Sveshnikoff, Acta Physicochimica U.S.S.R. **3**, 257 (1935).
[5] P. Debye, Trans. Electrochem. Soc. **82**, 265 (1942).

state is achieved) is important in describing some reactions; for example, quenching of fluorescence in the photo-stationary state. A first attempt at this transient problem has been made by Umberger and LaMer.[6]

The purpose of this paper is to outline the principles of Smoluchowski's collision theory of reactions in solution, and to use it to derive formulae for collision frequency as a function of time in dilute solutions. The results will be applied to the theory of quenching of fluorescence.

I. GENERAL THEORY

Let us consider a solution containing two kinds of particles as solute, and suppose that a reaction occurs when a particle of one kind enters the "sphere of influence" of one of the other kind; that is, when their centers are separated by a distance R (usually assumed to be the sum of the radii of the two particles). Under this assumption the reaction rate is a function of the number of collisions per unit time. In general, the collision frequency depends on the Brownian motion of the particles. We base our collision frequency calculations on Smoluchowski's differential equation for the probability of finding a particle in a given region of space while it is experiencing a Brownian motion in the force field of another particle. The solution of this differential equation enables us to determine the probability of a collision between two particles in a given time interval. Assuming the independence of collisions, we see that the product of this probability by the number of particles of each type in the system during the collision interval gives the total number of collisions in the interval. Thus we are able to calculate the reaction rate at that time.

Smoluchowski's equation:[7]

$$\partial w_B/\partial t = D_2 \operatorname{div} \{\operatorname{grad} w_B - (\mathbf{F} w_B/kT)\} \quad (1)$$

describes the motion of a particle "B" in the force field of a stationary particle "A" separated from it by a distance r. Here $w_B(r, t)$ is defined so that $4\pi r^2 w_B(r, t)dr$ is the probability of finding the two particles separated by a distance between r and $r+dr$ at time t. k is Boltzmann's constant, T the absolute temperature, and D_2 the diffusion constant of particles of kind B in the solution. If the force $\mathbf{F}$ can be derived from a potential U,

$$\mathbf{F} = -\operatorname{grad} U, \quad (2)$$

(1) becomes

$$\partial w_B/\partial t = D_2\{\nabla^2 w_B + (w_B/kT)\nabla^2 U + (1/kT)(\partial w_B/\partial r)(\partial U/\partial r)\}. \quad (1a)$$

When A also experiences a Brownian motion, one must replace D_2 by $D = D_1 + D_2$, where D_1 is the diffusion constant for particles of kind A in the solution. It is convenient to introduce a new function $\alpha(r, t)$ defined by

$$\alpha(r, t) = w_B \exp\{U(r)/kT\}, \quad (3)$$

for after this substitution (1a) becomes (assuming the diffusion field to be spherically symmetrical)

$$\frac{\partial \alpha}{\partial t} = D\left\{\frac{\partial^2 \alpha}{\partial r^2} + \frac{\partial \alpha}{\partial r}\left(\frac{2}{r} - \frac{1}{kT}\frac{\partial U}{\partial r}\right)\right\}. \quad (4)$$

This equation has also been derived in a somewhat different manner by Umberger and LaMer.[6]

To calculate the collision frequency we use the initial condition:

at time $t=0$, particles of kind B are arranged in a Boltzmann distribution about one of kind A, thus

$$w_B(r, 0) = n_B(0) \exp\{-U(r)/kT\}, \quad (5a)$$

where $n_B(0)$ is the mean concentration in particles per cc of B's exterior to the sphere $r = |R|$. In terms of $\alpha(r, t)$ this is equivalent to

$$\alpha(r, 0) = n_B(0) = n_B; \quad (5b)$$

and Smoluchowski's boundary conditions:

(a) Very far from the particle A the concentration of B's remain at their initial value

$$w_B(\infty, t) = n_B \quad (6a)$$

or

$$\alpha(\infty, t) = n_B. \quad (6b)$$

This is strictly true only in the case where $n_B(0) \gg n_A(0)$, so that while the supply of A's is exhausted by the reaction the concentration

[6] J. Umberger and V. LaMer, J. Am. Chem. Soc. **67**, 1099 (1945).

[7] M. Smoluchowski, Ann. d. Physik **48**, 1103 (1915). See also S. Chandrasekhar, Rev. Mod. Phys. **15**, 1 (1943). This paper also contains a short exposition of Smoluchowski's theory of coagulation of colloids.

of B's is but slightly affected. Thus, while $n_B(t) \simeq n_B$ for all t, $n_A(t) \to 0$ as $t \to \infty$.

(*b*) The concentration of particles of kind B on the sphere of influence of an A is zero before a reaction involving that particular A occurs

$$w_B(R, t) = 0 \tag{7a}$$

or

$$\alpha(R, t) = 0. \tag{7b}$$

Under conditions (*a*) and (*b*), Eq. (1) is equivalent to the equation describing the diffusion of particles into a spherical hole of radius R from a spherically symmetrical steady source a large distance away.

The solution of (4) under these conditions enables one to calculate[6] the rate $I(t)$ at which particles of kind B arrive at the surface $|r| = R$ at time t:

$$I(t) = 4\pi r^2 D\left(\frac{\partial w_B}{\partial r} + \frac{w_B}{kT}\frac{\partial U}{\partial r}\right)_{r=R}$$

$$= 4\pi D R^2 \exp\{-U(R)/kT\}(\partial\alpha/\partial r)_{r=R} \tag{8}$$

and the collision frequency $\nu(t)$ at time t from

$$\nu(t) = I(t) n_A(t). \tag{9}$$

II. COLLISION FREQUENCY IN GENERAL FORCE FIELD

In this section we shall solve the differential Eq. (4),

$$\frac{\partial\alpha}{\partial t} = D\left\{\frac{\partial^2\alpha}{\partial r^2} + \frac{\partial\alpha}{\partial r}\left(\frac{2}{r} - \frac{1}{kT}\frac{\partial U}{\partial r}\right)\right\}, \tag{4}$$

under the initial condition (5b),

$$\alpha(r, 0) = n_B, \tag{5b}$$

and the boundary conditions (6b) and (7b):

$$\alpha(\infty, t) = n_B, \tag{6b}$$

$$\alpha(R, t) = 0. \tag{7b}$$

The steady-state solution of (4) (that corresponding to $\partial\alpha/\partial t = 0$) has been obtained by Debye[5] and is, as can be verified by direct substitution into (4), (6b), and (7b)

$$\alpha(r) = n_B\{1 - [S(r)/S(R)]\}, \tag{10}$$

where

$$S(r) = \int_r^\infty z^{-2} \exp\{U(z)/kT\} dz. \tag{11}$$

To obtain the transient solution of (4) we introduce a new function $f(r, t)$ defined by

$$\alpha(r, t)/n_B = 1 + [S(r)/S(R)][f(r, t) - 1]. \tag{12}$$

By substituting (12) into (4), (5b), (6b), and (7b) we see that $f(r, t)$ satisfies

$$\frac{\partial f}{\partial t} = D\left\{\frac{\partial^2 f}{\partial r^2} + \frac{\partial f}{\partial r}\left[\frac{2S'(r)}{S(r)} + \left(\frac{2}{r} - \frac{1}{kT}\frac{\partial U}{\partial r}\right)\right]\right\}, \tag{13}$$

$$f(R, t) = 0, \quad f(r, 0) = 1, \quad \text{and} \quad f(\infty, t) < \infty, \tag{13a}$$

where

$$S'(r) = \partial S/\partial r = -r^{-2} \exp\{U(r)/kT\}. \tag{14}$$

The transformation (12) is useful because in the range of large r the coefficient of $(\partial f/\partial r)$ becomes negligible, while in the range of medium r's corresponding to close approach of two particles, forces of the Coulomb type $U(r) \sim a/r$ cause the term $2S'(r)/S(r)$ to cancel the remainder of the coefficient of $\partial f/\partial r$, leaving a coefficient of lower order than that of $\partial\alpha/\partial r$ in (4). This is apparent if we write

$$S(r) \simeq \int_r^\infty z^{-2}(1 + a/zkT + a^2/2(zkT)^2 + \cdots) dz,$$

from which we obtain

$$2S'(r)/S(r) \simeq -2/r - a/r^2 kT - O(1/r^3);$$

thus, leaving terms of $O(1/r^3)$ when added to

$$\left(\frac{2}{r} - \frac{1}{kT}\frac{\partial U}{\partial r}\right) \simeq 2/r + a/kTr^2.$$

We shall on this account neglect the term involving $\partial f/\partial r$ in (15), waiting until the next section to estimate the error caused by this simplification. The solution of the approximate $f(r, t)$ equation $\partial f/\partial t = D\partial^2 f/\partial r^2$ under the conditions (13a) is

$$f(r, t) = \operatorname{erf}\{(r - R)/2(Dt)^{\frac{1}{2}}\}, \tag{15}$$

where

$$\operatorname{erf} y = 2\pi^{-\frac{1}{2}} \int_0^y \exp(-v^2) dv. \tag{15a}$$

Therefore,

$$\alpha(r, t)/n_B - 1 \simeq S(r)/S(R) \times\{-1 + \operatorname{erf}[(r - R)/2(Dt)^{\frac{1}{2}}]\}, \tag{16}$$

and from (8) the collision frequency $\nu(t)$ at time t is

$$\nu(t)=I(t)n_A(t)\simeq 4n_Bn_A(t)\pi D \times\left\{\frac{1}{S(R)}+\frac{R^2\exp\left[-U(R)/kT\right]}{(\pi Dt)^{\frac{1}{2}}}\right\}, \quad (17)$$

where $S(R)$ is given by (11). In the absence of interparticle forces, $U(R)=0$ and $S(R)=1/R$, reducing (17) to the classical Smoluchowski expression

$$\nu(t)=4\pi n_Bn_A(t)DR\{1+R/(\pi Dt)^{\frac{1}{2}}\}. \quad (17a)$$

III. COLLISION FREQUENCY WHEN $U(r)$ IS COULOMB POTENTIAL

The potential function of particular interest for studying reaction rates in very dilute solutions is the Coulomb potential

$$U(r)=z_Az_Be^2/\mathfrak{D}r, \quad (18)$$

where ez_A = charge on particle of kind A and ez_B = charge on particle of kind B.

It is convenient to define a length L as

$$L=z_Az_Be^2/\mathfrak{D}kT. \quad (19a)$$

L is positive when both kinds of particles have the same type of charge, and negative otherwise. With a Coulomb potential

$$S(r)=\int_r^\infty z^{-2}\exp(L/z)dz=(e^{L/r}-1)/L, \quad (19b)$$

so that (13) becomes

$$\frac{\partial f}{\partial t}=D\left\{\frac{\partial^2 f}{\partial r^2}+\frac{1}{L}\frac{\partial f}{\partial r}\left(\frac{2L}{r}-\frac{L^2}{r^2}\coth\frac{L}{2r}\right)\right\}. \quad (20)$$

It is to be noted that the coefficient of $(\partial f/\partial r)$ can be written as

$$\frac{1}{L}\left\{\frac{2L}{r}-\left(\frac{L}{r}\right)^2\coth\frac{L}{2r}\right\} \simeq(1/L)\left\{-\frac{1}{6}(L/r)^3+\frac{1}{360}(L/r)^5+\cdots\right\}$$

which for most values of L/r of interest is small. The boundary conditions (13a) are still valid.

Let $f(r,t)$ be divided into two parts

$$f(r,t)=f_1(r,t)+f_2(r,t), \quad (21)$$

such that $f_1(r,t)$ satisfies

$$\partial f_1/\partial t=D(\partial^2 f_1/\partial r^2), \quad (22)$$

the boundary conditions

$$f_1(R,t)=0 \quad \text{and} \quad f(\infty,t)<\infty, \quad (23a)$$

and the initial condition

$$f_1(r,0)=1. \quad (23b)$$

Then f_2 satisfies the initial and boundary conditions

$$f_2(R,t)=f_2(\infty,t)=f_2(r,0)=0. \quad (24)$$

By introducing the Laplace transform of $f_1(r,t)$:

$$F_1(r,s)=\int_0^\infty f_1(r,t)\exp(-st)dt, \quad (25)$$

one can reduce (22) to an ordinary equation

$$d^2F_1/dr^2-(s/D)F_1=-1/D,$$

with the boundary conditions $F_1(R,s)=0$ and $F_1(\infty,s)<\infty$. The solution of this equation is

$$F_1(r,s)=(1/s)\{1-\exp[-(r-R)(s/D)^{\frac{1}{2}}]\}. \quad (26)$$

Inverting the Laplace transform, we have[8]

$$f_1(r,t)=\operatorname{erf}[(r-R)/2(Dt)^{\frac{1}{2}}], \quad (27)$$

and as a first approximation

$$\alpha(r,t)/n_B\simeq 1+\left(\frac{e^{L/r}-1}{e^{L/R}-1}\right)\left\{-1+\operatorname{erf}\left(\frac{r-R}{2(Dt)^{\frac{1}{2}}}\right)\right\}, \quad (28)$$

which agrees with (16).

The determination of $f_2(r,t)$ is somewhat more complicated. Except in the region of very small r, (20) reduces to (22), so one could expect f_1 to be the main contribution to f, and to be quite larger than f_2. Then, substituting (21) into (20), remembering (22) and neglecting the product of the two small quantities, df_1/dr and that following (20), we have

$$\frac{\partial f_2}{\partial t}=D\left\{\frac{\partial^2 f_2}{\partial r^2}+\frac{\partial f_1}{L\partial r}\left(\frac{2L}{r}-\frac{L^2}{r^2}\coth\frac{L}{2r}\right)\right\}. \quad (29)$$

[8] Cf. the table of transforms in Churchill, *Modern Operational Mathematics in Engineering* (McGraw-Hill Book Company, Inc., New York, 1944), p. 295.

The initial and boundary values of f_2 are given by (20). This equation is solved in the appendix where it is shown that

$$f_2(r,t)=-\frac{2}{(\pi Dt)^{\frac{1}{2}}}\left\{\int_R^\infty \exp\left[-(r-3R+2y)^2/4Dt\right]\log\left(\frac{y}{L}\sinh\frac{L}{2y}\right)dy\right.$$
$$\left.-\int_r^\infty \exp\left[-(2y-R-r)^2/4Dt\right]\log\left(\frac{y}{L}\sinh\frac{L}{2y}\right)dy\right\}, \quad (30)$$
$$=-\frac{2}{(D\pi t)^{\frac{1}{2}}}\{\quad\}.$$

Thus,

$$-1+\alpha(r,t)/n_B\simeq\left(\frac{e^{L/r}-1}{e^{L/R}-1}\right)\left[-1+\operatorname{erf}\left(\frac{r-R}{2(Dt)^{\frac{1}{2}}}\right)-\frac{2}{(\pi Dt)^{\frac{1}{2}}}\{\quad\}\right].$$

We are now able to calculate the rate at which particles arrive at the surface $|r|=R$ from (8)

$$I(t)=4\pi DR^2\exp\{-U(R)/kT\}(\partial\alpha/\partial r)_{r=R}.$$

Since

$$\log\{(R/L)\sinh(L/2R)\}=\frac{2}{Dt}\int_R^\infty (y-R)\log\{(R/L)\sinh(L/2R)\}\exp\left[-(y-R)^2/Dt\right]dy, \quad (31)$$

we have

$$\left.\frac{1}{n_B}\frac{\partial\alpha}{\partial r}\right]_{r=R}=\frac{Le^{L/R}}{R^2(e^{L/R}-1)}+(\pi Dt)^{-\frac{1}{2}}+\frac{4\pi}{(\pi Dt)^{\frac{1}{2}}}\int_R^\infty (y-R)\exp\left[-(y-R)^2/Dt\right]\log\left(\frac{y\sinh L/2y}{R\sinh L/2R}\right)dy \quad (31a)$$

and

$$I(t)=4\pi Dn_B\left\{\frac{L}{e^{L/R}-1}+\frac{R^2e^{-L/R}}{(\pi Dt)^{\frac{1}{2}}}+\frac{4\pi R^2e^{-L/R}}{(\pi Dt)^{\frac{3}{2}}}\right.$$
$$\left.\times\int_R^\infty (y-R)\exp\left[-(y-R)^2/Dt\right]\log\left(\frac{y\sinh L/2y}{R\sinh L/2R}\right)dy\right\}. \quad (32a)$$

Integrating the right-hand term by parts, we obtain

$$I(t)=4\pi DRn_B\left\{\frac{L/R}{e^{L/R}-1}+\frac{Re^{-L/R}}{(\pi Dt)^{\frac{1}{2}}}+\frac{Re^{-L/R}}{(\pi Dt)^{\frac{1}{2}}}\int_R^\infty\left(\frac{2}{y}-\frac{L}{y^2}\coth\frac{L}{2y}\right)\exp\left[-(y-R)^2/Dt\right]dy\right\}. \quad (32b)$$

The integral

$$J(L/R,\,Dt/R^2)=\frac{R}{(\pi Dt)^{\frac{1}{2}}}\int_R^\infty\left(\frac{2}{y}-\frac{L}{y^2}\coth\frac{L}{2y}\right)\exp\left\{-\frac{(y-R)^2}{Dt}\right\}dy \quad (33)$$

is evaluated in Appendix II. The value of the third term in the bracket in (32b) is tabulated in Table I as a function of $\tau=Dt/R^2$ and is compared with the sum of the first two terms. Four typical ratios 3, 2, 1, and -1 have been chosen. According to Umberger and LaMer[6] $L/R=3$ corresponds approximately to the self-quenching of fluorescein and $L/R=2$ to the quenching of a fluorescein ion by an iodide ion. It is to be noted that over the entire time scale the perturbation term (33) gives a very small percentage contribution to the collision frequency $n_A(t)I(t)$ and for most purposes may be neglected, leaving

$$\nu(t)=n_A(t)I(t)\simeq 4\pi n_A(t)n_BDR\left\{\frac{L/R}{e^{L/R}-1}+\frac{Re^{-L/R}}{(\pi Dt)^{\frac{1}{2}}}\right\}. \quad (34)$$

TABLE I. Comparison of the sum of the two main terms in the bracket of (32b) with correction term, Δ, given by the integral in the same bracket.

L/R \ $\frac{\pi Dt}{R^2}$		10^{-4}	10^{-3}	10^{-2}	10^{-1}	1	10	10^{2}	10^{3}	10^{4}	∞
3.0	approx. 5.13	1.73	.655	.314	.207	.174	.162	.158	.157	.157	
	correction, Δ −.03	−.03	−.03	−.025	−.02	$-.02<\Delta<0$	$-.02<\Delta<0$	0	.0007	0	
2.0	approx. 13.8	4.59	1.67	.741	.448	.356	.327	.317	.314	.313	
	correction −.04	−.04	−.04	−.035	−.02	−.01	−.004	−.002	−.0003	0	
1.0	approx. 37.4	12.2	4.26	1.74	.950	.698	.619	.594	.586	.582	
	correction −.03	−.03	−.025	−.025	−.02	−.015	−.015	−.01	−.004	0	
0	approx. 101	32.6	11.0	4.16	2.00	1.32	1.10	1.03	1.01	1.00	
	correction 0	0	0	0	0	0	0	0	0	0	
−1.0	approx. 273	87.5	28.8	10.2	4.30	2.44	1.85	1.67	1.61	1.58	
	correction −.22	−.22	−.20	−.17	−.13	−.10	−.09	−.08	−.02	0	

The results in Table I confirm our original assumption that f_2 in (21) is small compared to f_1, so that (32a) can be accepted as a complete expression for $I(t)$.

IV. COLLISION FREQUENCY FOR SCREENED COULOMB POTENTIAL

The results of the last section are valid only for solutions so dilute that there are very few ions per unit distance between an arbitrarily selected pair. As the concentration increases the number of intermediate ions increases, screening the effect of one ion on another distant one. In this case, according to the Debye-Hückel theory of strong electrolytes

$$U(r)=-\frac{1}{2}\left\{\frac{\exp(\kappa R_2/2)}{1+\frac{1}{2}\kappa R_1}+\frac{\exp(\kappa R_1/2)}{1+\frac{1}{2}\kappa R_2}\right\}\frac{z_1z_2e^2e^{-\kappa r}}{\mathfrak{D}r}, \quad (35)$$

where R_1 and R_2 are radii of the two particles and κ the ionic strength of the solution. Following Debye,[5] if we let

$$\gamma=-\frac{1}{2}\left\{\frac{\exp(\frac{1}{2}\kappa R_2)}{1+\frac{1}{2}\kappa R_1}+\frac{\exp(\frac{1}{2}\kappa R_1)}{1+\frac{1}{2}\kappa R_2}\right\}, \quad (35a)$$

$$\kappa^2=(4\pi e^2/\mathfrak{D}kT)\sum n_iz_i^2, \quad (35b)$$

$S(r)$ becomes (from (11)):

$$S(r)=\int_r^\infty z^{-2}\exp\{(\gamma L/z)e^{-\kappa z}\}dz.$$

When κ is small,

$$S(r)\simeq\int_r^\infty z^{-2}\exp\{(\gamma L/z)(1-\kappa z+\cdots)\}dz,$$

$$=e^{-\kappa\gamma L}(e^{L\gamma/r}-1)/L\gamma.$$

Thus, the collision frequency is, from (17),

$$\nu(t)\simeq 4\pi n_Bn_A(t)D\left\{\frac{\gamma L\exp(\kappa L\gamma)}{(e^{L\gamma/R}-1)}+\frac{R^2\exp[-(\gamma L/R)e^{-R\kappa}]}{(\pi Dt)^{\frac{1}{2}}}\right\}. \quad (36)$$

On the basis of the numerical work discussed in the last section, we neglect the contribution of the perturbation terms to (36).

V. APPLICATION TO QUENCHING OF FLUORESCENCE

In the absence of a quencher fluorescence is a simple first-order reaction. When a solution of a

dye such as fluorescein is irradiated with light of the proper wave-length, it is excited into a higher energy state. After the light source is removed the excited molecules return to their normal states with the emission of radiation. This emission occurs in such a manner that if $n_A(t)$ is the number of excited molecules at time t, their rate of return to a normal state is proportional to the number excited at that time; that is,

$$dn_A(t)/dt = -n_A(t)/\tau_0,$$

where τ_0 is the rate constant for the reaction. Clearly

$$n_A(t) = n_A \exp(-t/\tau_0), \tag{37}$$

where $n_A = n_A(0)$ = number of excited molecules when light source is removed at time $t=0$.

If potassium iodide is added to the fluorescein solution at the moment the exciting radiation is removed, it is found that the light emitted by the excited molecules as they return to their ground stated is not as intense as in the absence of the KI. This quenching effect can be explained by assuming that when an iodide ion collides with an excited fluorescein molecule it absorbs the excess energy of the fluorescein, returning it to its ground state. Thus, an excited fluorescein molecule loses its excess energy either by collision or through fluorescence.

The number of collisions in time dt at time t is (17a):

$$\nu(t)dt \simeq 4n_B n_A(t)\pi D \times \left\{\frac{1}{S(R)} + \frac{R^2 \exp[-U(R)/kT]}{(\pi Dt)^{\frac{1}{2}}}\right\}dt = n_B n_A(t)\{\beta + \epsilon t^{-\frac{1}{2}}\}dt. \tag{38}$$

Thus, if each collision removes energy from an excited fluorescein molecule,

$$dn_A(t)/dt = -\{(1/\tau_0) + \beta n_B + \epsilon n_B t^{-\frac{1}{2}}\}n_A(t),$$

or at time t:

$$n_A(t) = n_A(0) \exp\{-t(\beta n_B + 1/\tau_0) - 2\epsilon n_B t^{\frac{1}{2}}\}. \tag{39}$$

In the case of a Coulomb potential

$$\beta = \frac{4\pi(L/R)(D_1+D_2)(R_1+R_2)}{(e^{L/R}-1)} \tag{40a}$$

and

$$\epsilon = 4R^2 e^{-L/R}[\pi(D_1+D_2)]^{\frac{1}{2}}. \tag{40b}$$

Employing Einstein's relation between viscosity of solvent and diffusion constant

$$D_j = kT/6\pi\eta R_j,$$

we have

$$\beta = \frac{2kT[2+(R_1/R_2)+(R_2/R_1)]}{3\eta(R/L)(e^{L/R}-1)} \tag{41a}$$

and

$$\epsilon = 4R^2 e^{-L/R}\left\{\frac{kT}{6\eta}\left(\frac{1}{R_1}+\frac{1}{R_2}\right)\right\}^{\frac{1}{2}}. \tag{41b}$$

The mean life of an excited fluorescein ion is, in the absence of quencher, τ_0, for

$$(1/n_A)\int_0^\infty n_A(t)dt = \int_0^\infty \exp(-t/\tau_0)dt = \tau_0. \tag{42}$$

In the presence of quencher it is

$$\tau^* = \int_0^\infty \exp\left\{-t\left(\beta n_B + \frac{1}{\tau_0}\right) - 2\epsilon n_B t^{\frac{1}{2}}\right\}dt = \frac{\tau_0 \exp x^2}{(1+\beta n_B \tau_0)}\int_0^\infty \exp[-(u^{\frac{1}{2}}+x)^2]du,$$

where

$$x = n_B\epsilon\{\tau_0/(1+\beta\tau_0 n_B)\}^{\frac{1}{2}}. \tag{42a}$$

By an obvious transformation

$$\tau^* = \frac{2\tau_0 \exp x^2}{1+\beta n_B\tau_0}\int_x^\infty (y-x)\exp[-y^2]dy = \frac{\tau_0}{1+\beta\tau_0 n_B}\{1 - x\pi^{\frac{1}{2}}(\exp x^2)(1-\operatorname{erf} x)\}; \tag{43a}$$

and when x is small,

$$\tau^* \simeq \frac{\tau_0}{1+n_B\beta\tau_0}(1-x\pi^{\frac{1}{2}}) = \frac{\tau_0}{1+\beta n_B\tau_0}\{1 - n_B\epsilon[\pi\tau_0/(1+\beta n_B\tau_0)]^{\frac{1}{2}}\}. \tag{43b}$$

As $n_B \to 0$

$$\left(\frac{\tau_0}{\tau^*} - 1\right) \to n_B\beta\tau_0 + n_B\epsilon(\pi\tau_0)^{\frac{1}{2}}. \tag{44}$$

Since the process of fluorescence is a very rapid one ($\tau_0 \sim 10^{-8}$ second), it is quite difficult to follow the decrease in $n_A(t)$ with time. One usually studies quenching of fluorescence in the *photo-stationary* state; that is, in a state in which the particles in the solution are kept excited by a constant source of light and in which the intensity of fluorescence remains constant. In any small time interval the same number of dye molecules become excited as lose their excess energy by either radiation or collision. It can be shown that under these conditions the ratio of the intensity of fluorescence in an unquenched solution to that in a quenched solution containing the same concentration of dye is equal to the ratio of the mean lives of the excited dye molecules in each of the solutions[3, 6]

$$I_0/I = \tau_0/\tau^*.$$

The quenching constant, k_Q, defined by

$$[(I_0/I)-1]/n_B = k_Q$$

is, in the range of low quencher concentration, therefore (from (44)),

$$k_Q = \beta\tau_0 + \epsilon(\pi\tau_0)^{\frac{1}{2}}. \tag{45a}$$

In particular, in the presence of Coulomb forces between particles, we obtain from[9] (41)

$$k_Q = \frac{2kT\tau_0\left(2+\frac{R_1}{R_2}+\frac{R_2}{R_1}\right)}{3\eta(R/L)(e^{L/R}-1)} + 4R^2e^{-L/R}\left(\frac{kT\pi\tau_0}{6\eta}\left(\frac{1}{R_1}+\frac{1}{R_2}\right)\right)^{\frac{1}{2}}. \tag{45b}$$

This expression differs from the classical one by the appearance of a term inversely proportional to the square root of the viscosity of the solvent. A similar expression can be obtained in the case of screened Coulomb forces by evaluating β and ϵ from (36) and (38).

Many experimental curves of k_Q plotted as a function of the reciprocal of the viscosity of the solvent have been collected in a paper of Davis and LaMer.[10] An example (see Fig. 1) is that obtained for the quenching of fluorescence of fluorescein by potassium iodide (original data from Sveshnikoff). It appears from (45) that two possible causes of the curvature in the experimental curves are

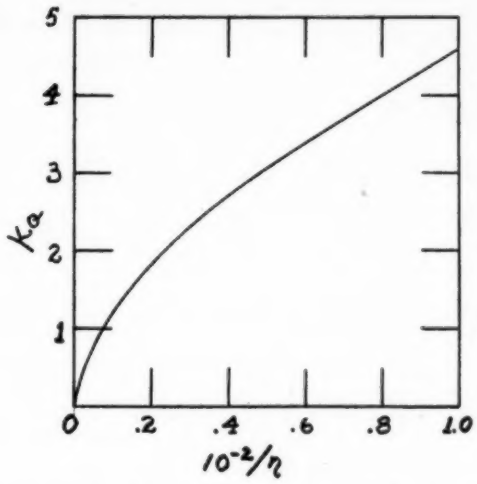

FIG. 1. Quenching of fluorescence of fluorescein by potassium iodide. Solvent is sucrose or glycerol solution. The volume molar concentration scale was used in determining k_Q (data from Sveshnikoff).

a. a significant fraction of the collisions between quencher and newly excited particles occur before a steady collision rate is achieved,

b. change in dielectric constant of solvent with change in viscosity.

Classically[10] the quenching constant curve should be a straight line. As was pointed out to the author by Dr. J. Q. Umberger, the first of the above two causes of the curvature is implicit in the theory of Sveshnikoff.[4] There an expression for τ^* is derived which is identical to (43) in the absence of forces between particles. However, in calculating the limiting low concentration expression for the quenching constant analogous to (45a) Sveshnikoff omitted the term corresponding to ϵ and therefore did not obtain the $\eta^{-\frac{1}{2}}$ component.

In conclusion the author wishes to thank Dr. J. Q. Umberger for his many informative discussions concerning quenching of fluorescence.

[9] In this special case k_Q was obtained previously by J. Q. Umberger (private communication).

[10] H. Davis and V. LaMer, J. Chem. Phys. **10**, 585 (1942).

APPENDIX I

Solution of the Differential Eq. (29)

From (29)

$$\frac{\partial f_2}{\partial t}=D\left\{\frac{\partial^2 f_2}{\partial r^2}+\frac{\partial f_1}{L\partial r}\left[\frac{2L}{r}-\frac{L^2}{r^2}\coth\frac{L}{2r}\right]\right\},$$

where

$$f_1(r,t)=\operatorname{erf}\left[(r-R)/2(Dt)^{\frac{1}{2}}\right]$$

and

$$f_2(R,t)=f_2(\infty,t)=f_2(r,0)=0.$$

Let us introduce the Laplace transform of $f_1(r,t)$ and $f_2(r,t)$,

$$F_j(r,s)=\int_0^\infty f_j(r,t)e^{-st}dt,$$

and use the expression (22b) for $F_1(r,s)$. Then (25) is transformed into the ordinary equation

$$\frac{d^2F_2}{dr^2}-\frac{sF_2}{D}=-\frac{1}{L(Dt)^{\frac{1}{2}}}\left\{\frac{2L}{r}-\frac{L^2}{r^2}\coth\frac{L}{2r}\right\}\exp\left\{-(r-R)(s/D)^{\frac{1}{2}}\right\},$$

and the boundary conditions become

$$F_2(R,s)=F_2(\infty,s)=0.$$

By direct substitution one can verify that

$$F_2(r,s)=-2(sD)^{-\frac{1}{2}}\exp\left\{(r-R)(s/D)^{\frac{1}{2}}\right\}\left[\int_R^r\log\left(\frac{y}{L}\sinh\frac{L}{2y}\right)\exp\left(-2(y-R)(s/D)^{\frac{1}{2}}\right)dy\right.$$

$$\left.-\left(1-\exp\left(-2(r-R)(s/D)^{\frac{1}{2}}\right)\right)\int_R^\infty\log\left(\frac{y}{L}\sinh\frac{L}{2y}\right)\exp\left(-2(y-R)(s/D)^{\frac{1}{2}}\right)dy\right].$$

Since the inverse Laplace transform of

$$F(r,s)=\int_0^\infty f(r,t)e^{-st}dt=s^{-\frac{1}{2}}\exp\left(-ks^{\frac{1}{2}}\right)$$

is

$$f(r,t)=(\pi t)^{-\frac{1}{2}}\exp\left(-k^2/4t\right),$$

one has immediately

$$f_2(r,t)=-\frac{2}{(\pi Dt)^{\frac{1}{2}}}\left\{\int_R^\infty\exp\left(-(r-3R+2y)^2/4Dt\right)\log\left(\frac{y}{L}\sinh\frac{L}{2y}\right)dy\right.$$

$$\left.-\int_r^\infty\exp\left(-(2y-R-r)^2/4Dt\right)\log\left(\frac{y}{L}\sinh\frac{L}{2y}\right)dy\right\}$$

as is given by (30) in the text.

APPENDIX II

Integration of $J(L/R, Dt/R^2)$

According to (33), $J(L/R, Dt/R^2)$ is defined by

$$J(L/R,Dt/R^2)=\frac{2R}{(\pi Dt)^{\frac{1}{2}}}\int_R^\infty\left\{\frac{1}{y}-\frac{L}{2y^2}\coth\frac{L}{2y}\right\}\exp\left\{-\frac{(y-R)^2}{Dt}\right\}dy.$$

Letting $\tau = Dt/R^2$ and $\mu = L/2R$, we have by an obvious transformation

$$J(2\mu, \tau) = 2(\tau\pi)^{-\frac{1}{2}} \int_0^\infty \left(\frac{\mu}{1+v} - \frac{\mu^2}{(1+v)^2} \coth \frac{\mu}{1+v} \right) \exp(-v^2/\tau) dv.$$

At early times (as $\tau \to 0$) the main contribution to the integral comes from the interval of small values of v, thus:

$$J(2\mu, \tau) \sim (1 - \mu \coth \mu) - (\tau/\pi)^{\frac{1}{2}}(1 - 2\mu \coth \mu + \mu^2 \operatorname{csch}^2 \mu) + (\tau/2)(1 - 3\mu \coth \mu + 3\mu^2 \operatorname{csch}^2 \mu - \mu^3 \operatorname{csch}^2 \mu \coth \mu).$$

At late times (as $\tau \to \infty$)

$$J(2\mu, \tau) \to 2(\pi\tau)^{-\frac{1}{2}} \int_0^\infty \left(\frac{1}{1+v} - \frac{\mu}{(1+v)^2} \coth \frac{\mu}{(1+v)} \right) dv = -2(\pi\tau)^{-\frac{1}{2}} \log \left(\frac{1}{\mu} \sinh \mu \right).$$

At intermediate times it seems convenient to substitute the series

$$x^2 \coth x = x + x^3/3 + x^5/45 - 2x^7/945 + x^9/4725 + \cdots$$

into $J(2\mu, \tau)$. Then, after integrating term by term one obtains

$$J(2\mu, \tau) = -2(\pi\tau)^{-\frac{1}{2}} \left(\frac{1}{3}\mu^2 I_3 + \frac{\mu^4}{45} I_5 - \frac{2\mu^6}{945} I_7 + \frac{\mu^8}{4725} I_9 + \cdots \right),$$

where

$$I_n = \int_0^\infty \frac{1}{(1+v)^n} \exp(-v^2/\tau) d\tau.$$

By integrating by parts one can show that I_5, I_7, etc. can be calculated from I_3. Thus for values of τ of interest one need only integrate I_3 numerically in order to determine $J(2\mu, \tau)$ completely.

Predissociations in Nitric Oxide

P. J. FLORY
Research Department, The Goodyear Tire and Rubber Company, Akron, Ohio
AND H. L. JOHNSTON
Department of Chemistry, The Ohio State University, Columbus, Ohio

(Received January 25, 1946)

GAYDON,[1-3] in a series of recent publications, has argued for a heat of dissociation of nitrogen of 9.764 ev, in place of the previously accepted value of 7.384 ev.[4] The heats of dissociation of nitric oxide calculated from these two values of D_{N_2}, in combination with thermochemical data and $D_{O_2}=5.09$ ev, are 6.49 and 5.29 ev, respectively. An obvious objection to the higher value of D_{NO}, and hence to Gaydon's D_{N_2} as well, is the previous suggestion of Kaplan[5] that the absence of β-bands in emission from vibrational level in the upper electronic state ($^2\pi$) beyond $v'=4$ is due to predissociation. This level corresponds to 6.12 ev, which is below the dissociation energy required by the higher value for D_{N_2}. Gaydon,[3] however, has now succeeded in locating emission bands of the β-system arising from upper levels for which $v'=5$ and 6, thus refuting previous *spectroscopic* evidence for predissociation in the β-system and thereby eliminating an objection to the higher dissociation energies.

Gaydon does not confine his renunciation of previous conclusions concerning predissociations of nitric oxide to those pertaining to the β-system. He apparently regards all evidence for predissociation from any of the excited levels of nitric oxide as worthless, dismissing it indiscriminantly as the product of "wishful thinking."

An investigation of the photo-decomposition of nitric oxide carried out by the present author[6] some time ago led them to the conclusion that at low pressures, using wave-lengths from 1800 to 2000A, the primary process is one of predissociation; under our experimental conditions the $\delta(1,0)$-band appeared to be principally responsible for the absorption causing decomposition. Gaydon[3] disposes of this work with the following remarks: "With the new knowledge that $B^2\pi$ [upper state of the β system] is not predissociated below $v=6$, and that state D [upper state of the ϵ bands] is of type $^2\Sigma^+$, and is not predissociated below $v=2$, it becomes clear that their [Flory and Johnston's] explanation of the photodissociation is certainly incorrect in detail and may be altogether wide of the mark. From inspection of the potential curves it would clearly be very difficult to imagine any repulsive curve which could predissociate $C^2\Sigma$ [upper state for the δ bands] below $v=1$ without also causing predissociation in $D^2\Sigma^+$ (the curve for which lies very close indeed to that for C) and $B^2\pi$. It may be noted that Flory and Johnston's observations are at variance with those of Macdonald (1928)."

Our measurements show conclusively that over the pressure range investigated, 0.02 to 7 mm, the rate of decomposition caused by the full radiation emitted by a low pressure mercury arc in quartz is directly proportional to the amount of Beer's law absorption, the rate being otherwise independent of pressure. The mere fact that rapid photo-decomposition occurs at these low pressures, where the mean lifetime with respect to collision far exceeds the life with respect to fluoresence, is strong indication of a monomolecular decomposition; the observed dependence of the rate on pressure firmly establishes this conclusion. The decomposition produced by the mercury arc was shown to be almost entirely due to radiation between 1800 and 1900A, the lower limit being imposed by absorption by quartz and air. Most of the decomposition appeared to be produced by wavelengths below 1850A. In this region the nitric oxide absorption spectrum is banded; hence, the

[1] A. G. Gaydon and W. G. Penney, Nature **150**, 406 (1943); A. G. Gaydon, *ibid.* **153**, 407 (1944).
[2] A. G. Gaydon, Proc. Phys. Soc. (London) **56**, 95 (1944).
[3] A. G. Gaydon, Proc. Phys. Soc. (London) **56**, 160 (1944).
[4] G. Herzberg and H. Sponer, Zeits. f. physik. Chemie **B26**, 1 (1934). See G. Herzberg, *Molecular Spectra and Molecular Structure* (Prentice-Hall, Inc., New York, 1941), pp. 477–9.
[5] J. Kaplan, Phys. Rev. **37**, 1406 (1931).
[6] P. J. Flory and H. L. Johnston, J. Am. Chem. Soc. **57**, 2641 (1935).

monomolecular dissociation must be a predissociation.

It was shown further that in this spectral region only the $\delta(1,0)$-band at 1830A is of sufficient intensity to account for the observed dependence of rate on nitric oxide pressure. (The spectrum of the mercury arc was rich in continuous radiation extending from the 1849A-resonance line to well below 1830A, in which region the weaker 1832A-line was included.) Hence, we concluded that predissociation occurred from the $v=1$ level of the $^2\Sigma$-state (upper state of the δ-bands). In conformity with this conclusion, no emission bands are known which arise from this or higher levels of the same electronic state, although intense absorption bands are known which involve these levels. The excitation energy associated with absorption by the $\delta(1,0)$-band is 6.77 ev, which is larger than either D_{NO} value.

Certain of our results obtained using filtered radiation from various spark sources showed that wave-lengths above 1900A, but probably below about 2000A, produced appreciable decomposition at nitric oxide pressures around 0.1 mm. They were considerably less effective than shorter wave-lengths, however; this might be expected merely from the markedly lower intensity of absorption in this region. We suggested at that time that β-band predissociation probably was responsible for decomposition by these longer wave-lengths, an interpretation which would seem to be incompatible with Gaydon's observation of emission bands from $^2\pi$, $v=5$ and 6 levels. However, the observation of emission bands does not necessarily preclude a weak predissociation which may occur only to the extent that the emission intensity is reduced, but not eliminated entirely.

Regardless of which bands are responsible for the effect, it is significant that wave-lengths above 1900A effect decomposition. It seems very doubtful to us that the observed effects here were confined to wave-lengths between this lower limit and 1910A, the wave-length corresponding to Gaydon's $D_{NO}=6.49$ ev. It would be extremely difficult to account for the decomposition at the low pressure employed by assuming a bimolecular process. Hence, these admittedly rather limited observations on the decomposition of nitric oxide by wave-lengths above 1900A cast doubt on the high value of D_{NO} proposed by Gaydon.

In conclusion we should like to point out that our results show conclusively that predissociation occurs when nitric oxide is irradiated with wave-lengths around 1800 to 1850A. The $\delta(1,0)$-band almost certainly is responsible for the overwhelming portion of this decomposition. Admittedly there may be some difficulty in postulating a repulsive state which dissociated $C^2\Sigma$, $v'=1$, while molecules in the neighboring $D^2\Sigma^+$, $v'=1$ (upper state for the ϵ-bonds) emit radiation; the latter apparently does not undergo predissociation at all, or does so with greater difficulty. Nevertheless, we wish to emphasize that this apparent incongruity does not justify dismissal of the photochemical results.

It should also be mentioned, contrary to Gaydon's statement, that our results do not conflict with those of Macdonald. His work was conducted at higher pressures, and, as we pointed out, a different spectral region probably was involved in his experiments.

Letters to the Editor

THIS section will accept reports of new work, provided these are terse and contain few figures, and especially few halftone cuts. The Editorial Board will not hold itself responsible for opinions expressed by the correspondents. Contributions to this section should not exceed 600 words in length and must reach the office of the Managing Editor not later than the 15th of the month preceding that of the issue in which the letter is to appear. No proof will be sent to the authors. The usual publication charge ($3.00 per page) will not be made and no reprints will be furnished free.

Loci of Emulsion Polymerization: The Diffusion of Organic Molecules from Emulsion Droplets through an Aqueous Phase into Soap Micelles

RICHARD S. STEARNS AND WILLIAM D. HARKINS
University of Chicago, Chicago, Illinois
February 4, 1946

AN important problem of emulsion polymerization in soap solutions is to determine the rate of diffusion of molecules from the surface of oil emulsion droplets through the aqueous phase into the position in which they are caught, i.e., in a soap micelle. The method used to determine the rate of diffusion is extremely simple and was outlined in an unpublished paper by Vinograd, Fong, and Sawer.[1] They measured by the use of a microscope the diameters of small drops of oil "submerged in soap solutions" and found that their diameters "decline *linearly* with time until 99 percent of the drop passes into the aqueous phase."

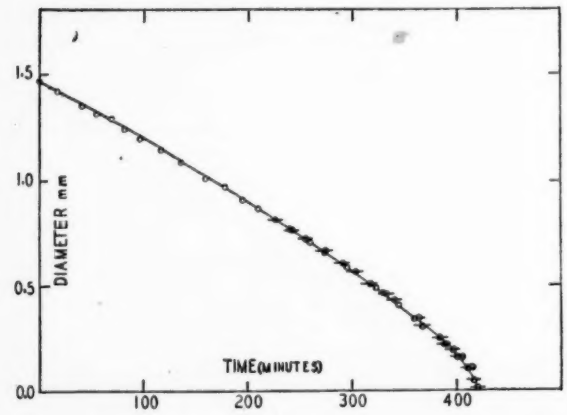

FIG. 1. Diffusion of ethyl benzene into 12.2 percent potassium laurate at 40°C. A second curve starting with a smaller initial drop diameter has been superimposed on the curve for the drop with a larger drop diameter by adding 226 minutes to the time axis.

Our work indicates a different relation: the rate of decrease of the diameter of the oil drop *increases with time* (Figs. 1 and 2), i.e., as the drop grows smaller. The rate of decrease of diameter for a drop of ethyl benzene in 12.2 percent potassium laurate solution at 40°C was increased from −0.00260 mm to −0.00430 mm per minute by a decrease in the diameter from 1.4 mm to 0.25 mm. The rate of diffusion is about twice as high at 40° as at 25°C.

In private communications to the writers Professor P. Debye has developed a theory for the diffusion of molecules from an oil drop into a soap solution. From the picture proposed by him the more rapid decrease of diameter for small than for large drops is what would be expected. His theory introduces a quantity defined by the relation:

$$\triangle^2 = D/\alpha,$$

in which D is the diffusion constant for the oil: in the special case cited, ethyl benzene, and α is a constant such that $\alpha n dt$ is the number of molecules of the oil which are caught per cc during the time dt by the soap at a place where the concentration of the oil is n. The quantity $\triangle$ is then representative for the characteristic thickness of the diffusion layer.

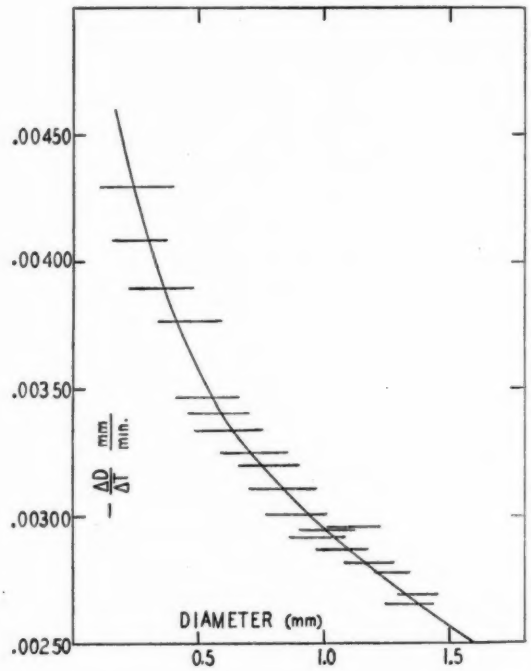

FIG. 2. Chord plot of data of Fig. 1, showing increase in the rate of diffusion with decrease in the size of the drop.

It is of interest that the calculated value of $\triangle$ found by the use of the linear variation of the diameter d of the drop of ethyl benzene is of the order of 50A, while from a representative curve, similar to that of Fig. 1 except that the concentration of the potassium laurate was 10.6 per-

cent, Debye calculated that Δ is about .06 mm or 6×10^5 A. What is now needed is to make certain that all of the conditions in our experiments are in accord with what is demanded by Debye's theory, which is developed on the basis of a spherical drop suspended in the soap solution.

On account of the difference between the density at 25°C of ethyl benzene (0.862) and of the soap solution (1.0082 for 12.2 percent potassium laurate) there is a slight departure of the drops from the spherical form. However, the drop becomes more spherical as it becomes smaller, and, coincidentally, the curvature in the diffusion curve of Fig. 1 increases. Also, while photographs of the profile of the drop have been taken, there has been as yet no accurate determination of the area of contact between the top of the drop and the glass plate against which it rests.

A drop of ethyl benzene suspended in an aqueous 10.6 percent solution of soap is covered with a tightly packed monolayer of molecules of soap with the $C_{12}H_{25}$-chain oriented toward the oil and the $-COO^-K^+$ toward the aqueous phase. The monolayer of soap is about 16A thick (neglecting the relatively few K^+ ions which form the outer part of the diffuse ionic layer). Such a very thin diffusion layer ($\Delta\sim50$A) would allow capture of ethyl benzene molecules by only the edges of those soap micelles which are in contact with the surface of the oil drop. In a 10.6 percent solution of potassium laurate about 15 percent of the volume is filled with solubilizing micelles (provided almost all of the soap is present as solubilizing micelles, which is not certain).*

The variation of the rate of diffusion of ethyl benzene is shown in Fig. 3 as a function of soap concentration at a

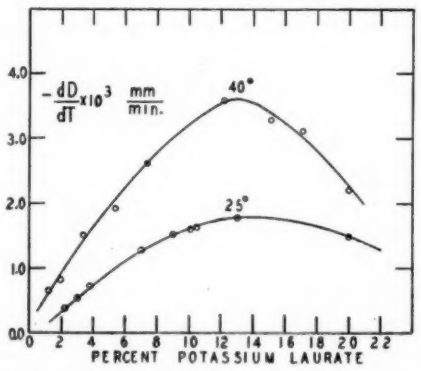

FIG. 3. Diffusion of ethyl benzene into potassium laurate as a function of soap concentration at a constant drop diameter of 0.5 mm.

constant drop diameter of 0.5 mm and at 25°C and 40°C. Both curves exhibit a maximum at a soap concentration of about 15 percent. The rate of diffusion of an oil into a soap solution is increased greatly by the presence of small amounts of salts such as potassium chloride.

[1] September 11–15, 1944, Meeting of the American Chemical Society.

* *Note:* Vinograd has communicated to us a mathematical analysis by Dr. J. N. Wilson, based on Fick's equation for diffusion. According to Wilson, a constant rate of change of the diameter of the drop, such as that obtained by Vinograd, represents a value of Δ such that $\Delta/d << 1$, i.e., a thin diffusion layer.

Loci of Emulsion Polymerization: Diffusion of Organic Molecules from Emulsion Droplets through an Aqueous Phase into Polymer Latex Particles

WILLIAM D. HARKINS AND RICHARD S. STEARNS
University of Chicago, Chicago, Illinois
February 4, 1946

IN recent communications Harkins[1] has developed a general theory of the loci of reaction in emulsion polymerization. According to this theory, when micellar soap is present, most of the polymer particle *nuclei* are *initiated* by polymerization of monomer layers of the general order of 10A thick, solubilized in soap micelles. The polymer molecules thus formed are sufficiently large to be ejected from the micelles into the aqueous phase outside, where they form extremely small (size *unknown*, *possibly* of the order of 25A diameter) polymer particle nuclei, which dissolve monomer. Such polymer-monomer particles become the locus in which, under ordinary conditions, almost all of the polymer is synthesized.

That the particles thus formed are extremely small was shown by an experiment in which 0.75 g of styrene was completely dissolved in 100 g of a 6 percent solution of potassium laurate. All of the styrene, except the small amount dissolved in the aqueous phase, was present in the micellar oil layers. After complete polymerization, the polymer appeared outside the micelles, but the solution, due to the small size of the polymer-latex particles, was almost as clear as the initial soap solution. The particles were so small that no method yet used has given their size.

However, when the same amount of styrene was polymerized in either (1) water alone or (2) a solution of the soap at 0.2 percent concentration (below the critical concentration for micelles), the solution became extremely opaque and very white, indicative of very large polymer particles. The extremely thin micellar oil layers in the presence of a higher concentration of soap—6 percent or more in this case—allow only very small polymer particles to form. However, if more and more styrene is emulsified in the 6 percent soap solution, and polymerization caused to proceed by the use of a catalyst, etc., the solution becomes more and more opaque as the polymer particles become larger. They may, for example, attain diameters of 1000A or even more. Data obtained by use of the electron microscope, from light scattering and by surface tension methods, which show the rate of growth of the polymer particles with the yield of polymer have been obtained and will be presented in later papers.

It is obvious that such small polymer particles cannot change into large particles with a constantly increasing total mass of polymer, unless monomer is constantly added to the polymer particles, while the monomer thus added undergoes polymerization. If all of the above is true, there must be a constant diffusion of monomer molecules from the emulsion oil droplets into the polymer particles after their ejection from the soap micelles. If polymer particles free from monomer become saturated with an oil such as ethyl benzene, which does not polymerize, the diffusion occurs in both directions and the monomer droplets no longer decrease in size.

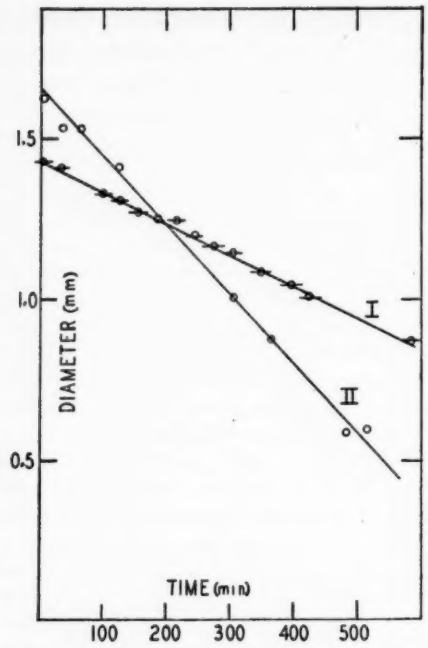

FIG. 1. Diffusion of ethyl benzene into latex solutions at 25°C. Curve I: 98 percent conversion. Curve II: 67 percent conversion.

Experiments were carried out in which polymer particles were substituted for the soap micelles used in the earlier work. The polymer particles were formed from a mixture of 75 percent isoprene and 25 percent styrene in a soap solution with an initial soap concentration of 3 percent and 100 parts monomer to 180 parts water. Samples of latex were used at 67 and 98 percent conversion to polymer. The former already contained 33 percent and the latter only 2 percent of monomer.

The rate of diffusion at 25°C from a drop of ethyl benzene with an initial diameter of 1.5 mm but calculated as the slope of the best straight line was found to be 2×10^{-3} mm decrease of diameter per minute in the polymer solution of 67 percent conversion and 1.0×10^{-3} mm in that of 98 percent conversion. These diffusion rates are not very accurate on account of the difficulty encountered in the observation of the boundary of the drop due to the opacity of the solution. Within the limits of Fig. 1 the rate of decrease of diameter of the drop is linear, but it seems probable that the rate will be found to increase as the drop decreases still further in diameter.

In these polymer solutions no micellar soap and very little dissolved soap is present. On account of the extremely great area of the latex particles almost the whole of the soap is adsorbed at the interface between the latex particles and the aqueous phase.

The relations presented in this and in the preceding letter are often neglected in the development of the kinetics of emulsion polymerization. When 3 percent soap with 100 g of monomer and 180 g of water is used, all free monomer commonly disappears by solution in the polymer particles by the time the yield of polymer reaches about 60 percent.

[1] W. D. Harkins, J. Chem. Phys. **13**, 381 (1945); **14**, 47 (1946).

The Critical Concentration for the Formation of Micelles as Indicated by the Absorption Spectrum of a Cyanine Dye *

MYRON L. CORRIN, HOWARD B. KLEVENS, AND WILLIAM D. HARKINS
University of Chicago, Chicago, Illinois
February 7, 1946

RECENTLY Sheppard and Geddes[1] reported that the absorption spectrum of aqueous pinacyanol chloride is shifted from that exhibited in aqueous solution to that characteristic of its solutions in non-polar solvents by the addition of cetyl pyridinium chloride. They consider that the "addition of a micelle-forming hydrophile colloid effects conversion of the dye from an aggregated—probably dimeric—to a monomeric state." We have determined the absorption spectra of the same cyanine dye in aqueous solutions of potassium laurate and potassium myristate of varying soap concentration at a dye concentration of 1×10^{-4} molar and a temperature of 25.6°. The extremely rapid change in the spectrum in each of these soap solutions is found to occur at the critical concentration for the formation of micelles, and this appears to give the simplest method for the determination of the critical concentration.

With increasing soap concentration, the observed spectra show a very pronounced shift over a short range of concentration to the form typical of the dye solutions in a non-polar medium. With potassium laurate the spectrum is markedly different from that of the dye in water at a soap concentration of 1×10^{-3} molar. In more concentrated solutions a band appears at 4800A; this band disappears

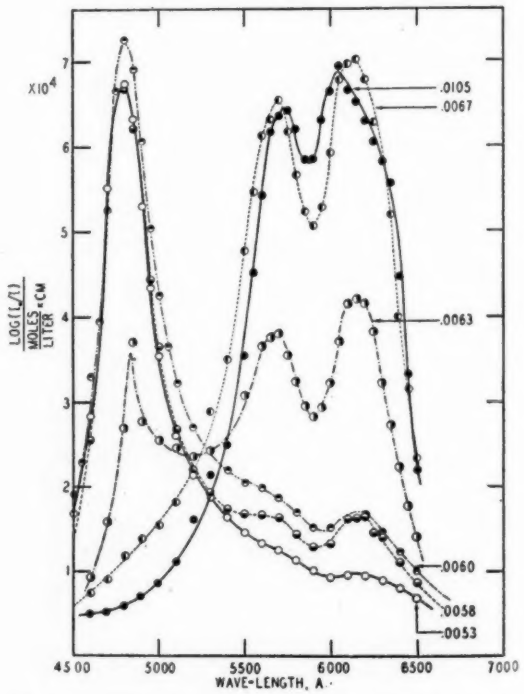

FIG. 1. Absorption spectra of 1×10^{-4} pinacyanol chloride in aqueous potassium myristate solutions.

and two bands at 5700A and 6150A appear when the soap concentration is varied from 2.3×10^{-2} to 2.4×10^{-2} molar; these latter higher wave-length bands are typical of pinacyanol chloride solutions in organic solvents. The behavior of potassium myristate as indicated in Fig. 1 is similar to that of the laurate. The transition of the former occurs at a soap concentration of 6.0×10^{-3} molar.

The observed phenomena can be illustrated in a more striking fashion by plotting the intensities of the three characteristic bands as a function of soap concentration as in Fig. 2. The smallness of the concentration range over which the change occurs is quite clearly indicated.

The simplest explanation that may be offered considers the change in nature of the absorption spectra as due to the formation of soap micelles which solubilize the dye.[2] In water an equilibrium exists between the monomer and dimeric forms of the dye.[3] When soap micelles are present, however, the dye may be solubilized within their hydrocarbon layers. It is thus in a non-polar environment, even though separated from water by only the length of a soap molecule (about 16A in case of the laurate). The dye will then be partitioned between the water and micelles with increasing dye solubilization as more micelles are formed.

Thus, the soap concentration at which the spectral transition occurs may be considered the critical concentration for the formation of micelles. The critical concentration at 25°C as determined by this method is 2.3 to 2.4 $\times10^{-2}$ molar for potassium laurate and 6.0×10^{-3} molar for potassium myristate. Unfortunately, no accurate published data by other methods on such values for potassium myristate are available for comparison.

The sharp nature of the change offers evidence that a considerable portion of ionic soap present before micelles are formed is transformed into micelles, once the proper soap concentration is attained. It would be improbable, for example, that the addition of 2×10^{-4} mole of potassium myristate per liter of solution could form enough micellar material to cause a spectral change so pronounced as that observed in going from a 5.8×10^{-3} to 6.0×10^{-3} molar solution of the soap.

The behavior of the soap-dye system in very dilute soap solutions (below 5×10^{-3} M for laurate) is quite complicated and is not, as yet, amenable to any simple explanation. It is hoped, however, to clarify this situation by further investigation. It is possible that soap solutions may exhibit some solubilizing properties at concentrations lower than those at which the marked spectral change occurs. If this is found to be true, it would indicate some micellar organization in these solutions in conformity with the views of McBain.[4]

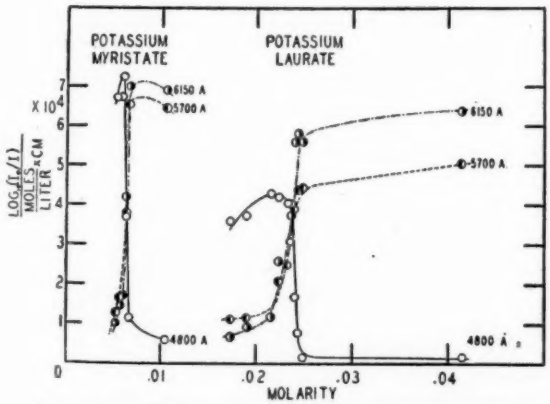

FIG. 2. Intensities of band maxima *vs.* soap concentration.

Further studies on the effect of temperature, dye concentration, and similar variables are in progress and will be presented together with a more complete discussion of the theory in a subsequent paper. The modification of the spectrum of the cationic dye by the anionic soaps is very much greater than that found with cetyl pyridinium chloride. An increase of temperature of 10°C to 35.8°C was found to decrease the critical concentration of potassium myristate only slightly to about 5.7×10^{-3} molar. However, this apparent change in critical concentration with temperature may not be real, but due to a different partitioning with temperature of the dye between the water and the micelles.

* The work reported in this paper was done in connection with the Government Research Program on Synthetic Rubber under contract with the Office of Rubber Reserve, Reconstruction Finance Corporation.

[1] S. E. Sheppard and A. L. Geddes, J. Chem. Phys. **13**, 63 (1945).
[2] W. D. Harkins, R. W. Mattoon, M. L. Corrin, J. Colloid Sci. **1**, (January 1946).
[3] S. E. Sheppard, Rev. Mod. Phys. **14**, 303 (1942).
[4] S. A. Johnston and J. W. McBain, Proc. Roy. Soc. **A181**, 119 (1943).

Estimation of the Surface Area of Solid Particles

HANS M. CASSEL
Speedry Products Company, New York 6, New York
February 11, 1946

IN replying to my letter of April 14, 1945,[1] Messrs. Harkins and Jura[2] have submitted data, previously not published, which prove that capillary condensation does not occur when loosely packed titanium dioxide powder is exposed to saturated steam. In the light of Bangham's observations[3] on mica it is reasonable to assume that this is also true in the case of tight packing. Accordingly, we have to face the alternative, as pointed out in my letter, that the adsorbent studied is not perfectly wettable, analogous to the behavior of mica. In other words, if the liquid phase were once formed by supersaturation, the contact angle at the vapor-film-liquid boundary would be greater than zero. Consequently, the "surface tension" (if it were measurable!) of the polylayer produced in the saturation procedure must be different from that of normal water. These films, as has been recognized by Bangham and, independently, by Frumkin,[4] form a phase different from liquid water, and are not "duplex films," as defined by Harkins. Consequently, no prediction of the magnitude of thermal effects resulting from the submersion of such films can be made without further investigation.

In principle, the "absolute method" is open to the same objection as the calculations of Emmett-Brunauer-Teller,[5] i.e., it contradicts the existence of first-order phase transitions from the adsorbed to the liquid state.

[1] H. M. Cassel, J. Chem. Phys. **13**, 249 (1945).
[2] W. D. Harkins and G. Jura, J. Chem. Phys. **13**, 449 (1945).
[3] D. H. Bangham and S. Mosallam, Proc. Roy. Soc. **A165**, 552 and **A166**, 558 (1938); D. H. Bangham and Z. Sawaris, Trans. Faraday Soc. **34**, 554 (1938).
[4] A. Frumkin, Acta Physicochimica U.S.S.R. **9**, 313 (1938).
[5] H. M. Cassel, J. Chem. Phys. **12**, 115 (1944); J. Phys. Chem. **48**, 195 (1944).